AD_____

Award Number: DAMD17-99-2-9010

TITLE: Mediation of Sulfur Mustard Cellular Toxicity by ATP: A Possible Mechanism of Action of Sulfur Mustard Toxicity

PRINCIPAL INVESTIGATOR: Paul M. Lundy, Ph.D.
R. Frew W. Gong
C. Vair L. Mi
P. Nelson T. Sawyer

CONTRACTING ORGANIZATION: Canadian Commercial Corporation
Ottawa, Ontario K1A 0S6 Canada

REPORT DATE: December 2002

TYPE OF REPORT: Final

PREPARED FOR: U.S. Army Medical Research and Materiel Command
Fort Detrick, Maryland 21702-5012

REPORT DOCUMENTATION PAGE

Form Approved
OMB No. 074-0188

1. AGENCY USE ONLY (Leave blank)	2. REPORT DATE	3. REPORT TYPE AND DATES COVERED
	December 2002	Final (16 Nov 98 - 15 Nov 02)

4. TITLE AND SUBTITLE

Mediation of Sulfur Mustard Cellular Toxicity by ATP: A Possible Mechanism of Action of Sulfur Mustard Toxicity

5. FUNDING NUMBERS

DAMD17-99-2-9010

6. AUTHOR(S) :

Paul M. Lundy, Ph.D., R. Frew, W. Gong, C. Vair, L. Mi, P. Nelson, T. Sawyer

7. PERFORMING ORGANIZATION NAME(S) AND ADDRESS(ES)

Canadian Commercial Corporation
Ottawa, Ontario K1A 0S6 Canada

E-Mail: Paul.Lundy@drdc-rddc.gc.ca

8. PERFORMING ORGANIZATION REPORT NUMBER

9. SPONSORING / MONITORING AGENCY NAME(S) AND ADDRESS(ES)

U.S. Army Medical Research and Materiel Command
Fort Detrick, Maryland 21702-5012

10. SPONSORING / MONITORING AGENCY REPORT NUMBER

11. SUPPLEMENTARY NOTES

Original contains color plates: All DTIC reproductions will be in black and white.

12a. DISTRIBUTION / AVAILABILITY STATEMENT

Approved for Public Release; Distribution Unlimited

12b. DISTRIBUTION CODE

13. Abstract ***(Maximum 200 Words)*** *(abstract should contain no proprietary or confidential information)*

The effect of HD on cell death was examined in a variety of tests in a number of phylogenetically distinct cell types. HD caused concentration dependant apoptosis with increasing numbers of necrotic cells at higher concentrations. A variety of techniques were used to examine HD induced cellular biochemical responses in attempts to identify a critical determinant of initiation of these events. Much of the work describes attempts to relate HD induced changes in intracellular calcium levels with cell death and also to determine the role of cell surface ionotropic ATP receptors (calcium pores), which when stimulated might be responsible for the calcium influx since upon stimulation they mimicked many of the apoptotic effects of HD. Examination of the intracellular biochemical events known to be related to induction of apoptosis such as the role of certain caspases and DNA'ases were also carried out. Some studies describe the characterization of a cytolytic pore complex in certain cells and the effects of HD on this pore. Other studies were prompted by our initial findings of the importance of cationic environment on ATP toxicity. This work identified the extreme importance of ionic environment (including pH) on HD toxicity.

14. SUBJECT TERMS:

sulfur mustard, ATP receptors, calcium, apoptosis

15. NUMBER OF PAGES

176

16. PRICE CODE

17. SECURITY CLASSIFICATION OF REPORT	18. SECURITY CLASSIFICATION OF THIS PAGE	19. SECURITY CLASSIFICATION OF ABSTRACT	20. LIMITATION OF ABSTRACT
Unclassified	Unclassified	Unclassified	Unlimited

Table of Contents

GENERAL BACKGROUND

The hypothesis that originally formed the basis for the work proposed in this cooperative research project, was based on the observation that sulphur mustard (HD) potently and irreversibly potentiated the effect of ATP on smooth muscle preparations (Lundy *et al.,* 1998) and also caused a sustained elevation of free intracellular Ca^{2+} ($[Ca^{2+}]_{INT}$) in certain tissue types (Hamilton *et al.,* 1998). These results were intriguing for four reasons: 1: It appeared that both ATP and HD interacted with the P_2X subtypes of the ATP receptor; 2: Both extracellular ATP and HD are broad spectrum cytolytic compounds; 3: both ATP and HD cause an increase in $[Ca^{2+}]_{INT}$ 4: stimulation of P_2X receptors led to a cascade of biochemical events which are very similar to events resulting from HD exposure, including the activation of those which can be identified as being confirmatory in the definition of apoptosis and necrosis.

Recent evidence suggests that extracellular ATP is a broad spectrum cytotoxic agent that kills cells and promotes apoptosis by activation of distinct cell surface P_2 purinoceptors (Burnstock, 1998). Some of these receptors, notably the P_2X sub-family are ionotropic channels, acting, for example, to transport calcium through the cell membrane causing a variety of physiological effector responses, such as muscle contraction or nerve transmission (Burnstock, 1998; Evans *et al.,*1992). At least two of the ATP receptors in this sub-family, in addition to their physiological roles, are also thought to mediate programmed cell death (apoptosis). The P_2X_1 subtype has been proposed to initiate apoptosis following activation and has been shown to be upregulated in cells undergoing this phenomenon (Chvatchko *et al.,* 1996; Zambon *et al.,* 1994). This particular receptor has marked sequence homology (Valera *et al.,* 1994; Brake *et al.,* 1994) to the product of the gene known as RP-2, which has been shown to encode for apoptosis (Owens *et al.,* 1991). The P_2X_7 receptor, on the other hand, is not only an ionotropic receptor which is permeable to ions such as calcium, but it also coupled to a non-specific membrane pore, which, following activation by ATP and its analogues, opens to allow the entrance into the cytoplasm of large molecules, up to about 900 daltons (Wiley *et al.,* 1996). The literature suggests that activation of this receptor may initiate cell lysis (necrosis), or what has also been termed colloidal osmotic lysis and it

has also been specifically linked to the development and expression of apoptosis. It is believed that the cytotoxic activity of ATP is generally the result of the stimulation of one or both of these ATP receptors.

HD, similar to ATP is also a broad spectrum cytotoxic agent, whose mechanism of cytotoxic activity is not clear (Papirmeister *et al.*, 1991). We proposed to examine the mechanism of the cytotoxic activity of HD and its relationship to P_2X receptors as the result of our original observations outlined above.

This report is divided into sections that can generally be described by the flow diagrams in Figures 1 and 2. We first outlined the type of cell death resulting from exposure to HD in a wide variety of phylogenetically different cell types. Since these cell types all demonstrated that at least part of the cell death described was apoptotic in nature the effect of HD on related events (Fig. 1) such as the effect on caspase activation and on DNA'ase activity were examined (Fig. 2). In addition, the role of other possible initiating events in HD induced apoptosis were examined in some detail, such as the role played by calcium which has been implicated in HD and ATP induced cytotoxicity and cytotoxicity in general (Kass and Orrenius, 1999). Certain tissues were examined for their cytolytic response to HD and for the presence of P_2X_1 and P_2X_7 receptors and their possible contribution to the toxicity observed. These examinations led to the definition and pharmacological identification of a membrane complex which when activated at various loci initiated both apoptosis and necrosis, as well as calcium influx. The results of attempts to manipulate the activity of this complex by HD were reported. The definition of P_2X_7 receptors in preparations from the central nervous system were also carried out. During these studies we consistently noticed that many of the effects of HD and those following activation of the P_2X_7 receptor were affected quite noticeably by the ionic environment in which the activity was measured. Experiments were then carried out to examine the role of ionic composition and pH on the effects of HD (Fig. 2).

It is well documented that the P_2X_1 (and possibly P_2X_7) extracellular receptor which mediates the contraction of the isolated smooth muscle preparations such as vas deferens and the urinary bladder (Lundy *et al.*, 1998) functions as an ionotropic channel which when activated, allowing the influx of calcium into the interior of the cell (Valera

et al., 1994). Furthermore, ATP activated calcium influx is widespread in a number of tissues in which ATP also causes cell death (Dowd, 1995). The implication is that ATP induced cell death may be triggered by calcium influx or a rise in $[Ca^{2+}]_{INT}$, There is now also considerable speculation that calcium may play an important role in the initiation of HD induced cell death (Papirmeister *et al.*, 1991; Hua *et al.*, 1993; Hamilton *et al.*, 1998) although good evidence of a cause-effect relationship is lacking (Sawyer and Hamilton, 2000). The role of calcium in the initiation of cell death through calcium mediated enzyme activation is very well documented (Orrenius and Nicotera, 1987, Kass and Orrenius 1999) and suggested to us that calcium overload, as a result of stimulating ATP receptors either by ATP, by ATP and HD together or indeed by HD itself, could activate calcium dependent proteases, phospholipases and endonucleases, and thereby initiate apoptosis, necrosis or perhaps both types of cell death.

METHODS

Cell Culture and Cytotoxicity Assays

CHO-K1 Cell Line Culture Seed cultures were obtained from the American Type Culture Collection. The cells were grown in 10% FCS in DMEM supplemented with streptomycin (100 (μg/ml) and penicillin (100 IU/ml) and the medium was changed as required. Stock cultures were closely monitored and not allowed to grow to confluency prior to subculture. Test cultures were seeded so that cells were used just prior to, or at confluency.

Human Skin Keratinocyte Culture Primary cultures of human skin keratinocytes were prepared from neonatal foreskins. Tissue was obtained on the day of circumcision and incubated at 4°C for 24 hr in 25 U/ml dispase (Collaborative Research, Bedford, MA). The epidermis was removed and the cells segregated by a further 5 min incubation in 0.25% trypsin at 37°C. The trypsin was deactivated by the addition of 20% serum in medium and the cell suspension was centrifuged. The cell pellet was resuspended in Keratinocyte Serum Free Medium (KSFM, Gibco BRL, Grand Island, NY) and filtered through 70 μM nylon mesh. 75 cm^2 flasks were seeded at 5 x 10^5 cells/8 ml KSFM supplemented with gentamicin (50 μg/ml) and Fungizone (0.25 μg/ml) and incubated in a 37°C humidified incubator in a 5% CO_2/95% air atmosphere. Cultures were re-fed every 2 - 4 days, as required. First passage cultures were seeded from log growth primary cultures at a density of 1000 cells/well in 96-well Costar multiwell plates, 10,000 cell/well in 24 multiwell plates, 50,000 cells/dish in 35 mm culture dishes, or at 2.5 x 10^5 cells per 75 cm^2 culture flask. Apoptotic cell death was assessed in subconfluent cultures 16 hr after HD exposure.

Chemical Treatment and Cytotoxicity Studies On the day of chemical treatment the cultures were treated with freshly prepared treatment medium so that the desired final HD concentration was reached at 0.25% ethanol (v/v). The viability of HD-exposed cultures was determined 24 hr after exposure. To assess cytotoxicity, alamarBlue (AccuMed International Inc.,Westlake, OH) was added (10%, v/v) and the cultures were allowed to

incubate with the dye for the last 2 – 3 hr of the treatment time period. The absorbences (570 nm - 600 nm) were then read on a Thermomax titerplate reader (Molecular Devices, Sunnyvale, CA). For the assessment of BzATP toxicity, CHO-K1 cells were treated with the drug dissolved in defined sucrose buffer (see below) for varying time intervals. 24 hours later cell viability was assessed using either the alamarBlue assay or LDH release. The 24 hr toxicity of maitotoxin (in culture medium) was also assessed in CHO-K1 cells using alamarBlue. Median lethal concentration (LC_{50}) values were determined graphically from experiments utilizing 6 wells per data point. Sulphur mustard was prepared by Defence Research and Development Canada - Suffield at greater than 98% purity.

Apoptosis Detection Techniques

Genomic DNA Analysis Test cell samples were lysed in 50 µl of lysis buffer (50 mM Tris, pH 7.5, 20 mM EDTA, and 1% Nonidet P-40) for 30 sec. After centrifugation at 2,000x*g* for 5 min at room temperature, the fragmented DNA in the supernatant was collected. After repeating the centrifugation step once, the supernatant was further treated at 56°C for 2 hr with RNase A (5 mg/ml) and SDS (1%), followed by digestion with proteinase K (2.5 mg/ml) at 37°C for 2 hr. DNA was precipitated and electrophoresed in 1.5% agarose gels containing 0.5 mg/ml ethidium bromide and visualized under UV light. A 100-bp DNA ladder (Bio-Rad, Mississauga, Ontario, Canada) was used as a size marker.

LMPCR-DNA Ladder Protocol DNA was isolated from treated and control keratinocyte cultures using DNAzol (Invitrogen, San Diego,CA). To each 75 cm^2 flask containing approximately 2 x 10^6 cells, 3 ml of DNAzol were added with trituration. After 5 min, the DNAzol containing the cell lysate was transferred to clean centrifuge tubes, and 0.5 ml of absolute ethanol per ml DNAzol were added. After a 10 min centrifugation at 14,000 x g, the supernatant was discarded, and the remaining pellet containing DNA washed with 75% ethanol. Following a second centrifugation, the supernatant was again discarded, and the pellet dried briefly at room temperature. The

DNA was resuspended with 40 µl 8 mM NaOH, followed by dilution with 60 µl TE (10:1, pH 7.6). DNA was quantitated by OD_{260} and stored at -20°C until use.

100 µl Ligation reactions were prepared with 1 µg DNA extract using the ligation buffer/adapter mix provided in the Apo-Alert DNA ladder kit (Clontech, Palo Alto, CA). The ligation reactions were incubated in a ramp-down protocol from 55°C to 10°C over the course of 1 hr. T4 ligase (2 units) was added, and the reactions incubated overnight (18 hr) at 16 °C. The DNA was cleaned up using GFX minicolumns (Amersham Biosciences, Baie d'Urfe, PQ), and eluted from the columns in a final volume of 50 µl sterile water. 10 µl of the purified DNA were used in a 50 µl PCR reaction, using the PCR premix (containing buffer, primers, and nucleotides) from the Apo-Alert kit. Following a 2 min hot start at 72 °C, 2 units of Taq polymerase (Amersham Biosciences, Baie d'Urfe, PQ) were added, and the reactions cycled 30 times as follows: 94 °C x 1 min, 72 °C x 4 min; followed by a 72 °C finishing extension for 15 min.

PCR products were assessed for DNA ladders diganostic of apotosis by 1.5% agarose gel electrophoresis in 1X TBE with Sybr-gold staining, comparing PCR products from untreated cells to cells treated with HD of varying concentrations. Calf thymus DNA was provided in the kit as a positive control.

TUNEL Reaction For *in situ* nick end labeling (TUNEL reaction) cells were plated onto 25 mm Thermonox plastic culture coverslips and allowed to grow to subconfluency prior to experimental use. After HD treatment the medium was removed and the coverslips were washed twice with PBS, and then fixed with 4% paraformaldehyde for 30 min. The cells were then permeabilized for 2 min with 0.1% triton X-100, 0.1% sodium citrate and after air drying, 50 µl of TUNEL reaction mixture (Roche Molecular Biochemicals, Laval, Quebec, Canada) was added so as to cover all cells. The coverslips were incubated at 37°C in a humidified chamber for 60 min and then rinsed 3 times with PBS prior to analysis by fluorescence microscopy.

Soluble DNA Soluble DNA was measured by the method described by Cui *et al.* (1994) with modifications. The cells were grown in 24 well plates and log phase growth cultures

were radiolabeled by incubation with [^{3}H]thymidine (1 μCi/ml, Amersham Canada Ltd.,Oakville, Ont, Canada) overnight at 37°C in a humidified 5% CO_2 incubator. The medium containing [^{3}H]thymidine was then removed and the cells rinsed once with PBS. After drug treatment, aliquots of the culture medium (1ml/well, part A) were saved for radioactivity measurement and the cells were lysed in 0.5 ml TET (10 mM TRIS-HCL pH 7.5, 2 mM EDTA, 0.2 % Triton X-100) at 4°C for 30 min. The cell-lysate was then centrifuged (22 min, 14,000x*g*) and the resulting supernatant (part B) was removed and counted. The lysate pellet (part C) was solublilized with 1N NaOH (0.3 ml/microfuge tube) and counted. The experiments were performed in triplicate. Soluble DNA (percentage) was calculated according to the following formula: (Part A (dpm) + Part B (dpm))/ (Part A (dpm + Part B (dpm) + Part C (dpm)) x 100.

Morphological Observations Cell cultures were grown to subconfluency in 24 well plates prior to experimentation. After HD treatment, the cells were washed with PBS and then stained with 10 μl dye mix (100 μg/ml acridine orange and 100 μg/ml ethidium bromide in PBS) as previously described (Duke and Cohen, 1992). The cells were then visualized and scored using fluorescence microscopy. A minimum of 200 cells was visualized and the incidence of each of the following four cellular states was recorded; i) viable cells with normal nuclei (VN; bright green chromatin with organized structure), ii) viable cells with apoptotic nuclei (VA: bright green chromatin which is highly condensed or fragmented), iii) nonviable cells with normal nuclei (NVN; bright orange chromatin with organized structure) and iv) nonviable cells with apoptotic nuclei (NVA; bright orange chromatin which is highly condensed or fragmented). The percentages of apoptotic and necrotic cells were then calculated according to the formula:

% apoptotic cells = (VA+NVA)/(VN+VA+NVN+NVA) x 100.

% necrotic cells = NVN/(VN+VA+NVN+NVA) x 100.

P2X Receptor Studies

Immunohistochemistry Protocols for immunohistochemical staining were obtained from Michael Iagallo (Histopathology Service Lab, UBC, personal communication,

1996). Rat tissues (synaptosomes and brain) were collected, rinsed in PBS, and fixed in 4% paraformaldehyde for 16 hr at 4°C. Tissues were then placed in PBS followed by PBS/10% sucrose (as a cryoprotectant) and frozen in OCT compound. Cryostat sections were cut at 8 μm and collected on adhesive coated microscope slides. Slides were then placed in PBS/0.01% Triton X-100, warmed to 37°C for 5 min to remove OCT compound, covered with Sequenza cover plates (Shandon, Pittsburgh, PA) and placed in a humidified Sequenza slide rack. Primary antibodies (anti- P_2X_1, anti- P_2X_2, anti- P_2X_4, and anti- P_2X_7, Alomone Labs, Jerusalem, Israel) were applied and incubated for 16 hr at room temperature. Slides were rinsed three times with PBS/Triton X-100. Secondary antibody (Oregon Green 488-labelled goat anti-rabbit, Molecular Probes, Eugene, OR) was applied to sections for 2 hr under the same conditions. Following incubation, the slides were washed in three changes of PBS/Triton X-100, and coverslipped using Prolong anti-fade mounting media. A negative procedural control, in which the primary antibody was omitted and replaced with diluent buffer only, was used with each series. After the final PBS rinse, the slides were mounted using Prolong anti-fade mounting media (Molecular Probe) and coverslipped. Slides were visualized using fluorescence microscopy and representative images taken with a Spot 2 digital camera (Diagnostic Instruments Inc., Sterling Heights, MI).

Synaptosome Preparation Synaptosomes were prepared using the Percoll® gradient method (Dunkley *et al.*, 1988). Briefly, the S_1 sucrose/EDTA supernatant was layered over a discontinuous Percoll® (Sigma, St Louis, MO) gradient consisting of 2 ml each of 3, 10, 15 and 23% (v/v) Percoll® dissolved in 0.32M sucrose containing 100 mg L^{-1} EDTA. This was centrifuged at 20,000x*g* for 5 min at 4°C in a Beckman preparative centrifuge. The 10/15% and 15/23% interfaces were combined and diluted four-fold with Hanks balanced salt solution (HBSS) at pH 7.3, and then centrifuged at 12,500x*g* for 25 min. The resulting pellet was resuspended in HBSS. Aliquots of the Percoll® purified or crude P_2 synaptosomes were deposited on glass microscope slides (500 μl, Cytospin) and used for fluorescence histochemistry (outlined below). The composition of HBSS was as

follows in mM: KCl 5.4, KH_2PO_4 0.5, NaCl 136, $NaHPO_4 .7H_20$, 0.34, D-glucose 5.6 and $CaCl_2$.

Western-Blotting Rat brain, or purified rat synaptosomes were mixed and incubated on ice for 20 min with 300-500 µl 1 x SDS gel loading buffer, containing 50 mM Tris-HCl (pH 6.8), 100 mM DTT, 2% SDS, 0.1% bromophenol blue and 10% glycerol. Protein concentration was measured using Coomassie Protein Assay Reagent (Pierce, Rockford, IL). The sample was heated in boiling water for 5 min and an equal amount of protein from each sample was electrophoresed on 8% SDS acrylamide gels and electrophoretically transferred to a nitrocellulose membrane. Prestained SDS-Page standards (Bio-Rad, Mississauga, Ontario, Canada) were used to ensure the successful transfer and measure the size of any signal thereafter. The membrane was blocked with PBS containing 0.1% Tween (PBST) and 5% skim milk overnight at 4°C and then washed for 10 min with PBST. This step was repeated an additional three times. The washed membrane was incubated with a 1:300 dilution of P_2X_1, P_2X_2, or P_2X_7 antibody in PBST solution for 90 min, washed again and incubated for 90 min with a peroxidase labeled anti-rabbit antibody (1:3000 dilution, included in ECL-Kit from Amersham Pharmacia Biotech, Baie d'Urfe, Quebec, Canada). The membrane was washed again and positive bands were visualized with the enhanced chemiluminescence reagents following the instructions of the manufacturer. P_2X_1 and P_2X_2 antibodies were obtained from Alomone Labs (Jerusalem, Israel) while P_2X_7 antibodies were obtained from two different sources (Alomone Labs, Jerusalem, Israel and Chemicon International, Inc., Temecula, CA), with similar results being obtained using both antibody sources.

Cytolytic Pore Studies

Buffer Solutions Physiological ionic buffer was made with the following composition in mM: KCl, 5; $MgSO_4$, 1; $CaCl_2$, 1; Na_2HPO_4, 1; D-glucose, 5.5; $NaHCO_3$, 5 and HEPES 20 (pH 7.4). *Sucrose buffer*: This low ionic strength medium was similar to that described by Michel *et al.,* (1996), and Surprenant *et al.,* (1996) in order to maintain lower concentrations of certain interfering ions. It consisted of the following in mM:

sucrose 280; $CaCl_2$ 0.5; KCl 5, D-Glucose 10, HEPES 10, N-methyl-D-glucamine 5, with the pH adjusted to 7.4.

Ethidium Bromide Uptake Studies CHO-K1 cells were allowed to grow until just confluent. The cells were gently trypsinized at room temperature and pelleted by centrifuging at 1000x*g* for 5 min. The pellet was suspended at a density of 10^6 cells/ml in 20 μM ethidium bromide dissoloved in either physiological ionic buffer or sucrose buffer. The cell suspensions were protected from light and kept on ice until used. At the time of experimentation 2 ml of cell suspension were placed into a quartz cuvette and fluorescence (excitation: 360nm/emmision: 480 nm) was acquired for 5 min prior to drug treatment and for at least 30 minutes afterwards. Confirmatory evidence of ethidium bromide uptake was obtained by visualizing the cells using fluorescence microscopy.

Ionic and pH Studies

Buffers All buffers used in the ionic studies were isoosmotic with F-12 culture medium, fwhich has a NaCl concentration of 130 mM and is 300 milliosmolar. Buffer composition consisted of 10 mM glucose, 10 mM HEPES, the test salt and sucrose so that the final solution was 300 milliosmolar, pH 7.4. The buffers were filter sterilized.

HD Exposures In studies that examined the effect of pH and ionic environment on the toxicity of HD, confluent cultures of CHO-K1 cells were used. Just prior to HD exposure the cultures were aspirated and the medium replaced with freshly pH'd medium. For ion studies, the cultures were rinsed once with the test ion buffer before HD exposure. Immediately following these steps, the cells were exposed to HD dissolved in the test pH or ion buffer. The exposure was carried out for 1 hr at 37°C, and then the cultures were changed into normal culture medium. For those experiments looking at the effects of pH and ion concentration on metabolic viability, toxicity was assessed 24 hr post-exposure using the alamarBlue cytotoxicity assay.

For experiments examining the effect of sodium chloride concentration on HD degradation as a function of time, HD solutions were made up in 32.5, 65.0 or 130 mM

sodium chloride buffer solutions. For studies looking at the effect of pH, HD treatment solutions were made up using culture medium adjusted to pH 7.5 and pH 9.5. At 1, 10, 20, 30, 40, 50 and 60 min after the different HD solutions were made up, cultures were exposed for 1 hr. After exposure, the HD treatment solutions were removed and replaced with culture medium. Toxicity was assessed 23 hr later using the alamarBlue cytotoxicity assay.

Intracellular Chloride Ion Studies Di-H MEQ was produced from 6-methoxy-*N*-ethylquinolinium iodide (MEQ, Molecular Probes) according to the manufacturer's recommended protocol. Cells were incubated with 50 μM DiH-MEQ in loading buffer (Hank's Balanced Salt solution, 10 mM HEPES pH 7.4 and 1 mM CaCl) for 10 min at 37°C. Cells were then rinsed with fresh loading buffer and incubated for a further 15 min. Cells were rinsed twice and resuspended in appropriate buffer at a concentration of approximately $5x10^5$ cells/mL. Intracellular Cl^- was monitored at 344 nm excitation and 440 nm emission with a Delatscan fluorometer and Felix software (Photon Technology International, Trenton, NJ). The MEQ fluorescence was calibrated for each buffer with 10 μM tributyltin chloride (Sigma-Aldrich, St Louis, MO).

Statistical Analysis Data was routinely analyzed by one-way analysis of variance (ANOVA) followed by *post hoc* Tukey-Kramer HSD Multiple or Dunnet's Comparison testing using JMP (SAS Institute, Cary, NC) software.

SULPHUR MUSTARD TOXICITY IN VARIOUS CELL TYPES

SUMMARY

In this section of the report we describe the concentration dependant cytotoxic effects of HD in a variety of cultured tissues. Results include the calculation of the LC_{50} for HD in the tissues examined including human keratinocytes, neurons, CHO-K1 cells, J774 cells (and later in the report also thymocytes). The cell death in all cases was due to a proportion of both mechanisms of cell death, apoptosis and necrosis. The former was the predominant type of cell death relative to necrosis, particularly at the lower HD levels examined. It was necessary to confirm the presence of apoptosis using a battery of apoptotic biochemical markers since no one of these tests can be taken as proof of apoptosis (Renvoize *et al.*, 1998). Each cell type exposed to HD at predetermined concentrations was examined by the apoptotic markers outlined in Table 1. A great deal of attention was devoted towards obtaining the "ladders" of fragmented DNA on agarose gels from human skin cells, that have become a prototypical indicator of apoptotic cell death. Despite our best efforts, and routine success with at least four other cell types in obtaining HD induced DNA ladders, we could not reproducibly detect these patterns of DNA fragmentation from HD treated keratinocytes. We suspect that this is a common problem encountered by laboratories using this cell type. This difficulty was solved by first amplifying the DNA fragments using ligase mediated PCR, prior to gel electrophoresis. Using this technique, the characteristic banding of the 180 bp oligomers was routinely visible over the background smearing of the randomly fragmented DNA.

Table 1: HD-induced Apoptotic Cell Death *in vitro*

	J774	CHO-K1	Neurons	Keratinocytes
Annexin V	YES	YES	YES	YES
TUNEL	YES	YES	YES	YES
DNA Ladders	YES	YES	YES	YES
Soluble DNA	YES	YES	N/A	YES
Morphology	YES	YES	YES	YES

The effects of HD on soluble DNA levels were not assessed in chick embryo neurons since this assay requires proliferating cells. Except for this assay, HD induced a concentration response for all assays in all cell types.

RESULTS

HD treatment resulted in concentration dependent cytotoxicity in all four of the cell types examined here as measured by the alamarBlue assay. Figure 3 shows a representative concentration response curve obtained for each of the different test cell types following treatment with HD. The macrophage-derived cell line J774 was much more sensitive than the CHO-K1 cells to the effects of HD, with LC_{50} values typically within the 50-75 μM range (panel b) compared to a LC_{50} range of 250-350 μM for the CHO-K1 and keratinocytes. Both keratinocytes and neurons showed differential sensitivity to HD, depending on the length of time they had been in culture (panel a and c). In contrast to keratinocytes, which became markedly more resistant to HD as they achieved confluency (panel c) neuronal cells became more sensitive to the toxicity of HD

as they matured. A summary of these results is presented in Table 2.

Table 2: Cellular Toxicity of HD in Various Cell Types (LC_{50} μM).

Cell Type	Stage	LC_{50} μM
Neurons	Immature	40.6
	Mature	14.5
Keratinocytes	Proliferating	45.1
	Confluent	215.4
CHO-K1	Sub-confluent	204.9
J744	Sub-confluent	63.4

All studies of apoptosis were carried out with just-confluent cultures of the cell lines, with immature neurons (one day *in vitro*) and with proliferating cultures of human keratinocytes (three to four days *in vitro*). HD-induced fragmentation of DNA was visualized using agarose gel electrophoresis and Fig. 4a-d shows the typical ladder patterns obtained when neurons (a), J774 cells (b), CHO-K1 cells (c) and keratinocytes (d) were treated with HD. Although we could consistently and easily obtain the DNA "ladder" patterns that have become the prototypical indicator of apoptotic cell death from at least four other cell types when they were treated with HD, this was not the case with HD treated keratinocytes, unless the DNA fragments were amplified using ligase mediated PCR prior to gel electrophoresis. This methodology was therefore used for all studies using keratinocytes hereafter. Fragmentation was also assessed quantitatively by using a soluble DNA assay utilizing tritiated thymidine. With the exception of neurons (which could not be labeled), HD induced a concentration-dependent increase in fragmentation in every cell type, which appeared to plateau at the higher HD concentrations (Fig. 5a-c).

Figure 6 illustrates examples of the results obtained following the assay of fragmented DNA using the TUNEL reaction and fluorescent (Fig. 6a-c) or light microscopic (Fig. 6d-f) detection. In CHO-K1 cells, apoptotic nuclei are stained with fluorescein, and clumping chromatin can easily be discerned as intensely dyed inclusions. In human keratinocytes, light microscopy is used and the brown product of the peroxidase reaction indicates apoptotic nuclei. This assay lends itself well to quantitation and Fig.7a-d shows that the number of apoptotic cells (as a percent of total cell number) increases with increasing HD concentration in all cell types. Figure 8a-c shows examples of HD induced morphology in rat thymocytes. Similar concentration responses were also observed with the other three cell types (data not shown). Fig 9 a-d shows the results obtained following quantitation of the two types of cell death in each of the four cell types which shows that the total cell death increases with HD concentration and that the percentage of cell death is shifted from apoptosis towards necrosis as the concentration increases. Fig. 10 shows examples of Annexin V binding to apoptotic CHO-K1 cells. Control cells are generally negative. At low HD concentrations, the fluorescein-labeled phospholipid-binding proteins recognize the externalized phosphatidylserine residues that are a hallmark of early stage apoptotic cell death and stain the cells green. As the concentration of HD becomes higher, the cell membranes of necrotic cells lose integrity and increasing numbers of cells also become stained with propidium iodide (red/brown colour). Similar concentration responses were also observed with the other three cell types (data not shown)

DISCUSSION

HD was toxic to all cell types that were exposed to it. This was not surprising since the acute toxicity of HD *in vivo* and *in vitro* has been widely reported in the literature. It is known from animal experiments and certainly from accidental and intentional human exposures in military conflicts (for reviews see Dacre and Goldman, 1996; Willems, 1989), that HD affects not only the obvious targets, which are the skin and eyes, but a wide variety of other tissues, including the GI, respiratory and immune systems and the brain (Papirmeister *et al.*, 1991). It has also been reported that HD and HD analogues can cause cytotoxicity through apoptotic cell death (Dabrowska *et al.*,

1996; Rosenthal *et al.,* 1998). The present studies extend these findings and show clearly and conclusively, using a wide range of tests that exposure to HD causes both apoptosis and necrosis in cells obtained from the immune system, the skin, and the CNS. Not all cells were equally sensitive to the cytotoxic effects of HD, but the signs of apoptosis began to appear at concentrations of HD that were found to induce cytotoxic effects in assay systems such as alamarBlue. In all cell types, increasing concentrations of HD resulted in a larger proportion of cells becoming necrotic, but it is not presently clear whether these cells progressed through an apoptotic stage during the degenerative process.

Many techniques are now available with which to measure apoptosis, including detection of cell surface proteins (Annexin V), assessment of membrane integrity using various dye exclusion tests (trypan blue, ethidium bromide, propidium iodide, acridine orange), morphological assessments using light or electron microscopy, measurements of DNA fragmentation using radiological (soluble DNA), electrophoretic (DNA ladders) or immunological (TUNEL) means and molecular biological methods to measure the regulation of a variety of genes associated with apoptotic cell death. In many cases, not all endpoints normally associated with apoptotic cell death may be induced by a specific agent or conversely, an endpoint normally associated with apoptosis will be detected in cells undergoing necrotic cell death. Since the nature of apoptotic cell death is often dependent on the target tissue and the inducing agent, assessment of a battery of endpoints is preferable when investigating mechanisms of cell death (Renvoize *et al.,* 1998). One significant difficulty that we encountered was in obtaining DNA "ladders" from human skin keratinocytes. Although we could consistently and easily obtain the DNA "ladder" patterns that have become the prototypical indicator of apoptotic cell death from at least four other cell types when they were treated with HD, this was not the case with HD treated keratinocytes. Our best attempts resulted in only very faint banding overlaying DNA smears when visualizing the gels – results that definitively would not be visible when documenting these results either photographically, or even digitally. We suspect that this is a common problem encountered by laboratories using this cell type. Personal communications from laboratories examining the effects of HD (W. Smith) or

UVB (D.F. Spandau) concerning induced DNA ladders have suggested that reproducibly obtaining good results with this methodology is not trivial. This difficulty was eventually solved by first amplifying the DNA fragments using ligase mediated PCR prior to gel electrophoresis. Using this technique, the characteristic banding of the 180 bp oligomers was routinely visible over the background smearing of the randomly fragmented DNA. We believe that this technical problem is due to the intrinsic variability of human keratinocytes in culture. The cells within each culture are not synchronized and thus respond variably to insult. In this case, strictly proliferating cells would be exceptionally sensitive to a given HD concentration, while other cells progressing towards terminal differentiation would display less sensitivity.

A number of recent studies have shown that HD induces several of the hallmarks of apoptotic cell death in cell culture. In one of the earliest works, Dabrowska and coworkers (1996) showed, using gel electrophoresis of DNA, as well as morphological criteria, that endothelial cells were induced to undergo an exclusively apoptotic cell death at low HD concentrations (< 250 μM), while at higher HD concentrations (> 500 μM), cells were undergoing both apoptosis and necrosis to an equal extent. Similar results have also been found in Hela cells (Sun *et al.,* 1998). Other laboratories (Michaelson, 2000; Meier and Millard, 1998) have used DNA gel electrophoresis exclusively to show that HD caused immune cells (thymocytes and lymphocytes) to degrade their DNA into the "ladder" patterns that have become the most prevalent endpoint used in apoptosis studies. Michaelson (2000) further showed that DNA fragmentation in thymocytes exposed to HD was time dependent, with initial formation of large fragments (50-700 kilobasepairs) followed several hours later by further degradation to the internucleosomal ladder of oligomers of ~180 base pairs. Rosenthal and coworkers (1998) investigated the effects of HD on human skin keratinocyte gene expression and found that two genes intimately linked to apoptotic cell death were affected. Thus, p53 was induced while the expression of Bcl-2 was suppressed. In addition, they showed that HD induced caspase-3 activation and poly (ADP-ribose) polymerase cleavage, both indicators of apoptotic cell death. In later sections of this report we have confirmed some of these results in certain of our cell lines.

The present studies expand and complement previous work and confirm that HD induces several different hallmarks of apoptotic cell death in cell culture. Furthermore, the selection of cell types in this study shows that HD exerts cytotoxicity in a remarkably conserved fashion. Thus, HD induces apoptotic cell death as assessed using morphology (acridine orange/propidium iodide), DNA fragmentation (DNA ladders, TUNEL assay, soluble DNA) and cell surface markers (Annexin V) in cells derived from different species (mouse, hamster, chicken, human), and from different organ/tissues (ovary epithelial, macrophage, brain neuron, skin keratinocyte), using different cell culture types (immortalized cell lines versus primary or first passage culture). That HD exerts its toxicity in such a conserved fashion *in vitro* strengthens the likelihood that similar mechanisms of cell death are also operative *in vivo*, a notion supported by recent findings that HD also induces several characteristics of apoptotic cell death in HD exposed pig skin (Smith *et al.,* 1997) and in hairless guinea pig skin (unpublished observations, this laboratory).

Although the different cascades of events that lead to apoptotic cell death are not fully understood it is clear that they can be regulated by a number of different biochemical determinants, including nitric oxide (NO), reactive oxygen species (ROS), caspase activation and intracellular calcium levels. Modulation of these endpoints offers the possibility that the prevention or treatment of HD induced apoptosis may be possible. Nitric oxide has received an enormous amount of research attention due not only to its myriad physiological functions, but also because it has been implicated in a number of disease states and pathologies when produced in excessive amounts. It has been suggested that NO and its ability to form an array of reactive species (NO^+, NO, NO^-, $ONOO^-$) can induce apoptosis by destabilizing mitochondria with subsequent intracellular calcium imbalance (Brune *et al.,* 1999; Richter, 1998). Efforts have been made to link the toxicity of HD with its effects on the activity of nitric oxide synthase (NOS) and indeed, several inhibitors of this enzyme have been shown to have a marked protective efficacy against the toxic effects of HD in both neuronal and keratinocyte culture (Sawyer, 1998a; b; 1999; Sawyer and Risk, 2000; Sawyer *et al.,* 1996; 1998). However, the protection obtained appeared to be related to the chemical structure of

arginine and these studies showed that NO did not play a role in either the toxicity of HD or in the protective efficacy of the drugs used.

The induction of apoptosis due to oxidative stress, either through generation of ROS or through depletion of intracellular antioxidant levels ie., glutathione (GSH) is also supported by an enormous amount of data (Fawthrop *et al.*,1991), and efforts have been expended to link the cytotoxic effects of HD with the oxidative state of the target cells. Although it has been shown that intracellular GSH levels do decline following HD exposure, only very limited success has been achieved when intracellular GSH levels are boosted by pretreatment with GSH precursors such as N-acetylcysteine (NAC) or other cysteine ester GSH precursors . Interestingly, pretreatment of endothelial cells with NAC was shown to prevent apoptotic features of cell death but not those of necrosis (Dabrowska *et al.*, 1996). However, these studies were only carried out to six hours, a time frame that is unlikely to be reflective of the full expression time of HD toxicity and it is unclear what effect NAC would have on HD toxicity after longer time intervals. L-Thiocitrulline (Sawyer *et al.*, 1998; Sawyer and Risk, 2000) and thiourea (unpublished observations) have been shown to have excellent protective efficacy against HD cytotoxicity in both human skin keratinocytes and chick embryo neurons. These compounds do not exert their protective effects through NOS inhibition or by chemically reacting with HD, and their strictly prophylactic action does not suggest that they are interfering with the ongoing production of HD induced ROS. However, it is possible that the reducing activity of the thio-amino moiety of these molecules may lend itself to chemically reacting with a unique, but short-lived toxic ROS species within the lipid bilayer of the cell membrane. We are currently investigating this avenue of research.

In summary, HD induces a uniform pattern of cellular responses that are indicative of apoptosis over a broad spectrum of cell types. The remarkably conserved fashion in which HD induces apoptotic cell death indicates that strategies based on interfering with these pathways may be able to prevent or treat HD toxicity.

THE ROLE OF CASPASE INDUCTION AND DNA'ase ACTIVATION IN HD INDUCED CELL DEATH

SUMMARY

The results presented in previous sections of this report indicated clearly that HD induced apoptosis/necrosis in a wide variety of cell types. The experiments described in this section of the report were designed to examine factors that have been reported to be important in the induction of apoptosis. Several interleukin converting enzymes known as caspases have been specifically implicated as mediators of the initiation of apoptotic events through the subsequent activity of certain DNA'ases .The first group of experiments described in this section of the report document the effects of HD on caspase or proteasome (multi unit caspase) activation and the result of the activation or inhibition of these caspases on the disposition of HD treated cells. Experiments were then carried out which examined HD induced cytotoxicity with respect to the activation of caspase-3 and the resulting activation of DNA'ase. Apoptosis and caspase activation have also been reported to occur following stimulation of certain membrane bound ATP receptors (P_2X_1, P_2X_7 subtypes detailed later). The original intent of the study outlined in the cooperative agreement, was to examine the role of HD on ATP receptors since activation of extracellular ATP receptors led to cell death through biochemical events very similar to those induced by HD. In the course of studies concerning P_2X_7 receptors in CHO-K1 cells a second receptor associated with the P_2X_7/pore was identified which was uniquely sensitive to maitotoxin. These discoveries led to the proposal of the existence of a cytolytic complex consisting of two receptors and a cytolytic pore. The pharmacological description and the toxic effects following activation of the complex are then reported along with studies to determine the degree of interaction of HD on the various components of the complex.

INTRODUCTION

In the previous section of this report we outlined the biochemical markers which clearly indicated that cell death following HD was due in significant measure to the

induction of apoptosis, the proportion being somewhat variable from one cell type to another. Apoptosis, or "cell suicide", is the process that refers to the orderly biochemical process employed by organisms to rid themselves of damaged or aged cells that are no longer optimally functional. Apoptosis is characterized by distinct biochemical events which result in a number of well characterized cellular morphological changes such as chromatin condensation, membrane blebbing, chromatin aggregation and the appearance of apoptotic bodies, a series of events resulting in cell death. The primary initiating signal in this cascade is unknown with certainty and may vary from cell to cell, but may be due to the stimulation of one or more distinct membrane events such as changes in calcium metabolism (see later section) or the activation of cell surface receptors such as those responding to extracellular ATP (previous discussion). The initiating signal leads to the activation of caspases or proteasomes, as well as the activation of one or more endonucleases (DNAases) leading to the DNA fragmentation typical of apoptosis (Fipipski *et al.*, 1990). Proteasomes are multi-catalytic high molecular mass protease complexes which, upon alteration of their activity, may induce or inhibit apoptosis (Shinohara *et al.*, 1996 and references therein; Hirsch *et al.*, 1998). Inhibitors of proteasomes, such as MG-132 or lactacystin have been shown to inhibit apoptosis induced by glucocorticords and several other cytotoxic agents (Hirsch *et al.*,1998). The viability of CHO-K1 cells incubated with MG-132 or lactacystin prior to exposure to concentrations of HD were examined and quantitated.

Further identification of those endonucleases (DNAase) responsible for DNA fragmentation have been made including DNAase I, II, cyclophilin and DNase-γ (Peitsch *et al.*, 1993; Barry and Eastman, 1993). Recently, another endonuclease that is activated specifically by caspase-3 during apoptosis has been described in human and mouse. This protein in human cells has been identified as DNA fragmentation factor 40, a 40 kDa subunit (DFF40, Liu *et al.*, 1998), whereas the mouse homologue is known as caspase-activated DNase (CAD, Enari *et al.*, 1998). CAD/DFF40 exists in the cytoplasm as an inactive complex associated with an endogenous inhibitor known as ICAD (Inhibitor of CAD) in the mouse (Sakahira *et al.*, 1998) or DNA fragmentation factor 45, a 45 kDa in humans (DFF45, Liu, 1998). ICAD/DFF45 is a dual function subunit that serves both as

a specific chaperone to mediate the correct folding of the complex and as an inhibitor of CAD/DFF40. Cleavage of the molecule removes the association of the inhibitor from the complex and results in the formation of the active CAD/DFF40 (Enari *et al.*, 1998; Halenbeck *et al.*, 1998; Zhang *et al.*, 1998). The cleavage is believed to be initiated following exposure of ICAD/DFF40 to caspase-3 that is believed to be a critical step in propagating the apoptotic signal following certain stimulae.

RESULTS

Caspase and Proteasome inhibition

The viability of CHO-K1 cells incubated with MG-132 or lactacystin prior to exposure to HD (100-400 μM) were examined using the alamarBlue assay. HD produced a concentration dependant increase in cell death which was apparently unaffected by the two proteasome inhibitors at concentrations from 1-50 μM (Fig 11).

In addition to the role played by proteasome activity in the control of apoptosis, much interest has been directed towards the control of cell death by individual caspases. These proteases have been widely implicated as mediators of the initiation of apoptosis (perhaps following activation by elevated intracellular Ca^{2+} levels). Proteases have become excellent candidates to perform functions relating to apoptosis. Since HD is obviously a consistent inducer of apoptosis, and because other apoptotic inducers can be inhibited by caspase inhibitors, we examined the effects of caspase inhibitors on the viability of CHO-K1 cells following HD. Neither of the proteasome inhibitors caused reduction of HD induced DNA fragmentation quantitated by the measurement of soluble DNA concentrations (Fig. 12).

HD (400 μM) produced a significant induction of the activity of caspase-3 which was unaffected by the proteasome inhibitors MG-132 or lactacystin (Fig. 13). Further studies were then carried out utilizing both specific and more general caspase inhibitors. Cells were preincubated with HD and a selection of inhibitors of caspases. As pointed out above, HD exposure resulted in caspase-3 induction, which suggested a significant role for caspase-3 in the HD induced progression of apoptosis. Although HD caused caspase-3 induction during apoptosis, HD toxicity (Fig. 15) was not affected by inhibitors

of caspase-3 even though the inhibitors reversed caspase induction (Fig. 14). ZVAD-fmk, which is a general cytosolic caspase inhibitor that affects caspases 1,3, 7,8, and 9 also failed to inhibit HD induced apoptosis (Fig. 15). The more specific caspase-8 inhibitor (IFTD-CHO) and the caspase-9 inhibitor (LEHD-CHO) also failed to affect HD induced apoptosis (Fig. 15). Again, these results strongly suggest that HD induced initiation of apoptosis does not appear to share some of the biochemical events seen following more commonly studied apoptotic stimulae such as radiation or dexamethasone which have reported to be sensitive to caspase inhibition (Bruno *et al.*, 1992; Fearnhead *et al.*, 1995; Weaver *et al.*, 1993).

DNA'ase Activation

For the DNA'ase studies J774 cells were utilized. J774 cells are a macrophage derived cell line, which like thymocytes, have also been reported to undergo cell death on exposure to external ATP (Murgia *et al.*, 1993; Steinberg *et al.*, 1987; Zambon *et al.*, 1994). This cell type therefore also provides a useful tool with which to examine HD, if HD induced toxicity is indeed mediated by ATP receptors. Moreover, as is the case with thymocytes, ATP induced cell death in J774 cells also appears to be preceded by an increase in intracellular calcium levels which may occur through activation of the P_2X_7 ATP ionic pore in this tissue. In this respect, J774 cells differ from thymocytes in that they contain the P_2X_7, but not the P_2X_1 type of receptor. Our results are completely consistent with the ability of HD to induce concentration-related apoptosis in this tissue as measured by DNA fragmentation, a positive TUNEL assay and staining with ethidium bromide. These results clearly demonstrate that although P_2X_1 ATP receptors may play a role in the initiation of apoptosis in a number of cell types, cell death may be induced in cells in which these receptors are absent or which contain P_2X_7 receptors.

DNA degradation is one of the first and most consistent hallmarks of apoptosis. This process results from cleavage of DNA into increasingly smaller size fragments of decreasing molecular weights through the activation of DNA'ases. The best characterized of these DNA'ases is a 40 kDa polypeptide which has been known as caspase activated DNA'ase or CAD. In normally functioning cells this polypeptide exists

in an inactive form as the result of its association with an inhibitor subunit called ICAD (Inhibitor of caspase activated DNA'ase). Following the induction of apoptosis the CAD/ICAD peptide is cleaved by the executioner caspase-3. The subsequent release of activated CAD then fragments DNA. Purified CAD is sufficient to induce DNA fragmentation and chromatin condensation. Since it has been demonstrated in another section of this report that HD exposure leads to activation of caspase-3, studies were carried out here to re examine the effects of HD on caspase activation and CAD/ICAD cleavage and subsequent DNA fragmentation. The experiments were designed to examine the possible role of time related DNA'ase activation and the correlation of these events with the development of apoptosis in cells exposed to HD.

The Effect of HD on Activation of Caspase-3 and Cleavage of CAD/ICAD

Experiments were carried out to examine the effect of HD on caspase-3 activity and on the cleavage of the polypeptide DNA'ase precursor CAD /ICAD. The studies were designed to compare the time related appearance of the changes in activity of these biochemical markers with the induction of apoptosis following exposure to HD of J774 cells.

HD (100 μM) caused significant time dependent increases in caspase-3 activity. The results in Fig.15A show that 2 hr after HD treatment, caspase-3 activity was elevated more than 2 fold, and after 3 and 4 hr reached much higher levels relative to control values. After similar exposure times cleavage of ICAD was also detected. In the control samples, Western blots showed the presence of a peptide fraction of approximately 45 kDA that corresponded to the presence of CAD/ICAD, and a second peptide of about 36kDA, that may be an isoform of the complex. At subsequent time periods an additional fragment appeared of between 20 and 30 kDA suggesting the partial cleavage of the 45kDA polypeptide. Following 3 or 4 hrs exposure to HD, an additional large fragment of 20-30 kDA and a smaller fragment of less than 20kDA were observed in the Western blots. Furthermore, the intact ICAD (45Kda) and a possible isoform of ICAD fragment (≅36 Kda) were found in all samples. In order to determine whether CAD/ICAD cleavage in this system was associated with subsequent activation of CAD,

the DNase activity of S-100 fractions prepared from J774 cells exposed to HD for 4 hr or from untreated cells was assessed. These fractions were examined for their effects by incubation with a mouse liver nuclei preparation to determine whether the nuclei would serve as a substrate for fragmentation by the activated DNA'ase. Mouse liver nuclei incubated with S-100 fraction derived from HD treated J774 cells became fragmented, forming a typical DNA ladder (Fig. 16C, lane 4). In contrast, the nuclei incubated with S-100 from untreated J774 cells remained intact (Fig. 16C, lane 3). In addition DNA ladders were not present in either in S-100 preparation without added nuclei (lane 1) or in mouse liver nuclei preparation without added S-100 (Fig. 16C, lane 2). Mouse liver nuclei incubated alone in buffer with no S-100 fraction showed no DNA cleavage (lane 5). These results clearly suggested that HD treatment resulted in the induction of caspase-3 and the appearance of an active S-100 fraction capable of initiating DNA cleavage.

The correlation between caspase-3 activation, cleavage of ICAD/CAD and cell apoptosis following HD treatment was also examined. HD exposed cultures were collected at similar time intervals outlined in Fig. 16 and apoptotic markers were examined, including HD induced DNA ladder formation, TUNEL assay and morphologic observation. The results shown in Fig. 17A indicate that HD caused internucleosomal DNA fragmentation, producing a DNA ladder characteristic of cell apoptosis in J774 cells, after 3 and 4 hr of exposure. No ladders were detected from untreated J774 cells or from cells collected following 2 hr exposures to HD. Parallel evidence was obtained from the TUNEL assay and morphologic observation. In the TUNEL assay, apoptotic cells identified by the presence of condensed brown nuclei, were found 3 and 4 hours following HD exposure. (Fig. 17 B, top panel: 3hr and 4hr). The data was then quantified and shown as HD induced increase in the percentage of apoptotic cells (Fig. 17B bottom panel). The percentage of apoptotic cells increased dramatically 3 & 4 hours following HD treatment. Staining the cells with acridine orange/ethidium bromide revealed typical morphologic changes indicative of apoptosis, e.g., shrunken cell bodies with condensed or fragmented chromatin, (Fig. 17 C).

DISCUSSION

Role of caspases/proteasomes on HD toxicity

The role of caspases has long been a subject of investigation to researchers interested in the aetiology of apoptosis in general and HD induced cell death in particular. Proteasomes are multi-catalytic high molecular mass complexes consisting of groups of caspases.which, upon alteration of their activity, may induce or inhibit apoptosis (Shinohara *et al.,* 1996; Hirsch *et al.,* 1998). Inhibitors of proteasomes have been shown to inhibit apoptosis induced by glucocorticords and several other apoptosis inducing stimulae (Hirsch *et al.,* 1998). Although there is a limited amount of research activity devoted towards the role played by proteasomes in apoptosis, a great deal of interest has been directed towards the control of cell death by one or more of several caspases. These proteases have now been widely implicated as mediators of the initiation of apoptosis, perhaps as the result of activation by elevated intracellular Ca^{2+} levels (examined in a later section). Since the toxicity of a variety of apoptotic inducers such as dexamethasone can be reduced by caspase inhibitors, we examined the effects of these inhibitors on the viability of CHO-K1 cells following HD exposure.

The proteasome inhibitors, lactacystin and MG-132 were ineffective in modulating HD induced toxicity, as were the specific caspase inhibitors. Caspase-8 and caspase-9 are procaspases and act upstream of caspase-3. Therefore the lack of activity for the specific caspase-8 inhibitor (IFTD-CHO) and caspase-9 inhibitor (LEHD-CHO) can be explained by assuming that more than one pathway leads to caspase-3 activation or that HD directly activates caspase-3. Indeed, as previously reported (Rosenthal *et al.,* 1998), HD has been shown to activate caspase-3, results which initially suggested that this protease played a significant role in the development of HD induced toxicity. However, even though ZVAD-fmk inhibited HD induced caspase-3 activity, it surprised us to find that it failed to confer any protection against HD toxicity. The lack of protective activity of the general cytosolic caspase inhibitor ZVAD-fmk, which affects caspases 1, 3, 8, 7, and 9, seems to be inconsistent with its published characteristics. Previous reports suggest that apoptosis caused by a variety of stimulae can be attenuated by inhibitors of caspases (Bruno *et al.,* 1992; Fearnhead *et al.,* 1995; Weaver *et al.,*

1993). Once again, the present results strongly suggested that HD induced initiation of apoptosis is not similar to apoptosis induced by more commonly studied stimulae such as dexamethasone.

Role of CAD/ICAD in HD induced apoptosis

A number of biochemical changes have been reported to result from HD exposure which suggests mechanisms for its toxic effects including caspase activation (Rosenthal *et al.*,1998, this report), PARP cleavage, elevated p53 and decreased BCL-2 activity (Rosenthal *et al.*,1998).

In the present study, attempts were made to examine some of the HD induced biochemical events which may be related to DNA,ase activation. It is well known that caspases play an important or critical role in the apoptotic cascade. Caspases such as caspase-8 or -9 are considered as 'initiator' caspases, which either directly or indirectly activate downstream 'effector' caspases like caspase-3, 6 and 7 (Cohen, 1997; Fraser and Evan, 1996; Srinivasula *et al.*, 1996). The 'effector' caspases then cleave intracellular substrates, such as CAD/ICAD and PARP (Sakahira *et al.*, 1998; Enari *et al.*, 1998) which appear to be critical in the final steps in apoptosis. Caspase-3 is considered to be an important "downstream" effector which acts as a primary executioner caspase. This caspase may activate the next important step which appears to be the activation of a DNAase resulting in DNA fragmentation and the appearance of the DNA ladders typical of apoptosis (Slee *et al.*, 2001). In J774 cells HD caused a time related increase in caspase-3 activity similar to activation seen in other cells (Rosenthal *et al.*, 1998). It was also possible to demonstrate with western blotting techniques the presence of a polypeptide with the characteristics of the inactive form of the 45 Kda DNA'ase inhibitor complex ICAD/CAD and a 36 kDa fragment, presumably an isoform of ICAD. Following exposure of J774 cells to HD, this inactive complex also became cleaved in a time related manner. The 45Kda fraction became increasingly fragmented with time following exposure to HD. The data also showed that DNA fragmentation was not detected in the absence of caspase-3 activation and that there appeared to be only an intermediate cleavage of the complex to a 20-30 kDa fragment when relatively small

increases in caspase-3 were measured at 2 hr. However, the appearance of <20 Kda ICAD fragment accompanying caspase-3 activation was observed at later time points and appeared to be essential for apoptotic execution. Previous studies have indicated that the generation of this 20 Kda fragment was correlated with DNA ladder formation (Gu *et al.*, 1999). These results clearly suggest that caspase-3 acts at an execution-stage during apoptosis and that complete cleavage of CAD/ICAD is required for DNA fragmentation. Clear evidence of DNA fragmentation was observed only at those time periods at which very large increases in caspase-3 activity became evident. On the other hand, other caspases such as caspase-6 and -7 may also cleave ICAD/DFF45 (Liu *et al.*, 1999; Woo *et al.*, 1998), which may explain the partial cleavage of CAD/ICAD to a 30 Kda fragment which did not result in measurable amounts of DNA fragmentation.

Studies were also carried out in J774 cells exposed to HD, and certain hallmarks of apoptosis were examined at similar times post exposure to those reported for ICAD/CAD cleavage and caspase-3 induction. HD caused time related DNA ladder formation, large increases in the proportion of apoptotic cells measured by TUNEL reaction and increased fluorescent staining of cells by acridine orange /ethidium bromide. It was interesting to note that all of the parameters measured appeared to be closely correlated with each other from a temporal point of view. The results taken together strongly suggest that HD exposure leads to caspase-3 induction, subsequent activation of the DNA'ase CAD and apoptosis in the J774 cell type.

It was also clear that DNA cleavage in the mouse liver nucleus preparations was dependant on incubation with S-100 fraction from J774 cells incubated with HD, and then only after incubation times which were consistent with the development of apoptosis in the cells (3, 4 hr). The fragmentation of the mouse DNA was correlated positively with the evidence from western blots, suggesting that the requirement for nuclear fragmentation was a prior activation of caspase-3 and CAD/ICAD cleavage which also occurred at 3 and 4 hr. This was evidenced by ladder formation in mouse liver nuclei only when exposed to HD treated J774 cell S-100 fractions. The results also indicated that the DNA ladders observed in this cell free system were not the result of any activity in the S-100 fraction or from the untreated mouse liver nuclei controls. Although we

cannot rule out the possibility that other DNAases may be involved in these observations, the finding of CAD/ICAD cleavage strongly indicate the CAD is the DNA'ase responsible for DNA fragmentation after HD exposure.

These data indicated that the execution of cell apoptosis occurred at those times which corresponded with activation of caspase-3 and CAD/ ICAD cleavage, revealing a strong link between activation of caspase-3, CAD/ICAD cleavage and the initiation of apoptosis in J774 cells in response to HD. These results also suggest some inconsistencies which we have observed while carrying out these experiments. For example, despite the induction of caspase-3 activity and the subsequent logical progression of other apoptosis related activity, results reported earlier in this report show that we were unable to demonstrate a reduction in HD toxicity following caspase-3 inhibition, which would certainly be predicted by the results shown in this section of the report. It appears intuitive that HD induced caspase-3 activation and the subsequent cleavage of the normally inhibited CAD/ICAD complex into an active form of DNA'ase presented here, is not likely merely coincidental in the mechanism of HD induced apoptosis

P_2X_1 and P_2X_7 ATP RECEPTOR ACTIVATION AND CELL DEATH

This section will outline experiments that were carried out in order to identify tissues which contained ATP receptors of the kinds we hypothesized might mediate some of the toxic effects of HD. These receptors, P_2X_1 and or P_2X_7 subtypes of the ATP family of receptors which when activated are known to mediate apoptosis/necrosis, result in caspase activation, mediate a rise in intracellular calcium levels, induce the secretion of interleukins and activate phospholipases, and endonucleases. Many if not all of these receptor mediated effects are mimicked by HD and all of the above effects can logically be implicated to play a role in HD induced cell death. Part A is a relatively short section which deals with attempts made to use rat thymocytes as a tissue model in which to identify the toxicity of HD, to identify ATP receptors in the tissue and to attempt to relate these two factors. Thymocytes were not a particularly useful cell type (see below) and we then carried out similar protocols utilizing the CHO-K1 cell type for our studies outlined in part B.

A. Role of P_2X_7 receptors in HD and adenine nucleotide (ATP) cytotoxicity

Thymocytes, and the response of thymocytes to HD, were chosen for study for several related reasons. Thymocytes have been extensively studied with respect to two very important aspects of our work: i) their response to ATP and to the classical inducer of apoptosis, dexamethasone and ii) the ATP receptors responsible for the cytotoxicity of these two compounds have been well studied. The literature clearly suggests that thymocytes exposed to ATP undergo apoptosis and it has been postulated that the apoptotic events are initiated by the stimulation of the membrane P_2X_1 receptor (Zheng *et al.*, 1991; Pizzo *et al.*, 1991) and also by the up-regulation of the P_2X_1 receptor mRNA (Chvatchko *et al.*, 1996). Furthermore, ATP induced cytotoxicity has been reported to be predictably modified by manipulating receptor and agonist (ATP) activity. For example, reducing the activity of ATP at the P_2X_1 receptors with appropriate blocking agents such as suramin or by decreasing ATP levels by increasing ATP metabolism, has been reported to inhibit the apoptotic cell death produced by ATP and its analogues

(Chvatchko *et al.*, 1996). Intracellular calcium elevation, which we have shown previously to result from HD exposure, has also been suggested to play a critical role in the initiation of apoptotic events in general (Kass and Orrenius, 1999; Dowd, 1995; Orrenius *et al.*, 1989). It has been postulated that an initial event in the induction of ATP induced apoptosis involves the ATP induced influx of calcium through the activation of an ATP receptor, although absolute cause and effect relationship exists between calcium influx and cell death. The results presented here reveal that HD causes a concentration and time dependent apoptosis (and necrosis) in thymocytes determined by several definitive assays.

A- Role of P_2X_1 receptors in HD and adenine nucleotide (ATP) cytotoxicity).

We undertook experiments to identify the type of P_2X receptors that exist in thymocytes. Fig. 18 shows RT-PCR RNA extracts stained with ethidium bromide. The 693 bp is specific for P_2X_7 and the 434 bp is specific for P_2X_1 receptor. Further evidence of the functional expression of ATP sensitive P_2X receptors is shown by the ATP induced uptake of the fluorescent dye YOPRO-1 (Fig. 19). In this figure the left-hand panels show the brightfield image of the thymocytes and the right-hand panels depict the cells that were fluorescently labeled by YOPRO-1. Panel A and B show cells incubated with YOPRO without ATP. The middle panel shows cells exposed to 1 mM and the bottom panel to 10 mM ATP, showing increased numbers of fluorescent cells. The dose-response relationship between dye uptake and ATP concentration is shown in Fig. 20.

Discussion: Thymocyte cell death

One of the main problems we encountered with the thymocytes consisted of our inability to demonstrate apoptosis (or cell death for that matter) in thymocytes exposed to ATP. Although ATP induced apoptosis in thymocytes has been widely reported in the literature (Zheng *et al.*, 1991) we have not been able to demonstrate ATP induced cell death using alamarBlue, an assay indicative of metabolic viability. This particular method indicates that the cells are still alive, indeed thriving, at concentrations of ATP up

to 12.5 mM following 24 hours of exposure. Moreover the demonstration of a concentration related increase in the uptake of YOPRO a dye which acts on cellular DNA which is normally indicative of cell death further complicated our attempts since all of the "surrounding" data indicated that cell death should have been readily seen.

In the second report submitted (2000) we detailed the difficulties we encountered in documenting ATP induced cell death in these cells since we were unsuccessful in duplicating literature reports with respect to the toxic effects of nucleotide (ATP) analogues on thymocyte toxicity. This led to a major shift in emphasis toward the study of CHO-K1 cells different cell types were then examined.

B CHO-K1 cells

The second and by far the largest part of this section deals with studies on CHO-K1 cells. CHO-K1 cells were selected for study for several reasons, including the results of our previous studies (in this report) which outlined both their sensitivity and the role of apoptosis and necrosis in their toxic response to HD. Furthermore, CHO-K1 cells had a well documented calcium influx pathway (Michel *et al.*, 1996) which was beneficial to our studies since part of our hypothesis involved the proposal that HD toxicity may be initiated through calcium influx resulting from the opening of an ATP activated ionic pore (Lundy *et al.*, 1998). Also, previous studies (reported prior to this section) showed that this cell type was one in which HD was able to initiate caspase induction.

First we confirmed the existence of P_2X_7 receptors in this tissue and subsequently carried out a number of experiments in which the toxicity of P_2X_7 agonists and HD were examined under different environmental conditions. At the same time we examined the role played by ions in the calcium influx induced by nucleotides in pinched off nerve endings (synaptosomes) which also were found to contain P_2X_7 receptors (studies to be outlined in Annex).

Effects of a selective P_2X_7 receptor antagonist on HD induced cell death

Initial studies were carried out in order to confirm the existence of P_2X_7 receptors in CHO-K1 cells. Fig. 21 shows the RT PCR transcript expression of total RNA from

CHO-K1 cells. Lane 1 shows the 100 base pair molecular weight markers and lane 2 is the amplified fragment of 594 base pair (P_2X_1) which was very faint and the amplified 660 base pair of the P_2X_7 (panel B). Lane 3 shows the negative control response. Oxidized ATP is a selective inhibitor of agonist activity at the P_2X_7 receptor. Preincubation with this receptor antagonist was found to have some interesting effects on HD induced cell death. Initially we incubated CHO-K1 cells with various concentrations of HD or HD in the presence of oATP. Fig. 22 shows typical ladder production in cells treated with increasing concentrations of HD (Lane 1-4). A 2 hr preincubation with either 300 or 500 μM oATP greatly abolished or eliminated the HD induced ladder formation (lane 6-8) whereas oATP by itself did not cause ladder formation. Following these experiments further work using similar protocols were used to quantitate cell death and the proportion of cells dying in the presence of HD as opposed to the numbers in the presence of the P_2X_7 inhibitor oATP. We also report here the results of experiments in which the buffer in which the ATP analogues were exposed to the cells has been altered from the point of view of ionic concentration. In these studies we switched exclusively to benzyl ATP, which is a much more potent agonist than other ATP analogues on the P_2X_7 receptor. By manipulating the ionic strength of the buffer it was then possible to demonstrate cell death which we could not demonstrate in high ionic strength buffers (see thymocytes, previous section). Experiments were then carried out to ensure that BzATP toxicity was indeed the result of its effects on only the P_2X_7 receptor by utilizing oATP which was extremely effective in preventing BzATP-induced toxicity, confirming the mechanism of action as taking place at the level of the P_2X_7 receptor.

This phenomenon is also shown in Figure 23, where DNA fragmentation is quantitated using the TUNEL reaction. Vehicle control or oATP treatment only, resulted in the expression of very limited number of TUNEL positive cells. In contrast, HD increased the percentage of TUNEL positive cells in a concentration-dependent fashion. Pretreatment with either concentration of oATP (2 hr), dramatically decreased the incidence of TUNEL positive cells in agreement with the results on Fig. 22. Figure 24 depicts the effects of oATP on the morphological changes induced by HD in CHO-K1 cells. HD induced a concentration-dependent increase in total cell death, as well as

apoptotic cell death. In the presence of HD alone the incidence of necrotic cell death was much less prevalent than cells undergoing apoptosis (top panel). The pretreatment with oATP (300 μM middle panel, 500 μM lower panel) increased the proportion of necrotic cells with a corresponding decrease in those cells showing apoptosis. However, the oATP pretreatment did not reduce total cell death (Fig. 25), but clearly decreased apoptosis and caused necrosis to become the predominant mode of cell death (Fig. 24). The lack of the overall reduction in HD induced cell death by oATP shown in Fig. 25, appears therefore to be due merely to a shift in apoptotic to necrotic cell death.

The effective concentrations of oATP used in the previous figures to block the P_2X_7 receptor were determined experimentally. The results presented in Fig. 26 reveal that as the concentration of the specific P_2X_7 agonist BzATP in sucrose based buffer (see later section) was increased above a threshold toxic dose of about 5 μM, there was a sharp increase in cell death that was somewhat dependant on the length of incubation time. BzATP induced cell toxicity appeared to reach maximal values following about 30 min of incubation for any given concentration of BzATP examined. These results will appear again in a subsequent section and will be discussed further.

Figure 27 shows the protective effects of oATP pretreatment on BzATP induced cytotoxicity and therefore indicating block of the P_2X_7 receptor at 300 or 500 μM. The toxicity of BzATP was reversed in a concentration-dependant manner with concentrations of 100 μM oATP or larger. Therefore the effective concentrations of oATP which blocked the P_2X_7 receptor were determined to be 300 and 500 μM and were used to obtain the results in Figs. 22, 23 and 24.

Discussion

P_2X_7 Inhibition: Effect on the HD Toxicity Profile:

oATP effectively inhibited the DNA fragmentation and apoptotic morphological changes typically induced by exposure of CHO-K1 cells to HD. The P_2X_7 inhibitory activity of oATP was confirmed by its ability to inhibit BzATP-induced cytotoxicity, as well as BzATP-induced ethidium bromide uptake (next section, Fig. 31). However, despite the inhibitory effects of oATP on HD induced apoptosis, it was also clear that the

overall toxicity of HD was unaffected. These results suggested that the cells that had originally followed the apoptotic pathway underwent cell death through a different mechanism following the blockade of the P_2X_7 receptor. This, in fact, was confirmed by our morphological data, which clearly showed that the pathway to cell death became predominantly necrotic in nature when the cells were incubated with oATP prior to HD exposure. A number of recent studies have demonstrated a link between P_2X_7 receptor activation and initiation of the biochemical cascade leading to apoptosis (Di Virgilio 1995; Zheng *et al.*, 1991; Ferrari *et al.*, 1999; Coutinho-Silva *et al.*, 1999; Schulze-Lohoff *et al.*, 1998). In addition, several studies have now identified situations where a shift from apoptosis to necrosis has occurred following prolonged stimulation of the P_2X_7 receptor or in situations where apoptotic events have been somehow impeded. Other recent studies have also identified the simultaneous development of both necrotic and apoptotic features following P_2X_7 activation (Schulze-Lohoff *et al.*,1998; Ferrari *et al.*, 1999) and the proportion of each can be affected by a variety of factors such as length of exposure and strength of the apoptotic signal.

Our studies thus appear to support at least a small or a modulatory role for the P_2X_7 receptor in HD-induced cell death although blocking the receptor had no real effect on the overall toxicity of HD. Under normal circumstances, HD induces a primarily apoptotic cell death through actions at the P_2X_7 receptor (and probably other sites). However, when this receptor is blocked (ie., with oATP), the pathway is shunted to one that is primarily necrotic in nature and no apparent change is observed in the overall cell death. The shunting of HD induced toxic effects from apoptosis to necrosis has been pointed out in other sections of this report and has been commented on in the conclusions.

In the next section evidence is presented which pharmacologically defines a complex consisting of this P_2X_7 receptor along with a second receptor sensitive to maitotoxin linked to a common pore which opens upon the stimulation of either receptor. The pore dilation mediated by the P_2X_7 receptor "side" results primarily in apoptotic but also a proportion of necrotic cell death. The other is a receptor whose activation results primarily in a necrotic cell death and whose prototypical agonist is maitotoxin. We

undertook this study employing a hypothesis that P_2X_7 inhibition by oATP may shunt HD induced cell death to one that is primarily determined by the maitotoxin activated side of the pore that demonstrates necrosis. This would result in a diminished apoptotic death and at the same time increase necrosis without altering overall cell death.

Pharmacological Identification of a P_2X_7/Maitotoxin Receptor Activated Cytolytic Membrane Pore in the Initiation of both Apoptosis and Necrosis.

Although a great deal of research has been carried out characterizing how cells die using these pathways, the particular mechanisms by which cells initiate or select a particular route of cell death appear to be poorly understood. This is particularly true for cell death induced by HD, for although both apoptosis and necrosis are involved, the initating stimulae are not at all well understood.

Cell death may be initiated through a variety of signaling mechanisms including the activation of external membrane bound receptors and/or ionic pores. The role of ionic pores in the initiation of cell death has been well studied, particularly those pores which regulate intracellular calcium levels (rev. see Kass and Orrenius, 1999). For example, maitotoxin (MTX), the most potent marine toxin yet described, has been reported to cause a variety of physiological events as the result of its ability to cause an increase in intracellular calcium concentrations (Tagliatela *et al.*, 1990) and in some cases necrotic cell death that is initiated through a mechanism also dependent on external calcium concentrations (Kutty *et al.*, 1988; Estacion and Schilling, 2001) through activation of a non-specific membrane cation channel that may in fact, be a MTX receptor (Morales-Tlalpan and Vaca, 2002; Martinez-Francois *et al.*, 2002). Clear examples of cell death initiated by receptor activation have also been well documented following exposure to ATP and its analogues, particularly 2'-3'-O- (benzylbenzyl) ATP (BzATP). These nucleotides are well known to initiate and promote both apoptosis and/or osmotic lysis (necrosis) in a very wide variety of cell types (Dubyak and El-Moatassim, 1993; Di Virgilio, 1995; Schulze-Lohoff *et al.*, 1998) through the activation of distinct cell surface ATP receptors (Di Virgilio, 1995; Burnstock, 1999). Some ATP receptors, notably in the P_2X sub-family, are ionotropic channels that act, for example, to transport calcium through the cell membrane (Burnstock, 1998) resulting in a variety of vital physiological effector responses, including muscle contraction and nerve transmission (Ralevic and Burnstock, 1998; Deuchars *et al.*, 2001; Lundy *et al.*, 2002). The P_2X_1 (Valera *et al.*, 1994; Brake *et al.*, 1994) and P_2X_7 (Di Virgilio 1995; Schulze-

Lohoff *et al.*, 1998) sub-types of P_2X receptors have been implicated in the mediation of ATP-induced cell death and may in fact play a wider role in cell death initiated by other toxic insults as well. Activation of the P_2X_7 receptor initially leads to the opening of an ionic channel, that in turn results in the secondary opening of a membrane pore. This pore, in its open state permeabilizes the membrane to a variety of larger molecular species (up to about 900 daltons, Wiley *et al.,* 1996) and the literature suggests that pore opening can lead to a cascade of events that eventually leads to either apoptotic or necrotic cell death (Di Virgilio, 1995; Zheng *et al.*, 1991; Coutinho-Silva *et al.*, 1999; Schulze-Lohoff *et al.*, 1998; Humphreys and Dubyak, 1996; Humphreys *et al.*, 2000).

Recent studies have suggested that there is a common link between activation of the MTX receptor (ion channel) and activation of the P_2X_7 receptor subtype which involves the secondary dilation of a pore common to both sites (Alzola *et al.*, 2001; Schilling *et al.*,1999a,b). The results presented in this report provide critical pharmacological identification of two distinct receptor sites with no apparent pharmacological interaction with one another. Furthermore, the data clearly defines a variety of factors that modulate the activity of either receptor and provides evidence for the direct association between the activation of either site and the subsequent dilation of what appears to be a common pore leading directly to the initiation of cell death

The definition of the two receptors and the control of subsequent activation of a pore leading to both apoptosis and necrosis led to studies carried out to determine the possible effects of HD on this complex. Since our studies have been carried out to examine the effects of HD on the P_2X_7 receptor (or the cytolytic pore connected to it), we examined the possibility that the initiation of the toxic effects of HD might in fact be this pore, or the receptor which controls pore dilation. Since maitotoxin also activates this pore, but by a totally different mechanism, it is conceivable that HD may act on the maitotoxin "side" of the pore, at least under certain conditions to cause it to open and initiate cytotoxicity.

RESULTS

Optimal ionic requirements for MTX and BzATP activity

Figure 28 illustrates the time- and ionic-dependence of EtBr uptake following exposure of CHO-K1 cells to BzATP or MTX, as measured by the detection of EtBr-DNA fluorescence signals. When cells incubated in sucrose buffer were exposed to 50 μM BzATP, a robust and time dependent increase in EtBr uptake was observed over the 30 min test period (Fig. 28A). In contrast, when the cells were incubated in PSS buffer containing physiological ion concentrations, even a much higher BzATP concentration (200 μM) failed to induce significant dye uptake over baseline values (Fig. 28B). Similar studies revealed that MTX activity was much less dependent on the ionic concentration of the test buffer than that of BzATP and that the presence of ions (in PSS buffer) actually enhanced MTX evoked EtBr uptake compared to that obtained in ion depleted sucrose buffer (Fig. 28C). Further confirmation of these findings was obtained using fluorescence microscopy (Fig. 29) to visualize the effects of MTX (125 pM) and BzATP (50 μM) on CHO-K1 cells under optimum ionic conditions (MTX/PSS, BzATP/sucrose). Few, or no fluorescent cells were noted with vehicle treatment (Fig. 29A,B). However, both MTX and BzATP treatment caused a time dependent uptake of EtBr when measured kinetically (Fig.29 G,H). Samples of these same cell suspensions taken at the end of a 30 min incubation period with the agonist, showed that most of the cells which could be seen by light microscopy (Fig. 29 E, 2F) were also fluorescent following exposure (Fig. 29 C,2D).

Studies carried out to determine the toxicity of BzATP in CHO-K1 cultures also showed the dependence of BzATP action on the ionic concentration of the buffer/medium bathing the cells. When the cultures were exposed to BzATP in F-12 culture medium (~130 mM NaCl), no toxicity could be detected even at 100 μM concentrations as indicated using LDH release (Fig. 30). In contrast, in a non-ionic sucrose buffer, BzATP induced near maximal 24 hr toxicity with only a 30 min exposure before the sucrose treatment buffer was aspirated and replaced with F-12 culture medium. BzATP induced a similar toxic response in sucrose buffer as assessed using the alamarBlue viability assay (shown in Fig. 33) and all further assays of cytotoxicity in this study were carried out using this reliable and less labor intensive method.

The effect of antagonists on MTX and BzATP induced EtBr uptake and toxicity

In order to further characterize the lack of interaction of MTX and BzATP induced effects on either receptor site as reflected by pore dilation and subsequent cytotoxicity, the effects of specific antagonists for each site were examined. When the selective P_2X_7 antagonist oATP was preincubated with cells 30 min prior to BzATP exposure (in sucrose buffer), EtBr uptake was totally inhibited over the 30 min incubation period (Fig. 31C vs. 31D). These cells exhibited no significant amount of staining under fluorescence microscopy (Fig. 31A) as compared to the BzATP induced staining shown in Fig. 31D. In contrast, the results in Fig 32 showed that oATP pretreatment had no significant inhibitory effect on the EtBr uptake in CHO-K1 cells treated with 125 pM MTX (in PSS buffer) as assessed either microscopically (Fig. 32A) or kinetically (Fig. 32D). Similar findings were also obtained when the effects of oATP on drug induced cytotoxicity were examined (Fig. 33). When CHO-K1 cells were incubated with BzATP in sucrose buffer for 1 h, the metabolic viability of the cells at 24 h (as measured by alamarBlue) declined in a concentration dependent fashion to less then 40 % of control values. However, preincubation of the cultures with oATP prior to BzATP treatment provided a concentration related protection that was maximal at 500 μM oATP (Fig. 33A). In contrast, oATP (Fig 33B) provided no protection against the toxic effects of MTX (in medium), even at concentrations that were completely protective against BzATP toxicity

Studies were carried out in order to examine the possible role of the calmodulin inhibitor W7 on the activation of the two receptor sites as well as in the initiation of cell death. When cells were preincubated for 15 min with 100 μM W7, BzATP induced EtBr uptake was unaffected (Fig. 34A vs 34C). In contrast, the rapid uptake of EtBr induced by 125 pM MTX was totally abolished by a 15 min preincubation with this concentration of W7 (Fig. 34B vs 34D), an effect that was found to be concentration dependent (Fig. 34E). W7 was found to exert differential and selective effects on the cytotoxicity induced by MTX and BzATP similar to those on EtBr uptake. Preincubation of cells with W7 prior to MTX exposure was cytoprotective in a concentration dependent fashion (Fig. 35B), but was marginally effective in preventing BzATP toxicity (Fig. 35A).

Effect of external Ca^{2+} concentration on MTX and BzATP induced EtBr uptake and toxicity

Figure 36 shows the marked dependence on external calcium of MTX induced EtBr uptake in CHO-K1 cells. At a moderate MTX concentration (125 pM), a steep increase in uptake was apparent when the assays were carried out at 1.5 mM calcium (Fig. 36A). This calcium concentration was near optimal in facilitating EtBr uptake (results not shown). However, no measurable dye uptake was apparent when external calcium was omitted from the external medium (Fig. 36B). In additional experiments (results not shown), cells exposed to MTX in calcium free PSS failed to take up EtBr until calcium (1.5mM) was added to the cuvette at which time there was an immediate increase in the uptake of EtBr that ultimately reached maximal levels. BzATP, unlike MTX, induced EtBr uptake (Fig. 36C) in the absence of any added calcium to the sucrose buffer. Moreover, analysis of the three curves depicted in this figure failed to reveal any statistically significant effect of external calcium concentration on EtBr uptake (ANOVA). However, the shape of the EtBr uptake curves shown in Fig. 36C suggests some divergence in the uptake among the three curves at time periods greater than 20 min following agonist exposure. This appears to suggest the possibility of an increasing effect of external calcium with time and may correlate with the initiation of the second phase of the biphasic response observed following exposure to BzATP.

Fig. 37A shows a summary of results carried out in which BzATP toxicity was examined in sucrose buffer at various calcium concentrations (10 μM - 2.5 mM). BzATP was not toxic when the incubation was carried out in the absence of calcium. At 100 μM external calcium, a shallow decline in cell viability with BzATP concentration became evident, which was maximal at 500 μM calcium, but never progressed below ~40 % cell viability. The calcium dependence of MTX induced cell toxicity was different in character than that of BzATP (Fig. 37B). Although MTX was still extremely toxic even in the absence of calcium (LC_{50} = 2.4 +/- 0.6 nM, n = 3), the addition of calcium resulted in a profoundly concentration-dependent increase in toxicity so that by 2.5 mM calcium, LC_{50} values were decreased by over two log orders of magnitude (LC_{50} = 22.4 +/- 3.7

pM, n =3). In addition, and in contrast to BzATP cytotoxicity, MTX toxicity to the cells approached 100 % at higher concentrations.

Examination of the role of the cytolytic pore in HD induced cell death

CHO-K1 cells were incubated in the buffer containing 20 μM ETBR in the flourometer and a baseline fluorescent uptake measured and the effects of the addition of HD (400 μM) to the cuvette on EtBr EtBr influx. Cells were incubated with 400 μM HD for one hour and dye uptake was followed using both fluorimetry (Fig. 38) and microscopy (Fig. 39). At these concentrations and incubation periods no noticeable effects of HD could be observed by simple light microscopy. In neither case did HD cause an appreciable increase in fluorescence intensity in contrast to the effects of either maitotoxin or BzATP seen in previous figures. In other experiments the effects of combined exposure of cells to both HD and BzATP were examined (Fig. 40). Cells were incubated with 400 μM HD for 10 min followed by the addition of BzATP (100 μM) (panel B) and compared to the EtBr uptake seen following BzATP alone (panel A). These results were quantitated and the results are presented in Fig. 41 which shows no significant difference in the uptake of EtBr in the presence or absence of HD. Experiments were then carried out using somewhat higher concentrations of HD (800 μM) and incubating HD with the CHO-K1 cells for sufficient time periods (8hr) to observe initial HD induced toxic events in the cell such as cell rounding. These cells were then prepared and incubated in EtBr with sufficient concentrations of either receptor agonist (BzATP or maitotoxin) to cause marked EtBr uptake over a 30 min time period. Fig. 42 shows that treating cells with either BzATP or maitotoxin in addition to a large concentration of HD caused no additional rate of increase in EtBr.

The results above led to the description of a membrane bound cytolytic pore which schematically looks like the diagram drawn as Fig 43. However appealing this complex might appear to be in the generation of both apoptotic and necrotic cell death we could find no definitive effects of HD on any aspect of the proposed complex.

DISCUSSION

Effect of HD on a cytolytic complex.

The results of this study offer strong evidence for the existence of separate P_2X_7 and MTX receptors, which when activated, independently initiate the dilation of a membrane pore resulting in the uptake of large molecular weight substances such as EtBr in CHO-K1 cells. In addition, we have also shown that the pharmacological factors which determine receptor activation and pore dilation such as external calcium concentration, concentration of ions within the incubation buffers and specific pharmacological antagonists also modulate the viability of the cell in a parallel manner with both receptor stimulation and EtBr uptake, the consequence of receptor stimulation. Studies were initiated to examine the effects of the selective P_2X_7 agonists such as BzATP on the viability of CHO-K1 cells. Preliminary studies were carried out in traditional physiological buffer systems or in culture media, and the results indicated a lack of effect of BzATP on either EtBr uptake or cell death. Although previously published work had revealed the inhibitory effects of certain ionic species (notably monovalent cations) on agonist/ P_2X_7 receptor association (Michel *et al.,* 1999; Virginio *et al.,* 1997; Song and Chueh, 1996; Lundy *et al.,* 2002), it was not initially clear that the presence of high concentrations of monovalent cationic species would totally eliminate P_2X_7 mediated responses in this particular cell line. The pharmacological relevance of the inhibitory activity of ions on receptor activation to the *in vivo* situation has been suggested to be related to an increase in P_2X_7 receptor activity in certain pathological states that promote reduced extracellular ionic concentrations in the region of the receptor. For example, it has been reported that anoxic conditions result in the collapse of ionic gradients at the cell membrane, which results in a marked decrease in external ionic concentration (Voresek and Sykova, 1997; Morris and Trippenbach, 1993). The resulting decrease in ionic strength in the region of the receptor, might then promote P_2X_7 receptor stimulation, activation of the cytolytic pore and the initiation of cell death. The present results obtained *in vitro* demonstrate the requirement for a cation-deficient environment to enable BzATP-induced $P2X_7$ activation, pore dilation and subsequent cell death, supporting the notion that collapsing ionic gradients *in vivo* might lead to increased

agonist/ P_2X_7 interactions with appropriate consequences. In contrast, MTX receptor stimulation was favored following exposure of cells to the agonist at "normal" physiological ionic concentrations typified by high sodium concentrations, although activity was still significant even in buffer with low ionic concentrations.

The activation of the two receptors was also dependant to various degrees on the calcium concentration in the incubation medium. MTX induced receptor activation was clearly heavily dependant on external calcium concentrations but to a lesser degree on sodium concentration. This relationship is consistent with recent reports (Morales-Tlalpan and Vaca, 2002) which demonstrated that MTX could induce calcium influx in buffer with reduced sodium content, but that sodium influx was abolished in the absence of calcium. It appears therefore that calcium is critical for the initiation of MTX effects, while sodium is able to modulate this activity. In contrast, increasing sodium concentrations have been reported to directly inhibit activation of the P_2X_7 receptor (Song and Chueh, 1996; Virginio *et al.*, 1999) an inhibition which appears to be reflected in the present results revealed by marked inhibition of P_2X_7 stimulation in a buffer containing physiologically relevant concentrations of sodium, although no attempts were made in the present studies to alter sodium concentrations in a systematic manner. On the other hand, activation of the P_2X_7 receptor was not as dependent on external calcium concentrations as was MTX activation. The optimal activity of the two sites under very different ionic conditions, including the presence of calcium, suggests that this membrane receptor/pore complex may offer a sensitive regulatory mechanism to control cell viability under very different cellular environmental conditions or insults.

It is clear that the two receptors do not share the same rigorous requirement for calcium to induce activation, a fact that is further supported by the observation that the calcium dependency for the demonstration of MTX induced cytotoxicity (and EtBr uptake) appears to be much greater than that for BzATP. While the potent toxicity of MTX was very clearly and sensitively related to increasing concentrations of extracellular calcium (10 μM – 2.5 mM), there was no absolute calcium requirement for the demonstration for a least some level of toxicity to be expressed. In contrast, although BzATP toxicity never reached more than 40 % of the treated cells and the concentration

effect curves were rather shallow, toxicity did require the presence of at least a minimal extracellular concentration of calcium.

Perhaps the most compelling argument for the separation of the P_2X_7 and the MTX receptors comes from experiments in which different pharmacological antagonists were employed in order to observe the potency of the two agonists to induce EtBr uptake and cell death. oATP is a selective antagonist of the P_2X_7 receptor site (Murgia *et al.*, 1993). The results obtained in the present study clearly show that concentrations of oATP that were effective in totally abolishing the responses to BzATP activated EtBr uptake and cytotoxicity, had no effect on MTX induced activation of its receptor site with respect to either parameter. With the understanding that W7 may not express its effects on MTX solely through calmodulin inhibition (Schaeffer *et al.*, 1991), the differential inhibition of the two receptors by W7 offers a clear distinction between the two receptor sites. Also, W7 showed a clear concentration dependant inhibition of both MTX induced EtBr uptake and cell death, but had no significant effects on similar parameters following P_2X_7 receptor stimulation induced by BzATP. It is interesting that a second calmodulin antagonist, trifluprομazine (1-10 μM) also blocked the effects of MTX and that both W7 and trifloupromazine blocked the MTX induced rise in intracellular free calcium levels and toxicity, but have little or no effect on BzATP induced effects (Lundy *et al.*, unpublished observations). Although the mechanism of W7 and trifluprομazine in the toxicity and the pore opening properties of MTX is currently poorly understood, the fact that these calmodulin inhibitors are specific for the inhibition of MTX responses as opposed to BzATP responses, offers additional evidence that the two receptors have no detectable cross sensitivity to at least these inhibitors. Therefore it is proposed that the different ionic requirements for the optimal demonstration of the agonist activity, the differential requirement for calcium in the activation of either site, and the exclusive site specific effects of oATP and calmodulin inhibitors, all strongly suggest that not only are the sites separate in this cell line (see also Schilling *et al.*, 1999a,b), but that the activation or inhibition of these sites are clearly predictive of ultimate cell death.

It is interesting to speculate on the reasons that cells, including human skin fibroblasts (Schilling *et al.*, 1999a), CHO-K1 cells and likely many other cell types,

contain at least two completely different receptors involved in the initiation of cytolysis following the opening of a common membrane pore. Previous studies have shown that MTX leads to necrosis in the absence of any apoptotic cells (Kutty *et al.*,1988, Zhao *et al.*, 1999). In sharp contrast, stimulation of the P_2X_7 receptor leads to a biochemical cascade including caspase induction, DNA fragmentation, PARP cleavage, release of cytokines, the activation of phospholipases and the induction of apoptosis which is followed in a proportion of the affected cells by secondary necrosis (Di Virgilio, 1995; Song and Chueh, 1996; Coutinho-Silva *et al.*, 1999; Schulze-Lohoff *et al.*, 1998; Humphreys and Dubyak, 1996; Humphreys *et al.*, 2000). It is of interest to speculate on the possibility that the preferential activation of the two sites examined here and possibly the common pore, may occur under very different environmental or pharmacological/physiological circumstances. The presence of three separate entities; two receptors and a membrane pore, which may be involved in the control of cell viability may provide the cell with sensitive or subtle methods by which to modulate its survival. Activation of one or the other site or some combination of the three, may partly explain why certain insults cause cells to take a given route to cell death. Further evaluation of such speculation awaits further pharmacological identification of the MTX site, as well as a much clearer elucidation of its mechanism of action on intracellular biochemical changes leading to cell death.

Although the P_2X_7 receptor *in vivo* is activated by ATP and presumably other pharmacological agents, it has yet to be demonstrated whether the MTX-activated channel responds to other endogenous or exogenous agonists resulting in cell death. It is presently also unclear whether the diameter of the cytolytic pore can be modified directly without primary activation of a receptor. However, maitotoxin is known to have very interesting pharmacological activity in a variety of tissues related to signal transduction. For example, MTX and P_2X_7 receptors sites have both been clearly identified on nerve endings where they sub-serve calcium entry followed by neurotransmitter release (Tagliatella *et al.*, 1990; Lundy *et al.*, 2002; Deuchars *et al.*, 2001). Furthermore it appears inherently unlikely that MTX receptors are resident on terrestrial mammalian tissue solely to respond to a rare marine toxin. Therefore the identification of endogenous

substances or toxic principals such as HD that activate either of the two receptors or the common pore directly would be of considerable interest.

Effects of HD on the Common Cytolytic Pore

With the above in mind and because the biochemical and toxic outcomes of exposure of cells to HD or either of the receptor sites is very similar, studies were initiated to determine the effects of HD alone or in combination with either of the receptor agonists on the two receptor "sides " of the common cytolytic pore. These responses were also quantitated by the measurement of the uptake of ethidium bromide. Cells exposed to various concentrations of HD alone failed to respond with increased uptake of EtBr. In other experiments, cells were incubated with higher concentrations of HD (400 μM) in ethidium bromide solution for shorter periods of time and then exposed to BzATP 100 μM. which also resulted in no change in the EtBr uptake kinetics. Since these concentrations of HD incubated with cells for the stated time periods failed to induce observable morphological changes typical of HD toxicity, cells were also incubated at higher concentrations of HD for longer time periods sufficient to cause observable changes in cell structure. When these HD affected cells were incubated with maitotoxin or BzATP there was still no indication that there were significant changes in EtBr uptake. These results were disappointing with respect to the theory that the cytolytic complex described in these studies did not appear to be materially affected by HD

TABLE 3

Studies on the Activation of the P_2X_7/Maitotoxin Cytolytic Pore in CHO-K1 Cells

$P2X_7$ Activated Pore	Maitotoxin Activated Pore
Activated by BzATP + certain P2X agonists	Not activated by P_2X_7 agonists
Inhibited by P_2X_7 antagonists	Not affected by $P2X_7$ antagonists
More active in sucrose buffer; less active in high ionic strength buffers	More active in ionic buffer than in sucrose-based buffer
Uptake of ethidium bromide is time-dependent	Uptake of ethidium bromide is time-dependent
Ethidium bromide uptake demonstrates a very shallow concentration effect curve	Uptake of ethidium bromide is very concentration dependent
Stimulation results in cell death by apoptosis/necrosis	Stimulation results in cell death by necrosis
Receptor acts as an ionic channel. Subsequent pore opening is relatively Ca^{2+} independent	Receptor acts as ionic channel, ethidium bromide uptake directly proportional to external Ca^{2+}

Stimulation of Ca^{2+} Influx Through ATP Receptors on Rat Brain Synaptosomes: Identification of Functional $P2X_7$ Receptor Subtypes

In the previous sections we have outlined attempts made to identify P_2X_7 receptors in a variety of tissues in order to determine whether the receptor activity was altered in any significant manner following exposure to sulphur mustard. The results in the **Annex 1** describe the identity and location P_2X_7 receptors in neuronal tissues. A number of molecular methods, biochemical measurements and immunoflourescence studies are described which prove the existence of P_2X_7 receptors in nerve endings. It was postulated that these receptors might also be altered by HD in a manner consistent with the central nervous system effects previously reported to occur in humans exposed to HD. The results show that P_2X_7 receptors on nerve endings partially control the access of external calcium (calcium influx) into nerve endings and play a role in the control of neurotransmitter release which may be relevant to states of neuronal activity. The identification of these receptors and the calcium influx which they apparently, was also unaffected by exposure to HD (see Fig. 44).

THE ROLE OF CALCIUM IN SULPHUR MUSTARD INDUCED APOPTOTIC CELL DEATH

SUMMARY

For several years now, the role of calcium in the aetiology of sulphur mustard induced cell death has been controversial. Although it now seems to be accepted that this CW agent causes a modest, but irreversible elevation of intracellular calcium in several different cell types, the importance of this calcium release to the overall viability of the exposed cell is not known with certainty. There is evidence in the literature that supports the contention that this phenomenon is an important causal step in the development of HD induced toxicity, as well as evidence that refutes this stance. In year three, we generated preliminary data that appeared to suggest that although calcium modulation did not change the overall toxicity of HD, inhibition of HD induced intracellular calcium may reduce the DNA fragmentation characteristic of apoptotic cell death. During this past year, studies designed to examine this hypothesis were not supportive. Modulators of intracellular calcium, including BAPTA-AM, thapsigargin and W-7 definitively did not alter the metabolic viability of HD treated keratinocytes. Furthermore, they were ineffective in reducing HD-induced fragmentation as measured by the TUNEL assay. Most importantly, these calcium modulators also had little effect on the prototypical HD laddering pattern induced by HD when visualized on electrophoresed agarose gels. Morphological assessment of the effect of these drugs was also consistent in that no statistically significant differences were noted compared to HD only treated cells, although there were some indications that W-7 may reduce the cell death at higher HD concentrations. Although we intend to carry out further studies to confirm these data, at this point it appears that in neonatal human skin keratinocytes in culture, HD-induced intracellular calcium perturbation does not play a major role in HD-induced (apoptotic) cell death. Thus, therapies predicated on modulation of intracellular calcium will not likely be effective in reducing HD induced injury.

RESULTS

Figure 45 depicts the results of cytotoxicity studies using just-confluent cultures of human keratinocytes exposed to HD. In these experiments the effects of various treatments that are known to modulate intracellular calcium on mustard toxicity were examined. In naïve cultures HD induced a concentration dependent decline in cell viability with a LC_{50} of 209.1 +/- 5.5 μM (mean +/- SD, n = 3). Treatment of the cultures in medium containing varying calcium concentrations yielded LC_{50} values that declined slightly, but generally not statistically significantly with calcium concentration. The calcium chelator BAPTA-AM and the calmodulin inhibitor W7 (Fig. 45) did not alter the toxicity of HD in any way. The endoplasmic reticulum Ca^{2+} ATPase inhibitor thapsigargin slightly, but not statistically significantly increased the toxicity of HD.

HD induced a concentration dependent increase in TUNEL positive cells (Fig. 46). Treatment of the cultures in nominal zero calcium concentration, or pretreatment with 25 μM BAPTA-AM, 10 μM thapsigargin or 30 μM W-7 did not significantly alter the response of vehicle control cells compared to naïve cultures, and likewise did not alter the profile of HD-induced TUNEL positive cells. Similar results were obtained when HD induced DNA fragmentation was visualized using LMPCR and subsequent agarose gel electrophoresis (Fig. 47). Vehicle control cultures yielded DNA fragments that when amplified, were of random size, causing a uniform smear within the gel. 100 – 500 μM HD induced the ladder patterns consistent with apoptotic cell death, with definitive bands being visible corresponding to the 180 basepair kilobase kit postive control (calf thymus DNA) included in the last lane of Panel E (sample K). 100 – 400 μM HD treatment in medium containing no calcium, or pretreatment with BAPTA-AM, thapsigargin or W-7 did not alter the appearance of the banding. However, at 500 μM HD, the sharpness of the bands was reduced with BAPTA-AM and thapsigargin treatment and eliminated by zero calcium and W-7.

The effects of calcium modulation on HD toxicity were next assessed using morphological means (Fig. 48). Control cells were undergoing a small amount of cell death (< 5%). HD exposure decreased cell viability to ~ 30% at 200 μM, with the cells equally divided between apoptotic and necrotic cell death. Treatment in medium

containing no calcium, or pretreatment with BAPTA-AM or thapsigargin did not alter the total cytotoxicity observed, but did appear to shift the ratio of apoptotic to necrotic cell death to one where necrosis was predominant. However, these changes were not statistically significant. Likewise, 200 μM W-7 appeared to signicantly decrease the number of cells undergoing both apoptotic and necrotic cell death. Statistical analyses of these results, however, showed that these results were not significant.

DISCUSSION

Several different laboratories utilizing a variety of cell culture systems have examined the effect of HD (~ 100 μM - 1.0 mM) on cellular calcium levels and have come to varying conclusions as to the importance of calcium homeostasis in HD-induced cytotoxicity. The first laboratory to test the thiol-Ca^{2+} hypothesis found that in mouse fibroblast B77 cells, HD induced a modest, but immediate and sustained rise in intracellular calcium levels that was independent of external calcium concentrations (Hua *et al.*, 1993). However, follow-up work by Mol and coworkers was equivocal. In second passage cultures of human skin epidermal keratinocytes grown on 3T3 feeder-layers, they found little or no evidence of HD-induced intracellular calcium elevation and dismissed the small increases they detected as reflecting abnormal cellular physiology rather than acute toxicity (Mol, 1994; Mol and Smith, 1996). In contrast, intracellular calcium was consistently found to be elevated 2- 6 hr after HD exposure in a mouse neuroblastoma-rat glioma hybrid cell line (NG108-15) by Ray and colleagues (Ray *et al.*, 1995), who also found a similar elevation in human epidermal keratinocytes (Ray *et al.*, 1994). This same group has gone on to report that the cell-permeant calcium chelator BAPTA-AM not only prevented this intracellular calcium elevation, but was also effective in preventing HD-induced cytotoxicity (Ray *et al.*, 1996; 1997; 1998).

Recent studies in our laboratory (Hamilton *et al.*, 1998) have tended to confirm the initial findings of Hua *et al.* (1993). In first passage just-confluent cultures of neonatal human skin keratinocytes, it was found that HD does indeed cause an immediate, concentration-dependent and sustained elevation of intracellular calcium that appeared to originate from intracellular stores. Furthermore, the sensitivity to HD and

the time course of this calcium elevation roughly paralleled the effects of HD on cell viability, although the concentrations of HD that maximally elevated intracellular calcium would be considered supralethal (Hamilton *et al.*, 1998). In order to further assess the link between intracellular calcium and HD-induced cytotoxicity we examined the effect of modulating both external and internal calcium levels prior to HD culture exposure in both proliferating and just-confluent cultures of neonatal human skin keratinocytes (Sawyer and Hamilton, 2000). Our initial work attempted to replicate the work of Ray and coworkers with BAPTA-AM (Ray *et al.*, 1996; 1997; 1998). This cell-membrane permeable calcium chelator should modulate toxicity if intracellular calcium elevation is indeed causal or involved in the cascade of events that lead to HD toxicity. Preliminary studies paralleled this group's work and found that at 25 μM, BAPTA-AM was non-toxic in confluent cultures. Unexpectedly, however, pretreatment of cultures with this chelator failed to modulate HD toxicity in any way. We also carried out experiments with thapsigargin, an endoplasmic reticulum Ca^{2+} ATPase inhibitor that we have previously shown to eliminate the intracellular calcium elevation induced by HD (Hamilton *et al.*, 1998) and the ionophore ionomycin. Both pretreatments also failed to modulate HD toxicity in any way at any concentration used. Finally, the effects of modulating the calcium concentration of the medium bathing the cultures were then examined (0 – 100 μM), since internal calcium levels are known to be sensitive to external calcium. Once again, the concentration response of HD was not altered. The current studies have replicated these previous findings in just-confluent cultures of neonatal human skin keratinocytes, and also shown that the calmodulin inhibitor W-7, previously shown to eliminate HD induced DNA "laddering" in HD treated human keratinocytes (Rosenthal *et al.*, 1998), failed to alter HD induced toxicity.

The findings of Ray and coworkers have been recently supplemented with additional work carried out using human skin keratinocytes (Rosenthal *et al.*, 1998). These studies demonstrated that HD causes the cleavage of DNA into the distinct "ladder patterns" of DNA fragments on electrophoresed agarose gels, that have become one of the hallmarks of apoptotic cell death. Furthermore, they showed that both BAPTA-AM and the calmodulin inhibitor W-7, reduced or eliminated the formation of these "ladders".

In an attempt to resolve the apparent disconnect between the repeated reports that intracellular calcium modulation can alter resultant HD toxicity, and our data that indicates that it cannot, we examined the effect of intracellular modulation on HD induced DNA fragmentation and morphology at 16 hr. It was possible that our measurements of 48 hr cellular metabolic viability as quantitated by the alamarBlue cytotoxicity assay may not reflect the effects of calcium modulation at earlier time points.

Our efforts at quantitating apoptotic cell death used three different endpoints. Cellular morphology was examined to assess as to how HD induced cell death was taking place; either through apoptotic or necrotic pathways, while apoptotic DNA fragmentation was assessed using the TUNEL assay, an immunohistochemical assay detecting the "nicked ends" of fragmented DNA, and agarose gel electrophoretic visualization of LMPCR amplified DNA fragments. We have found that while we can easily visualize HD induced apoptotic DNA ladder patterns on electrophoresed agarose gels from a variety of different cell types, DNA ladders from HD treated keratinocytes are not reproducibly and clearly obtained unless the DNA fragments are first amplified by LMPCR. Using this methodology, HD treatment of keratinocytes routinely yields DNA laddering on electrophoresed agarose gels that is consistent with the fragmentation of DNA into the 180 basepair nucleosomes characteristic of apoptotic cell death.

The data obtained from experiments examining HD induced DNA fragmentation consistently illustrated the lack of effect of calcium modulation. HD induced a concentration related increase in TUNEL positive cells that was not significantly altered by zero extracellular calcium, BAPTA-AM, thapsigargin or W-7. Likewise, the distinct DNA ladder pattern induced by HD (100 –500 μM) was not changed, except at the highest HD concentration, where zero calcium and W-7 pretreatment eliminated the banding pattern. However, in these cases it is more probable that the combined insult of high HD concentration and drug pretreatment simply resulted in necrotic insult, rather than a protective effect, a conclusion supported by the cytotoxicity studies. The morphological studies also supported a lack of effect of calcium modulation on HD induced toxicity. Although calcium modulation appeared to shift the effect of 200 uM HD from one being approximately equally divided between apoptotic and necrotic cell

death, towards one being predominantly necrotic in nature, the changes were not statistically significant.

In summary, previous studies in this laboratory have shown that HD induces a rapid, sustained and concentration-dependent increase in intracellular calcium in neonatal human skin keratinocytes that appears to originate from intracellular sources. However, this study shows that perturbation of calcium homeostasis is not causal or directly involved in the development of HD induced apoptotic cell death, DNA fragmentation, or gross cytotoxicity, at least in this cell culture system. These findings suggest that therapeutic regimens specifically aimed at modulation of intracellular calcium, or interrupting calcium dependent apoptotic events will not be effective.

THE ROLE OF IONIC ENVIRONMENT IN SULPHUR MUSTARD INDUCED CELL DEATH

SUMMARY

The importance of ionic environment in the toxicity of ATP to cells in culture has been well documented in this report. In routine tissue culture medium, we were unable to demonstrate ATP toxicity, accept at very high concentrations. However, in buffers containing no sodium, but adjusted to physiological osmolality (~ 300 milliosmolal) with sucrose, ATP and its analogues were shown to be quite toxic. This was an integral part of our efforts to demonstrate that HD may exert its toxicity at the level of ATP receptors and thus, follow-up studies consisted of trying to characterize any interactions between ATP and HD. These met with difficulty since, to our surprise HD was virtually non-toxic to cells in culture when the exposures were carried out in the non-ionic sucrose buffers so necessary for ATP toxicity to be expressed.

The interesting finding that HD was essentially non-toxic in ion-free buffer, prompted us to examine the role of ionic environment, including pH, on HD toxicity in CHO-K1 cell culture. We show here that HD toxicity is strongly dependent on the ionic environment during the first hour of treatment. As one increased the sodium chloride concentration of the treatment buffer from zero to a physiological 130 mM, 24 hr HD LC_{50} values decreased from > 800 μM to ~ 100 – 130 μM. Furthermore, the toxicity of HD appeared to be strongly dependent on the *anionic* environment; exposure of the cultures to HD in sodium salt buffers yielded similar LC_{50} values regardless of cation identity. Likewise, exposure to HD in iodide salts (lithium, potassium, sodium, cesium, rubidium) yielded similar and much decreased LC_{50} values of ~ 8 – 12 μM. A simple explanation to these phenomena would be that the increased halide concentration shifts the equilibrium of the HD hydrolysis reaction to the left, resulting in an alteration of HD half-life with chloride ion, and the formation of bis (2-iodoethyl) sulphide and its products with iodide ion. However, studies showed that the half-life of HD toxicity in 32.5, 65.0 or 130 mM sodium chloride was virtually identical, suggesting that the ionic dependence of HD was biochemical in nature. Additional experimental work further

supported this conclusion. The prototypical chloride ion channel inhibitor DIDS significantly inhibited HD toxicity at concentrations as low as 400 μM, while the exposure of cells to HD in basic medium was also found to confer profound protective effects against its toxicity. These latter findings suggested that HD toxicity was perhaps mediated through the perturbation of intracellular chloride ion levels. However, experiments using fluorescent indicator dyes showed that this was not the case.

The role of solution chemistry in the dependence of HD toxicity on anionic environment needs to be more rigorously examined using analytical chemical techniques. However, at this point overwhelming evidence appears to support the conclusion that this dependence is biochemical in nature and that whatever site HD acts upon to initiate the cascade of events that leads to cell death, is sensitive to perturbations in its ionic environment. These findings may be of importance in the future in assisting in the characterization of this elusive mechanism of HD toxic action.

RESULTS

Figure 49A and 50C depict the effect of varying NaCl concentration on HD toxicity in CHO-K1 cells. Cultures were exposed to varying concentrations of HD in culture medium, or in defined sucrose buffers of increasing NaCl concentration for one hour. The cultures were then changed into culture medium and assayed for cell viability 23 hr post-HD exposure. The LC_{50} for HD in culture medium was ~ 130 μM, in contrast to a value of > 800 μM when the treatment was carried out in defined sucrose buffer. As the buffer NaCl concentration was increased, the toxicity of HD also became greater, so that by ~ 130 mM NaCl, the LC_{50} approximated that obtained in culture medium. The median effective concentration for NaCl was 10.8 mM +/- 2.9 mM with respect to increasing the toxicity of HD from that obtained in non-ionic sucrose buffer to one approaching the LC_{50} obtained in physiological F-12 culture medium. Similar studies were carried out in a variety of buffer solutions containing different salts and the results are depicted in Figures 50-56 and in Table 4. Although to this point the data has not been analyzed statistically, preliminary conclusions can be made. Experiments examining the

effects of the potassium and sodium salts of fluoride, bromide, iodide, aspartate, gluconate, glutamate and isothiocyanate on HD toxicity indicate that the cation has relatively little influence on HD toxicity, compared to the anionic species. This is particularly emphasized by the results obtained in the studies utilizing the iodide salts of lithium, potassium, sodium, cesium and rubidium (Table 4, Fig. 49B, 51C,D, 55A,B,C). Although HD toxicity is almost a log order of magnitude greater in these buffer solutions compared to all other test buffer solutions (at comparable salt molarities), the differences between the results obtained with the different iodide salts was negligible. The chloride salts of lithium, potassium, sodium, cesium, rubidium and choline were also examined (Table 4, Fig. 50C,D, 54A-D). Although the toxicity of HD treated in lithium chloride and sodium chloride buffers was somewhat increased compared to the other salts, the differences were not as dramatic as between anionic species. Similar trends were obtained when divalent chloride salt buffers were used as the HD treatment buffers (Fig. 56). The toxicity of HD increased as the concentration of calcium chloride or magnesium chloride was increased, with the former salt being more effective in restoring the toxicity of HD to those obtained in routine culture medium.

The protective effect of different classes of chloride ion channel inhibitors against HD toxicity was examined. The potent chloride ion channel inhibitors chlorotoxin and IAA-94 were ineffective in protecting against HD toxicity (Fig. 57). However, the chloride ion channel inhibitor DIDS showed protective efficacy in both F-12 culture medium, as well as in 130 mM sodium chloride treatment buffer (Fig. 58). In culture medium, protection was modest, but substantial at 1.0 mM DIDS. In contrast, significant protection was obtained against HD at 400 μM DIDS that increased to greater than 500 % at 1.0 mM DIDS.

The effect of NaCl concentration on the hydrolysis of HD was examined (Fig. 59). Varying concentrations of HD (50 – 800 μM) were dissolved in 32.5, 65.0 or 130 mM NaCl buffer and at different time intervals (2 – 60 min), CHO-K1 cells were exposed to these solutions. One hr post-exposure, the cultures were refed with culture medium and 23 hr later cell viability was examined. With each buffer, the toxicity of HD (as expressed by LC_{50} values) decreased exponentially with time. However, the rate of

decay of HD toxicity was virtually identical in the three buffers as evidenced by the parallel plots of log LC_{50} versus time. The derived half-lives of HD in the different buffer solutions (mean of three experiments) were 24.1 min (32.5 mM NaCl), 21.2 min (65.0 NaCl) and 22.3 min (130 mM NaCl).

Table 4. Effect of ionic environment on HD toxicity in CHO-K1 cells.*

	F^-	Cl^-	Br^-	I^-	Aspartate$^-$	Gluconate$^-$	Glutamate$^-$	Thiocyanate$^-$
Li^+	-	20.0 +/- 1.0	-	1.90 +/- 1.3	-	-	-	-
K^+	37.9 +/- 7.0	30.5 +/- 5.1	12.0 +/- 2.3	0.7 +/- 0.1	16.0 +/- 0.7	> 150.0	139.5 +/- 0.7	139.5 +/- 10.0
Na^+	> 65.0	10.8 +/- 2.9	17.4 +/- 0.9	0.7 +/- 0.1	18.0 +/- 8.3	> 150.0	> 150.0	> 150.0
Rb^+	-	31.8 +/- 2.7	-	3.9 +/- 1.2	-	-	-	-
Cs^+	-	26.9 +/- 0.7	-	0.7 +/- 0.2	-	-	-	-
Choline$^+$	-	32.9 +/- 5.9	-	-	-	-	-	-

* The data reflect mM EC_{50} values, where the "effect" is defined as the difference between the toxicity of HD in sucrose buffer (almost no toxicity) and its toxicity in physiological culture medium.

The effects of HD on intracellular chloride concentration was examined by loading CHO-K1 cells with the dye indicator MEQ. This fluorescence of this dye is quenched with increasing concentrations of chloride. As can be seen in Fig. 60, HD had little or no effect whether the incubations were carried out in defined sucrose, sodium chloride or sodium iodide buffers.

Figure 61 shows the effect of varying pH on the toxicity of HD when the incubations were carried out in culture medium. When the cultures were exposed to HD at a pH close to that of physiological pH (pH 7.5), the LC_{50} was 143.1 μM +/- 9.0 μM. HD was only slightly more toxic when the treatments were carried out in medium at acidic pH. In contrast, the toxicity of HD was dramatically reduced as the treatments were carried out in medium at pH greater than 8.5, so that at pH 9.5, HD was almost four times less toxic (LC_{50} = 593.7 μM +/- 53.7 μM). The effect of pH on the hydrolysis of HD was examined (Fig. 62). Varying concentrations of HD (50 – 800 μM) were dissolved in medium adjusted to pH 7.5 or pH 9.5 and at different time intervals (2 – 60 min), CHO-K1 cells were exposed to these solutions. One hr post-exposure, the cultures were refed with fresh culture medium and 23 hr later cell viability was examined. With each buffer, the toxicity of HD (as expressed by LC_{50} values) decreased exponentially with time. However, the rate of decay of HD toxicity was similar at both pH's as evidenced by the parallel plots of log LC_{50} versus time. The derived half-life of HD in pH 7.5 medium (mean of three experiments) was 20.3 min in pH 7.5 medium and 22.0 min in pH 9.5 medium.

DISCUSSION

The effect of ionic environment on P2 receptor function has been extensively studied in recent years and it is now well established that the action of ATP at the P2 receptor is largely determined by the presence of monovalent cations. Thus, in human lymphocytes, the response to ATP is enhanced when NaCl is replaced by KCl, choline chloride or N-methyl-D-glucamine chloride (Wiley *et al.*, 1992), while in murine macrophages a similar increase in the ability of ATP to stimulate phospholipase D is seen when NaCl is replaced with KCl or LiCl (Dubyak and El-Moatassim, 1993). A more recent study (Michel *et al.*, 1999) in HEK293 cells examined the effect of cations, as well as pH on $P2X_7$ receptor function. They found that the potency of BzATP was 19 times higher in NaCl-free buffer than in 140 mM NaCl containing buffer. Replacement of the sodium ion with either potassium of choline decreased the effect of the chloride salt.

They also found that receptor function was optimal at pH 7.5, declining at pH values below 6.5 or above 8.5.

Ironically, the effects of ionic environment on the toxicity of HD were diametrically opposed to those on P2 receptor function and resultant ATP potency/toxicity. Thus, in contrast to ATP, HD was virtually non-toxic in non-ionic buffer, and regained its toxicity (relative to that in culture medium) in a concentration-response fashion only as the NaCl concentration was increased. The chloride salt of lithium was about half as effective in rendering HD toxic, while potassium, rubidium, cesium and choline salts were equipotent and approximately one third as effective. Evidence that the anionic component of the salts was, in fact the primary determinant in the resultant toxicity of HD (as opposed to the cation), were the results obtained with iodides. All five salts of iodide were approximately equal in potency and rendered the toxicity of HD a log order of magnitude more toxic than in the sodium salts. Thus, the effects on HD toxicity were not related to P2 receptor function and instead, appeared to be due to perturbations of chloride ion activity. We thus screened several classes of chloride ion inhibitors for protective effects against HD. Although IAA-94 and chlorotoxin were not effective, the prototypical chloride ion channel inhibitor DIDS was moderately protective against HD when the incubations were carried out in culture medium. However, this protection was much more dramatic when the incubations were carried out in defined 130 mM NacL buffer; DIDS was significantly protective at concentrations as low as 400 μM, and gave greater than 500% protection at 1.0 mM. With this compelling evidence that the toxicity of HD was mediated through its effect on chloride ion channel activity, studies were next carried out to characterize these effects using the fluorescent dye MEQ. This fluorescence of this dye is quenched in a concentration related manner with chloride ion, and the intracellular chloride ion concentration of cells loaded with this dye can be quantitated. Unexpectedly, HD had little or no effect on MEQ fluorescence, whether the incubations were carried out in defined sucrose, sodium chloride or sodium iodide buffers. Thus, it does not appear that HD is exerting its toxicity through the modulation of chloride ion activity.

At this point it was tempting to ascribe the ionic effects on HD toxicity to alterations in the rate of HD hydrolysis by the chloride ion. The hydrolysis of HD is reversible and should be dependent on the chloride ion concentration of the environment (cited in Papirmeister *et al.*, 1991). To determine the half-life of the "active or toxic" species of HD, solutions of varying HD concentrations (50 – 800 μM) were made up in different NaCl buffers (32.5 – 130 mM). At varying time intervals (2 – 60 min) after HD solvation, aliquots of the solutions were used to treat cultures. One hr post-exposure, the HD treatments were replaced with medium and cell viability was assessed 32 hr later. If the rate of hydrolysis is playing a role in determining HD toxicity in these buffers, then the half-life of HD should reflect the significant difference in HD toxicity observed in these buffers. This in fact, was not the case. Although the LC_{50} of HD in 32.5 mM sodium chloride was approximately three times higher than in 130 mM sodium chloride, the log LC_{50} versus time plots were parallel and the derived half-lives for HD in these solutions were very similar. Clearly, differences in HD hydrolysis could not account for the dramatic differences seen in HD toxicity in these buffers.

The effects of varying pH on HD toxicity were also dramatic, and very different from those on ATP potency. In contrast to the pH dependency of ATP, where P2 receptor function is optimal at physiological pH and decreases at either acidic or basic pH, HD toxicity changed relatively modestly from pH 5.0 to pH 8.0 and then declined precipitously as the pH became more basic. This pH dependence is somewhat unusual from a physiological standpoint, and once again, it is tempting to speculate that modulating pH changes the hydrolysis rate of HD in solution. Similar half-life experiments were carried out to those described above with the sodium chloride buffers and once again, the rate of HD hydrolysis did not appear to play a role in determining toxicity. The half-lives of HD in medium adjusted to pH 7.5 or pH 9.5 were virtually identical, even though the toxicity of HD in these solutions is dramatically different.

At this point we do not how alterations in the ionic environment modulate the toxicity of HD. Although the use of seemingly non-physiological buffers makes the interpretation of results problematic, the use of these types of buffers has been well documented in ion channel research, although the justification for their use, especially

with respect to P2 receptor function, has generally been that during conditions of ischemia, ionic gradients collapse and potassium, sodium, chloride and calcium levels are altered so that P_2X_7 receptor function is enhanced. During these conditions HD toxicity would be decreased, perhaps as a result of a protective mechanism against other (natural) toxicants that share some traits with HD.

In summary, we report that the toxicity of HD is profoundly dependent on its ionic environment and present strong evidence that this dependence is biochemical in nature. These findings may be of importance in the future in assisting in the identification and characterization of the elusive mechanism of HD toxic action.

KEY RESEARCH ACCOMPLISHMENTS

The studies reported here clearly demonstrated that HD caused both apoptosis and necrosis in a wide variety of cell types. The proportion of each type of cell death was dependant to some degree on the concentration of HD to which the cells had been exposed. All of the hallmarks related to apoptosis appear to be present in HD induced toxicity

HD induced cell death was correlated with several biochemical changes such as caspase activation. However, manipulation of caspases or proteasomes was not sufficient to significantly alter HD induced toxicity.

It was also clear that HD induced activation of caspase-3 appeared to be necessary for subsequent activation of an important DNA'ase following the cleavage of CAD/ICAD.

Cell death following activation of the ubiquitous P_2X_7 receptor is dependent on the ionic environment suggesting that the receptor is activated to induce cell death in vivo in states of reduced ionic gradients at the cell membrane such as those proposed to occur in anoxic states.

HD leads to a variety of calcium related events such as an increase in the intracellular calcium concentration. However, as with several HD induced events a direct causative role of calcium in HD induced cell death could not be clearly demonstrated.

A membrane bound cytolytic complex consisting of two receptor sites linked to a common cytolytic pore was demonstrated in CHO-K1 cells. Although we could not demonstrate effects of HD on this complex it is felt that it will provide future avenues for important research into both apoptotic and necrotic mechanisms of cell death. These studies are ongoing

Several studies have clearly indicated an important role for the ionic environment in HD induced cell death and cell death in general.

Inhibition of the P_2X_7 ATP receptor did not inhibit HD induced cell toxicity but did control the route by which cell death was effected with respect to apoptoisis / necrosis.

CONCLUSIONS

The work reported in this document has led to several interesting and significant findings concerning the effects of HD on cells and cell biochemistry. However, many of these studies have also led to considerable frustration since HD was found to induce a wide variety of changes in just about all of the morphological and biochemical events which we undertook to study. Establishing cause and effect relationships between the easily observable biochemical events induced by HD, and the manipulation of these events in the hope to effect dramatic alterations in its toxicity proved to be difficult.

In the first section of the report it was clearly obvious that HD exposure to a wide variety of cells led to apoptosis. Apoptosis is well known to be the result of a cascade of events, including the elevation of intracellular calcium levels, the activation of certain caspases and DNA'ases, the uptake of vital dyes and in many cases the activation of cell surface receptors such as P_2X_1 and P_2X_7 receptors. We were able to demonstrate that HD resulted in many of these, what might be termed, causative events. For example, HD exposure resulted in increased intracellular calcium levels, described here and previously by other groups, induction of caspase-3 and subsequent activation of an important DNA'ase. However manipulation of the calcium increase using different tools (ie., blocking agents) and the reversal of HD induced caspase induction or DNA'ase activation, did not result in an alteration of cell toxicity as one would have predicted if these events were causative. In some cases such manipulation attenuated apoptosis, but merely shifted the primary mode of cell death to a necrotic one. Similarly, certain cells expressing cytotoxic ATP receptors were shown to undergo apoptosis following exposure to ATP analogues or to HD. Under either stimulus, the cells expressed increased calcium uptake, activation of intracellular caspases, endonucleases and peroxidases and interleukin release. Inhibition of the receptors by receptor antagonists, at best shunted the cell death from apoptosis to necrosis but did not affect overall toxicity.

During the course of our studies we identified a membrane bound complex consisting of two receptors that upon activation, caused the opening of a cytolytic pore. This resulted in the accumulation of a vital dye and also a biochemical cascade reminiscent of that induced by HD. However promising this discovery appeared to be

with respect to HD toxicity, HD appeared to have no direct effect on any of the components of this complex, nor did it potentiate the effects of the agonists at these sites. Finally, our early difficulties during these studies, where the extreme importance of cationic environment on ATP toxicity was demonstrated, has led us to findings that may have importance in the future. In contrast to ATP, where toxicity could *only* be detected in buffers with low cation concentration, HD elicited virtually no toxicity when CHO-K1 cultures were exposed in a defined sucrose, low salt buffer environment. This discovery prompted us to examine the dependence of HD on ionic environment in more detail. We found that the toxicity of HD is profoundly dependent specifically on the anionic environment in which the cells are placed, as well as the pH. The logical explanation to the anionic dependence of HD toxicity is that increasing halide concentration pushes the chemical hydrolysis reaction of HD to the left, thus altering HD half-life and the resultant toxicity. Our studies showed that the half-life of HD in 32.5, 65.0 or 130 mM sodium chloride was virtually identical, suggesting that the ionic dependence of HD was biochemical in nature. Studies using fluorescent dyes also showed that the ionic dependence of HD was not related to perturbations in intracellular chloride ion concentrations. It appears that HD exerts its toxicity through a biochemical site/mechanism that is sensitive to ionic environment.

REPORTABLE OUTCOMES

Lundy, P.M., Hamilton, M.G., Mi, L., Gong, W., Vair, C., Sawyer, T.W. and Frew, R. (2002). Stimulation of Ca2+ influx through ATP receptors on rat brain synaptosomes: Identification of functional P2X7 receptor subtypes. *British Journal of Pharmacology* **135**, 1616-1626.

Gong, W., Mi, L., Nelson, P., Hamilton, M.G., Lundy, P.M. and Sawyer, T.W. Sulphur mustard induces apoptosis in diverse cell types. *Journal of Applied Toxicology* (Accepted with revisions).

Lundy, P.M., Nelson, P., Mi, L., Frew, R., Vair, C. and Sawyer, T.W. (2002). Factors controlling cell death through activation of a $P2X_7$ /maitotoxin activated common cytolytic pore in CHO-K1 cells. *European Journal of Pharmacology* (submitted for publication).

Sawyer, T.W., Lundy, P.M., Mi, L., Nelson, P., Martin, L., Ford, B. and Bjarnason, S. Role of calcium in sulphur mustard induced apoptotic cell death. (In preparation).

Sawyer, T.W., Ford, B., Bjarnason, S., Vair, C. and Nelson, P. Effect of ionic environment on sulphur mustard toxicity. (In preparation).

Mi, L., Sawyer, T.W. and Lundy, P.M. Induction of apoptosis by sulphur mustard through activation of ICAD/CAD in J774 cells (In preparation).

Gong, W., Mi, L., Sawyer, T.W., Lundy, P. and Hamilton, M. Sulphur Mustard Induced Apoptosis in the CHO-K1 Cell Line. The Role of Caspase Inhibitors. Cancer Genetics and Tumor Suppression Genes, Cold Springs Harbour, NY, 2000.

Gong, W., Mi., L., Sawyer, T.W., Lundy, P. and Hamilton, M.G. Sulphur Mustard Induced Apoptotsis in CHO-K1 Cells. Bioscience Review, Hunt Valley, MD, 2000.

Mi, L., Gong, W., Lundy, P., Sawyer, T.W. and Hamilton, M.G. Effect of Calcium Manipulation on the Toxicity of Sulphur Mustard in J774 Cells. Bioscience Review, Hunt Valley, MD, 2000.

Gong, W., Mi, L., Nelson, P., Hamilton, M., Lundy, P. and Sawyer, T.W. Sulphur Mustard Induced Cell Death in Diverse Cell Types. Bioscience Review, Hunt Valley, MD, 2000.

Lundy, P.M., Nelson, P., Mi, L., Gong, W., Frew, R., Shei, Y. and Sawyer, T.W., Factors controlling cell death through activation of a cytolytic pore common to P2X7 receptors and a maitoxin activated ion channel in CHO-K1 cells. Bioscience Review, Hunt Valley, MD, 2002.

Lundy, P.M., Mi, L., Hamilton, M.G., Nelson, P., Gong, W. and Sawyer, T.W., Cell death following activation of a maitoxin activated cation channel or the ATP/P2X7 receptor stimulated cytolytic pore in CHO-K1 cells. Studies with HD. Bioscience Review, Hunt Valley, MD, 2002.

REFERENCES

Alzola, E., Chaib, N., Pochet, S., Kabre, E., Marino, A. and Dehaye, J-P. (2001). Modulation by propranolol of the uptake of ethidium bromide by rat submandibular acinar cells exposed to a $P2X_7$ agonist or to maitotoxin. *Cellular Signaling* **13**, 465-473.

Barry, M.A., and Eastman, A. (1993). Identification of deoxyribonuclease II as an endonuclease involved in apoptosis. *Archives of Biochemistry and Biophysics* **300**, 440-450.

Brake, A.J., Wagenbach, M.J. and Julius, D. (1994). New structural motif for ligand-gated ion channels defined by an ionotropic ATP receptor. *Nature* **371**, 519-523.

Brune, B., von Knethen, A. and Sandau, K.B. (1999). Nitric oxide (NO): An effector of apoptosis. *Cell Death and Differentiation* **6**, 969-975.

Bruno, L., Lassota, P., Giaretti, W., and Darzynkiewicz, Z. (1992). Apoptosis of rat thymocytes triggered by prednisolone, camptothecin, or teniposide is selective to G_0 cells and is prevented by inhibitors of proteases. *Oncology Research* **14**, 29-35.

Burnstock, G. (1998). History of extracellular nucleotides and their receptors. *In: The P_2 nucleotide receptors*. Editors Turner, J.T., Weisman, G.A. and Fedan J.S. Humana Press, Totawa, N.J.

Burnstock., G. (1999). Current status of purinergic signalling in the nervous system. In P. Illes & H. Zimmerman (Eds.). Progress in Brain Research. 120, Nucleotides and their receptors in the nervous system. Amsterdam, Elsevier, pp. 3-10.

Chvatchko, Y., Valera, S., Aubry, J.-P., Renno, T., Buell, G., and Bonnefoy, J.-Y. (1996). The involvement of an ATP-gated ion channel, P_2X_1 in thymocyte apoptosis. *Immunity* **5**, 275-283.

Cohen, G.M. (1997). Caspases: the executioners of apoptosis. *Biochemistry Journal* **326**, 1-16.

Coutinho-Silva, R., Persechini, P.M., da Cunha Bisaggio, R., Perfettini, J.-L., Torres de sa Neto, A.C., Kanellopoulos, J.M., Motta-Ly, I, Dautry-Varsat, A. and Ojcius, D.M. (1999). P_{2z}/P2x_7 receptor-dependent apoptosis of dentritic cells. *American Journal of Physiology* **276 (Cell Physiology 45)**, C1139-C1147.

Cui, S., Reichner, J.S., Mateo, R.B. and Albina, J.E. (1994). Activated murine macrophage induced apoptosis in tumor cells through nitric oxide-dependent mechanisms. *Cancer Research* **54**, 2462-2467.

Dabrowska, M.I., Becks, L., Lelli, J.L., Levee, M.G. and Hinshaw, D.B. (1996). Sulfur mustard induces apoptosis and necrosis in endothelial cells. *Toxicology and Applied Pharmacology* **141**, 568-583.

Dacre, J.C. and Goldman, M. (1996). Toxicology and pharmacology of the chemical warfare agent sulfur mustard. *Pharmacology Review* **48**, 289-325.

Deuchars, S.A., Atkinson, L., Brooke, R.E., Musa, H., Milligan, C.J., Batten, T.F.C., Buckley, N.J., Parson, S.H. and Deuchars, J. (2001). Neuronal P2X_7 receptors are targeted to presynaptic terminals in the central and peripheral nervous systems. *Journal of Neuroscience* **15**, 7143-7152

Di Virgilio, F. (1995). The P2 purinoceptor: an intriguing role in immunity inflammation and cell death. *ImmunologyToday* **16**, 524-528.

Dowd, D.R., (1995). Calcium regulation of apoptosis. In: Advances in Second Messenger and Phosphoprotein Research. Vol. 30, Ed: A.R. Means, Raven Hill Press Ltd., New York.

Dubyak, G.R. and el-Moatassim, C. (1993). Signal transduction via P2 purinergic receptors for extracellular ATP and other nucleotides. *American Journal of Physiology* **265**, C577-C606.

Duke, R.C. and Cohen, J.J. (1992). Morphological and biochemical assays of apoptosis. In: *Current Protocols in Immunology*, **Suppl. 3.17**, 1-16.

Dunkley, P.R., Heath, J.W., Harrison, S.M., Jarviem, P.E., Glenfield, P.J. and Rostas, J.A.P. (1998). A rapid Percoll gradient procedure for isolation of synaptosomes directly from an "S1" fraction: homogeneity and morphology of subcellular fractions. *Brain Research* **441**, 59-71.

Enari, M., Sakahira, H., Yokoyama, H., Okawa, K., I wamatus, A., and Nagata, S. (1998). A caspase-activated DNase that degrades DNA during apoptosis, and its inhibitor ICAD. *Nature* **391**, 43-50.

Estacion, M. and Schilling, W.P. (2001). Maitotoxin-induced membrane blebbing and cell death in bovine aortic endothelial cells. *BMC Physiology* **1**, 2.

Evans, R.J., Derkach, V. and Surprenant, A. (1992). ATP mediates fast synaptic transmission in mammalian neurons. *Nature* **357**, 503-505.

Fawthrop, D.J., Boobis, A.R. and Davies, D.S. (1991). Mechanisms of cell death. *Archives of Toxicology* **65**, 437-444.

Fearnhead, H.O., Rivett, A.J., Dinsdale, D. and Cohen, G. (1995). A pre-existing protease is a common effector of thymocyte apoptosis mediated by diverse stimulae. *FEBS Letters* **357**, 242-246.

Ferrari, D., Los, M., Bauer, M.K.A., Vandenabeele, P., Wesselborg, S. and Schulze-Osthoff, K. (1999). P2Z purinoceptor ligation induces activation of caspases with distinct roles in apoptotic and necrotic alterations of cell death. *FEBS Letters* **447**, 71-75.

Fipipski,J., Leblanc,J.,Youdale, T., Sikorska, M., and Walker, P.R. (1990). Periodicity of DNA folding in higher order chromatin structures. *EMBO Journal* **9**, 1319-1327.

Fraser, A., and Evan, G. (1996). A license to kill. *Cell* **85**, 781-784.

Gong, W., Mi, L., Nelson, P., Hamilton, M.G., Lundy, P.M. and Sawyer, T.W. Sulphur mustard induces apoptosis in diverse cell types. *Journal of Applied Toxicology* (Accepted with revisions).

Gu, J., Dong, R.P., Zhong, C., Mclaughlin, D.F., Wu, M.X., and Schlossman, S.F. (1999). Functional interaction of DFF35 and DFF45 with caspase-activated DNA fragmentation nuclease DFF40. *Journal of Biological Chemistry* **274**, 20759-20762.

Halenbeck, R., MacDonald, H., Roulston, A., Chen, T.T, Contoy, L., and Williams, L.T. (1998). CPAN, a human nuclease regulated by the caspase-sensitive inhibitor DFF45. *Current Biology* **8**, 537-540.

Hamilton, M.G., Dorandeu, F.M., McCaffery, M., Lundy, P.M. and Sawyer, T.W. (1998). Modification of cytosolic free calcium concentrations in human keratinocytes after sulphur mustard exposure. *Toxicology in Vitro* **12**, 365-372.

Hirsch, T., Dallaporta, B., Zamzuni, N., Susin, S.A., Ravagnan, L., Marzo, I., Brenner, C. and Kroemer, G. (1998). Proteasome activation occurs at an early, premitochondrial step of thymoctye apoptosis. *Journal of Immunology* **161**, 35-40.

Hua, A., Daniel, R., Jasseron, M.P. and Thiriot, C. (1993). Early cytotoxic effects induced by bis-chloroethyl sulphide (sulphur mustard): $[Ca^{2+}]_I$ rise and time-dependent inhibition of B77 fibroblast serum response. *Journal of Applied Toxicology* **13**, 161-168.

Humphreys, B. and Dubyak, G.R. (1996). Induction of the P2Z/ $P2X_7$ nucleotide receptor and associated phospholipase D activity by lipopolysaccharide and IFN-γ in the human THP-1 monocyte cell line. *Journal of Immunology* **157**, 5627-5637.

Humphreys, B.D., Rice, J., Kertesy, S.B. and Dubyak, G.R. (2000). Stress-activated protein kinase/JNK activation and apoptotic induction by the macrophage P2X7 nucleotide receptor. *Journal of Biological Chemistry* **275**, 26792-26798.

Kass, G.E.N. and Orrenius, S. (1999). Calcium signaling and cytotoxicity. *Environmental Health Perspectives* **107**, 25-35.

Kutty, R.K., Singh, Y., Santostasi, G. and Krishna, G. (1988). Maitotoxin-induced cell death involving loss of cell ATP following influx of calcium. *Toxicology and Applied Pharmacology* **101**, 1-10.

Liu,X., Li, P., Widlak, P., Zou, H., Luo, X., Garrard, W.T., and Wang, X. (1998). The 40-kDa subunit of DNA fragmentation factor induces DNA fragmentation and chromatin condensation during apoptosis. *Proceedings of the National Academy of Science (USA)* **95**, 8461-8466.

Liu,X., Li, P., Zou, H., Widlak, P., Garrard, W.T., and Wang, X. (1999). Activation of the apoptotic endonuclease DFF40 (caspase-activated DNase or nuclease). Oligomerization and direct interaction with histone H1. *Journal of Biological Chemistry* **274**, 13836-13840.

Lundy, P.M., Hamilton, M.G., Mi, L., Gong, W., Vair, C., Sawyer, T.W. and Frew, R. (2002). Stimulation of Ca^{2+} influx through ATP receptors on rat brain synaptosomes:

identification of functional $P2X_7$ receptor subtypes. *British Journal of Pharmacology* **135**, 1616-1626.

Lundy, P.M., Sawyer, T.W., Hand, B.T. and Frew, R. (1998). Effects of bis (2-chloroethyl) sulphide on ATP receptor-mediated responses in rat vas deferens: Possible relationship to cytotoxicity. *Journal of Pharmacological and Experimental Therapeutics* **285**, 299-306.

Martinez-Francois, J.R., Morales-Tlalpan, V. and Vaca, L. (2002). Characterization of the maitotoxin-activated cationic current from human skin fibroblasts. *Journal of Physiology* **538**, 79-86.

Meier, H.L. and Millard, C.B. (1998). Alterations in human lymphocyte DNA caused by sulfur mustard can be mitigated by selective inhibitors of poly(ADP-ribose) polymerase. *Biochim. Biophys. Acta* **1404**, 367-376.

Michaelson, S. (2000). DNA fragmentation pattern induced in thymocytes by sulphur mustard. *Chemico-Biological Interactions* **125**, 1-15.

Michel, A.D., Chessell, I.P. and Humphrey, P.P.A. (1999). Ionic effects on human recombinant $P2X_7$ receptor function. *Naunyn-Schmiedeberg's Archives of Pharmacology* **359**, 102-109.

Michel, A.D., Grahames, C.B.A. and Humphrey, P.P.A. (1996). Functional characterization of P2 receptors in PC12 cells by measurement of radiolabelled calcium influx. *Naunyn-Schmiedeberg Archives of Pharmacology* **354,** 562-571.

Mol, M.A.E. (1994). Does sulfur mustard cause any changes in the cytoplasmic free calcium levels of human epidermal keratinocytes. In *Proceedings of the NATO RSG-3 Panel VIII meeting.* Munich, Germany. pp. 25-28.

Mol, M.A.E. and Smith, W. (1996). Ca^{2+} homeostasis and Ca^{2+} signalling in sulphur mustard-exposed normal human epidermal keratinocytes. *Chemico-Biological Interactions* **100**, 85-93.

Morales-Tlalpan, V.and Vaca, L. (2002). Modulation of the maitotoxin response by intracellular and extracellular cations. *Toxicon* **40**, 493-500.

Morris, M.E. and Trippenbach, T, (1993). Changes in extracellular $[K^+]$ and $[Ca^{2+}]$ induced by anoxia in neonatal rabbit medulla. *American Journal of Physiology* **264**, R761-R769.

Murgia, M., Hanau, S., Pizzo, P., Rippa, M. and di Virgilio, F. (1993). Oxidized ATP, an irreversible inhibitor of the macrophage purinergic P2Z receptor. *Journal of Biological Chemistry* **268**, 8199-8203.

Orrenius, S., McConkey, D.J., Bellomo, G. and Nicotera, P. (1989). Role of Ca^{2+} in toxic cell killing. *Trends in Pharmacological Sciences* **10**, 281-285.

Orrenius, S. and Nicotera, P. (1987). Biochemical mechanisms of oxidative liver cell injury. *Bulletin of European Physiopathology and Respiration* **23**, 291-295.

Owens, G.P., Hahn, W.E., and Cohen, J.J. (1991). Identification of mRNA associated with programmed cell death in immature thymocytes. *Molecular and Cellular Biology* **11**, 4177-4188.

Papirmeister, B., Feister, A.J., Robinson, S.I. and Ford, R.D. (1991). *Medical Defense Against Mustard Gas: Toxic Mechanisms and Pharmacological Implications.* CRC Press, Boca Raton, Fl.

Peitsch, M.C., Muller, C. and Tschopp, J. (1993). DNA fragmentation during apoptosis is caused by frequent single-strand cuts. *Nucleic Acids Research* **18,** 4206-4209.

Pizzo, P., Zanovello, P., Bronte, V. and Di Virgilio, F. (1991). Extracellular ATP causes lysis of mouse thymocytes and activates a plasma membrane ion channel. *Biochemical Journal* **274**, 139-144.

Ralevic,V. and Burnstock., G. (1998). Receptors for purines and pyrimidines. Pharmacolocigal Reviews **50**, 413-492.

Ray, R., Benton, B.J., Anderson, D.R., Byers, S.L. and Petrali, J.P. (1998). Intervention of sulfur mustard (HD) toxicity by down regulation of cell proliferation and metabolic rates. In *Proceedings of the 1998 Medical Defence Bioscience Review.* pp. 123.

Ray, R., Benton, B.J., Anderson, D.R., Byers, S.L., Shih, M.L. and Petrali, J.P. (1996). The intracellular free calcium chelator BAPTA prevents prevents sulfur mustard toxicity in cultured normal human epidermal keratinocytes. In *Proceedings of the 1996 Medical Defense Bioscience Review.* pp. 1021-1027.

Ray, R., Benton, B.J., Broomfield, C.A., Anderson, D.R., Byers, S.L., Petrali, J.P. and Bhat, K.R. (1997). Calcium-dependent mechanisms of sulfur mustard toxicity and its protection. In *Proceedings of NATO RSG-3 Panel VIII meeting.* McLean, VA. pp. 479-486.

Ray, R., Legere, R.H., Majerus, B.J. and Petrali, J.P. (1995). Sulfur mustard-induced increase in intracellular free calcium level and arachidonic acid release from cell membrane. *Toxicology and Applied Pharmacology* **131**, 44-52.

Ray, R., Majerus, B.J. and Broomfield, C.A. (1994). Effect of sulfur mustard on intracellular free calcium level and membrane fluidity in normal human epidermal keratinocytes. *Canadian Journal of Physiology and Pharmacology* **72** (Suppl. 1), 22.3.

Renvoize, C., Biola, A., Pallardy, M. and Breard, J. (1998). Apoptosis: Identification of dying cells. *Cell Biology and Toxicology* **14**, 111-120.

Richter, C. (1998). Nitric oxide and its congeners in mitochondria: Implications for apoptosis. *Environmental Health Perspectives* **106, Suppl. 5**, 1125-1130.

Rosenthal, D.S., Simbulan-Rosenthal, C.M.G., Iyer, S., Spoonde, A., Smith, W., Ray, R. and Smulson, M.E. (1998). Sulfur mustard induces markers of terminal differentiation and apoptosis in keratinocytes via a Ca^{2+}-calmodulin and caspase dependent pathway. *Journal of Investigative Dermatology* **111**, 57-70.

Sakahira, H., Enari, M., and Nagata, S. (1998). Cleavage of CAD inhibitor in CAD activation and DNA degradation during apoptosis. *Nature* **391**, 96-99.

Sawyer, T.W. (1998a). Characterization of the protective effects of L-nitroarginine methyl ester (L-NAME) against the toxicity of sulphur mustard *in vitro*. *Toxicology* **131**, 21-32.

Sawyer, T.W. (1998b). Modulation of sulphur mustard toxicity by arginine analogues and related nitric oxide synthase inhibitors *in vitro*. *Toxicological Sciences* **6**, 112-123.

Sawyer, T.W. (1999). Synergistic protective effects of selected arginine analogues against sulphur mustard toxicity in neuron culture. *Toxicology and Applied Pharmacology* **155**, 169-176.

Sawyer, T.W. and Hamilton, M.G. (2000). Effect of intracellular calcium modulation on sulfur mustard cytotoxicity in cultured human neonatal keratinocytes. *Toxicology In Vitro* 14, 149-157.

Sawyer, T.W., Hancock, J.A. and D'Agostino, P.A. (1998). L-Thiocitrulline: A potent protective agent against the toxicity of sulphur mustard **in** *vitro. Toxicology and Applied Pharmacology* **151**, 340-346.

Sawyer, T. W., Lundy, P.M. and Weiss, M.T. (1996). Protective effect of an inhibitor of nitric oxide synthase on sulphur mustard toxicity in vitro. *Toxicology and Applied Pharmacology* **141**, 138-144,

Sawyer, T. W. and Risk, D. (2000). Effects of selected arginine analogues on sulphur mustard toxicity in human and guinea skin keratinocytes. *Toxicology and Applied Pharmacology* **163**, 75-83.

Schaeffer,P., Lugnier,C. and Stoclet, J-C. (1991). Interactions of calmodulin antagonists with calcium antagonists binding sites. *European Journal of Pharmacoogy* **206** 325-332

Schilling, W.P., Sinkins, W.G. and Estacion, M. (1999a). Maitotoxin activates a nonselective cation channel and a P2Z/P2X7-like cytolytic pore in human skin fibroblasts. *American Journal of Physiology* **277**, C755-C765.

Schilling, W.P., Wasylyna, T., Dubyak, G.R., Humphreys, B.D. and Sinkins, W.G. (1999b). Maitotoxin and P2Z/P2X7 purinergic receptor stimulation activate a common cytolytic pore. *American Journal of Physiology* **277**, C766-C77.

Schulze-Lohoff, E., Hugo, C., Rost, S., Arnold, S., Gruber, A., Brune, B. and Sterzel, R.B. (1998). Extracellular ATP causes apoptosis and necrosis of cultured mesangial cells via P2Z/$P2X_7$ receptors. *American Journal of Physiology*, **275 (Renal Physiology 44)**, F962-F971.

Shinohara, K., Tomioka, M., Nakano, H., Tone, S., Ito, H. and Kawashima, S. (1996). Apoptosis induction resulting from proteasome inhibition. *Biochemistry Journal* **317**, 385-388.

Slee, E.A., Adrain, C., and Martin, S.J. (2001). Executioner caspase-3, 6, and 7 perform distinct, non-redundant roles during the demolition phase of apoptosis. *Journal of Biological Chemistry* **276**, 7320-7326.

Smith, K.J., Graham, J.S., Hamilton, T.A., Skelton, H.G., Petrali, J.P. and Hurst, C.G. (1997). Immunohistochemical studies of basement membrane proteins and proliferation and apoptosis markers in sulfur mustard induced cutaneous lesions in weanling pigs. *Journal of Dermatological Science* **15**, 173-182.

Song, S-L. and Chueh, S-H. (1996). Antagonistic effect of Na^{+} and Mg^{2+} on P_{2Z} purinoceptor-associated pores in dibutyryl cyclic AMP-differentiated NG108-15 cells. *Journal of Neurochemistry* **67**, 1694-1701.

Srinivasula, S.M., Ahmad, M., Fernandes-Alnemri, T., Litwack, G., and Alnemri, E.S. (1996). Molecular ordering of the Fas-apoptotic pathway: the Fas/APO-1 protease Mch5 is a CrmA-inhibitable protease that activates multiple Ced-3/ICE-like cysteine proteases. *Proceedings of the National Academy of Science (USA)* **93**, 14486-14491.

Steinberg, T.H., Newman, A.S., Swanson, J.A. and Silverstein, S.C. (1987). ATP^{4-} permeabilizes the plasma membrane of mouse macrophages to fluorescent dyes. *Journal of Biological Chemistry* **262**, 8884-8888.

Sun, J., Wang, Y-X. and Sun, M-J. (1998). Apoptosis and necrosis induced by sulfur mustard in Hela cells. *Acta Pharmacol. Sin.* **20**, 445-448.

Surprenant, A., Rassendren, F., Kawashima, E., North, R.A. and Buell, G. (1996). The cytolytic P2Z receptor for extracellular ATP identified as a P2X receptor ($P2X_7$). *Science* **272**, 735-737.

Taglialatela, M., Canzoniero, L.M.T., Fatatis, A., Di Renzo, G., Yasumoto, T. and Annunziato, L. (1990). Effect of maitotoxin on cytosolic Ca^{2+} levels and membrane potential in purified rat brain synaptosomes. *Biochim. Biophys Acta* **1026**, 126-132.

Valera, S., Hussy, N., Evans, R.J., Adami, N., North, R.A., Suprenant, A. and Buell, G. (1994). A new class of ligand-gated ion channel defined by a P2x receptor for extracellular ATP. *Nature* **371**, 516-519.

Virginio, C., Church, D., North, R.A. and Surprenant, A. (1997). Effects of divalent cations, protons and calmidazolium at the rat $P2X_7$ receptor. *Neuropharmacology* **36**, 1285-1294.

Virginio, C., MacKenzie, A., North, R.A. and Surprenant, A. (1999). Kinetics of cell lysis, dye uptake and permeability changes in cells expressing the rat $P2X_7$ receptor. *Journal of Physiology* **519**, 335-346.

Voresek, I. and Sykova, E. (1997). Ischemia-induced changes in the extracellular space diffusion parameters K^+, and pH in the developing rat cortex and corpus callosum. *Journal of Cerebral Blood Flow Metabolism* **17**, 191-203.

Weaver, V.M., Lach, B., Walker, P.R. and Sikorska, M. (1993). Role of proteolysis in apoptosis: Involvement of serine proteases in internucleosomal DNA fragmentation in immature thymocytes. *Biochemistry and Cell Biology* **71**, 488-500.

Wiley, J.S., Chen, J.R., Snook, M.S. Gargett, C.E. and Jamieson, G.P. (1996). Transduction mechanisms of P2Z purinoceptors. In: P2 Purinoceptors: Localisation, Function and Transduction Mechanisms (pp 149-165), Wiley, Chichester.

Wiley, J.S., Chen, J.R., Wiley, M.J. and Jamieson, G.P. (1992). The ATP^{4+} receptor-operated ion channel of human lymphocytes: inhibition of ion fluxes by ameloride analogues and by extracellular sodium ions. *Biochemistry and Biophysics* **292**, 411-418.

Willems J.L. (1989). Clinical management of mustard gas casualties. *Annals Medicinae Militaris Belgicae* **3**, 1-61.

Woo, M., Hakem, R., Soengas,M.S., Duncan, G.S., Shahinian, A., Kagi, D., Hakem,A., McCurrach, M., Kaufman, S.A., Senaldi, G., Howard, T., Lowe,S., and Mak, T.W. (1998). Essential contribution of caspase 3/CPP32 to apoptosis and its associated nuclear changes. *Genes Dev* 12, 806-819.

Zambon, A., Bronte, V., Di Virgilio, F., Hanau, S., Steinberg, T.H., Collavo, D. and Zanovello, P. (1994). Role of extracellular ATP in cell-mediated cytotoxicity: A study with ATP-sensitive and ATP-resistant macrophages. *Cellular Immunity* **156**, 458-467.

Zhao, X., Pike, B.R., Newcomb, J.K., Wang, K.K.W., Posmantur, R.M. and Hayes, R.L. (1999). Maitotoxin induces calpain but not caspase-3 activation and necrotic cell death in primary septo-hippocampal cultures. *Neurochemical Research* **24**, 371-382.

Zhang, J., Liu,X., Scherer, D.C., Boivin, G.P., Van Kaer, L., Wang,X., and Xu, M. (1998). Resistance to DNA fragmentation and chromatin condensation in mice lacking the DNA fragmentation factor 45. *Proceedings of the National Academy of Science (USA)* **95**, 12480-12485.

Zheng, L.M., Zychlinsky, A., Liu, C.C., Ojcius, D.M. and Young, J.D-E. (1991). Extracellular ATP as a trigger for apoptosis or programmed cell death. *Journal of Cellular Biology* **112**, 279-288.

FIGURE LEGENDS

Figure 1: Examination of the type of cell death induced by HD

Figure 2: HD induced apoptosis was studied from the theoretical point of view that the initial events in the apoptotic cascade were consistent with the activation of one or more membrane bound ATP cytolytic receptors. As the figure indicates, studies were carried out to determine whether receptor activation might result in the subsequent elevation of intracellular calcium, which in turn activated caspases or activated a definable DNA'ase leading to the usual hallmarks of apoptosis. In the course of these studies the important novel identification of ATP receptors in the brain was achieved, as was the identification and pharmacological description of a membrane bound cytolytic complex consisting of two calcium sensitive receptors and a common cytolytic pore.

Figure 3: Toxicity of HD in various cell types. Cultures of neurons (a), J774 cells and CHO-K1 cells (b) and keratinocytes (c) were treated with HD and cytotoxicity was assessed 24 h (neurons, CHO-K1, J774) or 48 h (keratinocytes) later using alamarBlue assay. Results represent a typical experiment utilizing the means of six wells per data point (n = 3).

Figure 4: HD induced DNA fragmentation in various cell types. Cell cultures were treated with varying concentrations of HD, the cells were harvested and then the DNA fragments were extracted and separated on 1.5 % agarose gels. DNA fragments from keratinocytes were first ampliflied using LM PCR prior to electrophoresis. Control cultures (C) showed no DNA fragmentation. HD treatment induced the DNA ladders characteristic of apoptotic cell death in neurons (a), J774 cells (b), CHO-K1 cells (c) and neonatal human skin keratinocytes (d).

Figure 5: HD induced elevation of soluble DNA in various cell types. Cellular DNA was labelled with tritiated thymidine prior to HD treatment and subsequent quantitation of DNA fragmentation. Results are the mean +/- standard deviation of three separate experiments and are normalized against controls. In human keratinocytes (a), CHO-K1 cells (b) and J774 cells (c) HD induced a concentration dependent increase in DNA fragmentation that plateaued at higher HD concentrations.

Figure 6: Detection of HD induced apoptotic cell death in cell culture by the TUNEL reaction. CHO-K1 cells and human skin keratinocytes were treated with HD and then assayed for apoptotic cell death using the TUNEL reaction and fluorescent microscopy (4a-c) or light microscopy (d-f), respectively. No apoptotic cells in vehicle treated control cultures (a,d) were detected. Concentration-dependent increases in fluorescein labeled nuclei were observed in CHO-K1 cells treated with 400 μM HD (b) and 600 μM HD (c) with condensed chromatin clearly visible. Similarly, brown apoptotic nuclei are visible in keratinocytes treated with 200 μM HD (e) and 400 μM HD (f).

Figure 7: Quantitation of HD induced apoptotic cell death in various cell types by the TUNEL assay. With the exception of neuronal cells, very few vehicle treated control cells were apoptotic. The percentage of apoptotic cells increased with HD concentration in human keratinocytes (a), chick neurons (b), CHO-K1 cells (c) and J774 cells (d). Results represent the mean +/- standard deviation of at least three separate experiments.

Figure 8: Morphology of HD treated thymocytes. Cells were treated with HD and then morphology was assessed using ethidium bromide and acridine orange. Control cells (a) show normal green nuclei while 50 μM HD induced the appearance of apoptotic nuclei (b, bright yellow/green condensed or fragmented chromatin). At higher HD concentrations (200

μM, c) the cell membrane loses its integrity and ethidium bromide enters the cell, staining the chromatin orange.

Figure 9: Quantitation of HD induced apoptosis/necrosis using morphological criteria. The effect on the morphology of human skin keratinocytes (a), chick neurons (b), CHO-K1 cells (c) and J774 cells (d) was assessed using acridine orange and ethidium bromide.

Figure 10: Detection of HD induced apoptotic cell death using Annexin V in CHO-K1 cells. Control cells (a) are generally negative. At 200 μM HD (b) the fluorescein labeled antibodies recognize the externalized phosphotidylserine residues that signify early stage apoptotic cell death and stain the cells green. At higher concentrations of HD (c, 400 μM), the cell membrane loses integrity and increasing numbers of cells are also stained with propidium iodide (red/brown colour) indicating necrosis.

Figure 11: Effect of proteasome inhibition on HD induced cytotoxicity in CHO-K1 cells. CHO-K1 cells were incubated with MG132 or lactacystin for 15 min prior to HD treatment. The cells were then allowed to incubate for a further 24 h after HD treatment. The viability of the cells was then assessed using the metabolic indicator dye alamarBlue. Neither MG132 nor lactacystin significantly modified HD induced cell death. Results represent the mean +/- standard error of the mean of three experiments.

Figure 12: Effect of proteasome inhibition on HD induced soluble DNA in CHO-K1 cells. CHO-K1 cells were incubated with MG132 or lactacystin for 15 min prior to HD treatment. The cells were then allowed to incubate for a further 6 h after HD treatment. DNA fragmentation was quantitated as described in Methods. Treatment of the cells with 400 μM HD resulted in an increase in soluble DNA of approximately 300-400%. Treatment with the proteasome inhibitors did not significantly alter HD induced DNA

fragmentation. Results represent the mean +/- standard error of the mean of three experiments.

Figure 13: Effect of proteasome inhibition on HD induced caspase-3 activity in CHO-K1 cells. CHO-K1 cells were incubated with lactacystin or MG132 15 min prior to HD treatment. The cells were then treated with HD and allowed to incubate for a further 6 h. Exposure of the cells to 400 μM HD alone resulted in an elevation of caspase-3 activity. Pretreatment of both control and HD treated cells with either inhibitor did not alter the expression of constitutive or induced caspase-3 activity. Results represent the mean +/- standard error of the mean of three experiments.

Figure 14: CHO-K1 cells were incubated with the general caspase inhibitor ZVAD-fmk for 15 min prior to HD treatment. The cells were then treated with HD and allowed to incubate for a further 6 h. Exposure of the cells with 400 μM HD resulted in an elevation of caspase-3 activity. Pretreatment of both control and HD treated cells with ZVAD-fmk resulted in a significant depression in both constitutive and induced caspase-3 activity. Results represent the mean +/- standard error of the mean of three experiments.

Figure 15: Effect of caspase inhibitors on HD induced cytotoxicity in CHO-K1 cells. CHO-K1 cells were incubated with either the general caspase inhibitor, ZVAD-fmk, or the specific caspase inhibitors, IEHD-CHO and LEHD-CHO for 15 min prior to HD treatment. The cells were then allowed to incubate for a further 24 h after HD treatment. The viability of the cells was assessed using the metabolic indicator dye alamarBlue. None of the caspase inhibitors altered HD toxicity. Results represent the mean +/- standard error of the mean of three experiments.

Figure 16: HD induced activation of caspase-3 and cleavage of the DNA'ase activator ICAD/CAD dimeric protein in J774 cells. A) Caspase-3 activity

was measured following exposure of J774 cells to HD treatment (100 μM for 2-4 hrs) by its proteolytic activity on DEVD-PNA substrate. Values represent mean + SEM from three independent experiments. Value for control experiments (no HD) was calculated using OD of HD free cells minus OD of blank control.

B) Cleavage of CAD/ICAD following HD exposure was examined by Western blotting assay using a rabbit anti-ICAD polyclonal antibody. Cleavage of the 45 kDa protein into two fractions; one of 20-30 kDa and one of less than 20 kDa was observed after 4 hrs. Cleavage was examined at the same time points following HD as in panel A. Lane 1, control; Lane 2, 2 hours post treatment; Lane 3, 3 hours post treatment; Lane 4, 4 hours post treatment.

C) Nuclease activity of the S-100 fraction from untreated cells with no added mouse nuclei (lane-1); S-100 fraction incubated with HD without mouse liver nuclei (lane-2); S-100 incubated with nuclei from untreated mouse liver (lane-3); S-100 incubated with mouse liver nuclei following HD treatment (lane 4) and nuclei alone in buffer from untreated mouse liver (lane 5).

Figure 17: Detection of apoptotic cell death of J774 cells at different times following HD treatment. A) Agarose gel electrophoresis of DNA extracted from J774 cells treated with HD (100 μM) at 2,3 and 4 hr. Lane 1, control (HD free); Lane 2, 2 hours post treatment; Lane 3, 3 hours post treatment; Lane 4, 4 hours post treatment. B) TUNEL assay of J774 cells in untreated J774 cells and 2, 3 and 4 hr (100 μM) following HD treatment. Cells were observed at 40x magnification using light microscopy. Cells undergoing apoptosis were identified as those showing brown/condensed nuclei amid counter staining. Bottom panel shows quantitative data based on TUNEL assay. Values (means+SEM) represent the results from three independent experiments. C) Accridine orange/ethidium bromide staining of J774

untreated cells (C) and 2,3 and 4 hours following HD treatment. Cells were observed at 20x --magnification using fluorescence microscope.

Figure 18: Expression of P2X1 and P2X7 receptor protein in CHO-K1 cells. Total RNA was extracted from rat thymocytes and RT-PCR carried out (methods). Photograph represents ethidium bromide stained PCR products specific for P2X7 and P2X1 receptor mRNA respectively, in rat thymocytes.

Figure 19: ATP mediated YOPRO uptake in thymocytes. Isolated rat thymocytes were incubated with YOPRO-1 in the presence of 0.0 mM ATP (A,B), 1.0 mM ATP (C,D) or 10 mM ATP (E,F). Dye uptake increased with ATP concentration. Images A,C and E: brightfield. Images B, D and F: fluorescence.

Figure 20: ATP concentration response of YOPRO uptake in isolated rat thymocytes. Cells were incubated with increasing concentrations of ATP (0.1-10 mM) in the presence of the vital dye YOPRO. Labelled cells were counted manually and divided by the total number of cells in the field (Mean +- SEM, N=3).

Figure 21: Transcript expression of P_2X_1 and P_2X_7 receptors in CHO-K1 cells. RT-PCR was used to examine the transcript expression of P_2X_1 and P_2X_7 receptors in CHO-K1 cells. Reaction with the total RNA from CHO-K1 cells without reverse transcription was used as the negative control (lane 3, both panels). Lane 1 shows the 100 base pair molecular weight markers, while lane 2 shows the amplified fragment of 594 bp (P_2X_1, panel A) and 660 bp (P_2X_7, panel B), respectively.

Figure 22: Effect of oATP on HD induced DNA fragmentation in CHO-K1 cells. Cells were exposed to HD alone or to HD following a 2 hr exposure to the

P2X7 antagonist oATP (300 μM or 500 μM). Lane 2-4 show typical HD induced DNA ladders, which were generally abolished in the presence of oATP (lane 6-8). oATP by itself produced no laddering (lanes 10-12).

Figure 23: Effect of oATP on HD-induced TUNEL reaction in CHO-K1 cells. Cell cultures were incubated with oATP for 2 hr prior to HD treatment. Five hours after HD exposure the cells were assessed for apoptotic cell death using the TUNEL reaction. Results represent the mean +/- standard deviation of three experiments.

Figure 24: Effect of oATP on HD-induced morphology in CHO-K1 cells. Cell cultures were incubated with oATP for 2 hr prior to HD treatment. Five hours after HD exposure the cells were stained with acridine orange and ethidium bromide and their morphology assessed using fluorescence microscopy. Results represent the mean +/- standard deviation of three experiments.

Figure 25: Effect of oATP on HD-induced cytotoxicity in CHO-K1 cells. Cell cultures were incubated with oATP for 2 hr prior to HD treatment. 24 hours post-HD treatment cell viability was assessed using the alamarBlue cytotoxicity assay. Results are expressed as a percentage of the HD treated only LC_{50} and represent the mean +/- standard deviation of three separate experiments.

Figure 26: Effect of incubation time on BzATP-induced LDH release in CHO-K1 cells. Confluent cultures of CHO-K1 cells were exposed to increasing concentrations of BzATP in defined sucrose buffer. At varying time intervals, the treatment buffer was aspirated and replaced with culture medium containing no drug. Cell death was measured 24 hours after the start of exposure using the LDH release cytotoxicity assay. One set of samples was treated with BzATP in culture medium, and the exposure was

carried out for the full 24 hours. Results are representative of several separate experiments.

Figure 27: Effect of oATP on BzATP induced LDH release in CHO-K1 cells. Confluent cultures of CHO-K1 cells were treated with oAYP 2 hr prior to HD exposure. Cell death was measured 24 hr post-HDS treatment using the alamarBlue cytotoxicity assay. Data is normalized as the percent of the HD-only treated LC_{50}. Results represent the mean +/- standard deviation of three experiments.

Figure 28: Effect of buffer ionic concentration on MTX and BzATP induced EtBr uptake in CHO-K1 cells. Cells were suspended in either sucrose (A) or PSS (B) buffer containing EtBr and baseline fluorescence was acquired for 5 min prior to BzATP exposure. BzATP (50 μM) induced EtBr uptake only in cells suspended in the non-ionic sucrose buffer (A vs B). In contrast, MTX induced EtBr uptake was enhanced in PSS compared to sucrose buffer (C). Data in C represents the mean +/- SEM of four separate experiments.

Figure 29: Effect of the ionic concentrations of buffers on MTX and BzATP induced EtBr uptake in CHO-K1 cells. Cells were incubated in the optimal buffer for demonstrating the activity of the agonists MTX (PSS) and BzATP (sucrose). Cells in PSS buffer containing 20 μM EtBr, were exposed to 125 pM MTX, and dye uptake was measured by fluorescence microscopy at 30 min (C) or followed for 30 min by kinetic analysis (G). Cells were exposed to BzATP (50 μM) and EtBr uptake was measured by fluorescence microscopy at 30 min (D) or kinetically (H). Panels A and B show the lack of dye uptake in cells not exposed to either agonist, while Panels E and F depict light micrographs of the samples shown in C and D, respectively.

Figure 30: BzATP induced cytotoxicity in CHO-K1 cells. Cells were grown in 96 well titerplates until just confluent. Treatment was initiated by replacing the medium with sucrose based buffer containing concentrations of BzATP. The cells were incubated for various time periods and then the buffer was removed and the cells fed with culture medium. 24 hr toxicity was determined using LDH release as the endpoint. The results are the mean of 3 separate experiments.

Figure 31: Inhibitory effect of oATP on BzATP induced EtBr uptake in CHO-K1 cells. Cells were treated with 50 μM BzATP in sucrose based buffer containing 20 μM EtBr with or without a 30 min preincubation with 300 μM oATP. Panel C shows a representative tracing of the increase in fluorescence induced by BzATP, while Panel D shows the inhibition by oATP of BzATP induced dye uptake. Samples of the cell suspension in D were removed at 30 min and examined by both light (B) and fluorescence microscopy (A), revealed no fluorescent cells.

Figure 32: Lack of inhibition of MTX induced dye uptake by oATP in CHO-K1 cells. Cells were treated with 125 pM MTX in PSS buffer containing 20 μM EtBr . Panel C depicts a representative tracing of the increase in fluorescence induced by MTX, in the presence of 300 μM oATP while Panel D shows a summary of the effects of oATP on MTX induced EtBr uptake (mean +/- S.E.M., n = 4). Panel A is a representative fluorescent micrograph of cells at the end of the 30 min exposure seen in Panel C

Figure 33: Effect of oATP on BzATP and MTX induced cell death measured by alamarBlue in CHO-K1 cells 24 h after exposure. Just confluent cultures were treated with various concentrations of oATP for 1 hr prior to exposure to increasing concentrations of BzATP (A) or MTX (B). oATP and BzATP incubations were carried out in sucrose buffer, prior to aspiration then refed with medium. MTX exposures were carried out in

culture medium.The data for BzATP (A) is normalized as a percent of the toxicity of vehicle treated controls while MTX results (B) are expressed as a percentage of the vehicle pretreated MTX LC_{50} values. All data represents the mean +/- standard deviation from three experiments. Asterisks denote statistically significant protection compared to no pretreatment ($p < 0.05$, Dunnett's Multiple Comparison Test).

Figure 34: Effect of the calmodulin inhibitor W7 on BzATP and MTX induced EtBr uptake in CHO-K1 cells. Cultures were pretreated with 100 μM W7 for 30 min followed by exposure to 150 μM BzATP in sucrose based buffer (Panel A and C) or 125 pM MTX in PSS (Panel B,D and E, both containing 20 μM EtBr). Panels A and B depict representative tracings of the steep increase in fluorescence induced by BzATP and MTX, respectively untreated with agonists. W7 had no effect on BzATP induced dye uptake A vs C), but almost completely eliminated the MTX induced response (D). This inhibitory activity was found to be concentration dependent (Panel E, mean +/- S.E.M., n = 4).

Figure 35: Effect of W7 on BzATP (Panel A) and MTX (Panel B) induced cytotoxicity measured by alamarBlue assay at 24 hr, in CHO-K1 cells. Just confluent cultures were treated with various concentrations of W7 1 hr prior to exposure to increasing concentrations of BzATP (A) or MTX (B) in appropriate buffers. W7 and MTX incubations were carried out in culture medium with no subsequent medium change. The figure shows the potent W7 effects against toxicity of MTX as opposed to negligible effects on the BzATP induced response. Data is expressed as a percentage of the vehicle pretreated control LC_{50} values. All data represents the mean +/- standard deviation obtained in three experiments. Asterisks denote statistically significant protection compared to no pretreatment ($p < 0.05$, Dunnett's Multiple Comparison Test).

Figure 36: Effect of external calcium concentration on BzATP and MTX induced EtBr uptake in CHO-K1 cells. Cells incubated in PSS containing 1.5 mM calcium and exposed to 125 pM MTX exhibited steep increases in fluorescence (A), while cells bathed in calcium-free buffer showed no response to the toxin (B). In contrast, CHO-K1 cells suspended in sucrose buffer and exposed to BzATP exhibited no statistically significant dependence on calcium concentration (C, mean +- SEM, n = 3).

Figure 37: Effect of external calcium concentration on BzATP (Panel A) and MTX (Panel B) induced cytotoxicity in CHO-K1 cells. BzATP (1 hr) incubations were carried out in sucrose buffer containing various calcium concentrations. MTX incubations were carried out in medium containing increasing calcium concentrations. Cell death was measured 24 h post-treatment using the alamarBlue cytotoxicity assay. Both BzATP (A) and MTX (B) toxicity was shown to be dependent on external calcium concentration. Asterisks denote statistically significant differences in toxicity compared to that obtained in nominal zero calcium concentrations ($p < 0.01$, Dunnett's Multiple Comparison Test).

Figure 38: Effect of HD (400 μM) on ethidium bromide uptake in CHO-K1 cells. CHO-K1 cells were incubated in ethidium bromide (20 μM) and exposed to HD and EtBr uptake measured for 60 min. The data presented is representative of the results obtained from four experiments.

Figure 39: Fluorescence photomicrograph of CHO-K1 cells exposed to HD for 60 min. This is a fluorescence micrograph of a typical response of CHO-K1 cells following exposure to 400 μM HD for 1 hour. Four individual experiments are currently being combined and analyzed for the total fluorescence intensity.

Figure 40: Effect of HD on BzATP stimulated ethidium bromide uptake in CHO-K1 cells. CHO-K1 cells were incubated with BzATP (100μM) (A) alone for 1 hr or with HD (400 μM) for 10 min followed by and during the exposure to BzATP (B). The figure represents one of four experiments.

Figure 41: Time related influx of ethidium bromide in CHO-K1 cells exposed to BzATP alone or BzATP following preincubation with HD. Ethidium bromide uptake in CHO-K1 cells was measured in cells exposed to BzATP (100 μM) for 1 hr and repeated following a 10 min preincubation with HD 100 μM for 1 hour. These represent the mean +/- S.E.M. of 4.

Figure 42: CHO-K1 cells were incubated with 800μM HD for 5 hours and placed in sucrose buffer (A) or PSS (B) and incubated for 5 min.with EtBr. A concentration of either BzATP (A) or maitotoxin (B) was added and EtBr uptake was measured for 30 min which was a maximal response at the concentrations of the two agonists used.

Figure 43: Schematic diagram showing a summary of the results of studies which have been carried out to determine the existence of a cytolytic complex in CHO-K1 cells and its relation to cell death. The role of HD on the two receptors that open the cytolytic pore are shown as questionable since definitive effects of HD on this complex, with the exception of shunting of toxicity from apoptosis to necrosis following HD, has not been demonstrated.

Figure 44: Lack of HD effect on calcium influx in synaptosomes. Synaptosomes were exposed to ATP (1mM) and calcium influx was measured for 90 sec (right hand panels). The influx experiments were repeated in the presence of 100 μM –1 mM HD (15 min) in either unstimulated (resting synaptosomes) or in synaptosomes stimulated with ATP. Each bar

represents mean influx +- SEM obtained from 3 experiments done in triplicate.

Figure 45: Effect of calcium modulation on HD cytoxicity in human skin keratinocytes. Just-confluent cell cultures were exposed to HD in medium containing varying calcium concentrations (A) or cultures were pretreated for 1 hr with BAPTA-AM (B), thapsigargin (C) or W-7 (D) prior to HD exposure. 48 hr later the cultures were assessed for viability using alamarBlue. The results represent the mean +/- standard deviation of three experiments using tissue from three different donors, and are normalized against the LC_{50} of vehicle-pretreated, HD-exposed cultures. Asterisk denotes statistically different from 100 μM calcium control (Tukey-Kramer HSD Multiple Comparison Test, $p < 0.05$).

Figure 46: Effect of calcium modulation on HD-induced DNA fragmentation measured by the TUNEL reaction in human skin keratinocytes. Just-confluent cell cultures were exposed to HD in normal medium or medium containing no calcium, or cultures were pretreated for 1 hr with 25 μM BAPTA-AM, 10 μM thapsigargin or 30 μM W-7 prior to HD exposure. 16 hr post-HD exposure the cultures were fixed with 4 % paraformaldehyde and then assessed for TUNEL positive cells. The results represent the mean +/- standard deviation of three experiments using tissue from three different donors. No pre-treatment changed the response compared to HD-only treatments (Tukey-Kramer HSD Multiple Comparison testing, $p > 0.05$).

Figure 47: Effect of calcium modulation on HD-induced DNA fragmentation. Just-confluent cell cultures were exposed to HD in normal medium or medium containing no calcium, cultures were pretreated for 1 hr with 25 μM BAPTA-AM, 10 μM thapsigargin or 30 μM W-7 prior to HD exposure. 16 hr post-HD exposure total genomic DNA was extracted, amplified by

LM PCR and resolved by agarose gel electrophoresis. The gels were stained with Sybr-gold. The gels depicted are representative of results obtained from three different experiments using cells from three different donors.

Figure 48: Effect of calcium modulation on HD-induced morphology. Just-confluent cell cultures were exposed to HD in normal medium (A), medium containing no calcium (B) or in cultures pretreated for 1 hr with 25 μM BAPTA-AM (C), 10 μM thapsigargin (D) or 30 μM W-7 (E) prior to HD treatment. 16 hr post-HD exposure the cultures were HD-induced morphological changes using ethidium bromide/acridine dual labelling. The results represent the mean +/- standard deviation of three experiments using tissue from three different donors. No pre-treatment changed the response compared to HD-only treatments (Tukey-Kramer HSD Multiple Comparison testing, $p > 0.05$).

Figure 49: Effect of NaCl or NaI concentration on HD-induced cell death in CHO-K1 cells. Confluent cultures were rinsed once with the NaCl (A) or NaI (B) test buffer prior to HD treatment in the same buffer. The cultures were changed back into culture medium 1 hr post-HD treatment and assessed for cell viability 23 hr later using the alamarBlue cytotoxicity assay. Results are the mean +/- standard deviation of three experiments.

Figure 50: Effect of NaF, KF, NaCl and KCl concentration on HD-induced cell death in CHO-K1 cells. Confluent cultures were rinsed once with the test salt buffer prior to HD treatment in the same buffer. The cultures were changed back into culture medium 1 hr post-HD treatment and assessed for cell viability 23 hr later using the alamarBlue cytotoxicity assay. Results are normalized against the LC_{50} of HD in culture medium and represent the mean +/- standard deviation of three experiments.

Figure 51: Effect of NaBr, KBr, NaI and KI concentration on HD-induced cell death in CHO-K1 cells. Confluent cultures were rinsed once with the test salt buffer prior to HD treatment in the same buffer. The cultures were changed back into culture medium 1 hr post-HD treatment and assessed for cell viability 23 hr later using the alamarBlue cytotoxicity assay. Results are normalized against the LC_{50} of HD in culture medium and represent the mean +/- standard deviation of three experiments.

Figure 52: Effect of Na aspartate, K aspartate, Na glutamate and K glutamate concentration on HD induced cell death in CHO-K1 cells. Confluent cultures were rinsed once with the test salt buffer prior to HD treatment in the same buffer. The cultures were changed back into culture medium 1 hr post-HD treatment and assessed for cell viability 23 hr later using the alamarBlue cytotoxicity assay. Results are normalized against the LC_{50} of HD in culture medium and represent the mean +/- standard deviation of three experiments.

Figure 53: Effect of Na isothiocyanate, K isothiocyanate, Na gluconate and K gluconate on HD induced cell death in CHO-K1 cells. Confluent cultures were rinsed once with the test salt buffer prior to HD treatment in the same buffer. The cultures were changed back into culture medium 1 hr post-HD treatment and assessed for cell viability 23 hr later using the alamarBlue cytotoxicity assay. Results are normalized against the LC_{50} of HD in culture medium and represent the mean +/- standard deviation of three experiments.

Figure 54: Effect of LiCl, RbCl, CsCl and choline Cl on HD induced cell death in CHO-K1 cells. Confluent cultures were rinsed once with the test salt buffer prior to HD treatment in the same buffer. The cultures were changed back into culture medium 1 hr post-HD treatment and assessed for cell viability 23 hr later using the alamarBlue cytotoxicity assay.

Results are normalized against the LC_{50} of HD in culture medium and represent the mean +/- standard deviation of three experiments

Figure 55: Effect of LiI, RbI and CsI on HD induced cell death in CHO-K1 cells. Confluent cultures were rinsed once with the test salt buffer prior to HD treatment in the same buffer. The cultures were changed back into culture medium 1 hr post-HD treatment and assessed for cell viability 23 hr later using the alamarBlue cytotoxicity assay. Results are normalized against the LC_{50} of HD in culture medium and represent the mean +/- standard deviation of three experiments.

Figure 56: Effect of $CaCl_2$ and $MgCl_2$ on HD induced cell death in CHO-K1 cells. Confluent cultures were rinsed once with the test salt buffer prior to HD treatment in the same buffer. The cultures were changed back into culture medium 1 hr post-HD treatment and assessed for cell viability 23 hr later using the alamarBlue cytotoxicity assay. Results are normalized against the LC_{50} of HD in culture medium and represent the mean +/- standard deviation of three experiments.

Figure 57: Effect of chlorotoxin and IAA-94 on HD induced cell death in CHO-K1 cells. Cells were preincubated with varying concentrations of the chloride ion channel inhibitors chlorotoxin (A) or IAA-94 (B) for 1 hr prior to HD exposure. Both incubations were carried out in defined NaCl buffers. One hour post-HD exposure, the cultures were refed with culture medium and assessed for cell viability 23 hr later using the alamarBlue cytotoxicity assay. Results are normalized against the LC_{50} of HD in culture medium and represent the mean +/- standard deviation of three experiments.

Figure 58: Effect of DIDS on HD induced cell death in CHO-K1 cells. Cells were preincubated with varying concentrations of the chloride ion inhibitor DIDS in either F-12 culture medium or defined NaCl buffer, for 1 hr prior

to HD exposure. One hour post-HD exposure, the cultures were refed with culture medium and assessed for cell viability 23 hr later using the alamarBlue cytotoxicity assay. Results are normalized against the LC_{50} of HD in culture medium and represent the mean +/- standard deviation of three experiments.

Figure 59: Effect of NaCl concentration on the hydrolysis of HD. Varying concentrations of HD (50 – 800 μM) were dissolved in 32.5, 65.0 or 130 mM NaCl buffer. At different time intervals (2 – 60 min), CHO-K1 cells were exposed to the HD solutions. One hr post-exposure, the cultures were refed with culture medium and assessed for cell viability 23 hr later using the alamarBlue cytotoxicity assay. Results represent the mean of three experiments.

Figure 60: Effect of HD on intracellular chloride ion concentration. CHO-K1 cells were loaded with the intracellular chloride ion indicator dye MEQ prior to HD exposure in NaCl free sucrose buffer (A), 130 mM NaCl buffer (B) or 65 mM NaI buffer (D). In one set of experiments, the cells were incubated for 30 min with the chloride ion inhibitor DIDS prior to HD treatment in 130 mM NaCL buffer. Results are representative of the results obtained from three independent experiments.

Figure 61: Effect of pH on HD-induced cell death in CHO-K1 cells. Confluent cultures were changed into medium of the desired pH immediately prior to HD treatment. The cultures were changed back into medium of physiological pH (7.4) 1 hr post-HD treatment and assessed for viability 23 hr later using the alamarBlue cytotoxicity assay. Results represent the mean +/- standard deviation of three experiments.

Figure 62: Effect of pH on the hydrolysis of HD. Varying concentrations of HD (50 – 800 μM) were dissolved in medium adjusted to either pH 7.5 or pH 9.5.

At different time intervals (2 – 60 min), CHO-K1 cells were exposed to the HD solutions. One hr post-exposure, the cultures were refed with culture medium (~ pH 7.4) and assessed for cell viability 23 hr later using the alamarBlue cytotoxicity assay. Results represent the mean of three experiments.

Fig. 1

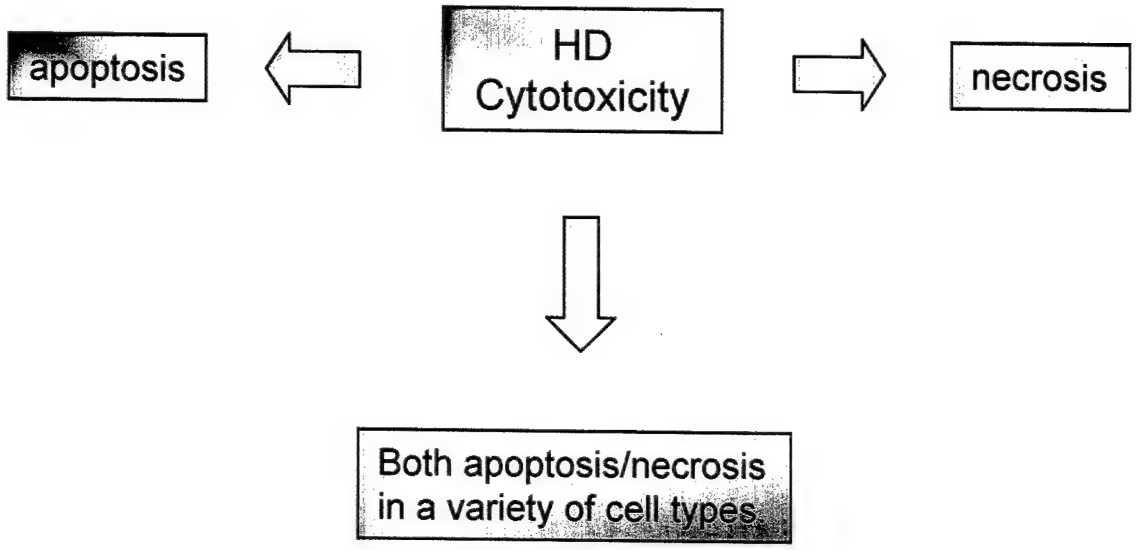
apoptosis
HD
Cytotoxicity
necrosis
Both apoptosis/necrosis
in a variety of cell types

Fig. 2

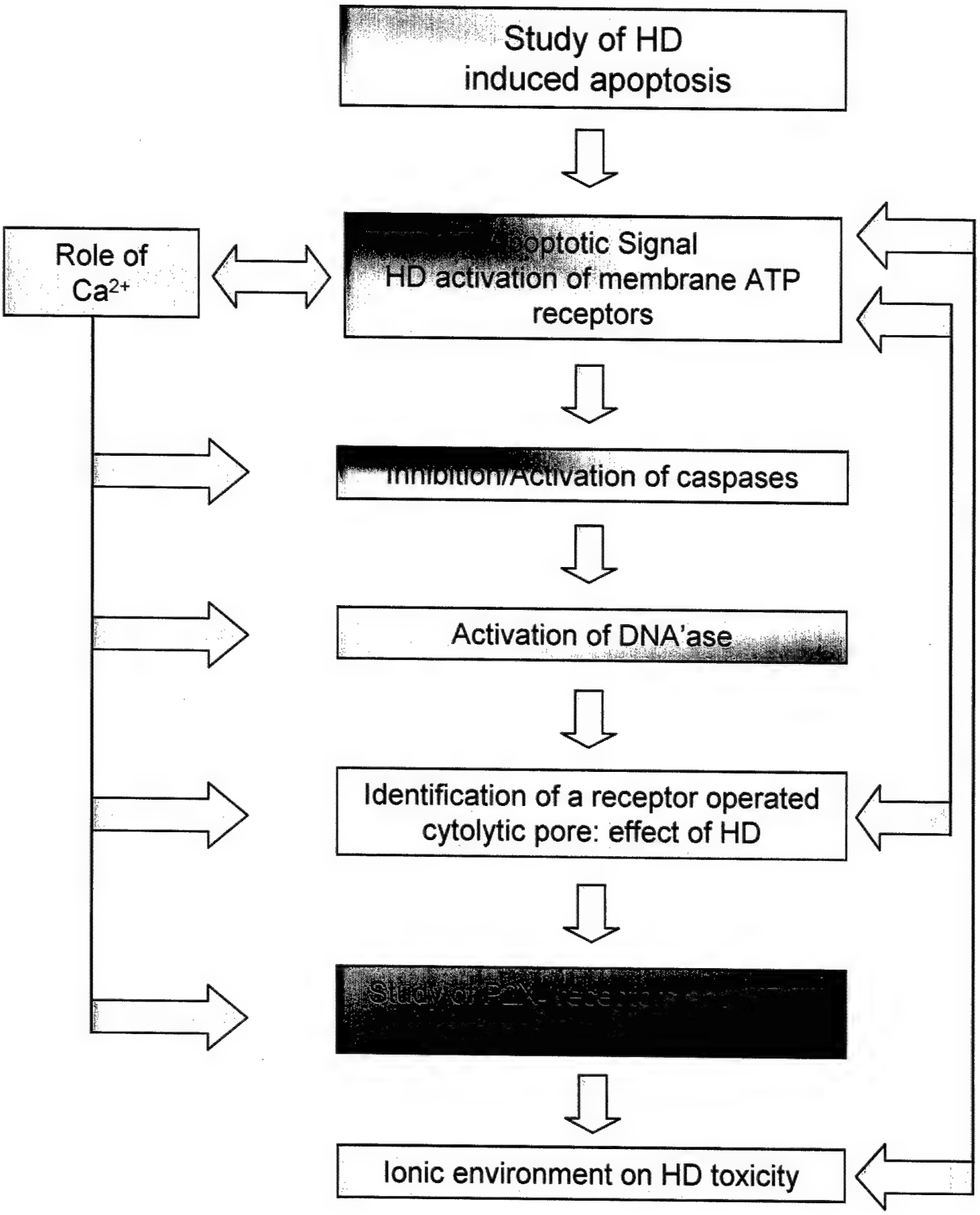
Study of HD induced apoptosis
Role of Ca^{2+}
Apoptotic Signal HD activation of membrane ATP receptors
Inhibition/Activation of caspases
Activation of DNA'ase
Identification of a receptor operated cytolytic pore: effect of HD
Ionic environment on HD toxicity

Fig. 3

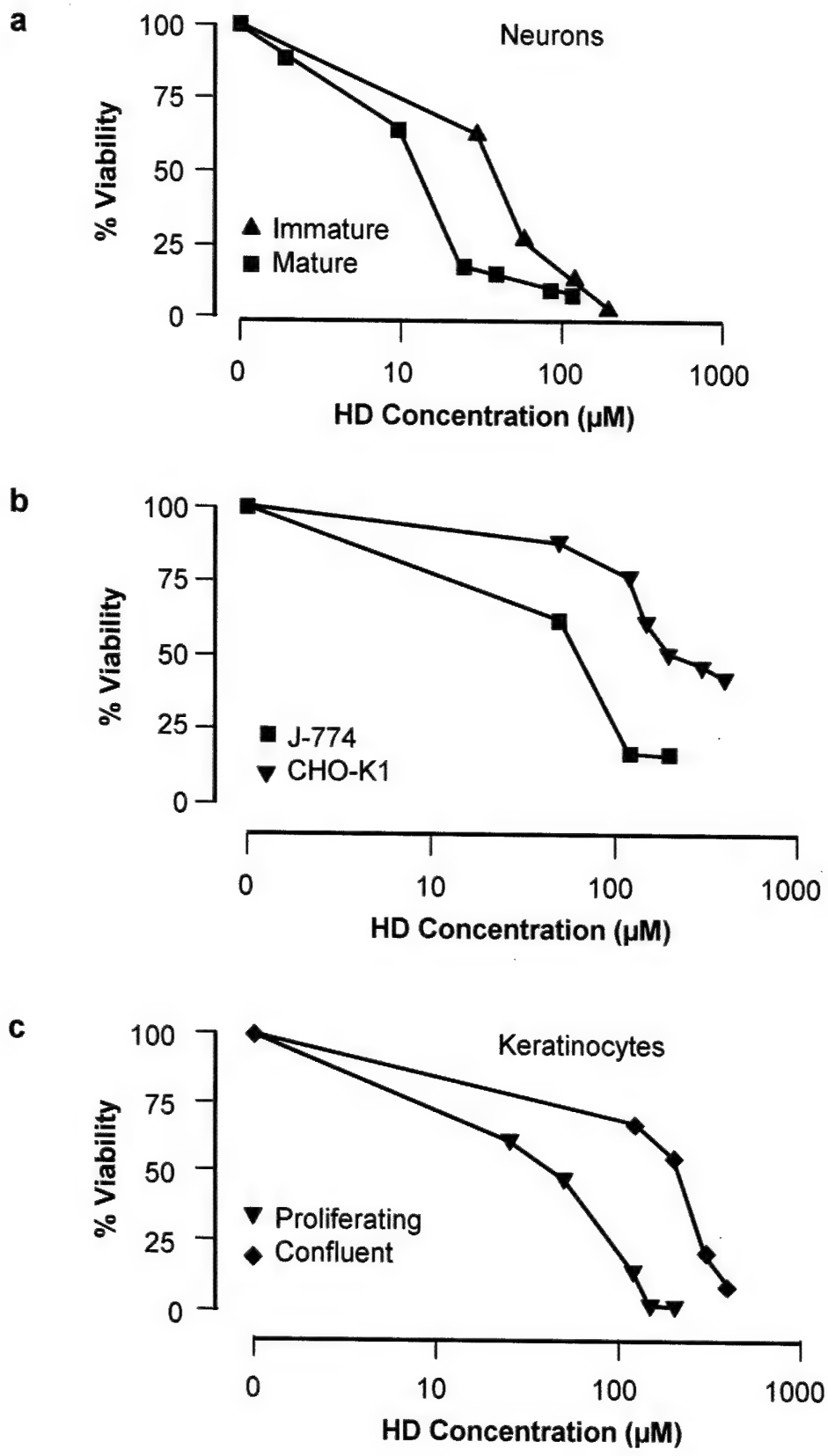
a
Neurons
% Viability
100
75
50
25
0
Immature
Mature
0
10
100
1000
HD Concentration (μM)
b
% Viability
100
75
50
25
0
J-774
CHO-K1
0
10
100
1000
HD Concentration (μM)
c
Keratinocytes
% Viability
100
75
50
25
0
Proliferating
Confluent
0
10
100
1000
HD Concentration (μM)

Fig. 4

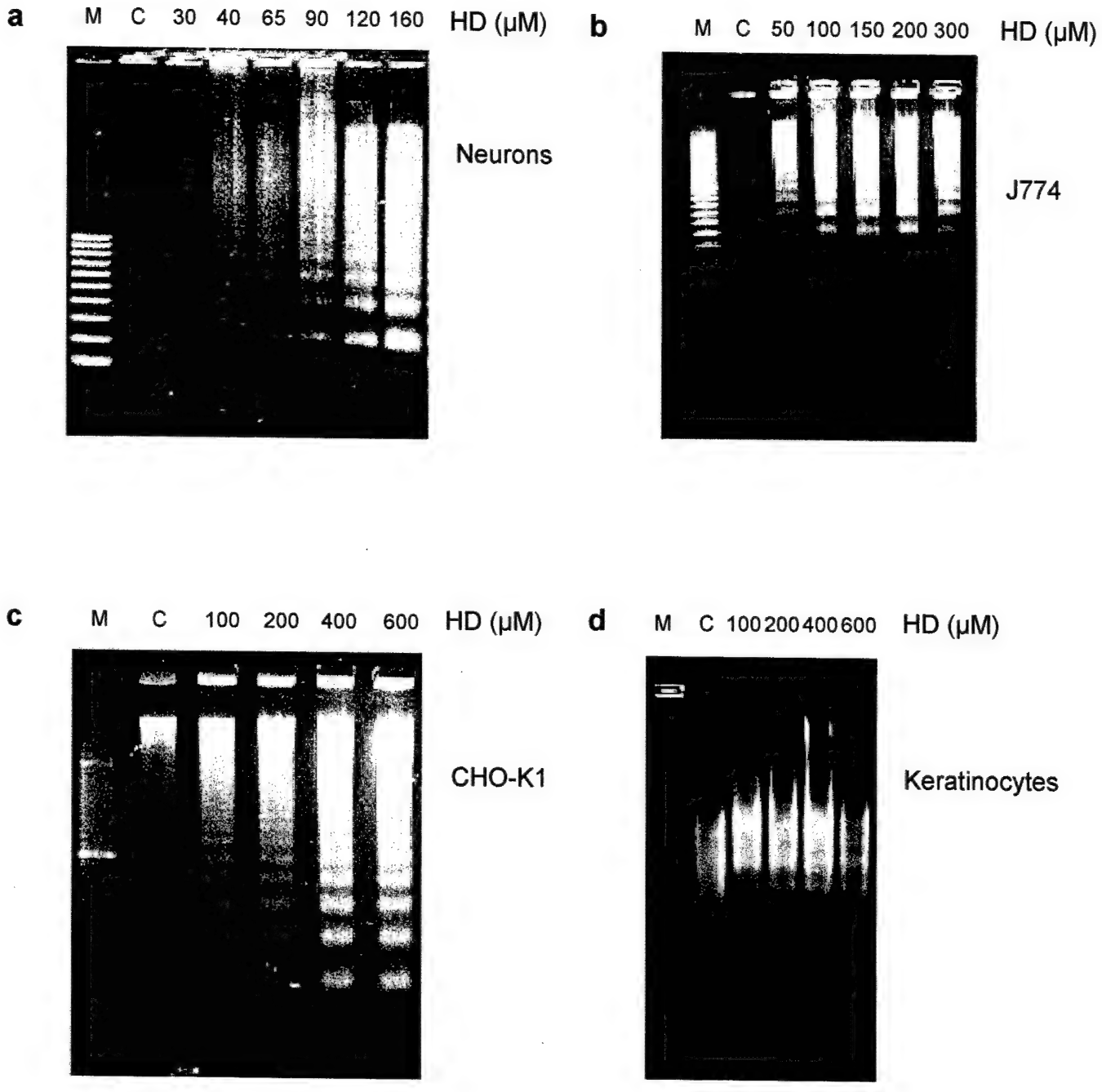
a
M C 30 40 65 90 120 160 HD (μM)
Neurons
b
M C 50 100 150 200 300 HD (μM)
J774
c
M C 100 200 400 600 HD (μM)
CHO-K1
d
M C 100 200 400 600 HD (μM)
Keratinocytes

Fig. 5

a

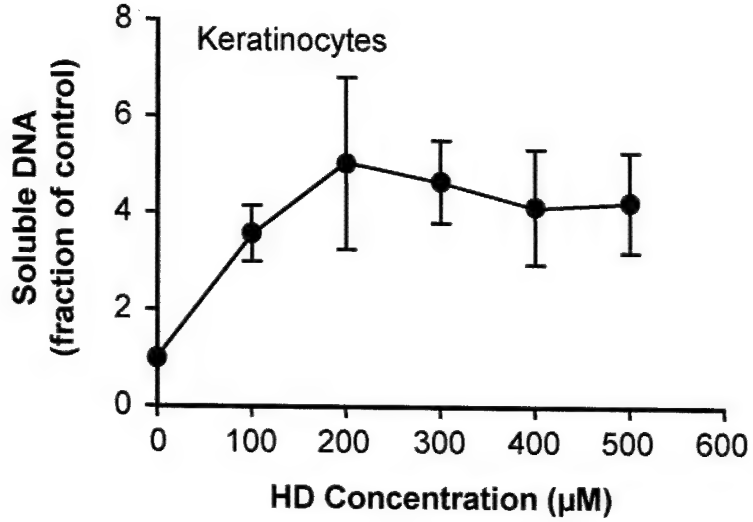
Keratinocytes
Soluble DNA (fraction of control)
0
2
4
6
8
0
100
200
300
400
500
600
HD Concentration (μM)

b

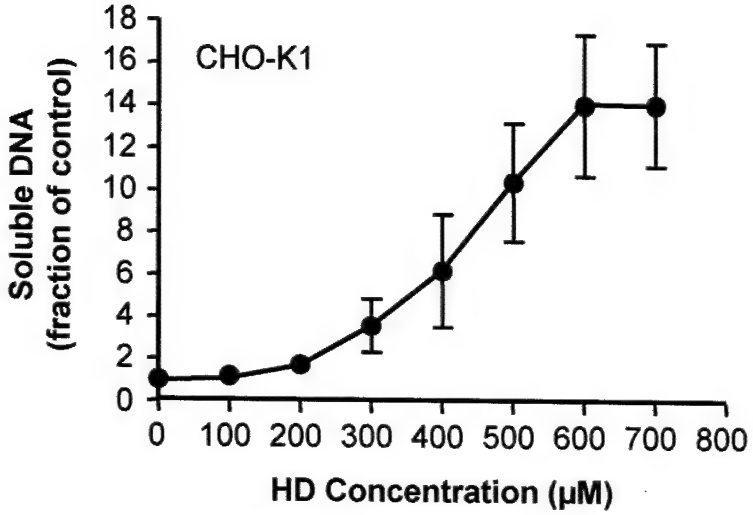
CHO-K1
Soluble DNA (fraction of control)
0
2
4
6
8
10
12
14
16
18
0
100
200
300
400
500
600
700
800
HD Concentration (μM)

c

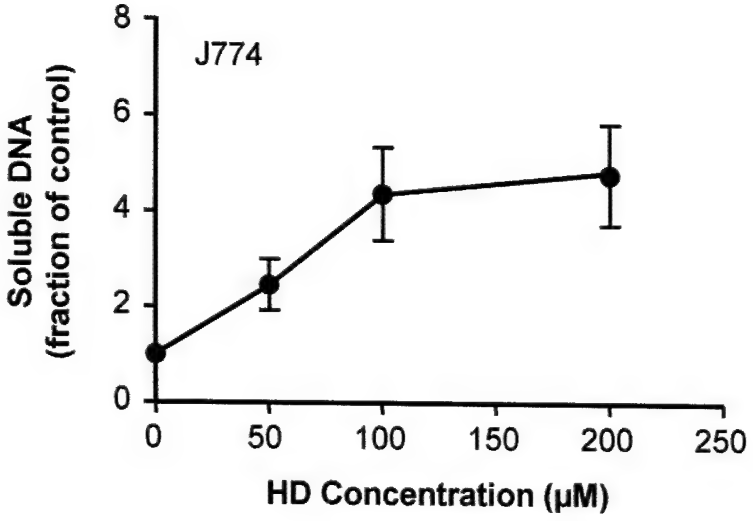
J774
Soluble DNA (fraction of control)
0
2
4
6
8
0
50
100
150
200
250
HD Concentration (μM)

Fig. 6

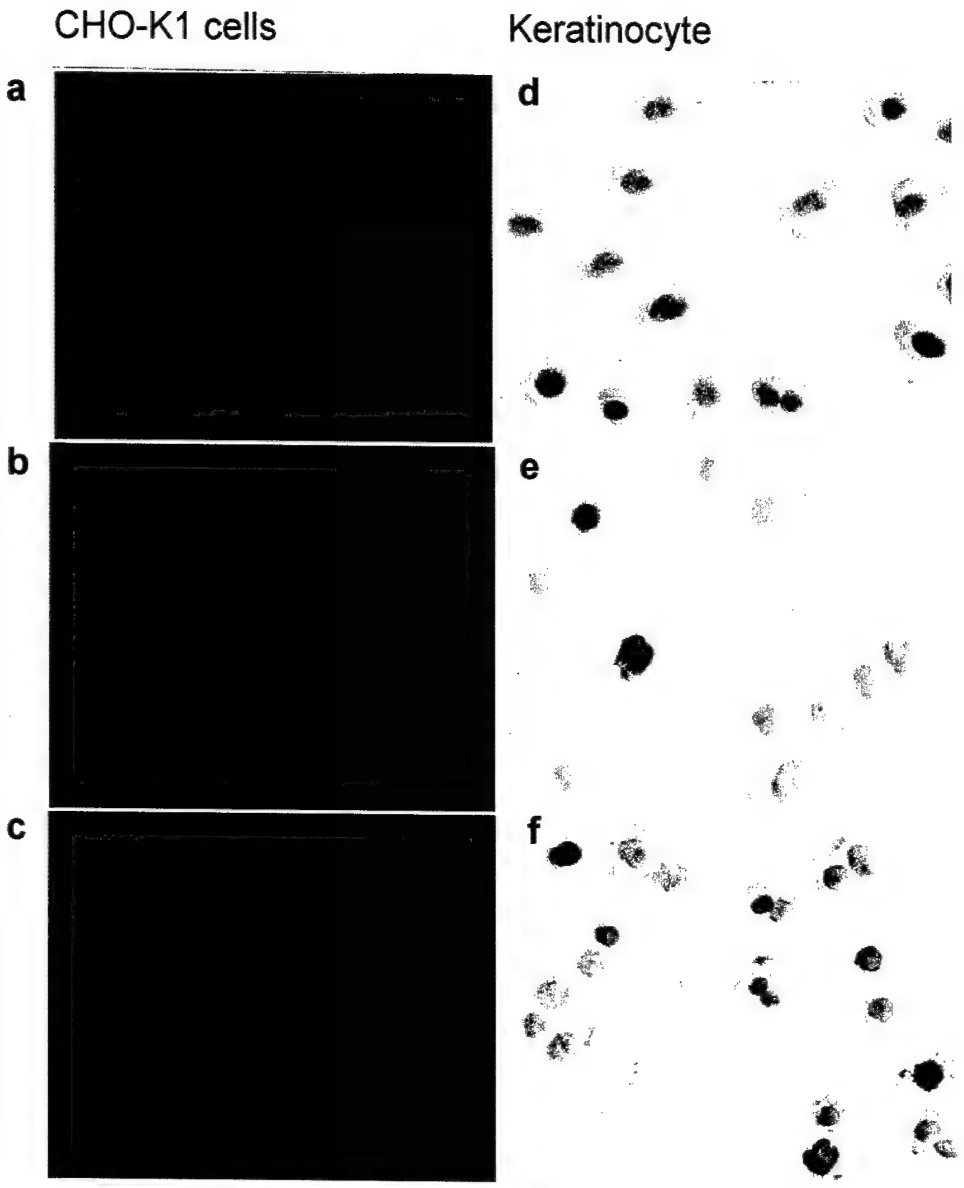

Fig. 7

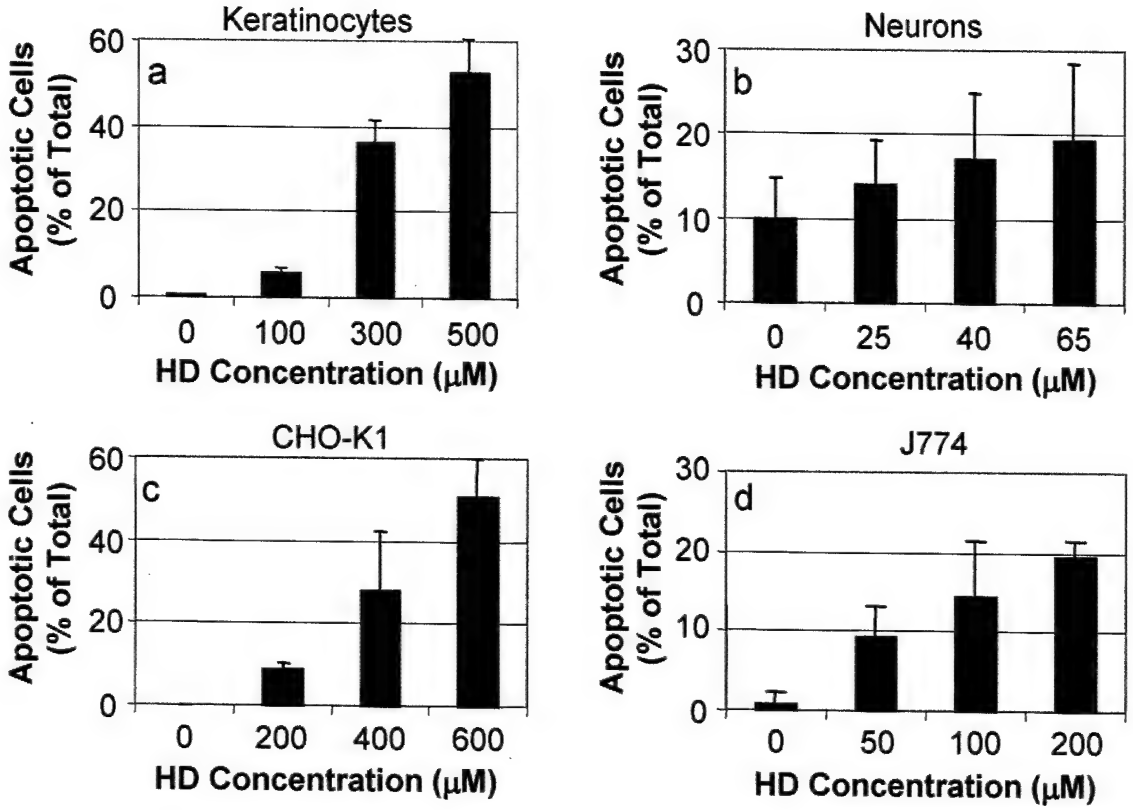
Keratinocytes
a
Apoptotic Cells (% of Total)
60
40
20
0
0
100
300
500
HD Concentration (μM)
Neurons
b
30
20
10
0
0
25
40
65
HD Concentration (μM)
CHO-K1
c
60
40
20
0
0
200
400
600
HD Concentration (μM)
J774
d
30
20
10
0
0
50
100
200
HD Concentration (μM)

Fig. 8

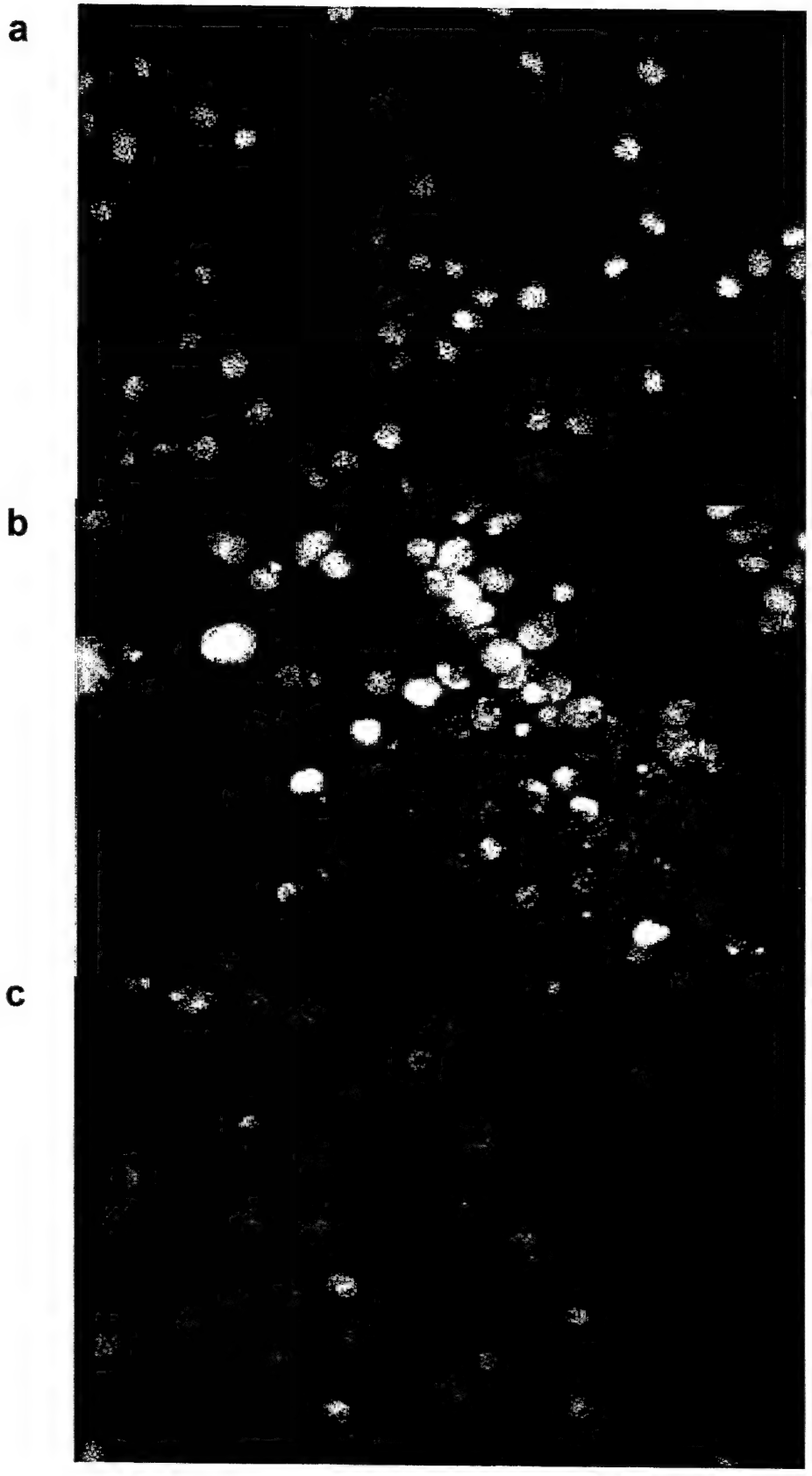

Fig. 9

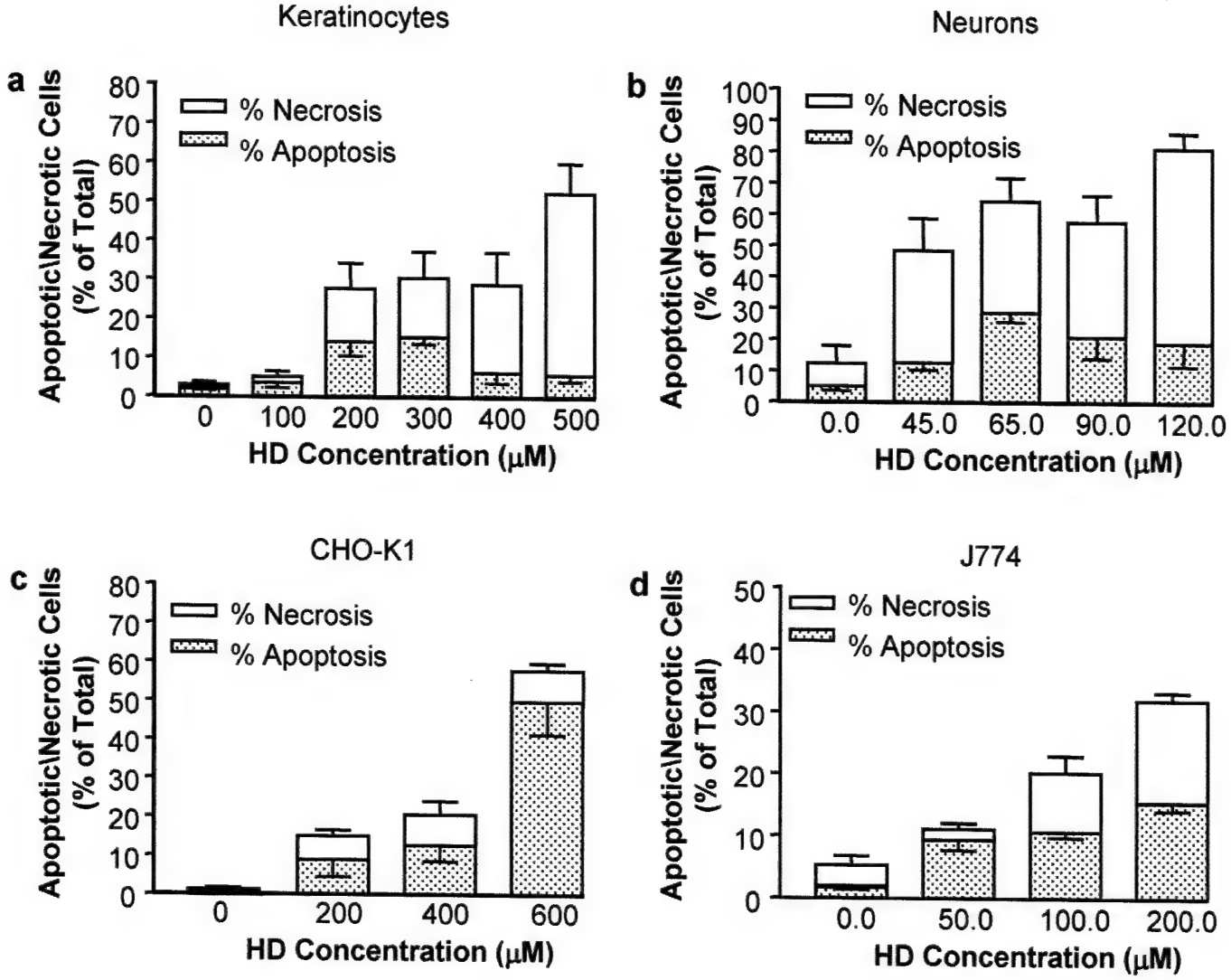
Keratinocytes
a
Apoptotic\Necrotic Cells (% of Total)
% Necrosis
% Apoptosis
0
10
20
30
40
50
60
70
80
0
100
200
300
400
500
HD Concentration (μM)
Neurons
b
Apoptotic\Necrotic Cells (% of Total)
% Necrosis
% Apoptosis
0
10
20
30
40
50
60
70
80
90
100
0.0
45.0
65.0
90.0
120.0
HD Concentration (μM)
CHO-K1
c
Apoptotic\Necrotic Cells (% of Total)
% Necrosis
% Apoptosis
0
10
20
30
40
50
60
70
80
0
200
400
600
HD Concentration (μM)
J774
d
Apoptotic\Necrotic Cells (% of Total)
% Necrosis
% Apoptosis
0
10
20
30
40
50
0.0
50.0
100.0
200.0
HD Concentration (μM)

Fig. 10

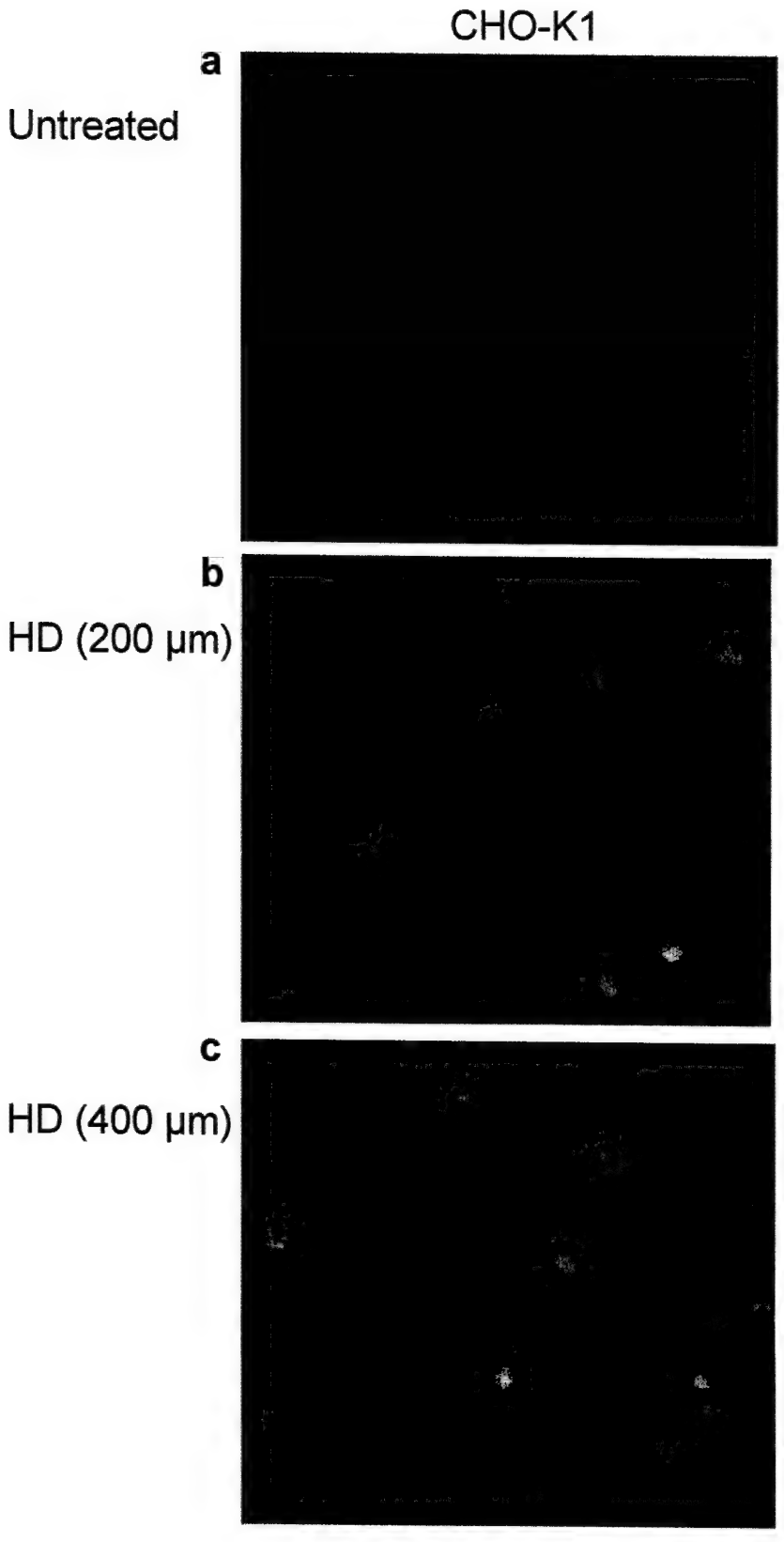

Fig. 11

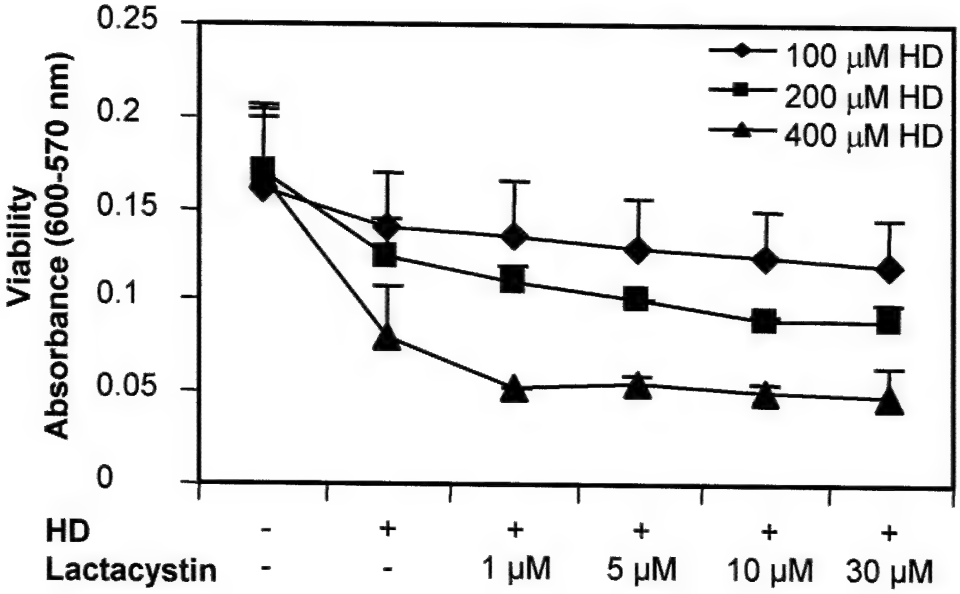
0.25
0.2
0.15
0.1
0.05
0
Viability
Absorbance (600-570 nm)
100 μM HD
200 μM HD
400 μM HD
HD - + + + + +
Lactacystin - - 1 μM 5 μM 10 μM 30 μM

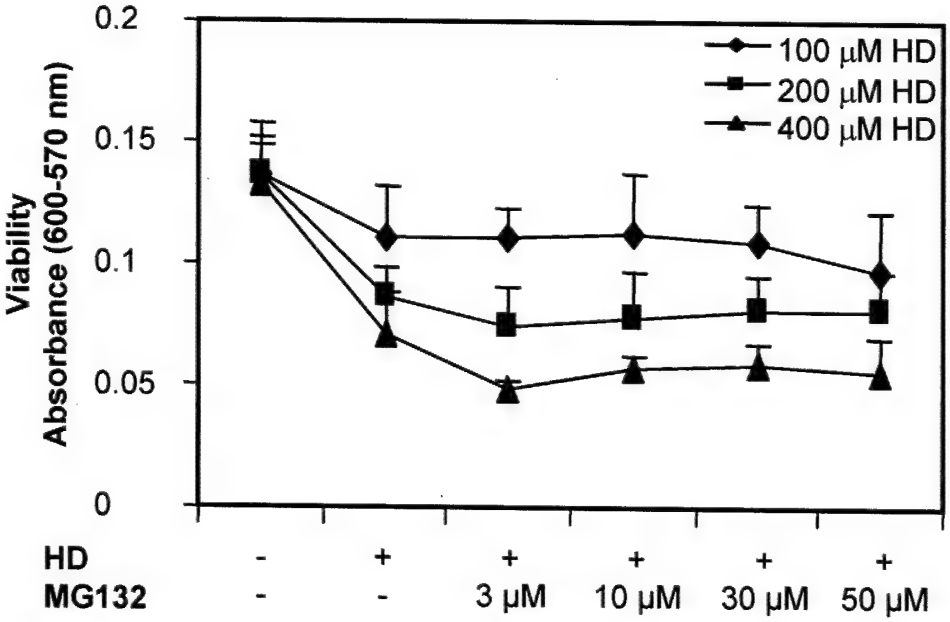
0.2
0.15
0.1
0.05
0
Viability
Absorbance (600-570 nm)
100 μM HD
200 μM HD
400 μM HD
HD - + + + + +
MG132 - - 3 μM 10 μM 30 μM 50 μM

Fig. 12

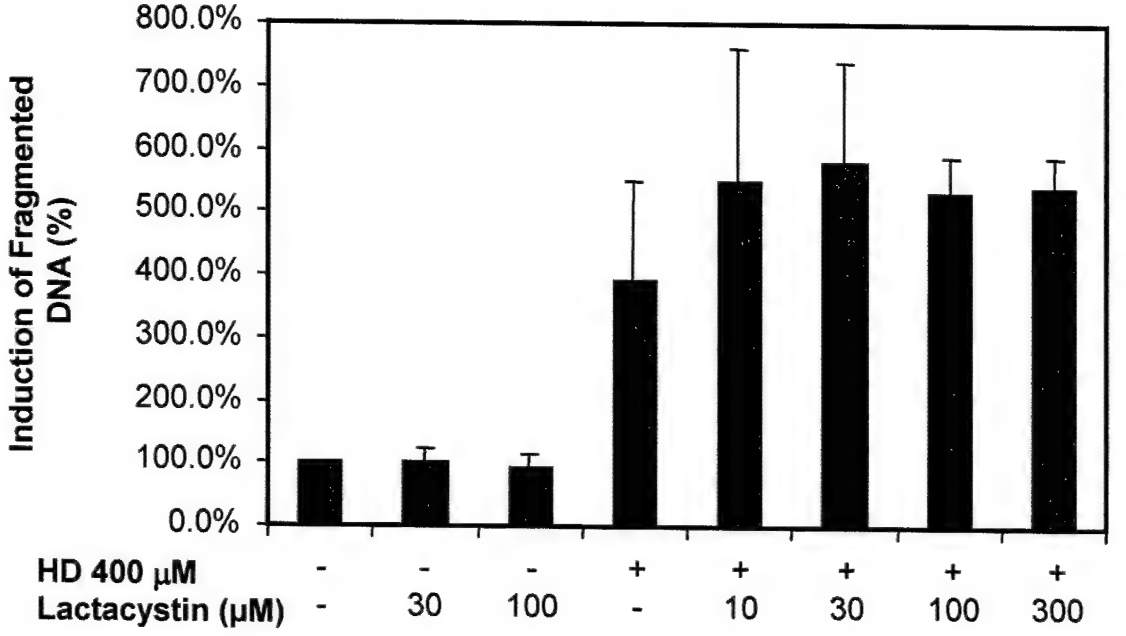
Induction of Fragmented DNA (%)
800.0%
700.0%
600.0%
500.0%
400.0%
300.0%
200.0%
100.0%
0.0%
HD 400 µM - - - + + + + +
Lactacystin (µM) - 30 100 - 10 30 100 300

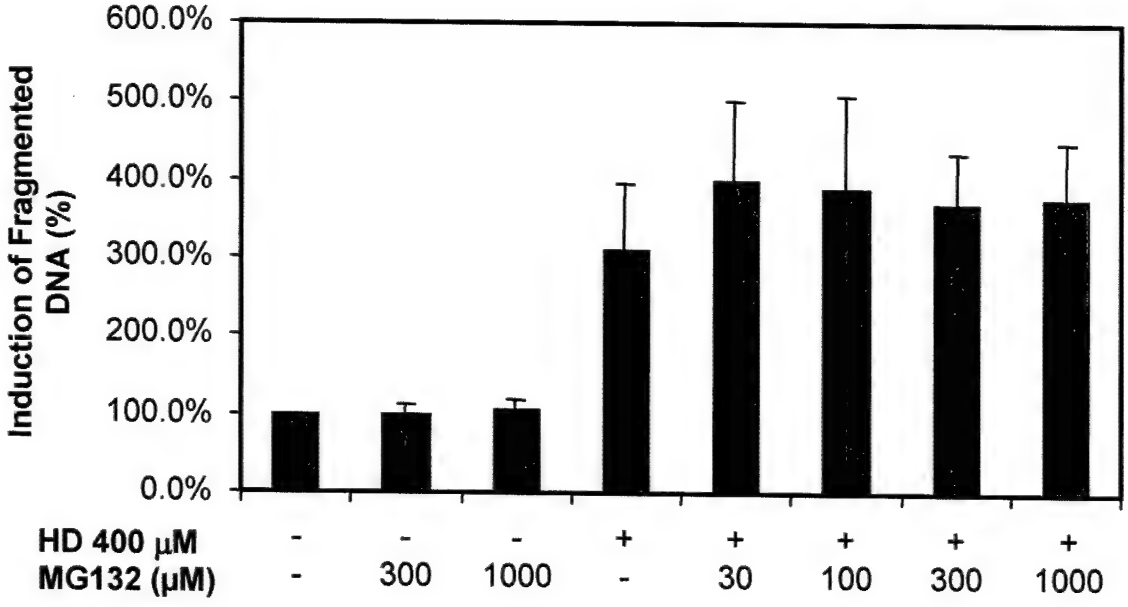
Induction of Fragmented DNA (%)
600.0%
500.0%
400.0%
300.0%
200.0%
100.0%
0.0%
HD 400 µM - - - + + + + +
MG132 (µM) - 300 1000 - 30 100 300 1000

Fig. 13

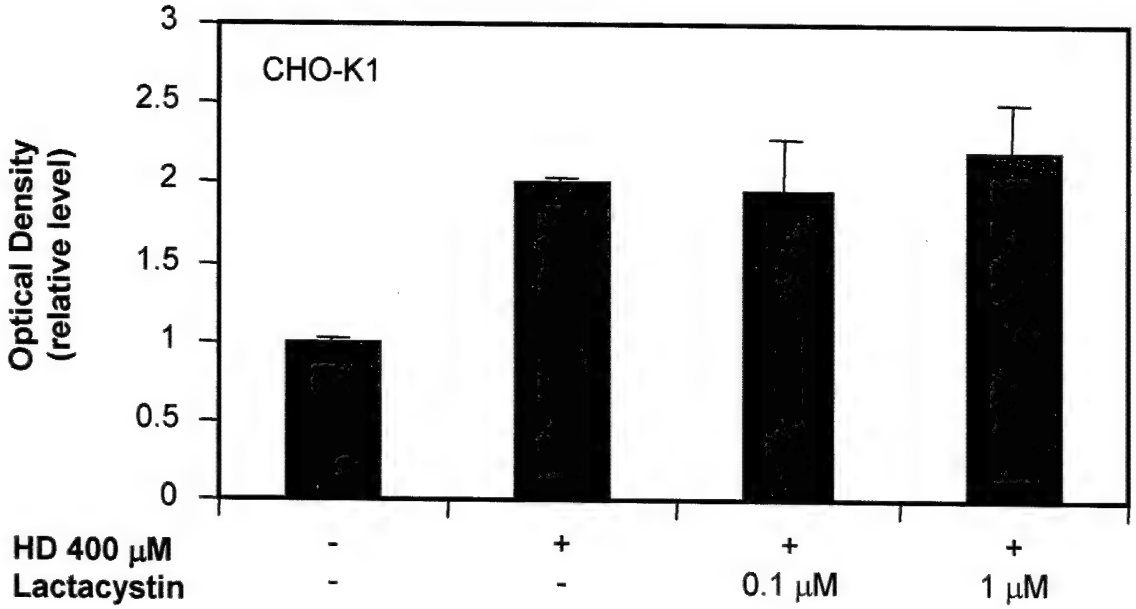
CHO-K1
Optical Density (relative level)
3
2.5
2
1.5
1
0.5
0
HD 400 μM - + + +
Lactacystin - - 0.1 μM 1 μM

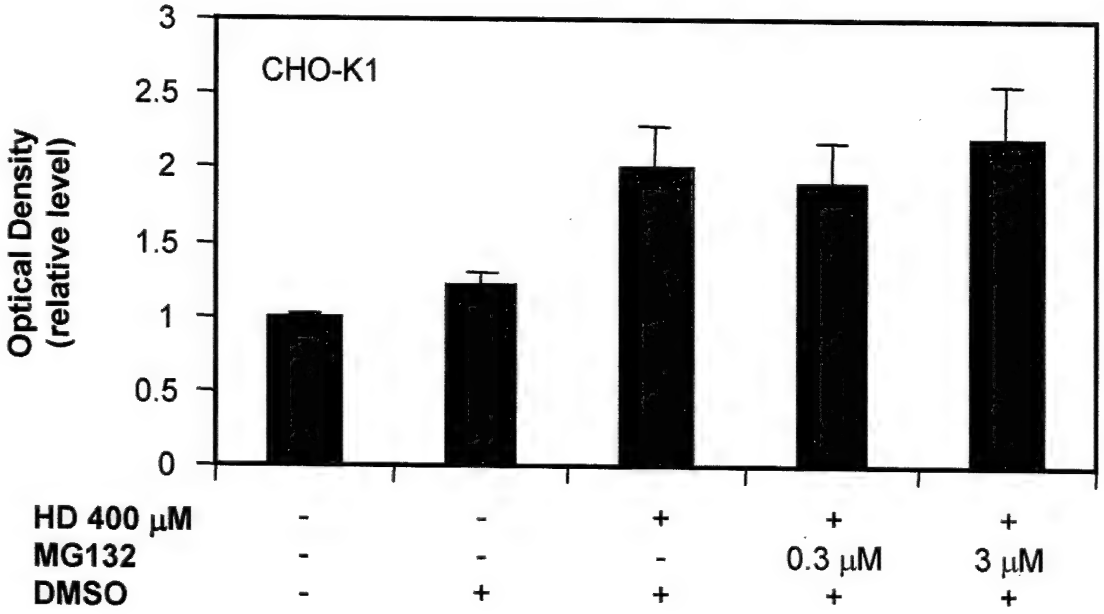
CHO-K1
Optical Density (relative level)
3
2.5
2
1.5
1
0.5
0
HD 400 μM - - + + +
MG132 - - - 0.3 μM 3 μM
DMSO - + + + +

Fig. 14

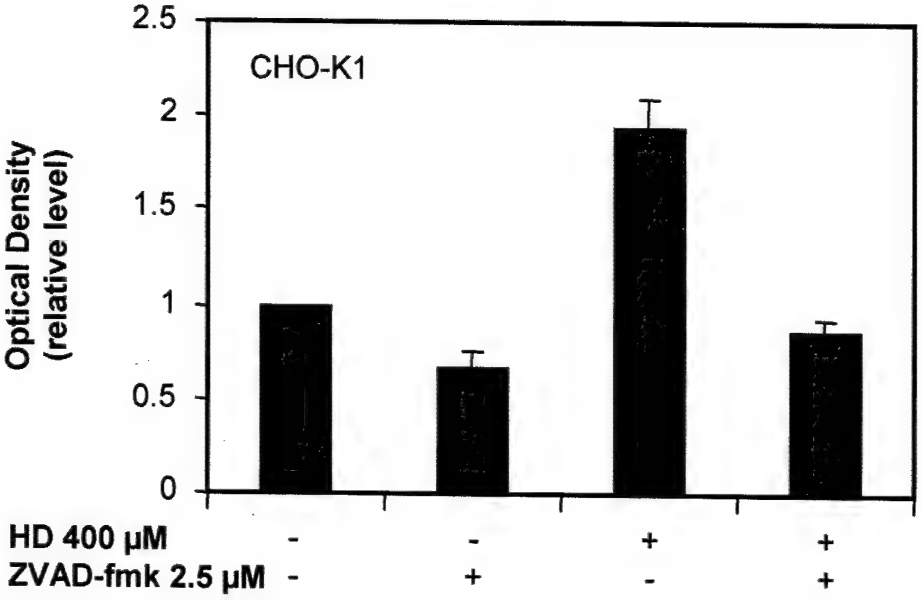
CHO-K1
Optical Density
(relative level)
2.5
2
1.5
1
0.5
0
HD 400 µM - - + +
ZVAD-fmk 2.5 µM - + - +

Fig. 15

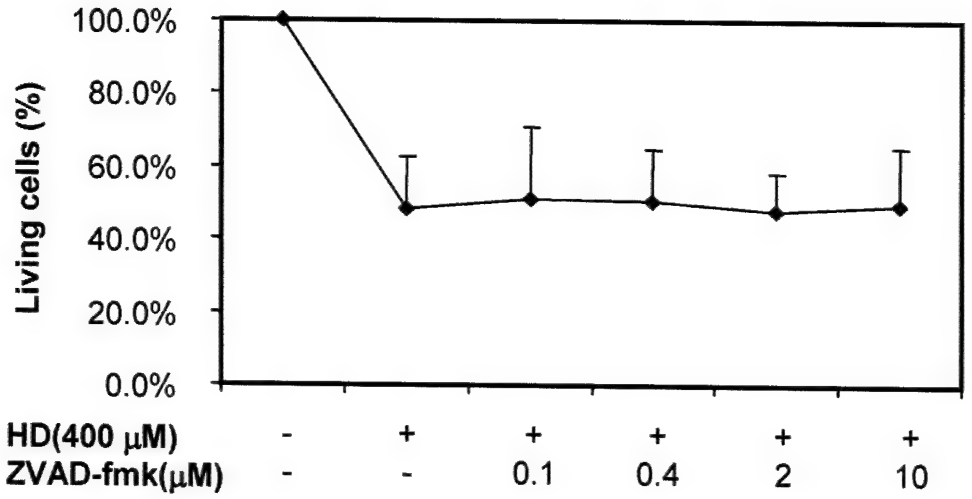
100.0%
80.0%
60.0%
40.0%
20.0%
0.0%
Living cells (%)
HD(400 μM) - + + + + +
ZVAD-fmk(μM) - - 0.1 0.4 2 10

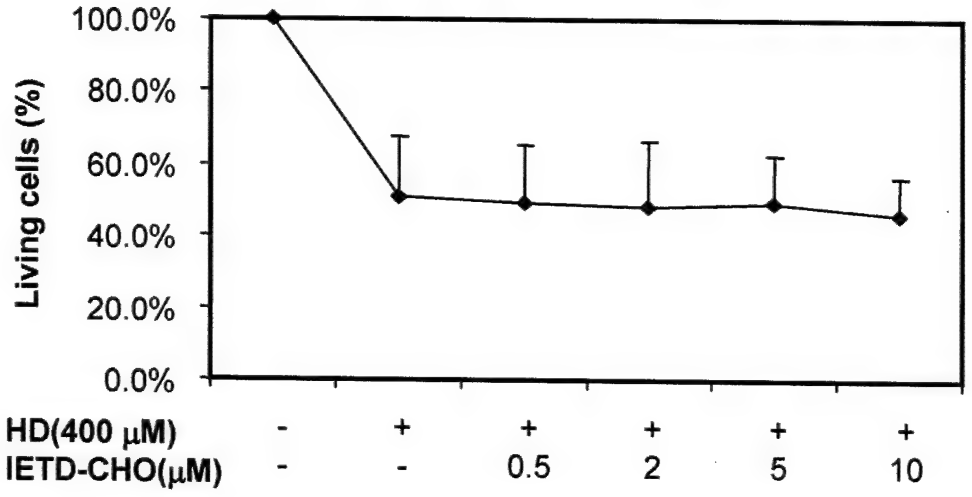
100.0%
80.0%
60.0%
40.0%
20.0%
0.0%
Living cells (%)
HD(400 μM) - + + + + +
IETD-CHO(μM) - - 0.5 2 5 10

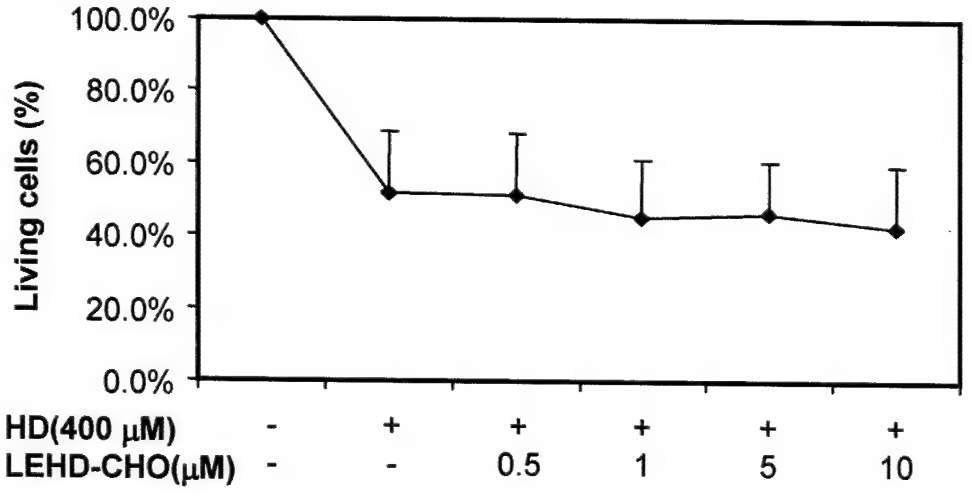
100.0%
80.0%
60.0%
40.0%
20.0%
0.0%
Living cells (%)
HD(400 μM) - + + + + +
LEHD-CHO(μM) - - 0.5 1 5 10

Fig. 16

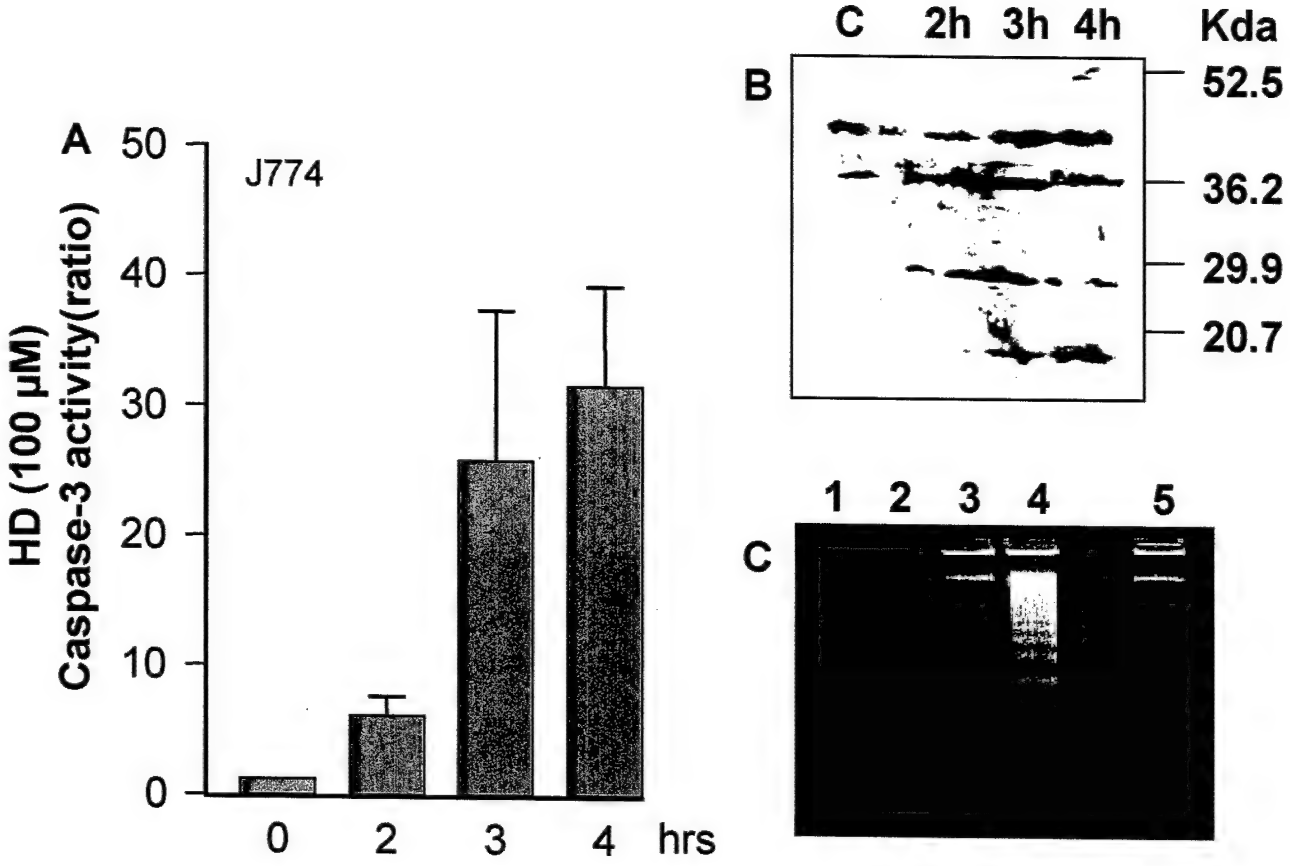
A
J774
HD (100 µM)
Caspase-3 activity(ratio)
50
40
30
20
10
0
0
2
3
4
hrs
B
C
2h
3h
4h
Kda
52.5
36.2
29.9
20.7
C
1
2
3
4
5

Fig. 17

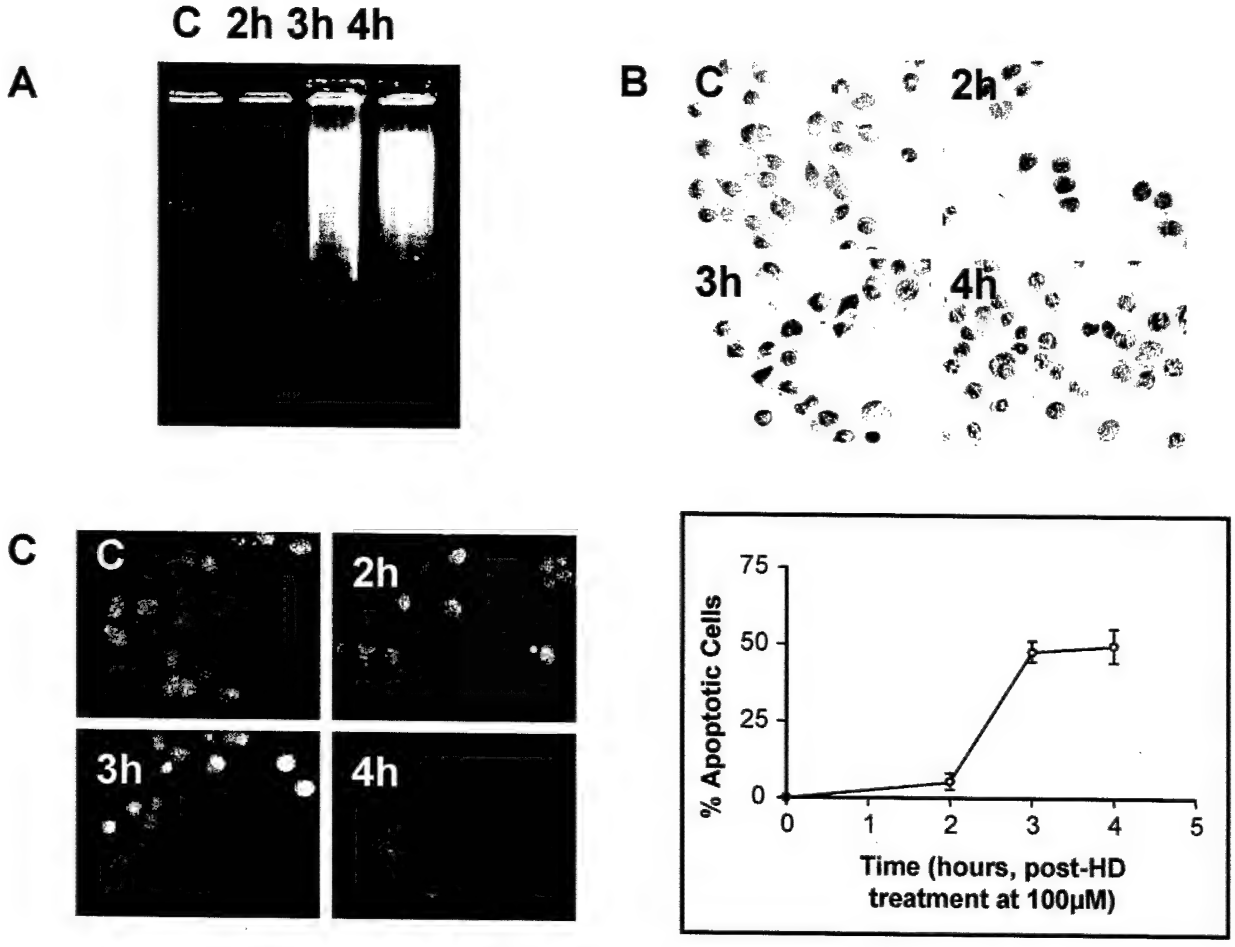
A
C 2h 3h 4h
B
C
2h
3h
4h
C
C
2h
3h
4h
% Apoptotic Cells
75
50
25
0
0
1
2
3
4
5
Time (hours, post-HD treatment at 100μM)

Fig. 18

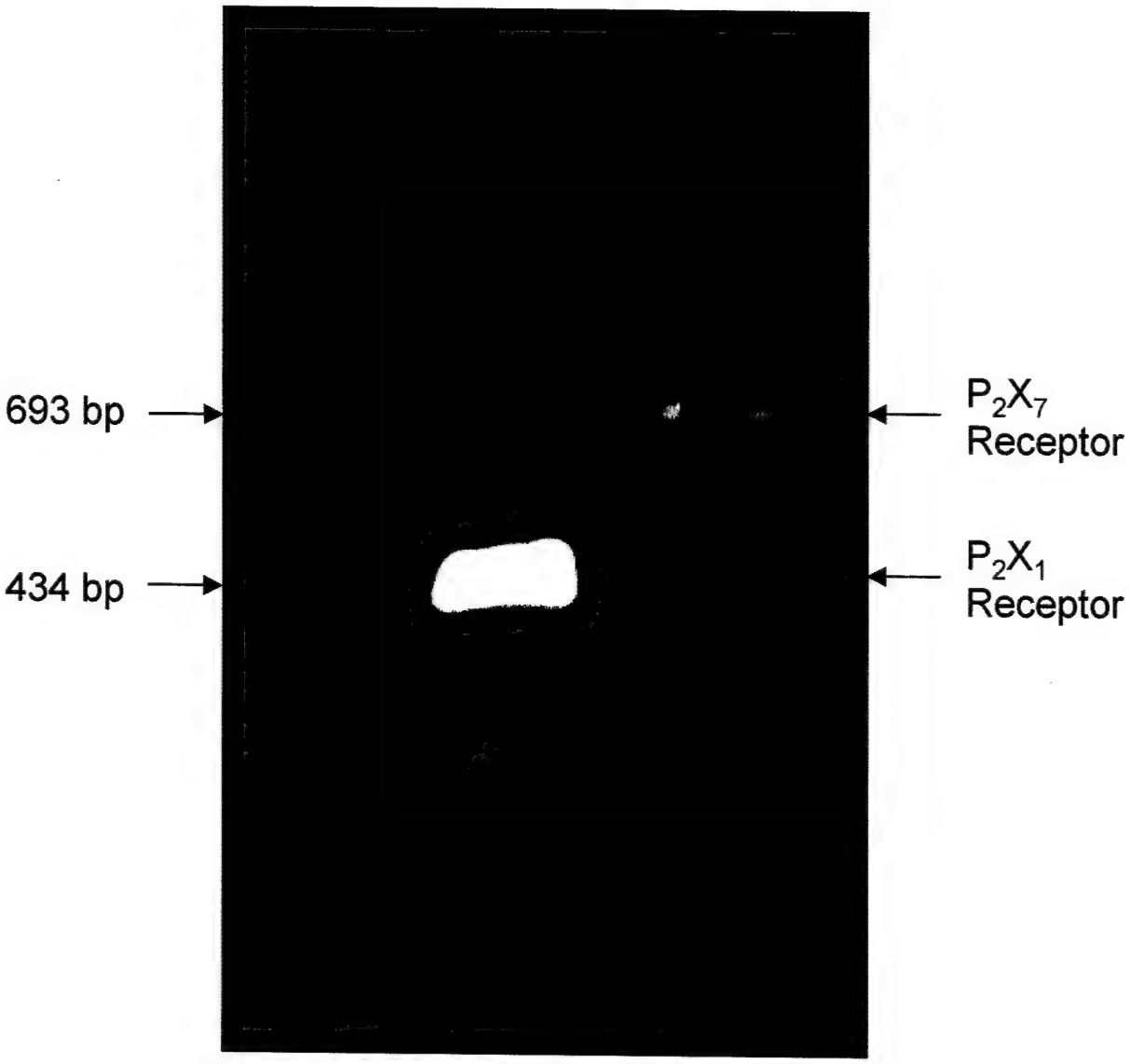

Fig. 19

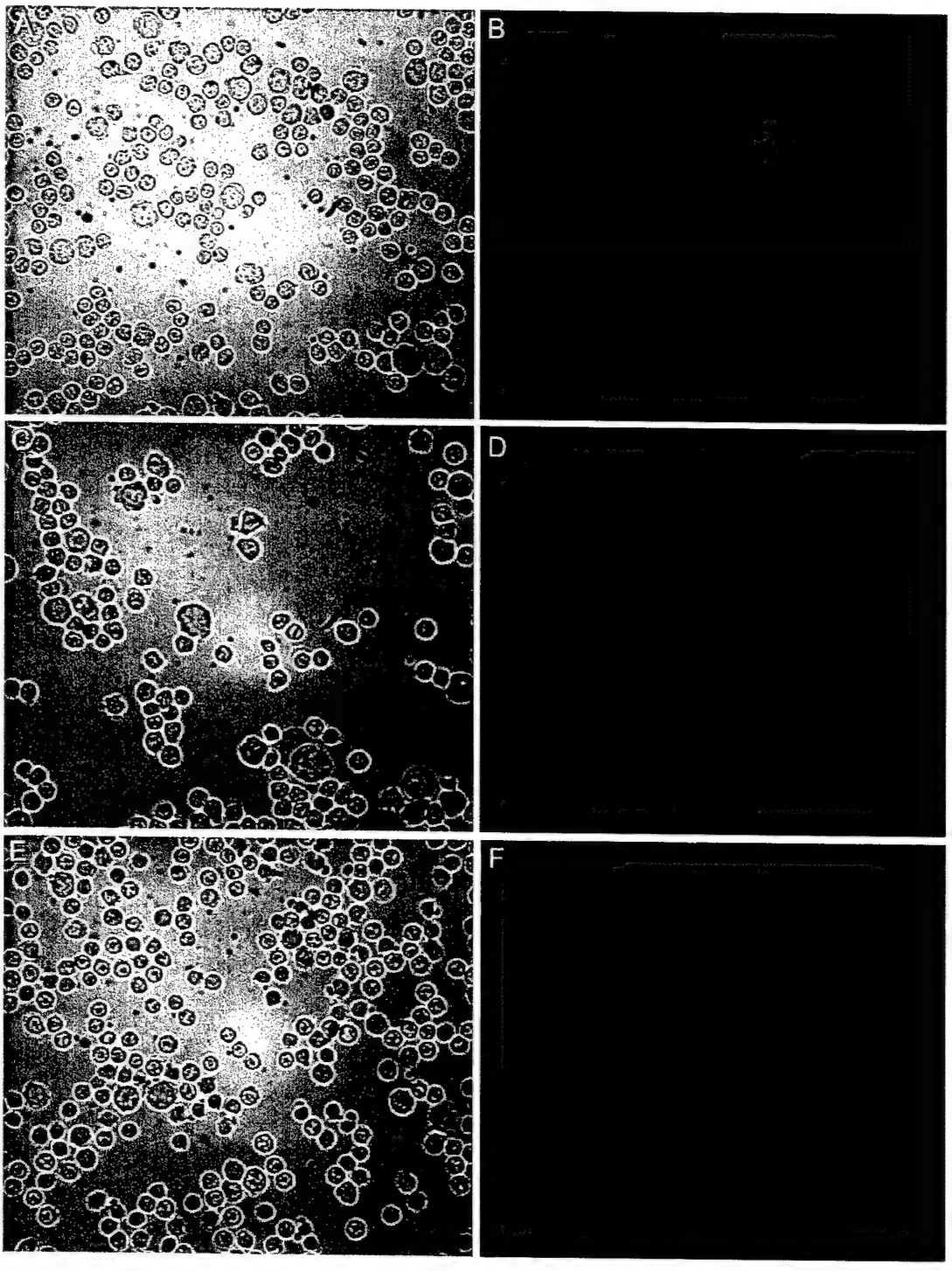

Fig. 20

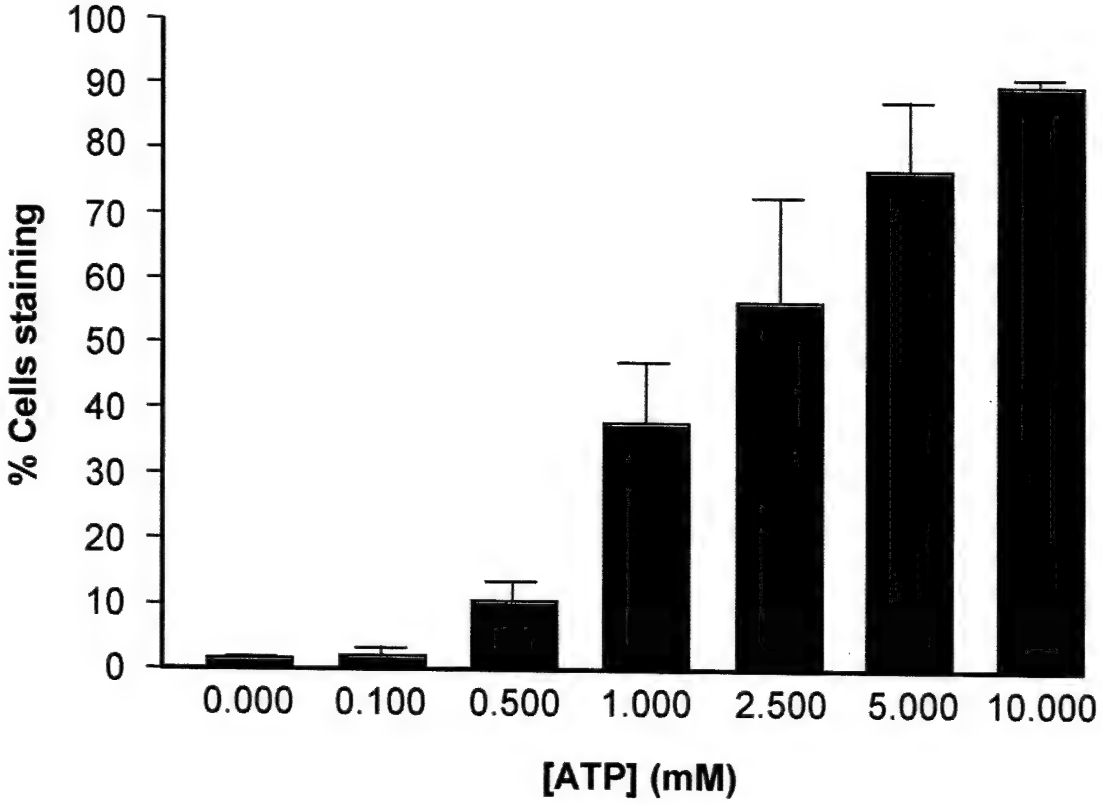
100
90
80
70
60
50
40
30
20
10
0
% Cells staining
0.000
0.100
0.500
1.000
2.500
5.000
10.000
[ATP] (mM)

Fig. 21

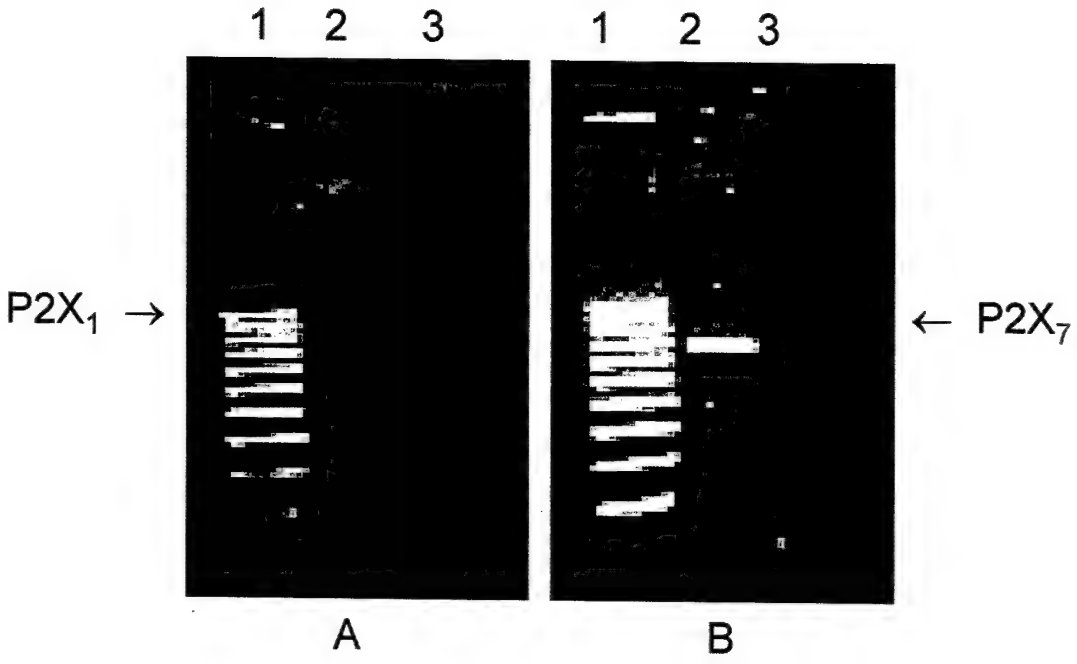

Fig. 22

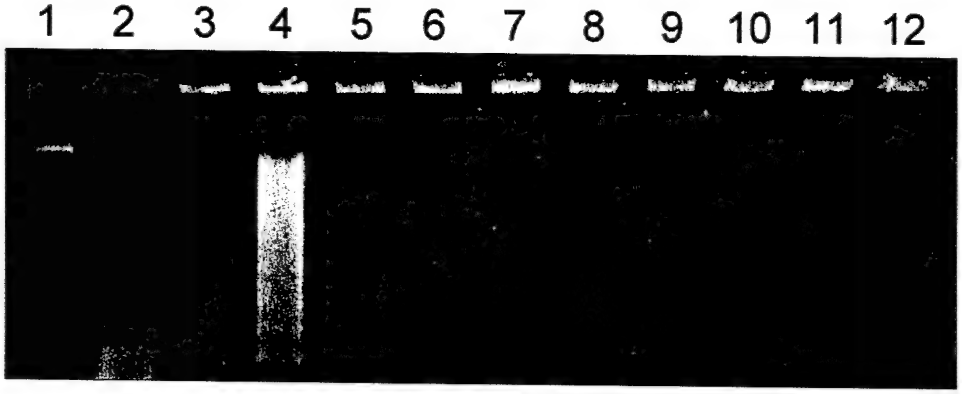
1 2 3 4 5 6 7 8 9 10 11 12
HD (μM) 0 200 400 600 0 200 400 600 0 200 400 600
300 μM oATP + + + +
500 μM oATP + + + +

Fig. 23

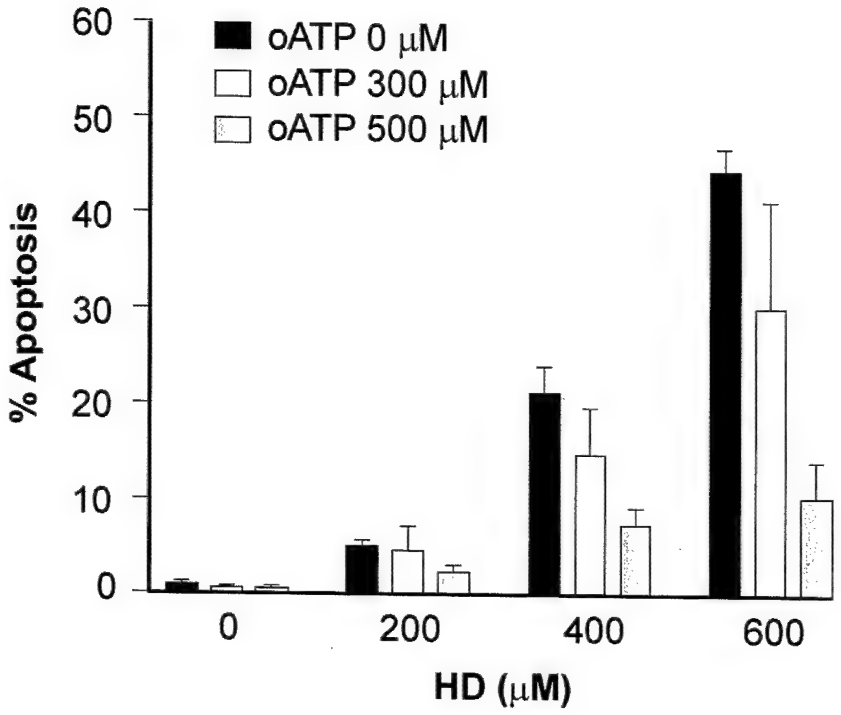
oATP 0 μM
oATP 300 μM
oATP 500 μM
% Apoptosis
60
50
40
30
20
10
0
0
200
400
600
HD (μM)

Fig. 24

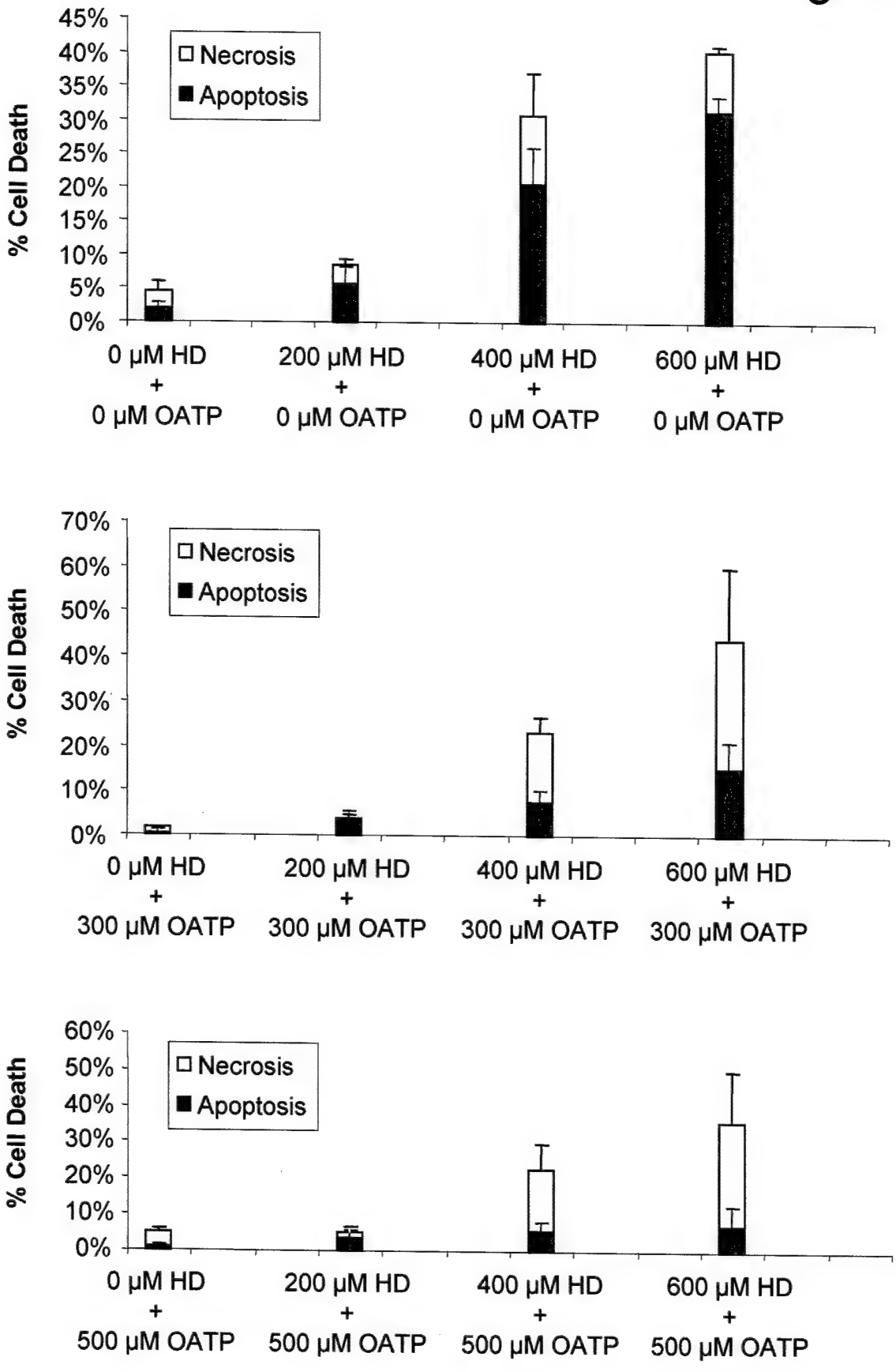
% Cell Death
Necrosis
Apoptosis
45%
40%
35%
30%
25%
20%
15%
10%
5%
0%
0 µM HD + 0 µM OATP
200 µM HD + 0 µM OATP
400 µM HD + 0 µM OATP
600 µM HD + 0 µM OATP
% Cell Death
Necrosis
Apoptosis
70%
60%
50%
40%
30%
20%
10%
0%
0 µM HD + 300 µM OATP
200 µM HD + 300 µM OATP
400 µM HD + 300 µM OATP
600 µM HD + 300 µM OATP
% Cell Death
Necrosis
Apoptosis
60%
50%
40%
30%
20%
10%
0%
0 µM HD + 500 µM OATP
200 µM HD + 500 µM OATP
400 µM HD + 500 µM OATP
600 µM HD + 500 µM OATP

Fig. 25

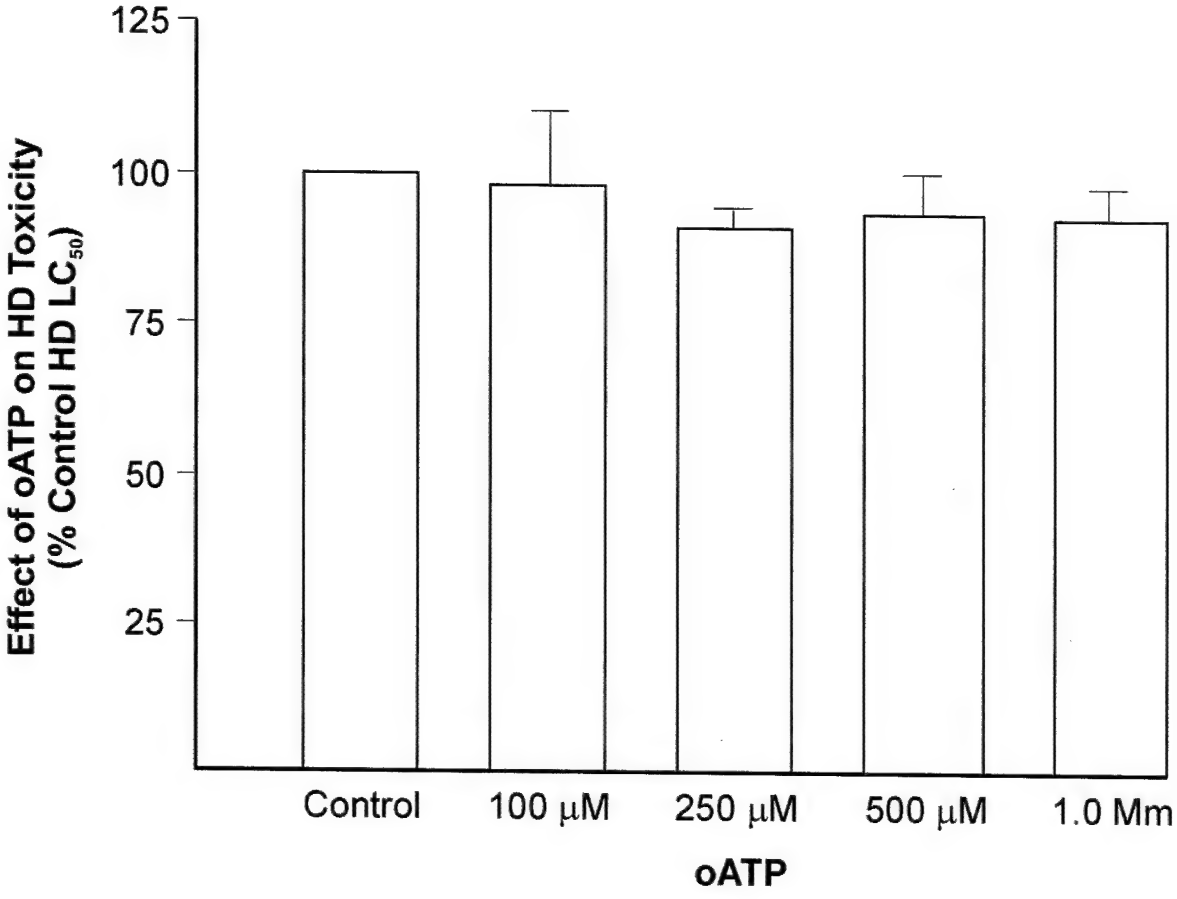
125
100
75
50
25
Effect of oATP on HD Toxicity
(% Control HD LC50)
Control
100 μM
250 μM
500 μM
1.0 Mm
oATP

Fig. 26

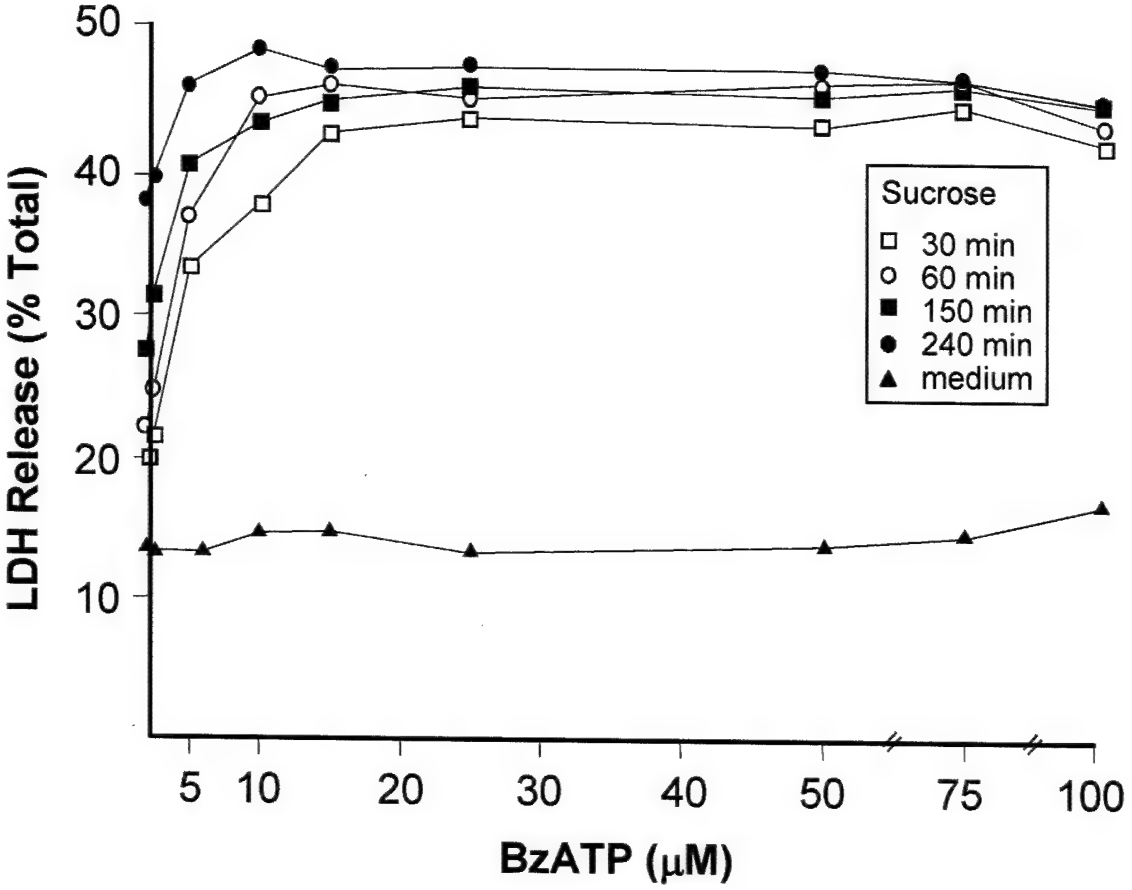
LDH Release (% Total)
50
40
30
20
10
5
10
20
30
40
50
75
100
BzATP (μM)
Sucrose
30 min
60 min
150 min
240 min
medium

Fig. 27

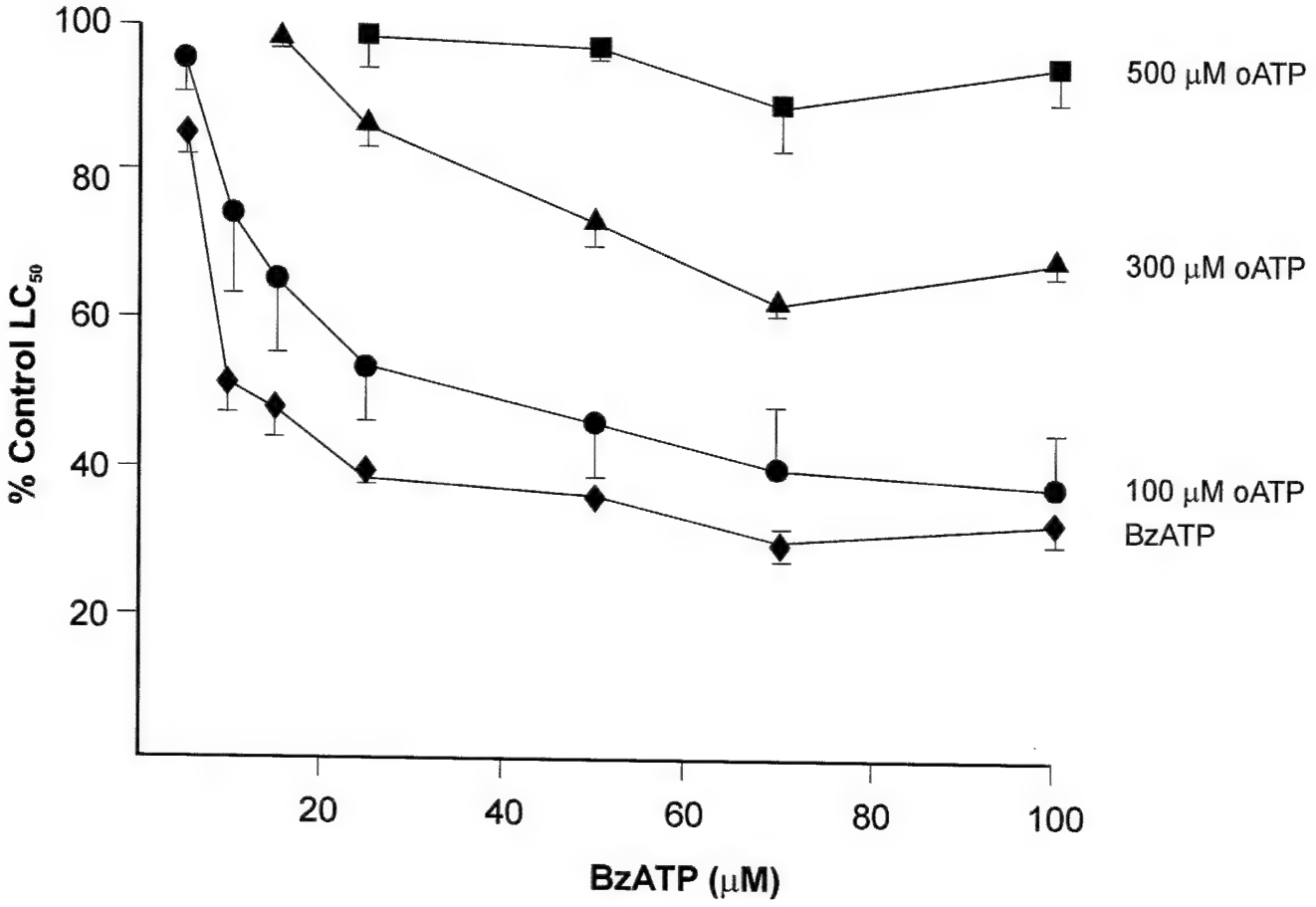
100
80
60
40
20
% Control LC50
20
40
60
80
100
BzATP (μM)
500 μM oATP
300 μM oATP
100 μM oATP
BzATP

Fig. 28

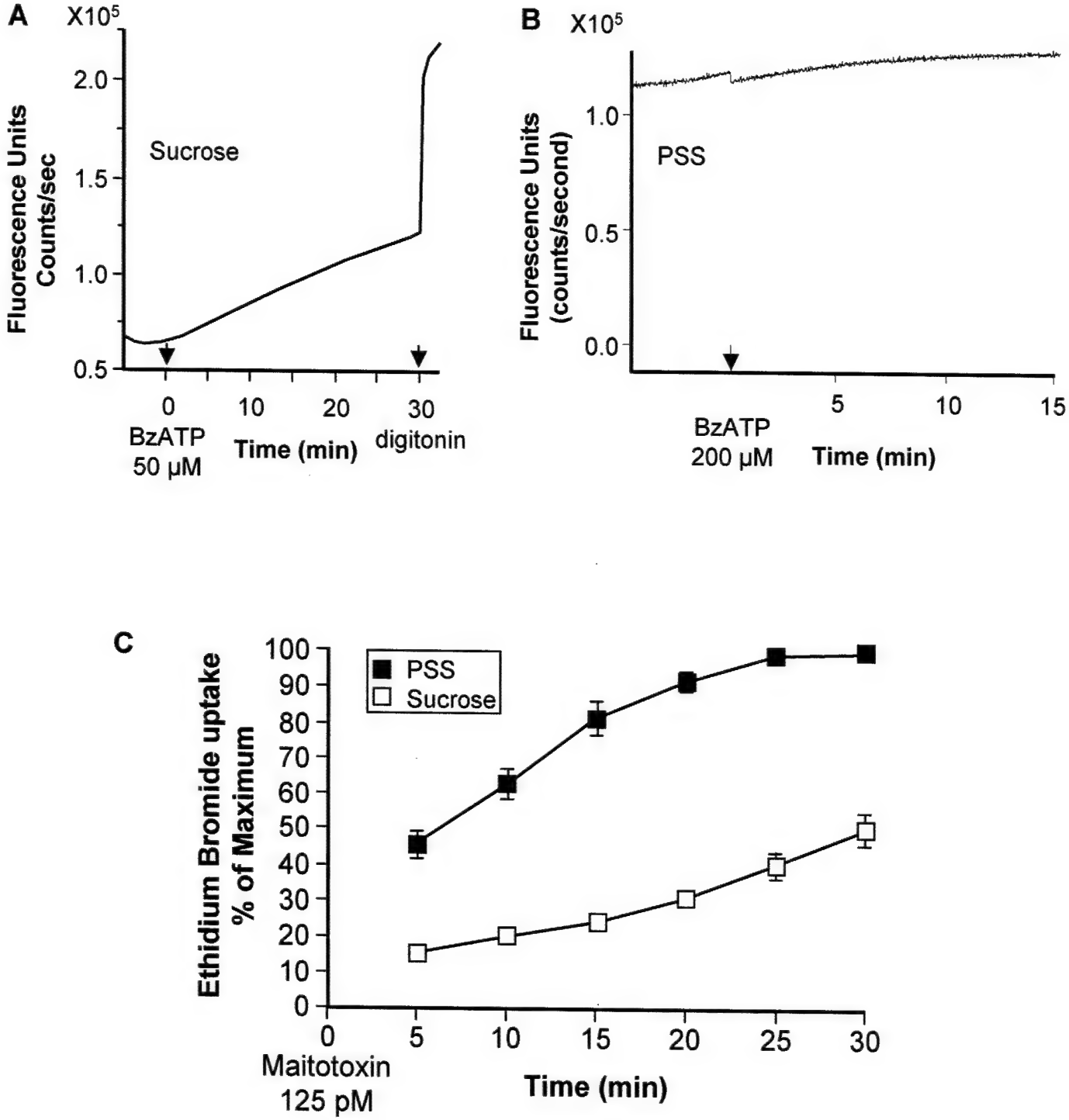
A
X10^5
2.0
1.5
1.0
0.5
Fluorescence Units
Counts/sec
Sucrose
0
BzATP
50 µM
10
20
30
digitonin
Time (min)
B
X10^5
1.0
0.5
0.0
Fluorescence Units
(counts/second)
PSS
5
10
15
BzATP
200 µM
Time (min)
C
100
90
80
70
60
50
40
30
20
10
0
Ethidium Bromide uptake
% of Maximum
PSS
Sucrose
0
Maitotoxin
125 pM
5
10
15
20
25
30
Time (min)

Fig. 29

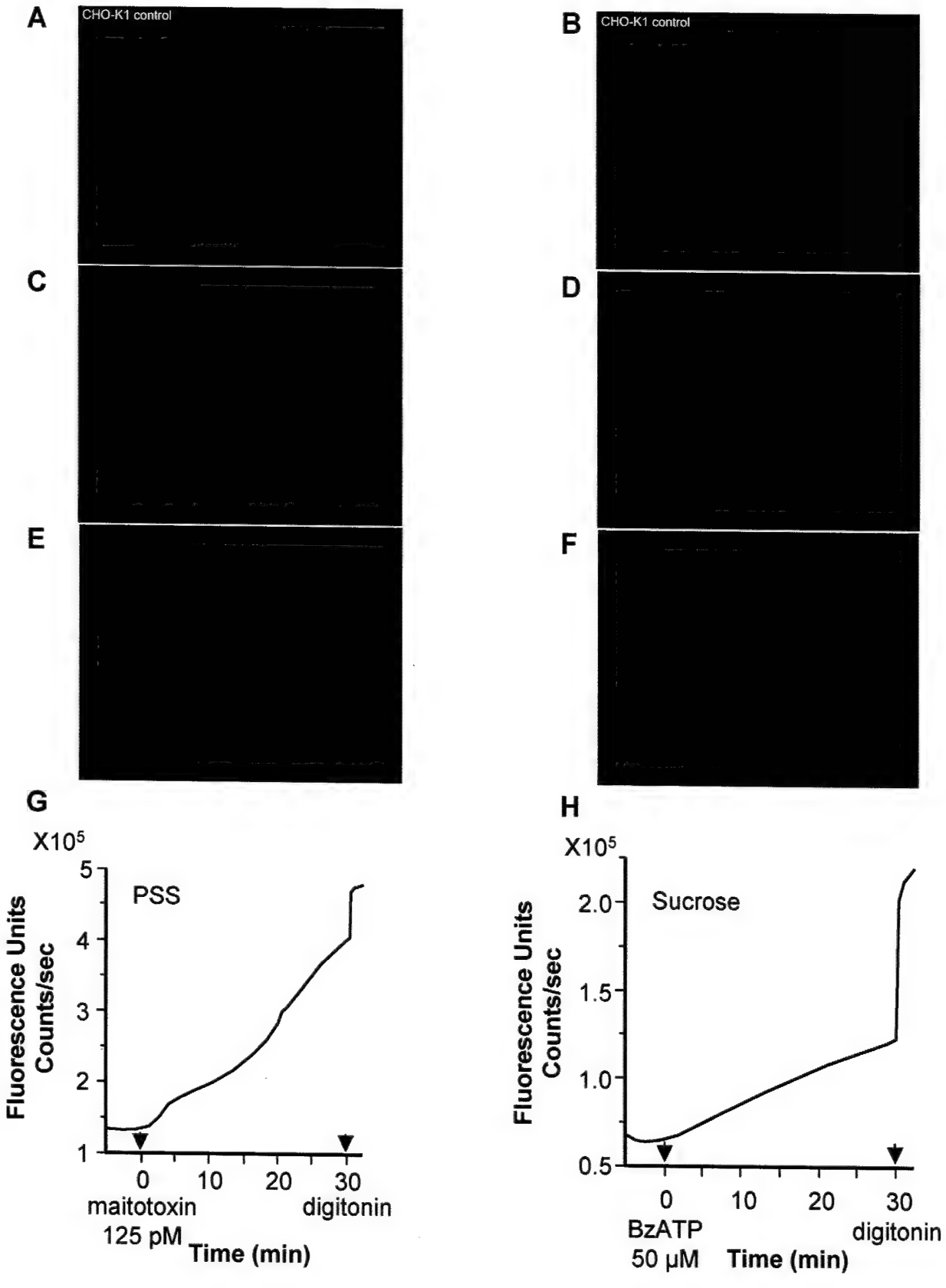
A
CHO-K1 control
B
CHO-K1 control
C
D
E
F
G
X10^5
5
4
3
2
1
PSS
Fluorescence Units
Counts/sec
0
10
20
30
maitotoxin
125 pM
digitonin
Time (min)
H
X10^5
2.0
1.5
1.0
0.5
Sucrose
Fluorescence Units
Counts/sec
0
10
20
30
BzATP
50 µM
digitonin
Time (min)

Fig. 30

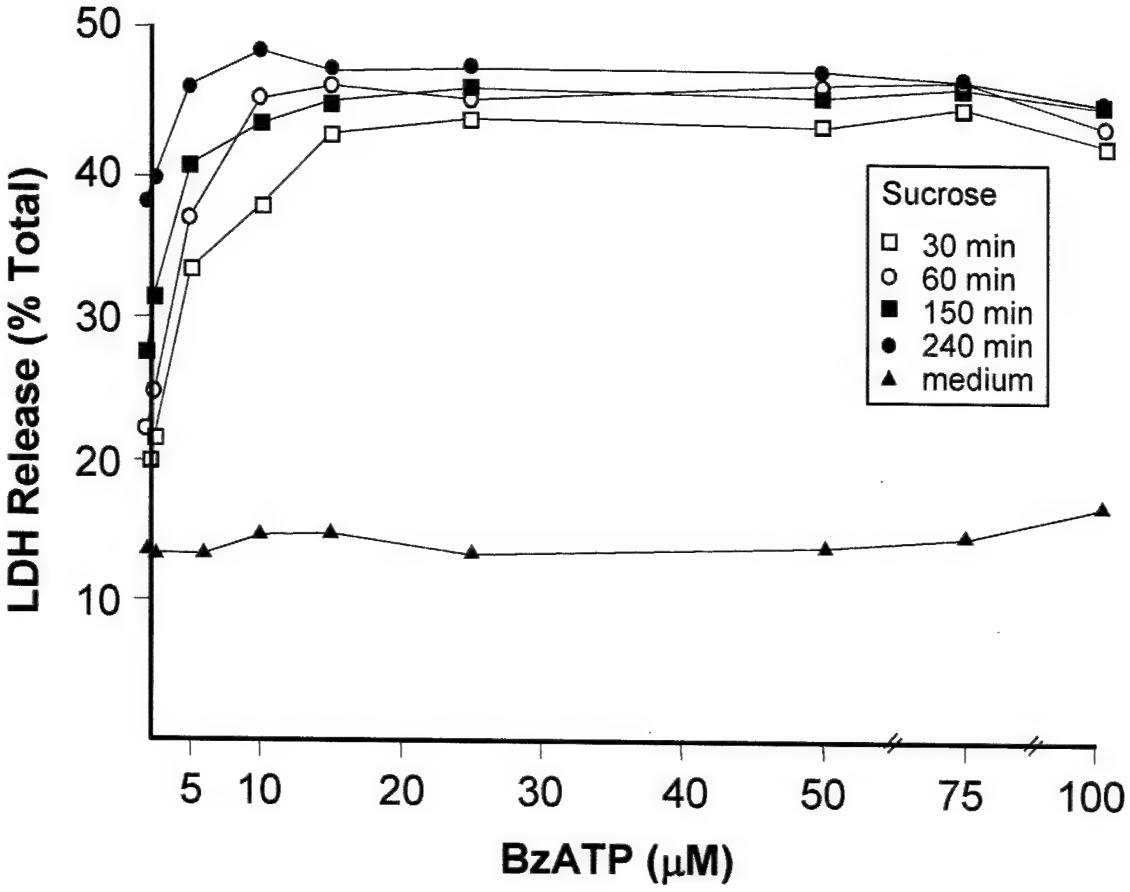
LDH Release (% Total)
50
40
30
20
10
5
10
20
30
40
50
75
100
BzATP (μM)
Sucrose
30 min
60 min
150 min
240 min
medium

Fig. 31

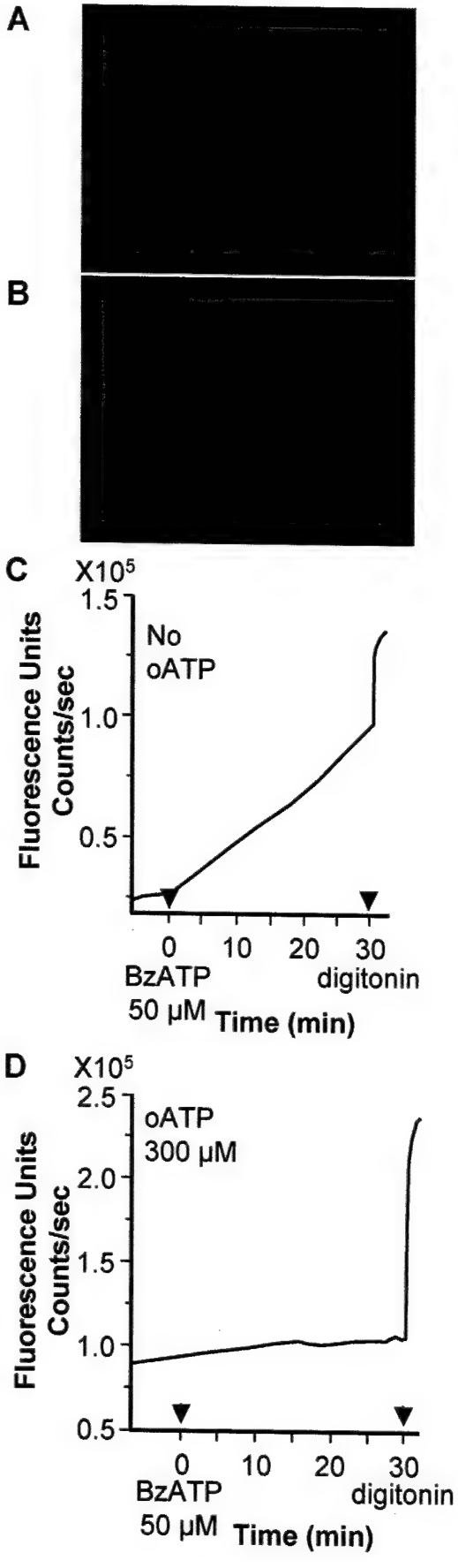
A
B
C
X10^5
1.5
1.0
0.5
Fluorescence Units
Counts/sec
No
oATP
0
10
20
30
BzATP
50 μM
digitonin
Time (min)
D
X10^5
2.5
2.0
1.5
1.0
0.5
Fluorescence Units
Counts/sec
oATP
300 μM
0
10
20
30
BzATP
50 μM
digitonin
Time (min)

Fig. 32

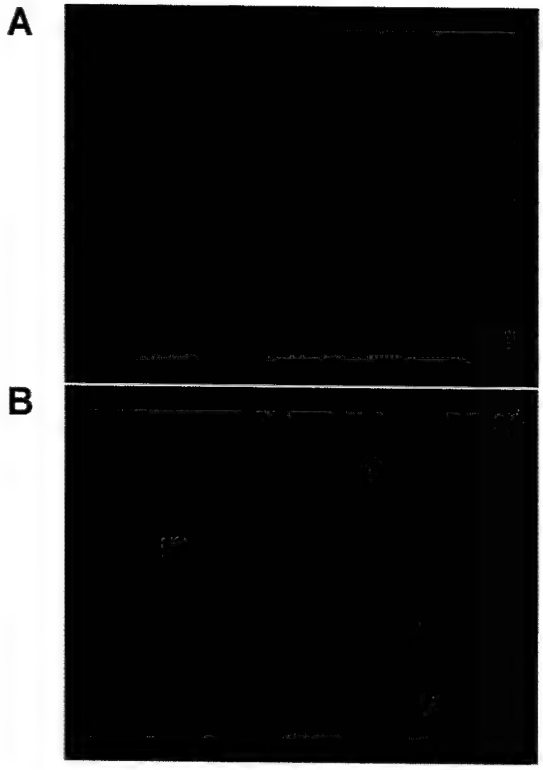
A
B

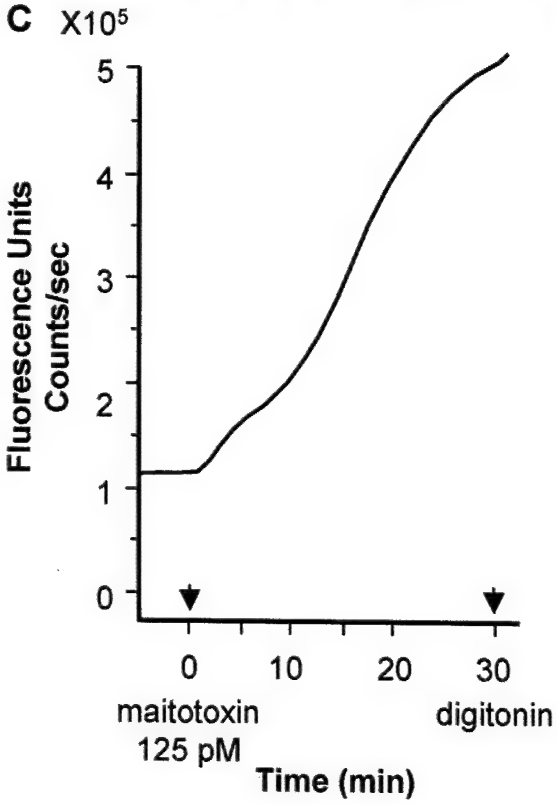
C
X10^5
5
4
3
2
1
0
Fluorescence Units
Counts/sec
0
10
20
30
maitotoxin
125 pM
digitonin
Time (min)

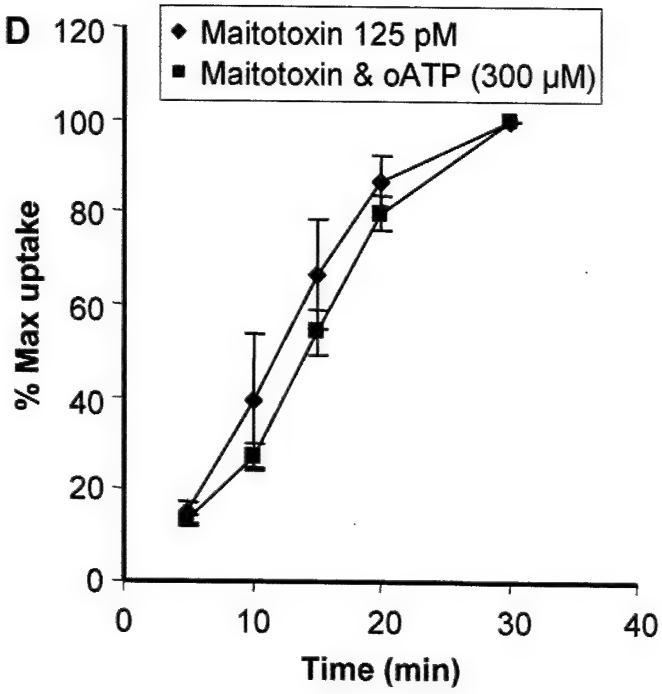
D
120
100
80
60
40
20
0
% Max uptake
Maitotoxin 125 pM
Maitotoxin & oATP (300 µM)
0
10
20
30
40
Time (min)

Fig. 33

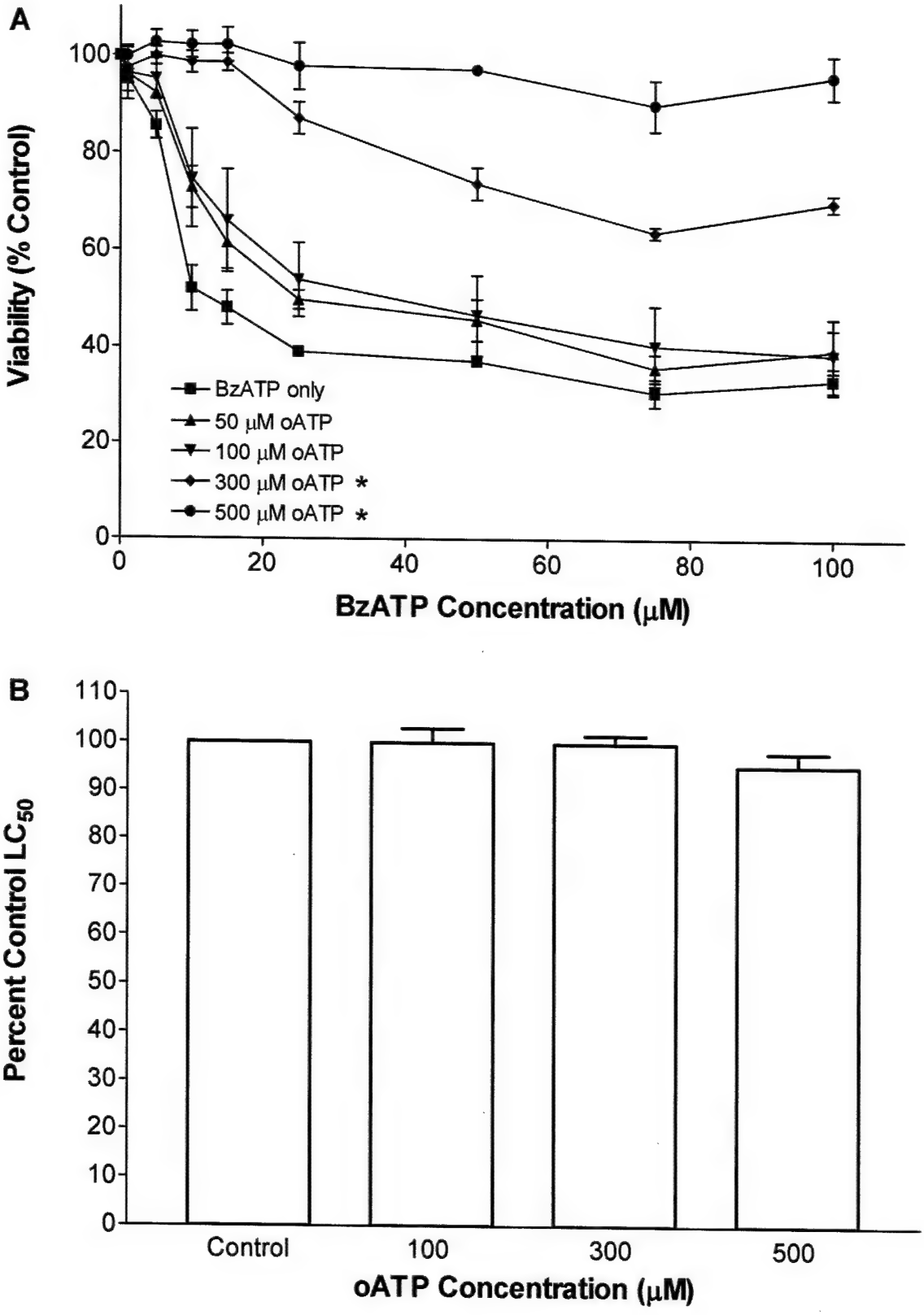
A
Viability (% Control)
100
80
60
40
20
0
0
20
40
60
80
100
BzATP Concentration (μM)
BzATP only
50 μM oATP
100 μM oATP
300 μM oATP *
500 μM oATP *
B
Percent Control LC50
110
100
90
80
70
60
50
40
30
20
10
0
Control
100
300
500
oATP Concentration (μM)

Fig. 34

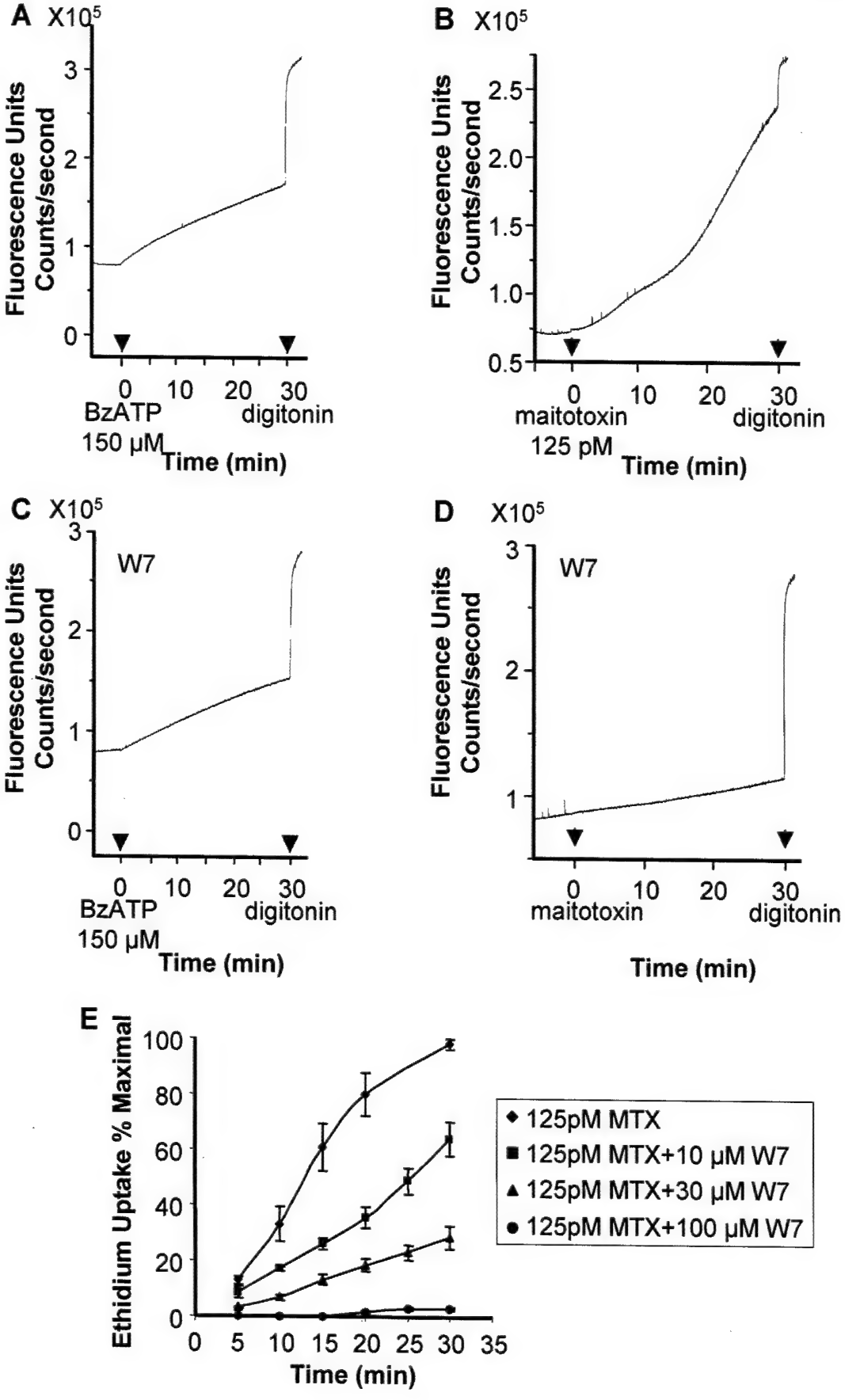
A
X10^5
Fluorescence Units
Counts/second
BzATP
150 µM
digitonin
Time (min)
B
X10^5
Fluorescence Units
Counts/second
maitotoxin
125 pM
digitonin
Time (min)
C
X10^5
W7
Fluorescence Units
Counts/second
BzATP
150 µM
digitonin
Time (min)
D
X10^5
W7
Fluorescence Units
Counts/second
maitotoxin
digitonin
Time (min)
E
Ethidium Uptake % Maximal
Time (min)
125pM MTX
125pM MTX+10 µM W7
125pM MTX+30 µM W7
125pM MTX+100 µM W7

Fig. 35

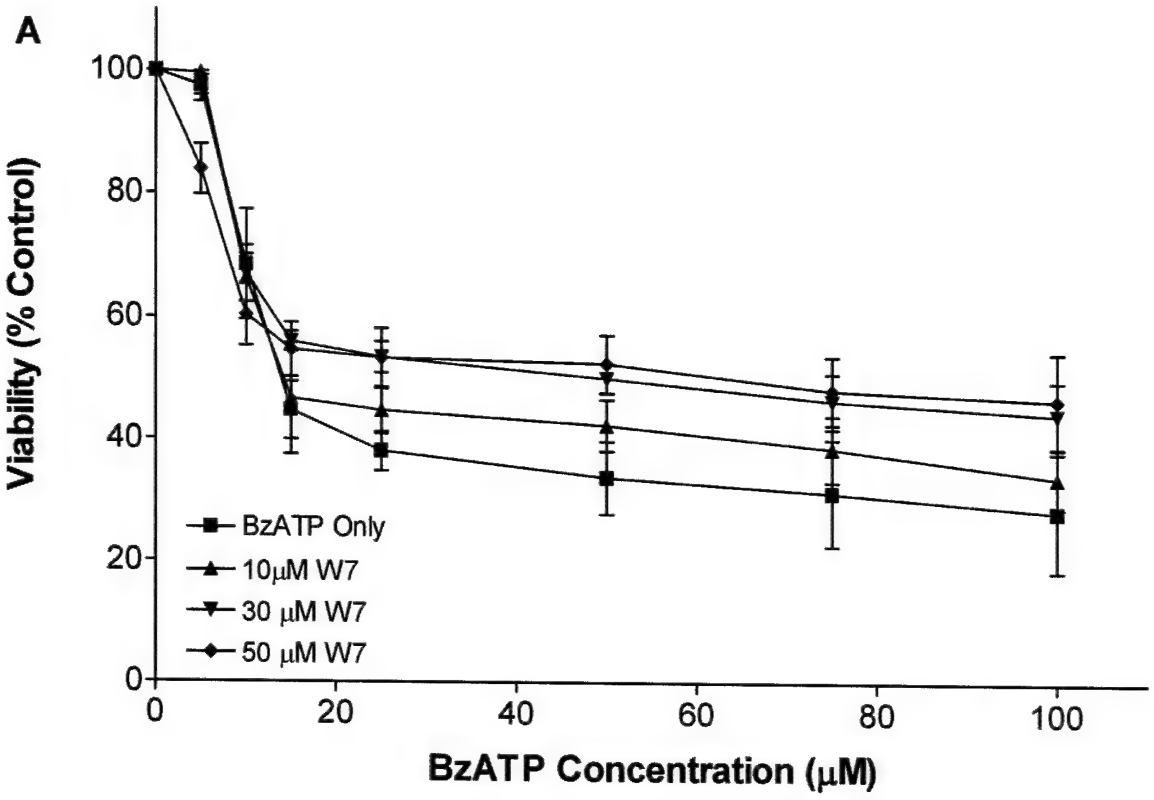
A
Viability (% Control)
100
80
60
40
20
0
0
20
40
60
80
100
BzATP Concentration (μM)
BzATP Only
10μM W7
30 μM W7
50 μM W7

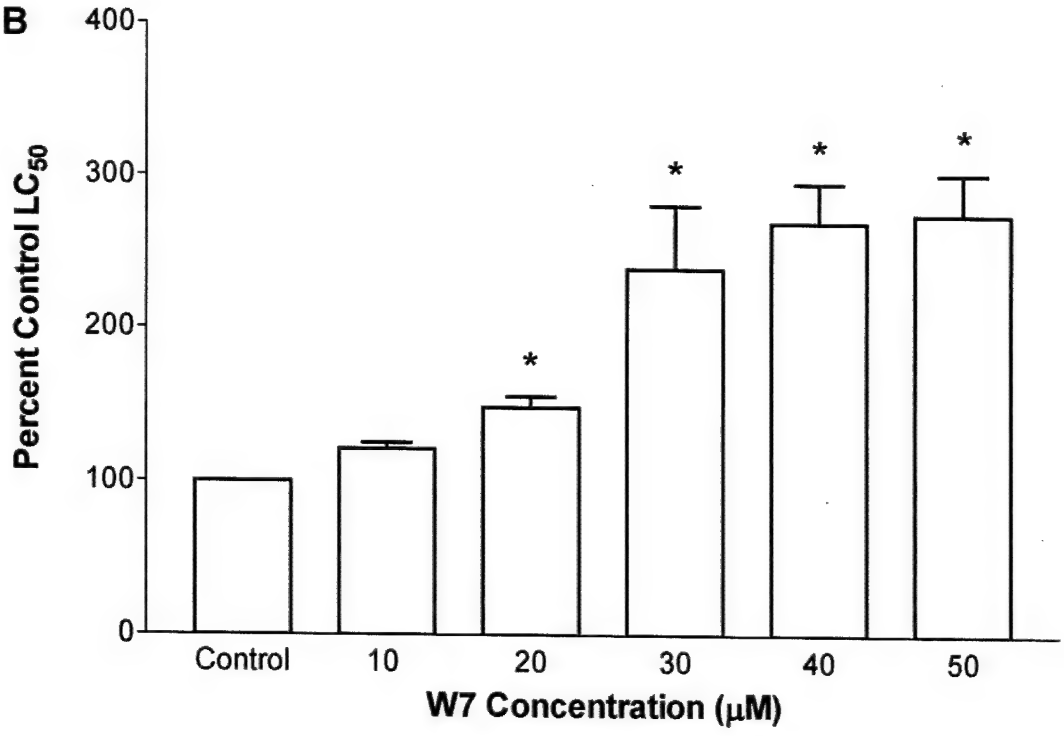
B
Percent Control LC50
400
300
200
100
0
*
*
*
Control
10
20
30
40
50
W7 Concentration (μM)

Fig. 36

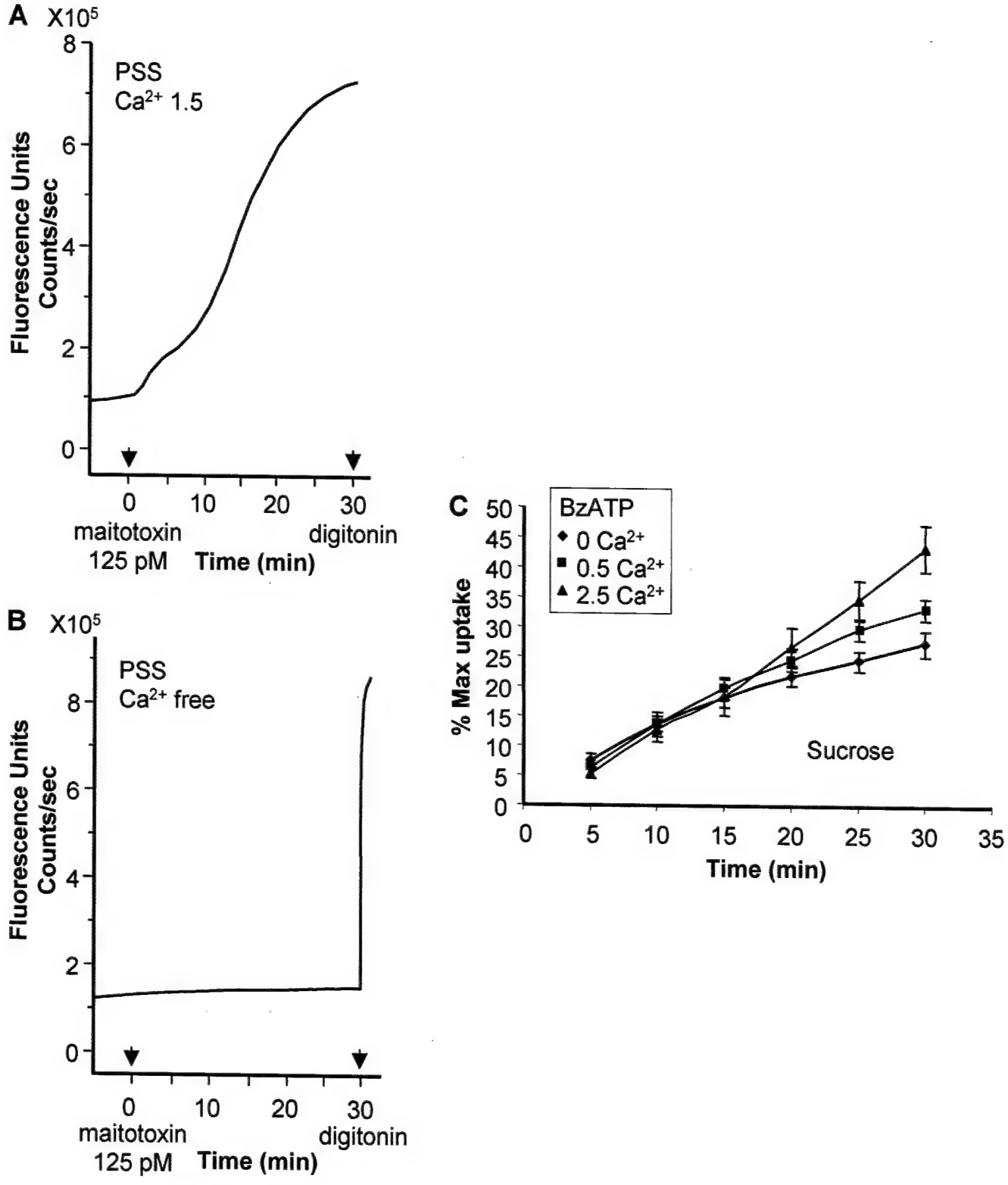
A
X10^5
PSS
Ca2+ 1.5
Fluorescence Units
Counts/sec
maitotoxin
125 pM
Time (min)
digitonin
B
X10^5
PSS
Ca2+ free
Fluorescence Units
Counts/sec
maitotoxin
125 pM
Time (min)
digitonin
C
BzATP
0 Ca2+
0.5 Ca2+
2.5 Ca2+
% Max uptake
Sucrose
Time (min)

Fig. 37

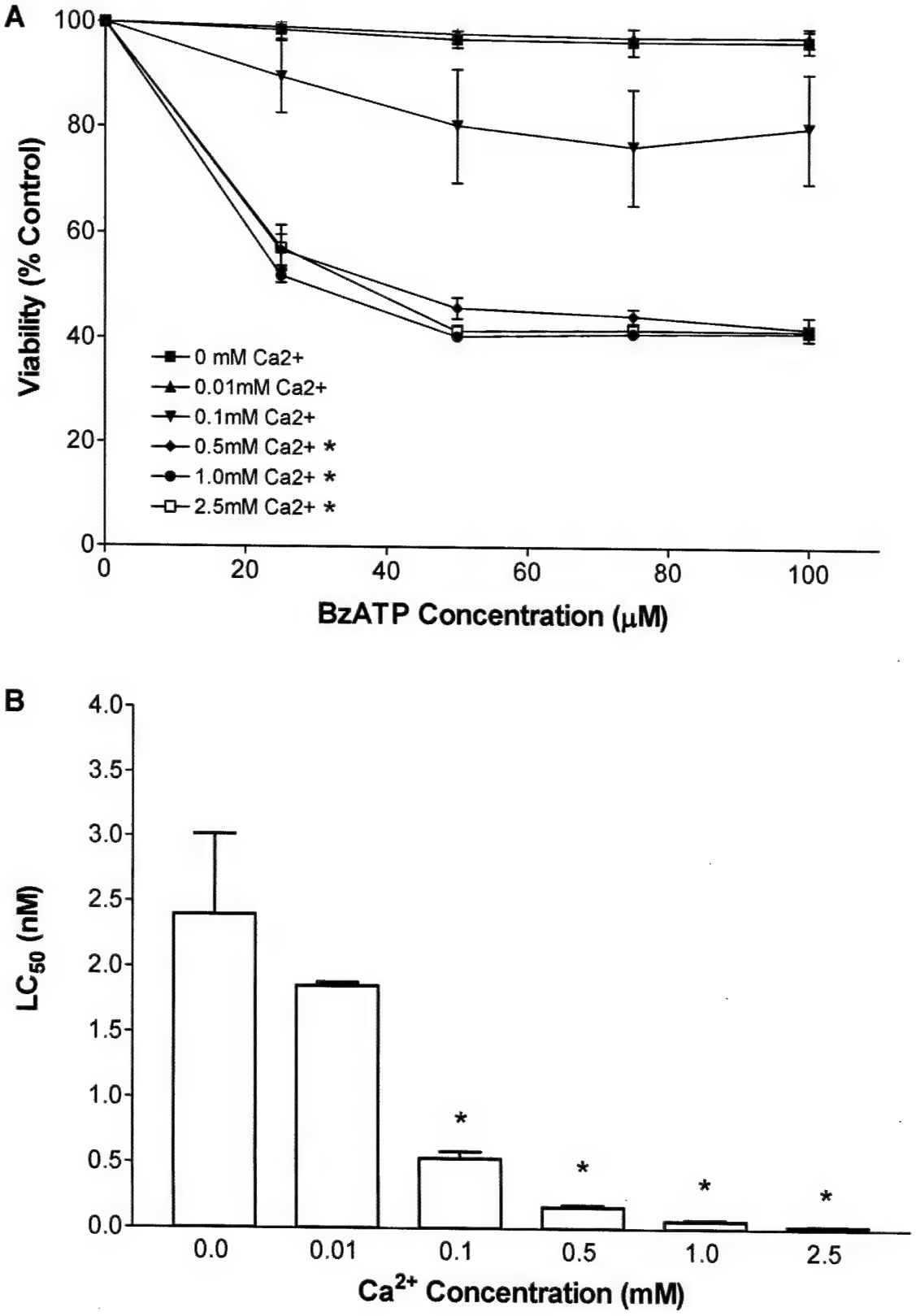
A
Viability (% Control)
100
80
60
40
20
0
0 mM Ca2+
0.01mM Ca2+
0.1mM Ca2+
0.5mM Ca2+ *
1.0mM Ca2+ *
2.5mM Ca2+ *
0
20
40
60
80
100
BzATP Concentration (μM)
B
LC50 (nM)
4.0
3.5
3.0
2.5
2.0
1.5
1.0
0.5
0.0
*
*
*
*
0.0
0.01
0.1
0.5
1.0
2.5
Ca2+ Concentration (mM)

Fig. 38

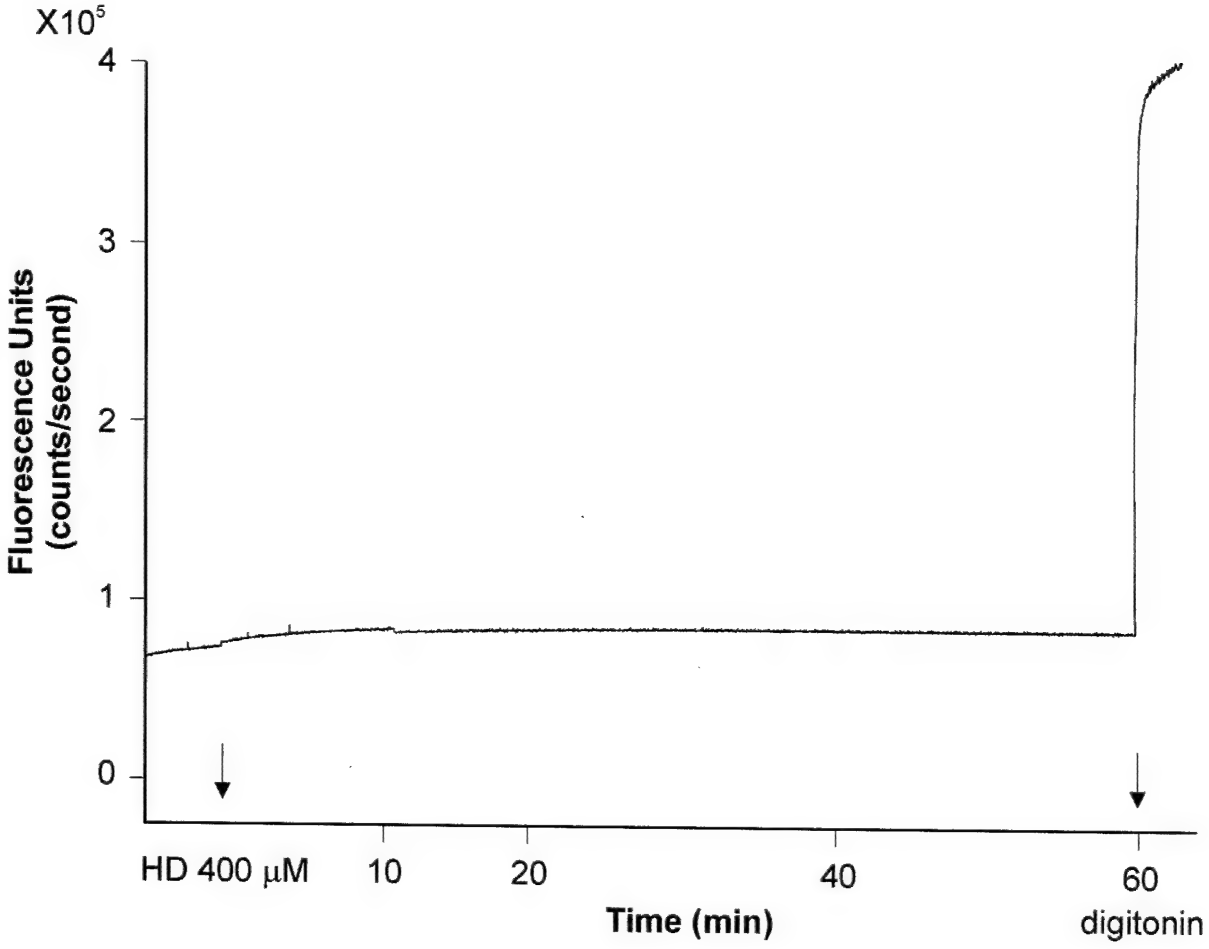
X10^5
4
3
2
1
0
Fluorescence Units
(counts/second)
HD 400 µM
10
20
40
60
digitonin
Time (min)

Fig. 39

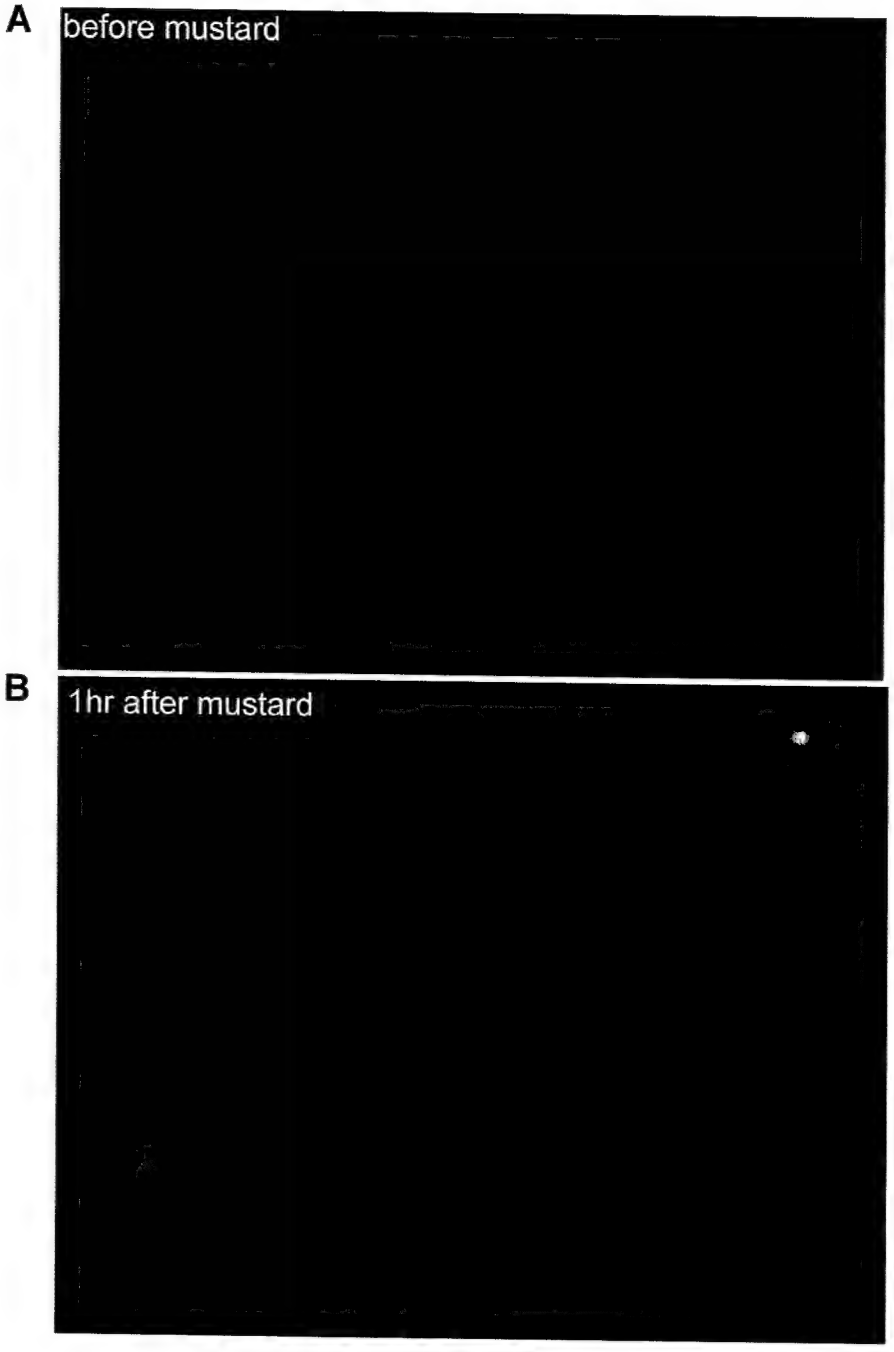

Fig. 40

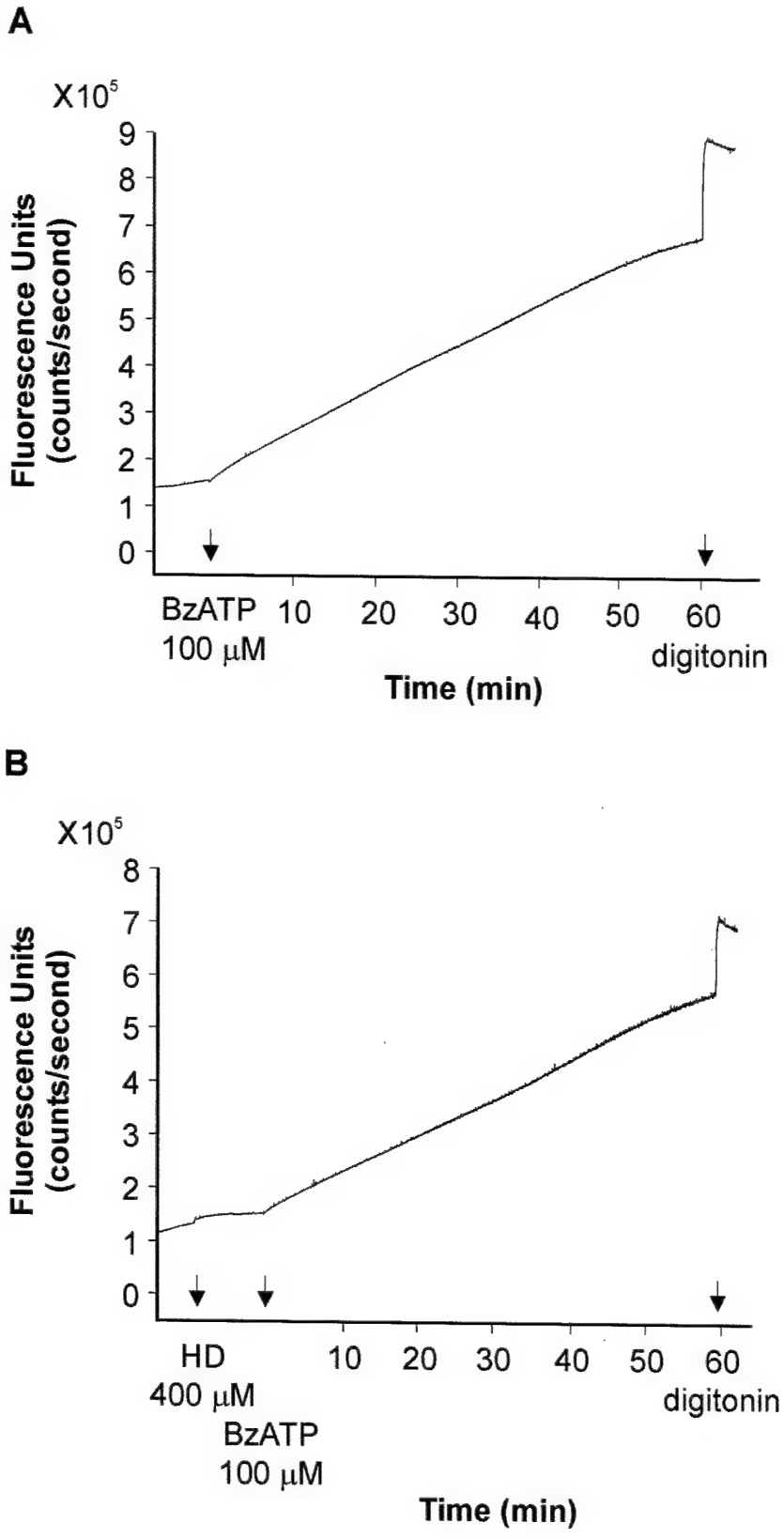
A
X10^5
9
8
7
6
5
4
3
2
1
0
Fluorescence Units
(counts/second)
BzATP
100 μM
10
20
30
40
50
60
digitonin
Time (min)
B
X10^5
8
7
6
5
4
3
2
1
0
Fluorescence Units
(counts/second)
HD
400 μM
BzATP
100 μM
10
20
30
40
50
60
digitonin
Time (min)

Fig. 41

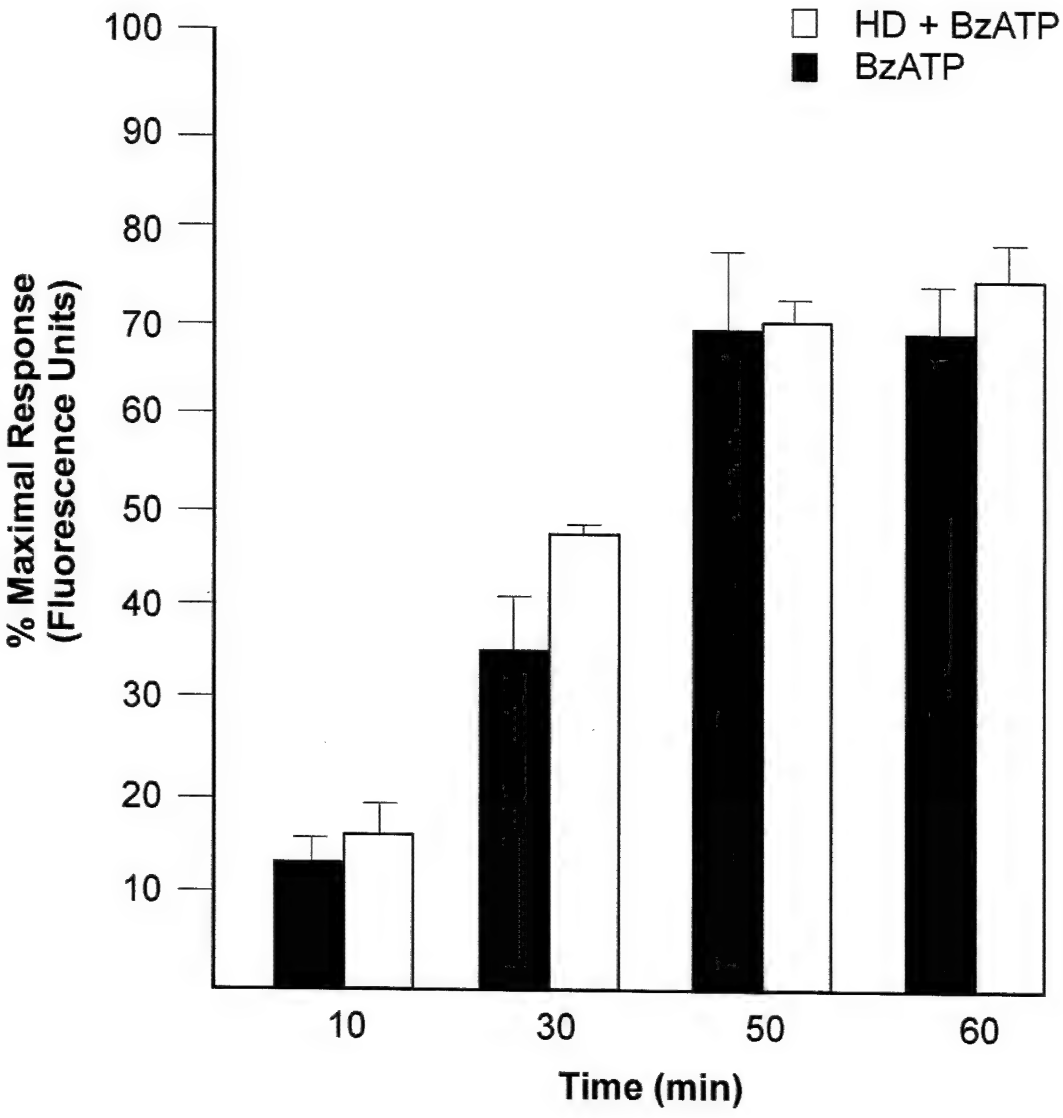
HD + BzATP
BzATP
100
90
80
70
60
50
40
30
20
10
% Maximal Response
(Fluorescence Units)
10
30
50
60
Time (min)

Fig. 42

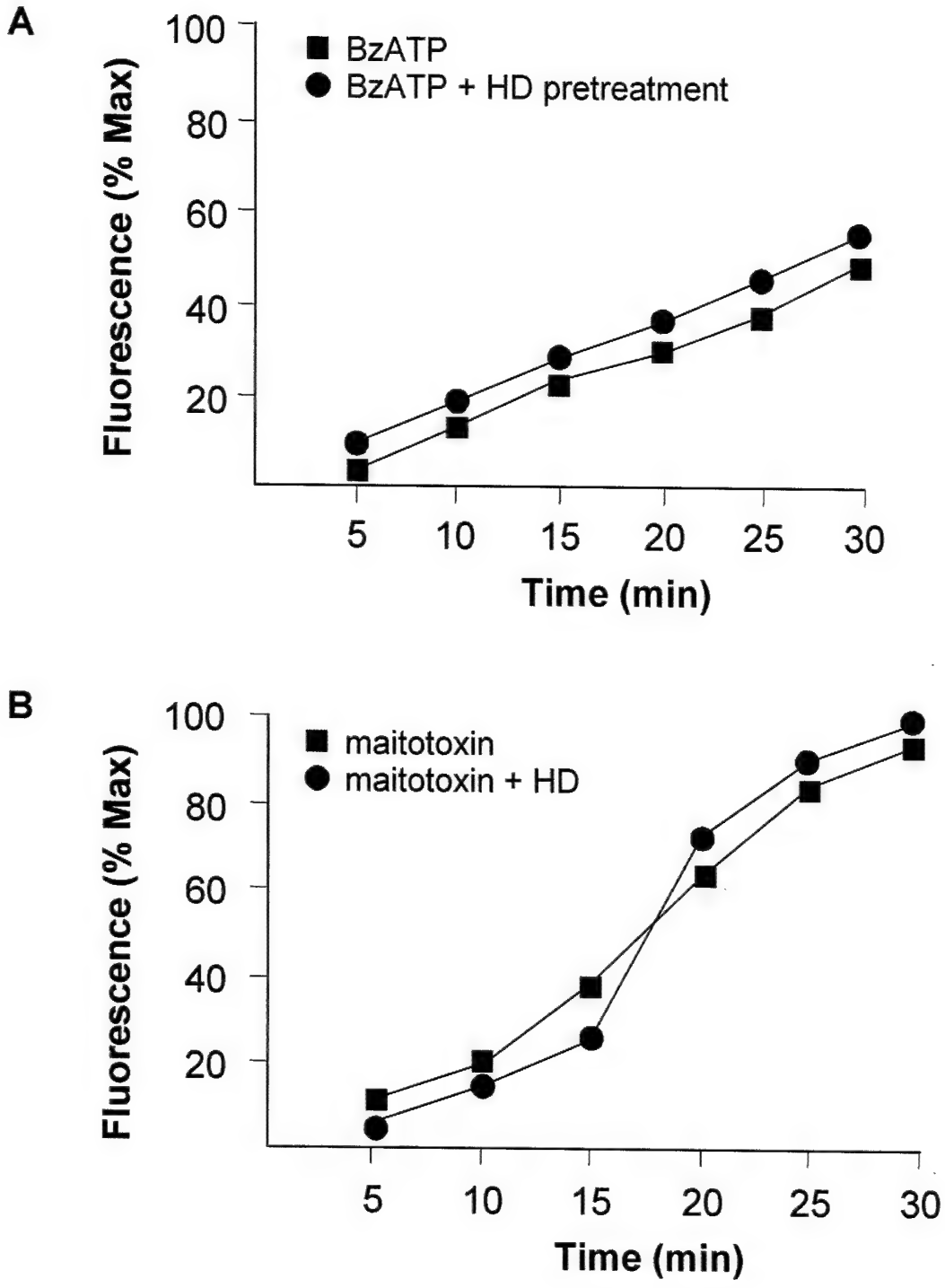
A
100
80
60
40
20
Fluorescence (% Max)
BzATP
BzATP + HD pretreatment
5
10
15
20
25
30
Time (min)
B
100
80
60
40
20
Fluorescence (% Max)
maitotoxin
maitotoxin + HD
5
10
15
20
25
30
Time (min)

Fig. 43

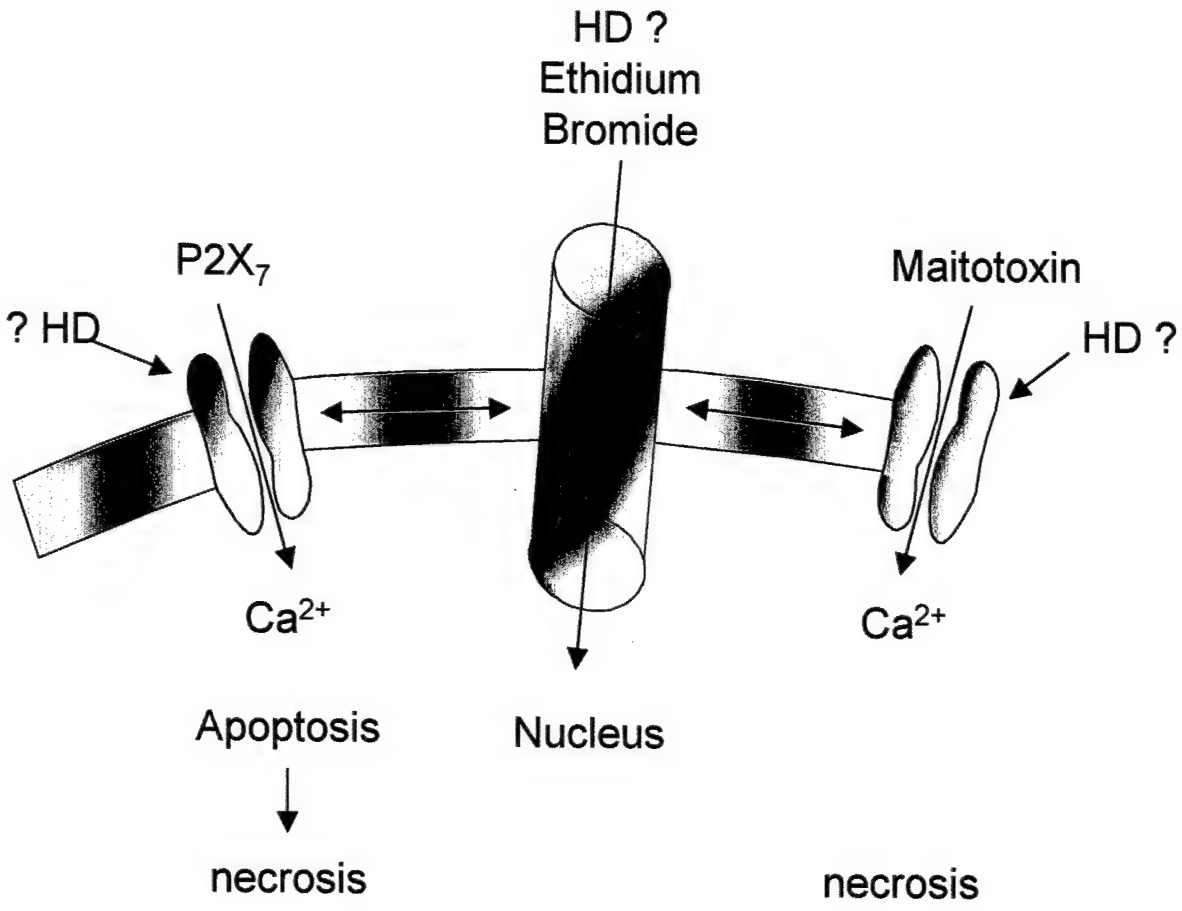
HD ?
Ethidium
Bromide
P2X7
? HD
Maitotoxin
HD ?
Ca2+
Ca2+
Apoptosis
Nucleus
necrosis
necrosis

Fig. 44

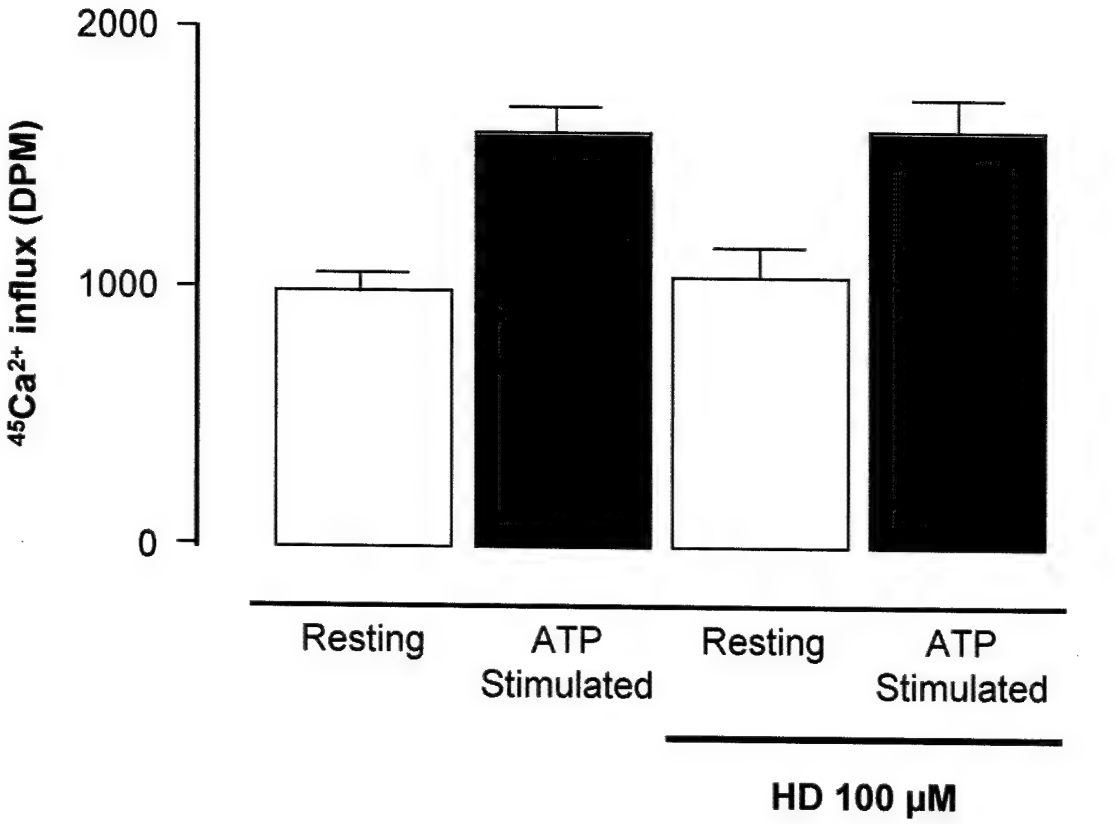
2000
1000
0
$^{45}Ca^{2+}$ influx (DPM)
Resting
ATP Stimulated
Resting
ATP Stimulated
HD 100 µM

Fig. 45

A)

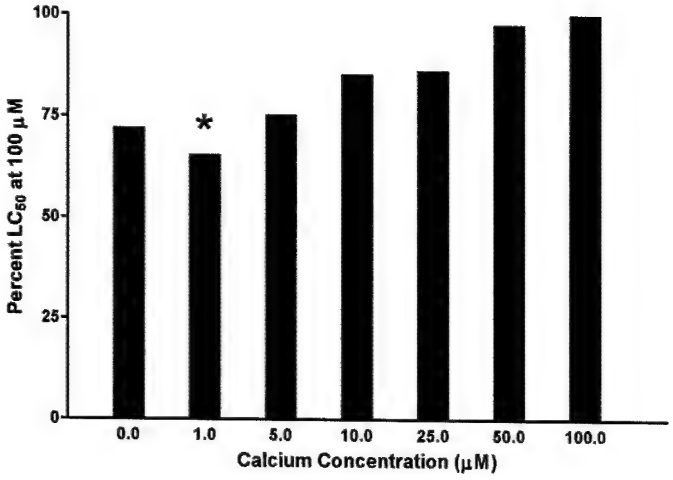
100
75
50
25
0
Percent LC_{50} at 100 µM
*
0.0
1.0
5.0
10.0
25.0
50.0
100.0
Calcium Concentration (µM)

B)

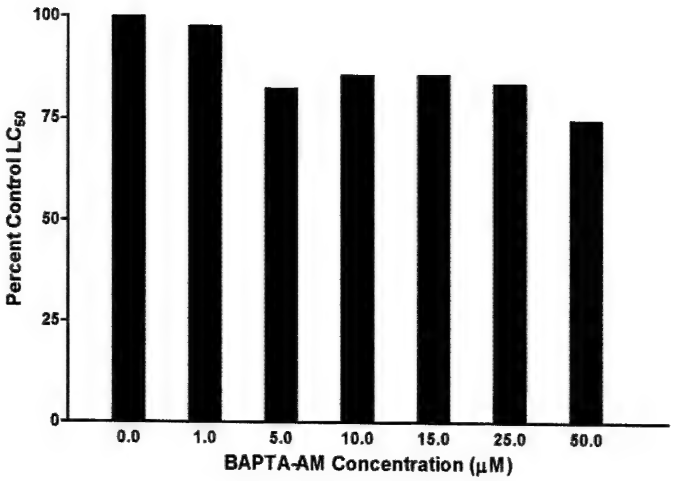
100
75
50
25
0
Percent Control LC_{50}
0.0
1.0
5.0
10.0
15.0
25.0
50.0
BAPTA-AM Concentration (µM)

C)

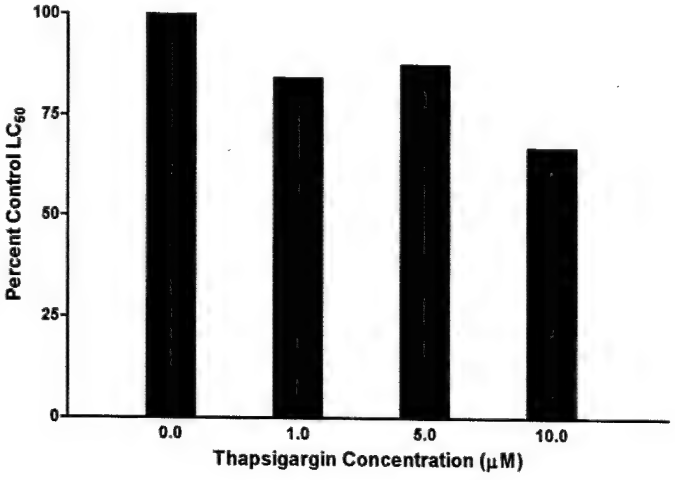
100
75
50
25
0
Percent Control LC_{50}
0.0
1.0
5.0
10.0
Thapsigargin Concentration (µM)

D)

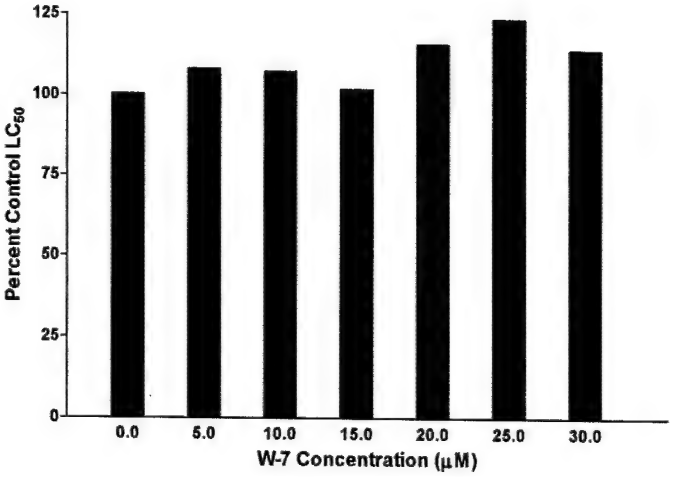
125
100
75
50
25
0
Percent Control LC_{50}
0.0
5.0
10.0
15.0
20.0
25.0
30.0
W-7 Concentration (µM)

Fig. 46

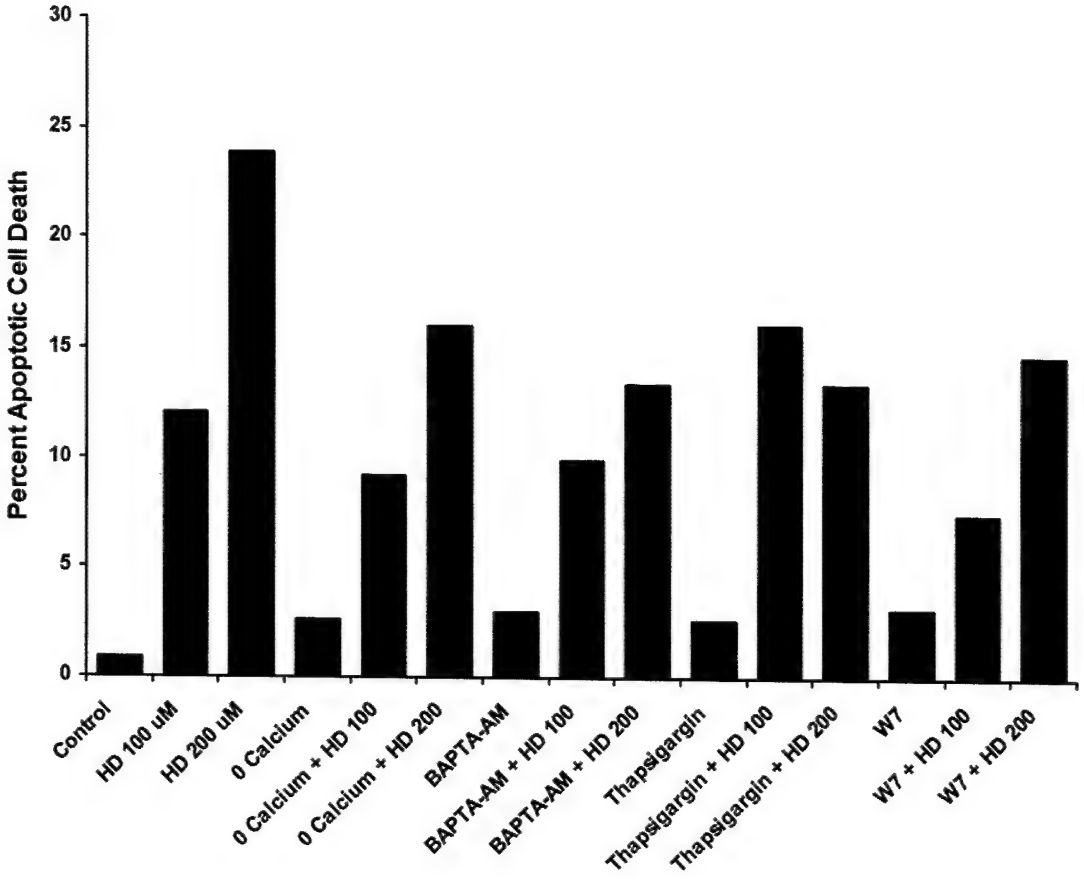
Percent Apoptotic Cell Death
30
25
20
15
10
5
0
Control
HD 100 uM
HD 200 uM
0 Calcium
0 Calcium + HD 100
0 Calcium + HD 200
BAPTA-AM
BAPTA-AM + HD 100
BAPTA-AM + HD 200
Thapsigargin
Thapsigargin + HD 100
Thapsigargin + HD 200
W7
W7 + HD 100
W7 + HD 200

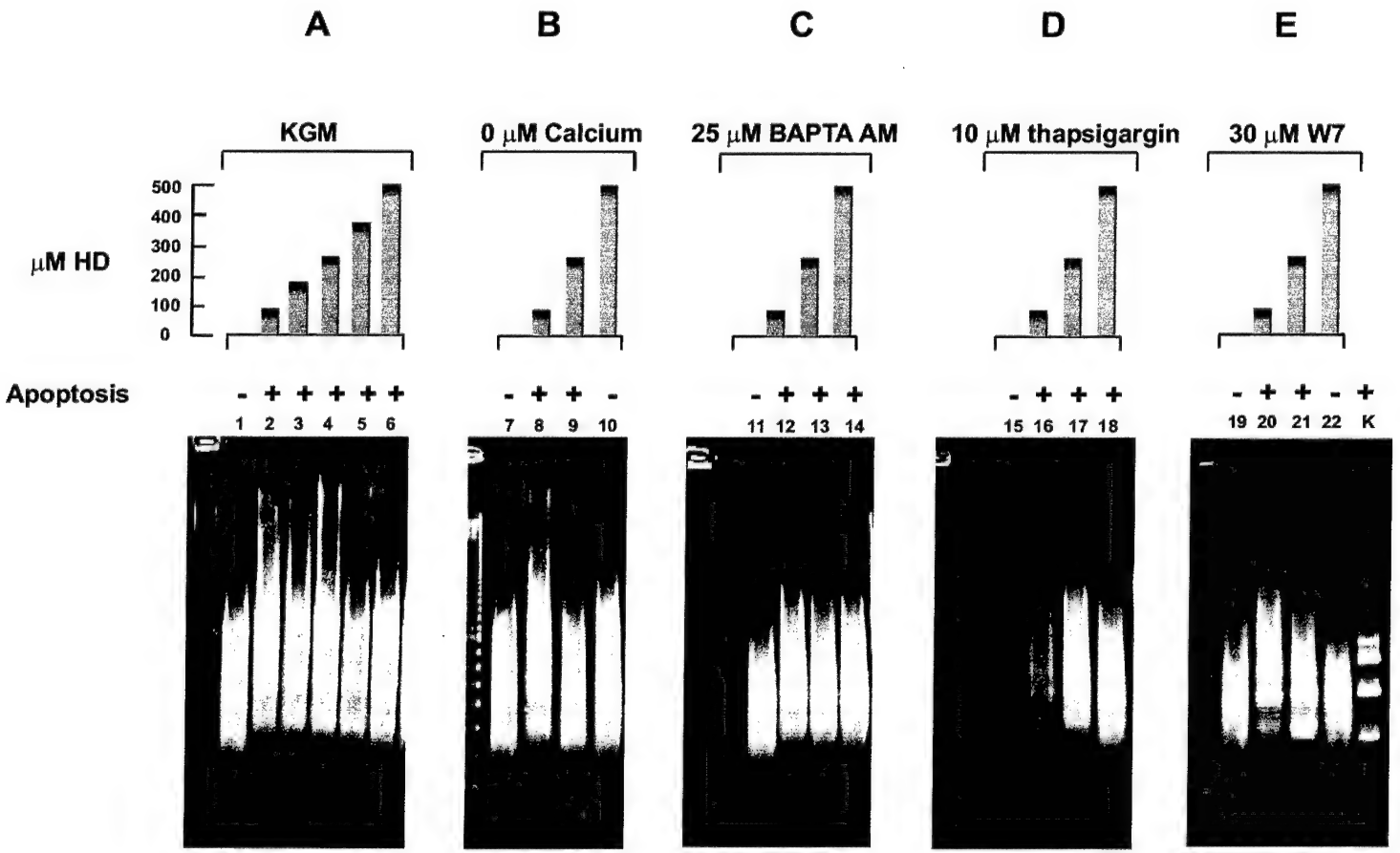
A
B
C
D
E
KGM
0 μM Calcium
25 μM BAPTA AM
10 μM thapsigargin
30 μM W7
μM HD
500
400
300
200
100
0
Apoptosis
- + + + + +
1 2 3 4 5 6
- + + -
7 8 9 10
- + + +
11 12 13 14
- + + +
15 16 17 18
- + + - +
19 20 21 22 K

Fig. 47

Fig. 48

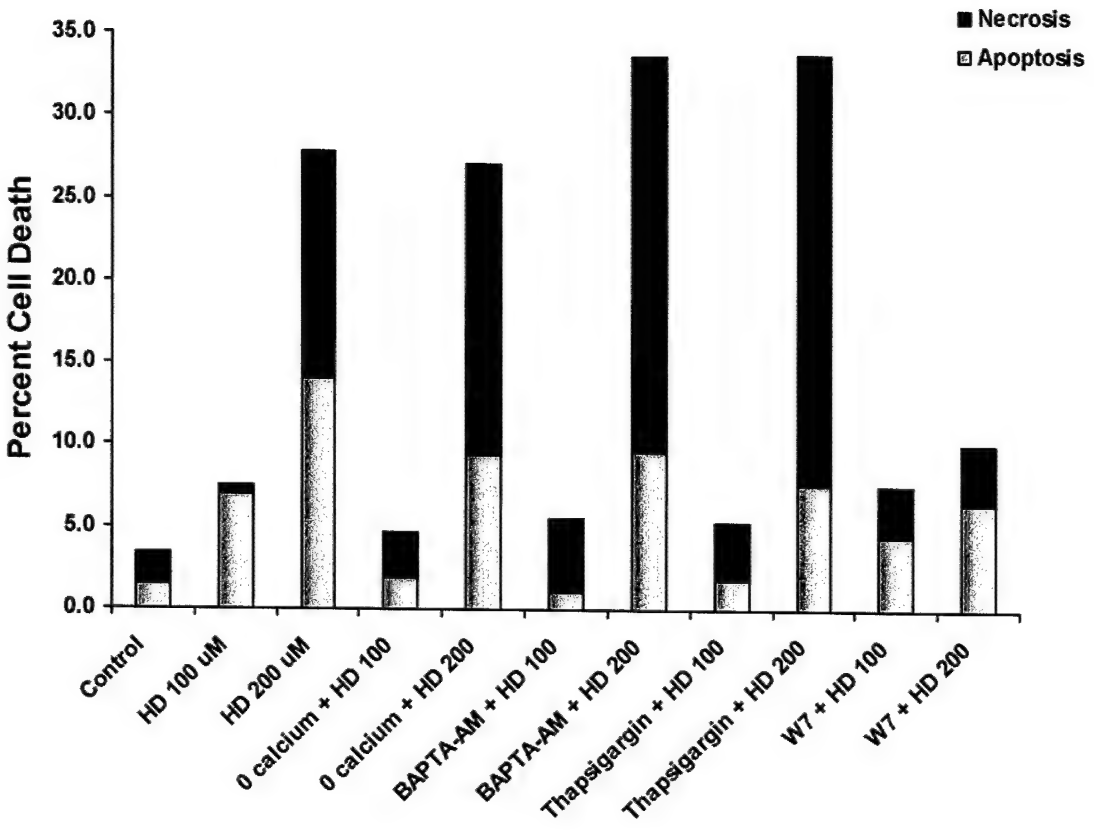
Necrosis
Apoptosis
Percent Cell Death
35.0
30.0
25.0
20.0
15.0
10.0
5.0
0.0
Control
HD 100 uM
HD 200 uM
0 calcium + HD 100
0 calcium + HD 200
BAPTA-AM + HD 100
BAPTA-AM + HD 200
Thapsigargin + HD 100
Thapsigargin + HD 200
W7 + HD 100
W7 + HD 200

Fig. 49

A

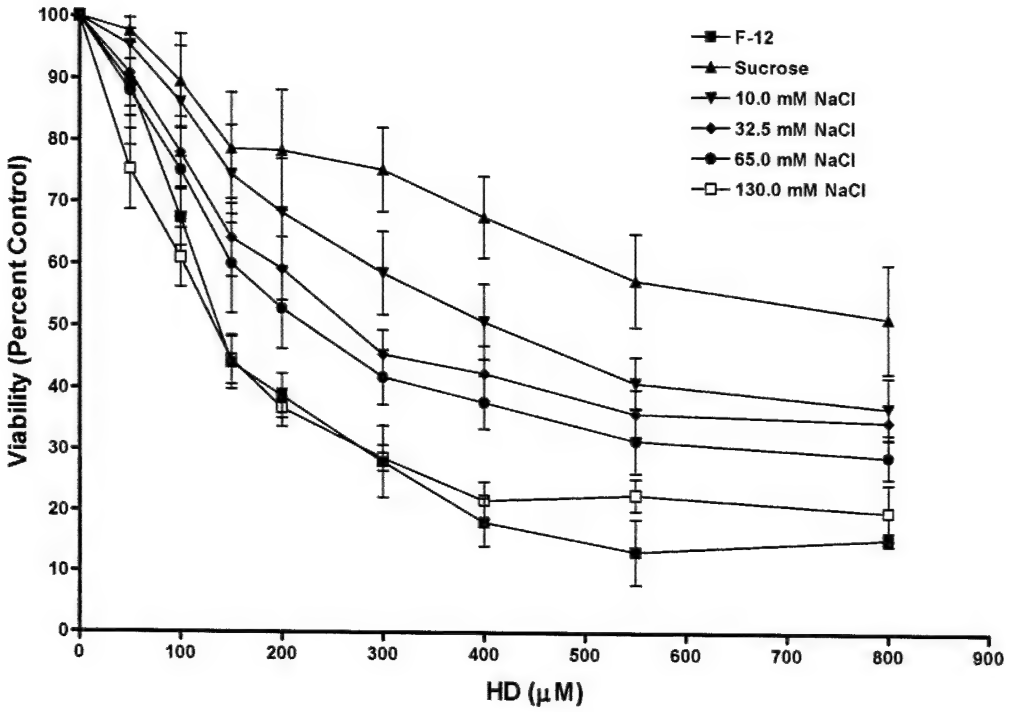
F-12
Sucrose
10.0 mM NaCl
32.5 mM NaCl
65.0 mM NaCl
130.0 mM NaCl
Viability (Percent Control)
HD (μM)

B

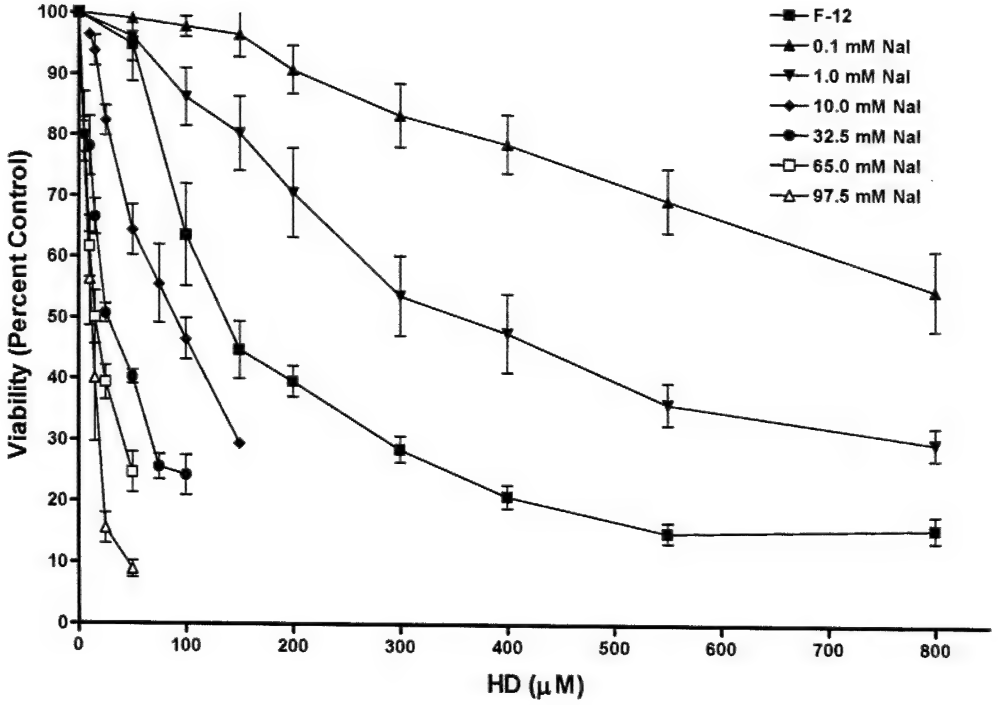
F-12
0.1 mM NaI
1.0 mM NaI
10.0 mM NaI
32.5 mM NaI
65.0 mM NaI
97.5 mM NaI
Viability (Percent Control)
HD (μM)

Fig. 50

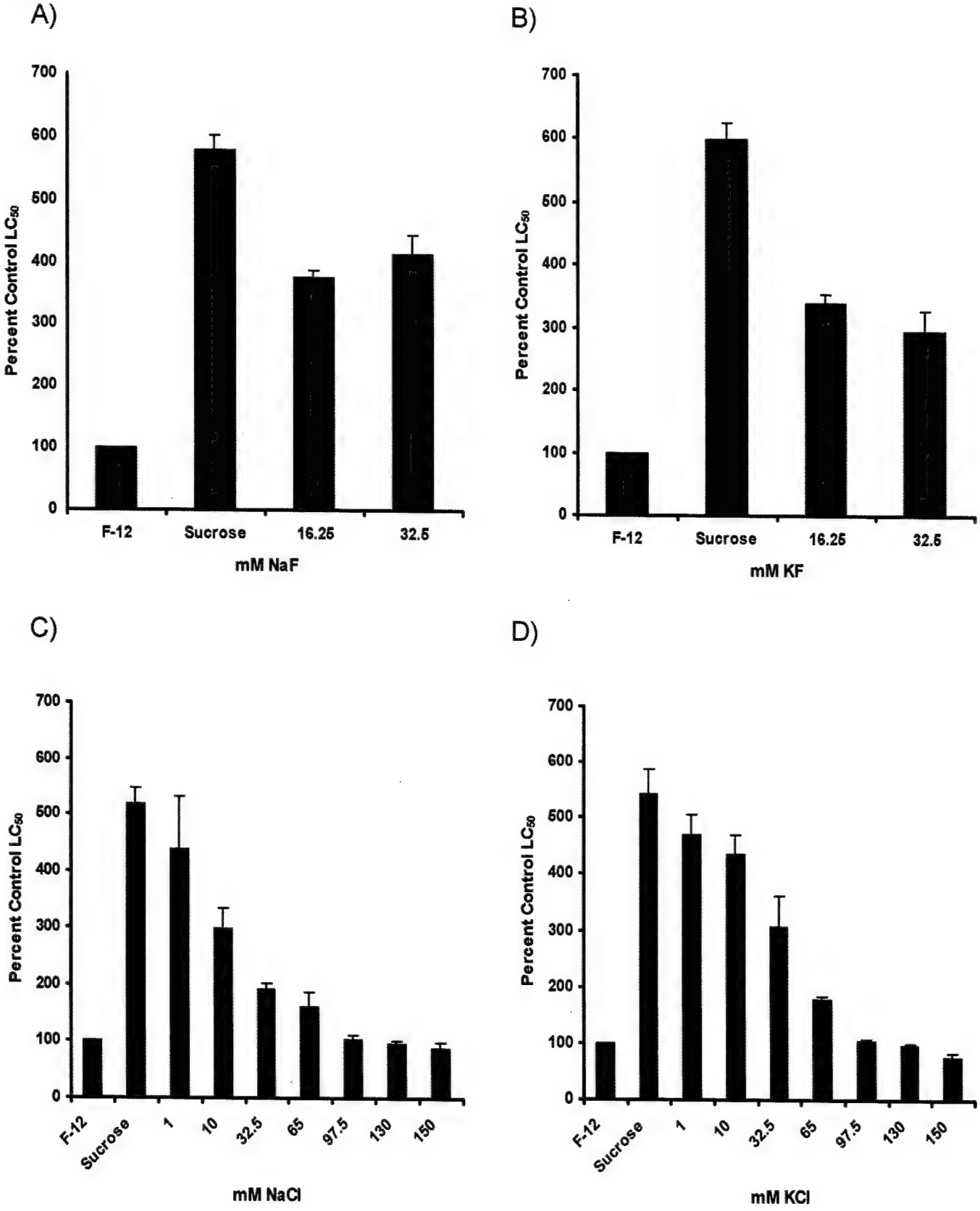
A)
B)
C)
D)
Percent Control LC50
700
600
500
400
300
200
100
0
F-12
Sucrose
16.25
32.5
mM NaF
mM KF
1
10
32.5
65
97.5
130
150
mM NaCl
mM KCl

Fig. 51

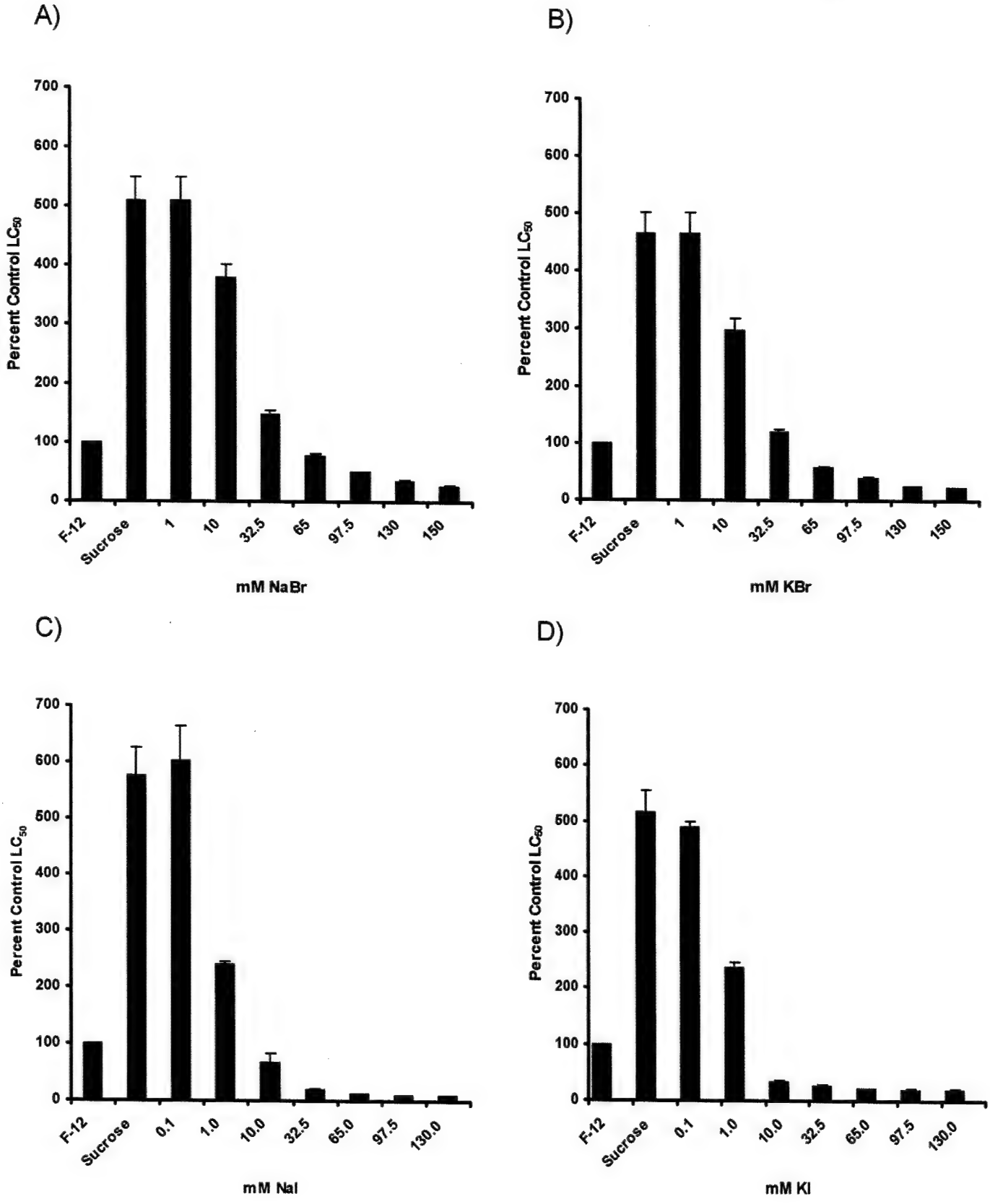
A)
B)
C)
D)
Percent Control LC50
700
600
500
400
300
200
100
0
F-12
Sucrose
1
10
32.5
65
97.5
130
150
mM NaBr
mM KBr
0.1
1.0
10.0
65.0
130.0
mM NaI
mM KI

Fig. 52

A)

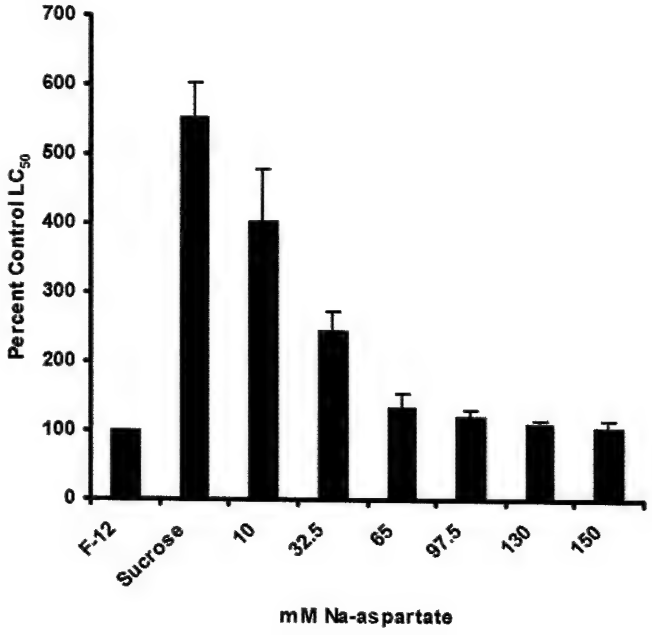
Percent Control LC_{50}
700
600
500
400
300
200
100
0
F-12
Sucrose
10
32.5
65
97.5
130
150
mM Na-aspartate

B)

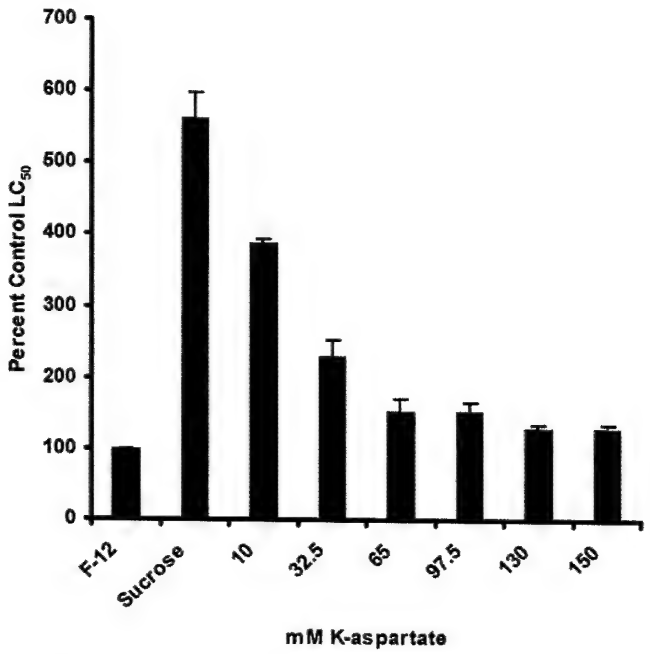
Percent Control LC_{50}
700
600
500
400
300
200
100
0
F-12
Sucrose
10
32.5
65
97.5
130
150
mM K-aspartate

C)

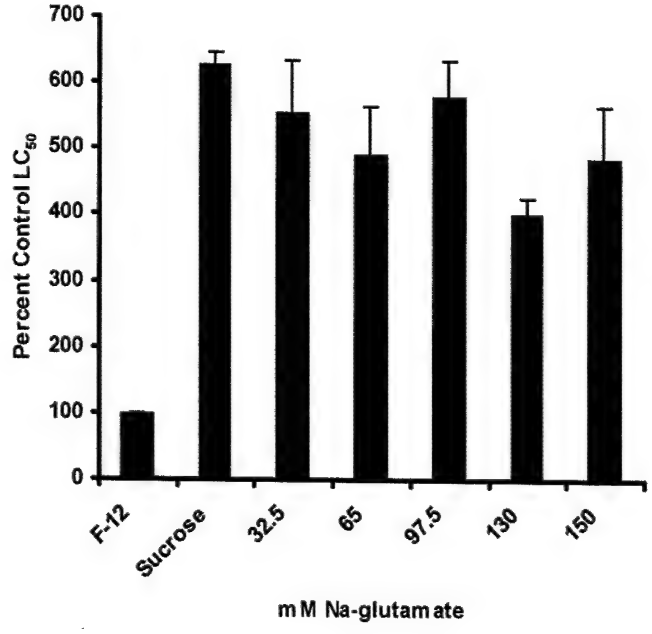
Percent Control LC_{50}
700
600
500
400
300
200
100
0
F-12
Sucrose
32.5
65
97.5
130
150
mM Na-glutamate

D)

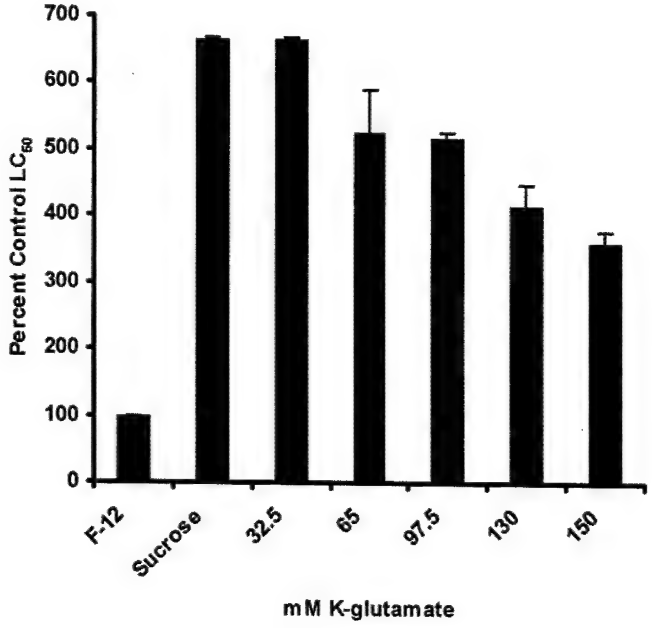
Percent Control LC_{50}
700
600
500
400
300
200
100
0
F-12
Sucrose
32.5
65
97.5
130
150
mM K-glutamate

Fig. 53

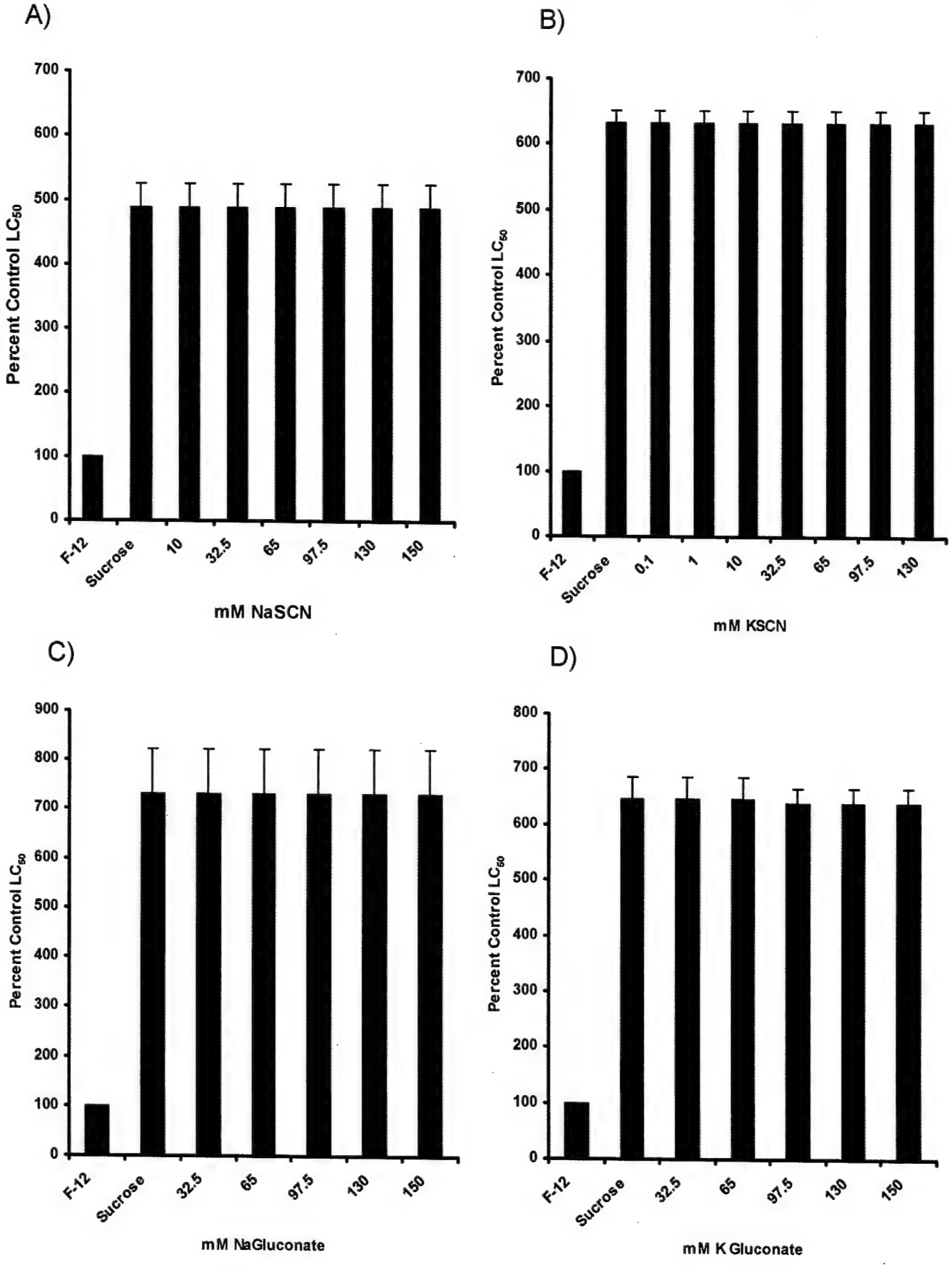
A)
Percent Control LC50
700
600
500
400
300
200
100
0
F-12
Sucrose
10
32.5
65
97.5
130
150
mM NaSCN
B)
Percent Control LC50
700
600
500
400
300
200
100
0
F-12
Sucrose
0.1
1
10
32.5
65
97.5
130
mM KSCN
C)
Percent Control LC50
900
800
700
600
500
400
300
200
100
0
F-12
Sucrose
32.5
65
97.5
130
150
mM NaGluconate
D)
Percent Control LC50
800
700
600
500
400
300
200
100
0
F-12
Sucrose
32.5
65
97.5
130
150
mM K Gluconate

Fig. 54

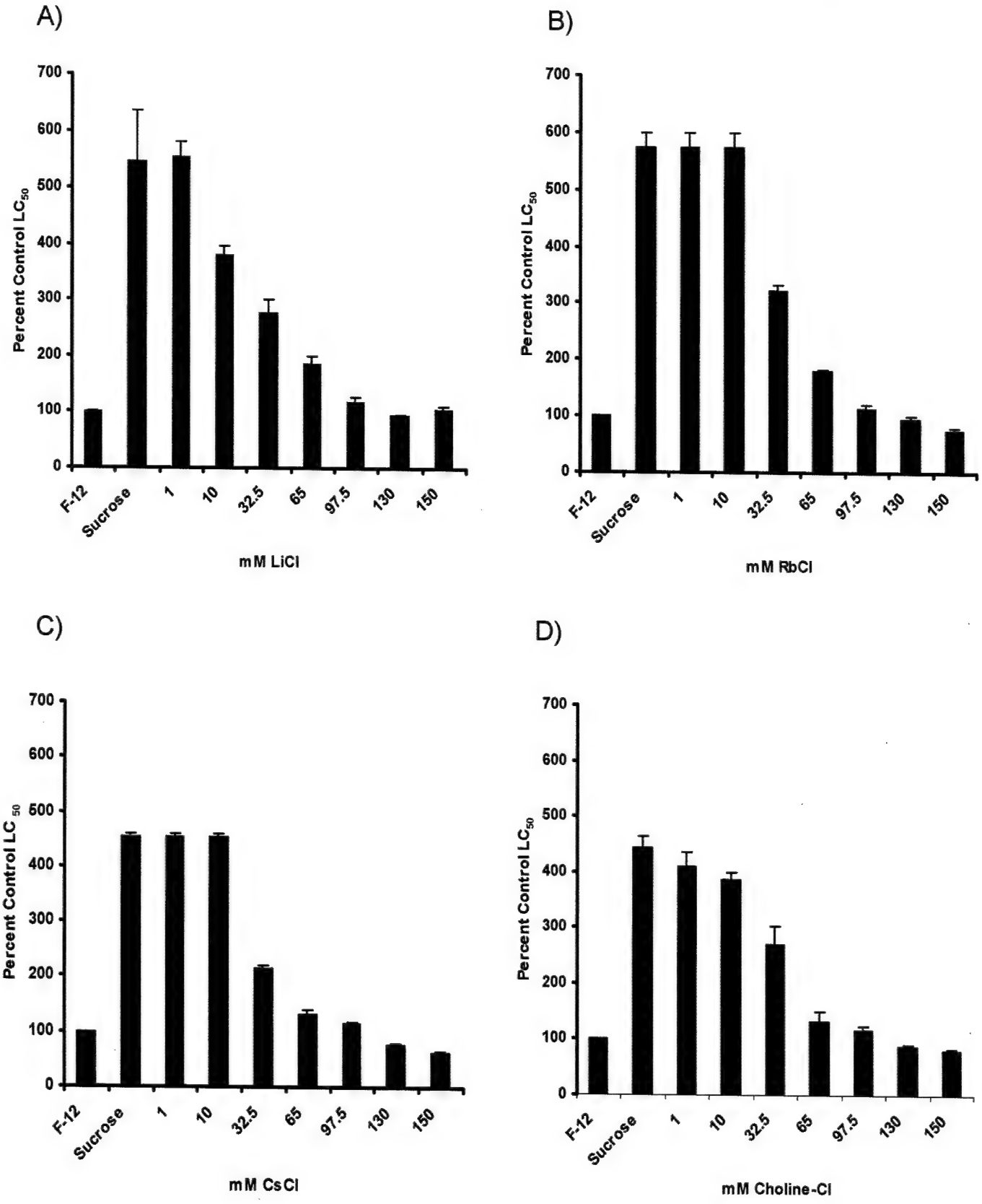
A)
B)
C)
D)
Percent Control LC50
700
600
500
400
300
200
100
0
F-12
Sucrose
1
10
32.5
65
97.5
130
150
mM LiCl
mM RbCl
mM CsCl
mM Choline-Cl

Fig. 55

A)

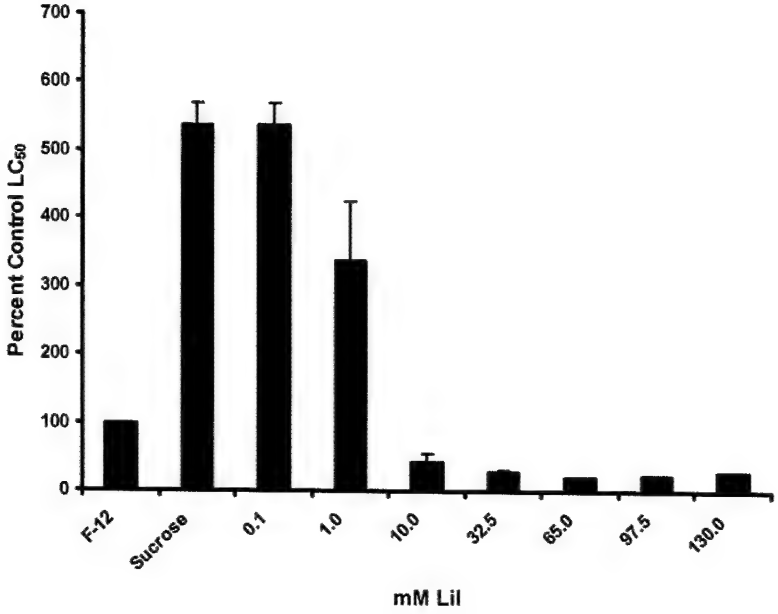
Percent Control LC50
700
600
500
400
300
200
100
0
F-12
Sucrose
0.1
1.0
10.0
32.5
65.0
97.5
130.0
mM LiI

B)

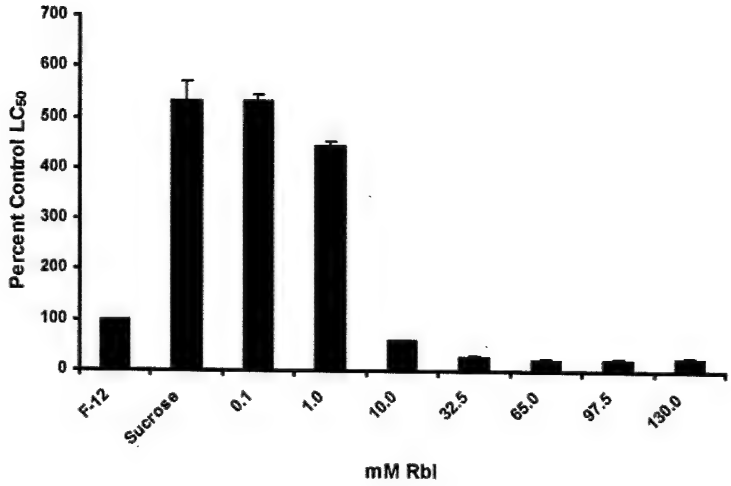
Percent Control LC50
700
600
500
400
300
200
100
0
F-12
Sucrose
0.1
1.0
10.0
32.5
65.0
97.5
130.0
mM RbI

C)

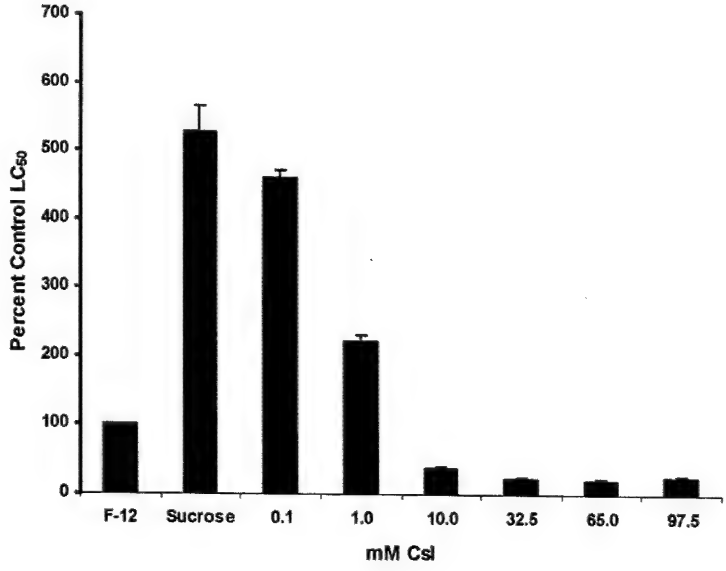
Percent Control LC50
700
600
500
400
300
200
100
0
F-12
Sucrose
0.1
1.0
10.0
32.5
65.0
97.5
mM CsI

Fig. 56

A)

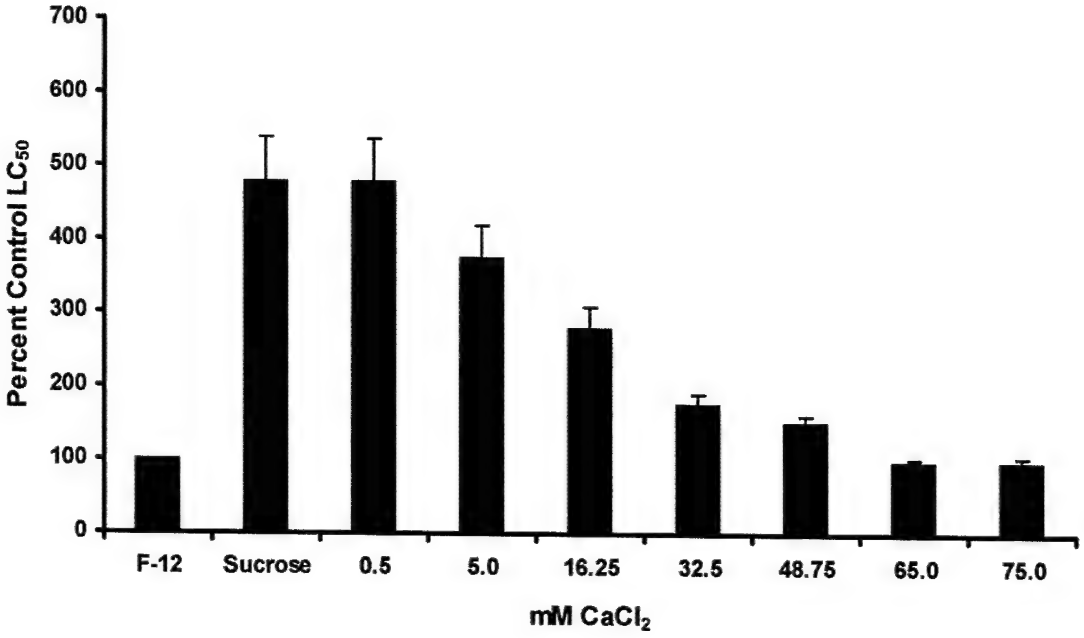
Percent Control LC_{50}
700
600
500
400
300
200
100
0
F-12
Sucrose
0.5
5.0
16.25
32.5
48.75
65.0
75.0
mM $CaCl_2$

B)

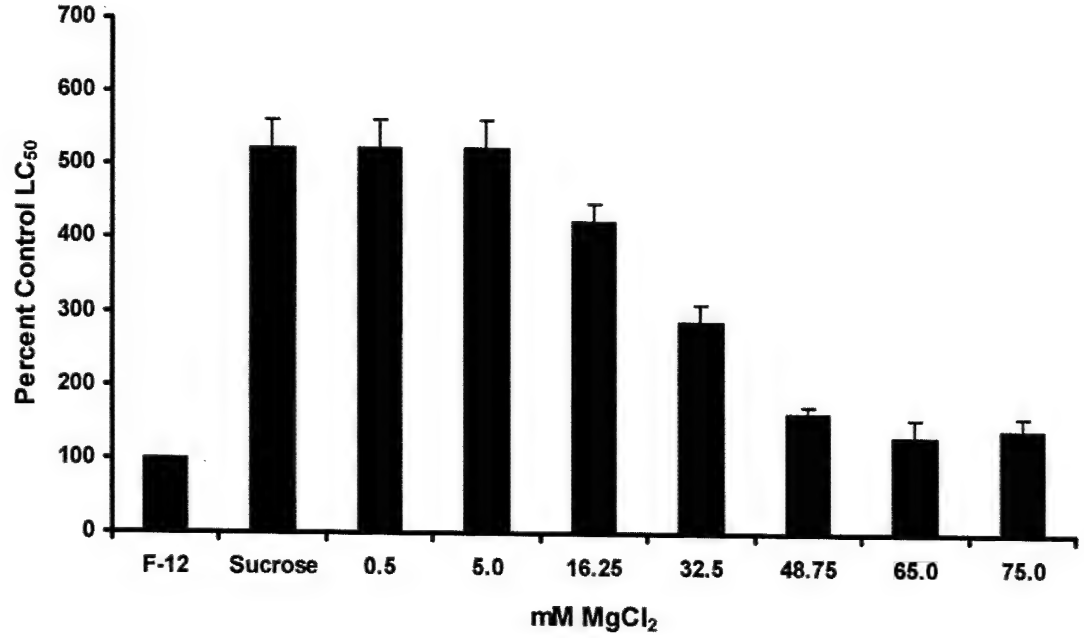
Percent Control LC_{50}
700
600
500
400
300
200
100
0
F-12
Sucrose
0.5
5.0
16.25
32.5
48.75
65.0
75.0
mM $MgCl_2$

Fig. 57

A)

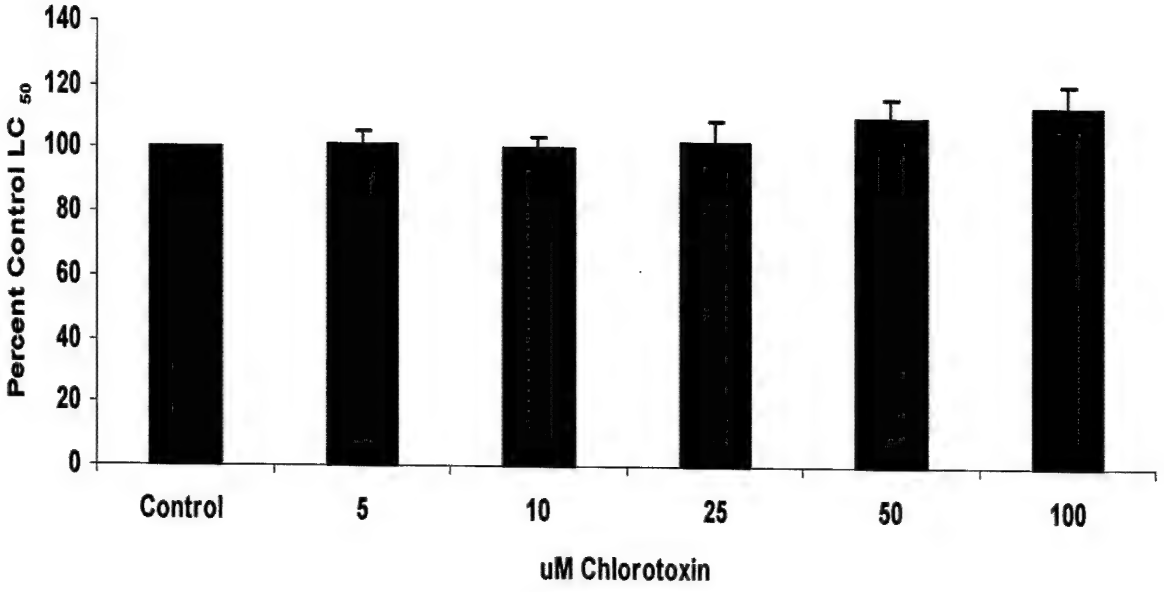
Percent Control LC 50
140
120
100
80
60
40
20
0
Control
5
10
25
50
100
uM Chlorotoxin

B)

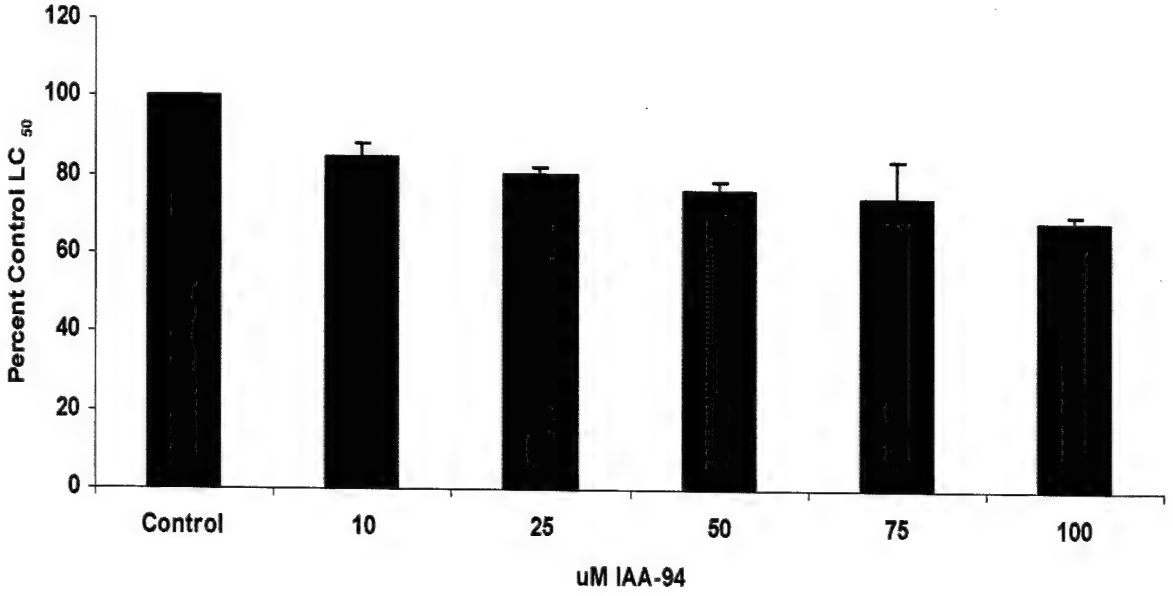
Percent Control LC 50
120
100
80
60
40
20
0
Control
10
25
50
75
100
uM IAA-94

Fig. 58

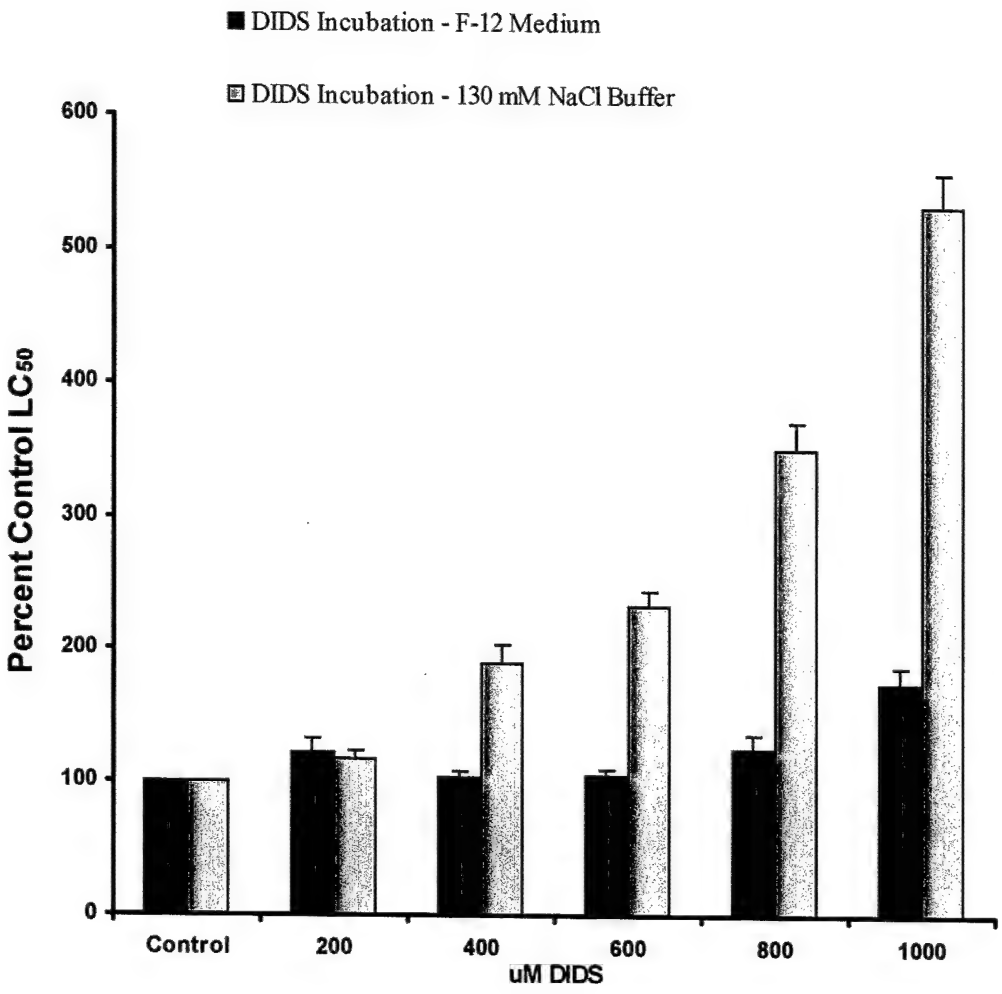
DIDS Incubation - F-12 Medium
DIDS Incubation - 130 mM NaCl Buffer
Percent Control LC50
600
500
400
300
200
100
0
Control
200
400
600
800
1000
uM DIDS

Fig. 59

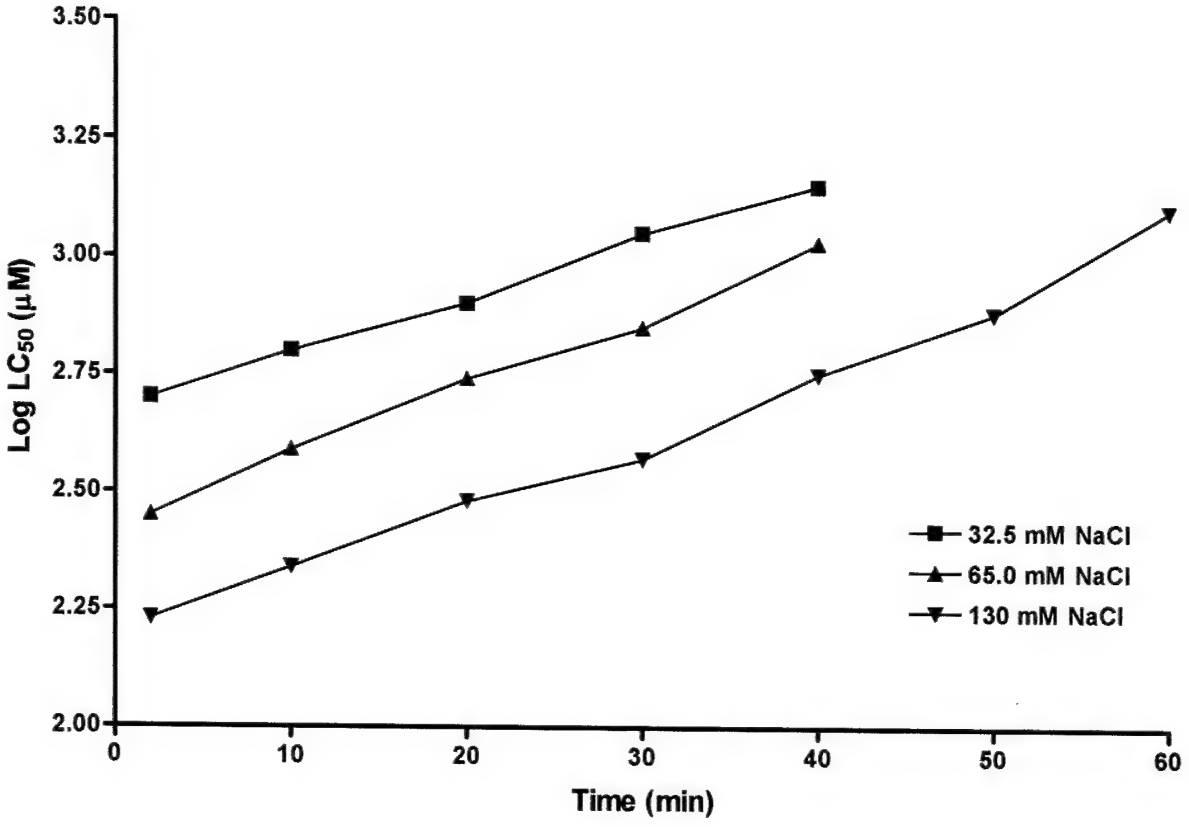
3.50
3.25
3.00
2.75
2.50
2.25
2.00
Log LC50 (μM)
0
10
20
30
40
50
60
Time (min)
32.5 mM NaCl
65.0 mM NaCl
130 mM NaCl

Fig. 60

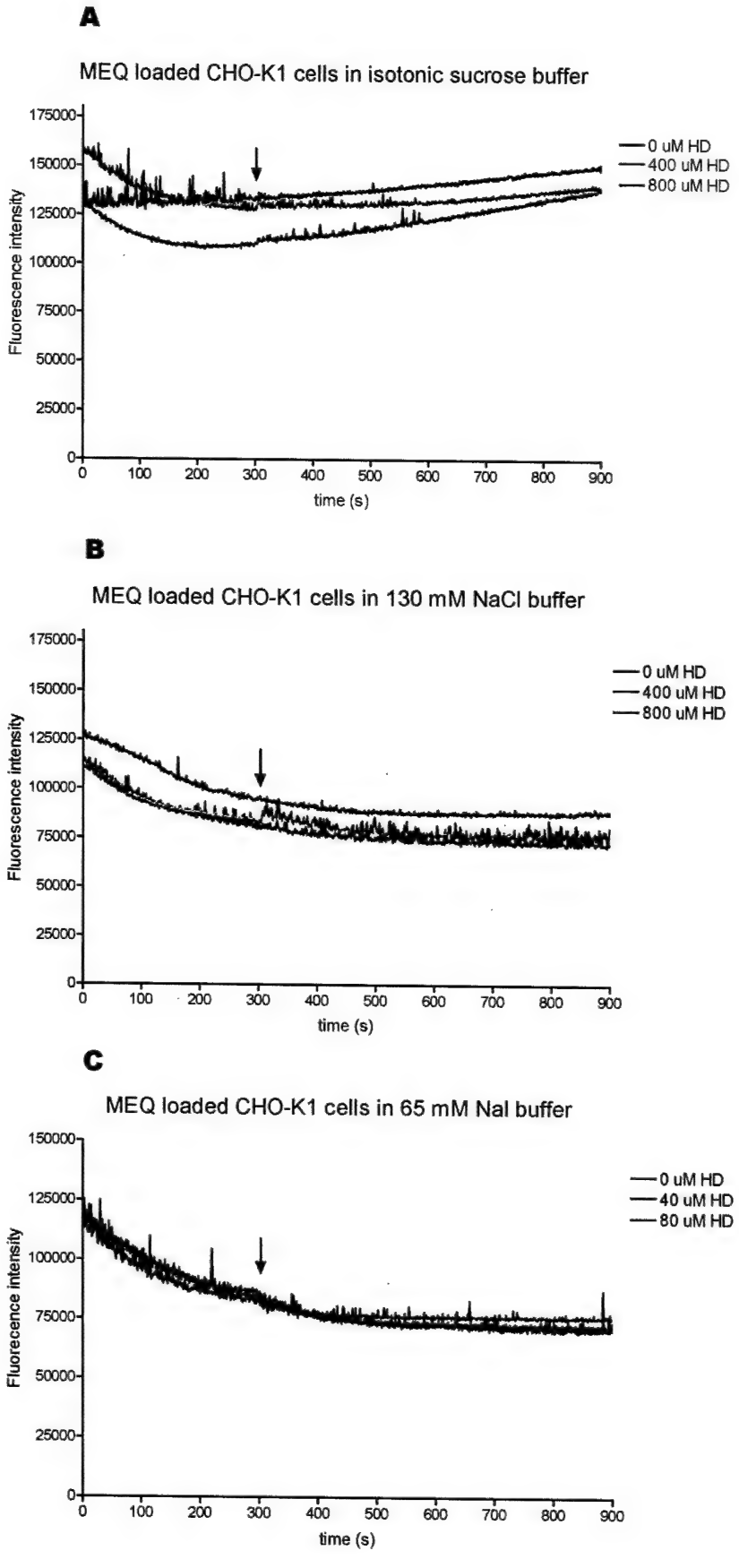
A
MEQ loaded CHO-K1 cells in isotonic sucrose buffer
Fluorescence intensity
time (s)
0 uM HD
400 uM HD
800 uM HD
B
MEQ loaded CHO-K1 cells in 130 mM NaCl buffer
Fluorescence intensity
time (s)
0 uM HD
400 uM HD
800 uM HD
C
MEQ loaded CHO-K1 cells in 65 mM NaI buffer
Fluorecence intensity
time (s)
0 uM HD
40 uM HD
80 uM HD

Fig. 61

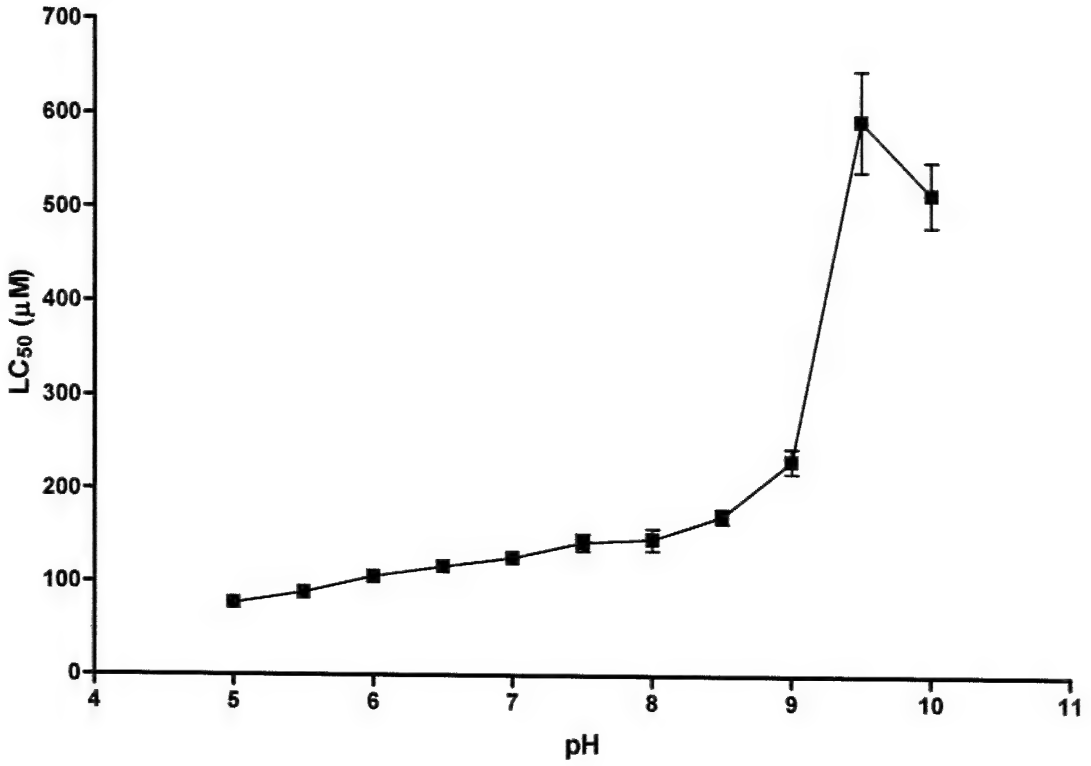

Fig. 62

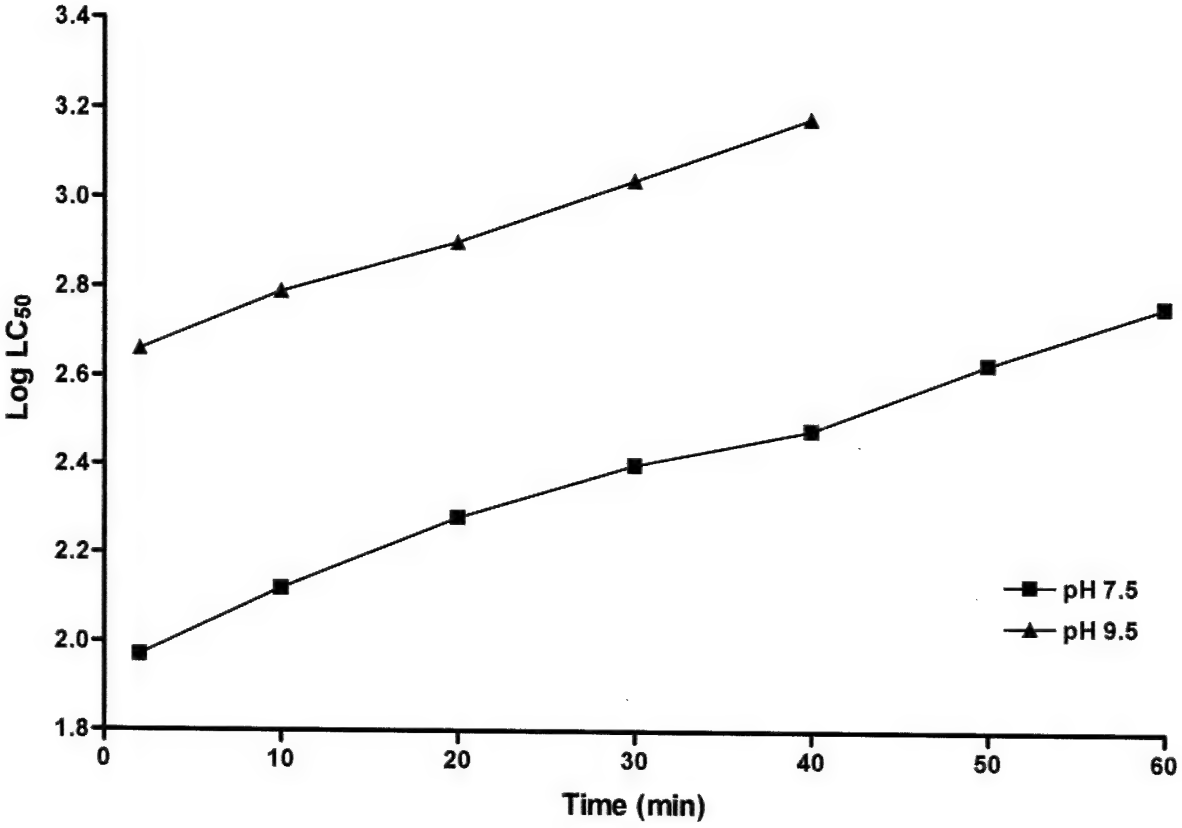
3.4
3.2
3.0
2.8
2.6
2.4
2.2
2.0
1.8
Log LC50
0
10
20
30
40
50
60
Time (min)
pH 7.5
pH 9.5

ANNEX 1

British Journal of Pharmacology (2002) 135, 1616–1626

www.nature.com/bjp

Stimulation of Ca^{2+} influx through ATP receptors on rat brain synaptosomes: identification of functional $P2X_7$ receptor subtypes

*,[1]Paul M. Lundy, [1]Murray G. Hamilton, [2]Lei Mi, [2]Wenrong Gong, [1]Cory Vair, [1]Thomas W. Sawyer & [1]Robert Frew

[1]Medical Therapy Group, Defence Research Establishment Suffield, P.O. Box 4000, Medicine Hat, Alberta, Canada T1A 8K6 and [2]Kinchyle Enterprises, Medicine Hat, Alberta, Canada T1A 8K6

1 ATP receptors of the P2X class have previously been identified on autonomic nerve endings and on a limited population of CNS neurons.

2 In the present study P2X receptors on mammalian cortical synaptosomes have been identified by a variety of functional and biochemical studies. In choline buffer ATP analogues caused concentration/time dependent Ca^{2+} influx. Relative to the effects caused by ATP, benzoylbenzoyl ATP (BzATP) was about seven times more active than ATP while 2-me-S-ATP and ATPγS were much less active. α,β-me- ATP and β,γ-me-ATP were virtually inactive. In sucrose buffer, relative to choline buffer, the activity of BzATP was more than doubled while activity in sodium buffer was reduced. Moreover, the P2X antagonists PPADS or Brilliant Blue G both significantly attenuated influx. These observations suggest the presence of P2X receptors on synaptosomes which subserve Ca^{2+} influx. This activity profile of the ATP analogues and the response to blocking agents are characteristic of responses of $P2X_7$ receptors.

3 Influx was unaffected by the VSCC inhibitors ω-CTx-MVIIC and (−) 202–791, indicating that ATP induced Ca^{2+} influx occurred primarily through P2X receptors.

4 $P2X_7$ receptor protein was identified by Western blotting and immunohistochemical staining. Purified preparations were devoid of significant concentrations of GFAP or the microglial marker OX-42 but contained greatly enriched amounts of syntaxin and SNAP 25.

5 The various pharmacological and biochemical studies were all consistent with the presence of functional $P2X_7$ receptors.

British Journal of Pharmacology (2002) **135**, 1616–1626

Keywords: Ca^{2+} influx; synaptosomes; P2X receptors; ATP analogues; ATP inhibitors; immunohistochemistry

Abbreviations: ATP, adenosine 5′triphosphate; ATPγS, adenosine 5′-O-(3-thiophosphate); BBG, Brilliant Blue G; BzATP, 2′&3′-O-(4-benzoylbenzoyl) adenosine 5′ triphosphate; ω-CTx-MVIIC, ω-conotoxin-MVIIC; GFAP, glial fibrillary acidic protein; HBSS, Hanks balanced salt solution; α,β-me-ATP, α,β-methylene-adenosine triphosphate; β,γ-me-ATP, β,γ methylene-L-adenosine triphosphate; 2-me-S-ATP, 2-methylthioadenosine triphosphate; PBS, phosphate buffered saline; PBST, phosphate buffered saline plus tween; PPADS, pyridoxal-phosphate-6-azophenyl-2′- 4′ disulphonic acid; VSCCs, voltage sensitive calcium channels.

Introduction

Ionotropic P2X purinergic receptors are located on a large number of different cell membranes and are believed to transduce the effects of extracellular ATP (adenosine triphosphate). There are currently seven identified, cloned subtypes of the P2X receptor. Some of these subtypes appear to mediate fast excitatory transmission in the peripheral autonomic nervous system between neurons and/or between neurons and smooth muscle cells (Evans *et al.*, 1992; Silinsky *et al.*, 1992; Galligan & Bertrand, 1994). ATP evokes the release of other autonomic neurotransmitters such as noradrenaline from peripheral neurons through activation of P2X receptor subtypes, which function as ATP gated ion channels or pores (Boehm *et al.*, 1995; Gibb & Halliday, 1996; Boehm, 1999; von Külgelgen *et al.*, 1993; 1999; Sperlágh *et al.*, 2000). Therefore, ATP receptors operating as cation channels may serve as an important alternate mechanism to the voltage sensitive calcium channels (VSCCs), through which the organism initiates or controls the release of neurotransmitters from a variety of autonomic nerves.

Evidence describing the presence of most P2X receptor subtypes on neurons in a number of brain areas exists (Ueno *et al.*, 1992; Edwards *et al.*, 1992; Séguéla *et al.*, 1996; Collo *et al.*, 1996, 1997; Burnstock, 1999; Kanjhan *et al.*, 1999). A role for undefined types of presynaptic P2X receptor subtypes in neurotransmission at a very few, well defined neuronal junctions has also been described (Motin & Bennett, 1995; Kidd *et al.*, 1998; Lê *et al.*, 1998; Khakh and Henderson, 1998, 2000; Gu & MacDermott, 1997; Hugel & Schlicter, 2000). Very recently, important new work has offered proof of $P2X_3$ as well as other undefined subtypes in midbrain synaptosomes (Diáz-Hernández *et al.*, 2001; Gómez-Villafuertes *et al.*, 2001).

In the present study, pharmacological and molecular biological evidence is presented for the existence of functional

*Author for correspondence; E-mail: Paul.Lundy@dres.dnd.ca

P2X receptors, specifically of the $P2X_7$ subtype (Surprenant *et al.*, 1996) on purified synaptosomal preparations of rat cortex. We have employed a number of pharmacological manipulations of responses proposed as reliable measures of P2X receptor function (Michel *et al.*, 1996; 1998; Virginio *et al.*, 1997; Jiang *et al.*, 2000; Hibell *et al.*, 2001). We have also employed Western blotting techniques and immunohistochemistry to confirm the presence of specific P2X subtypes in order to support the identification of receptors carried out by pharmacological methods. These findings constitute a variety of evidence for the existence and functional significance of $P2X_7$ receptors on central presynaptic elements.

Methods

Preparation of synaptosomes

Rat (male, Sprague–Dawley, wt 250–300 g) crude synaptosomes were prepared by homogenization of brain cortex in ice-cold 0.32 M sucrose using six strokes of a teflon/glass homogenizer. The homogenate was centrifuged at $1000 \times g$ for 10 min at 4°C. The supernatant was decanted and centrifuged at $12{,}400 \times g$ for 25 min and the resulting pellet (P_2) was resuspended in one of three different buffers of composition outlined below for the subsequent measurement of ATP induced calcium influx.

Purified synaptosomes were prepared using the Percoll® gradient method (Dunkley *et al.*, 1988). Briefly, the S_1 sucrose/EDTA supernatant was layered over a discontinuous Percoll® (Sigma, St Louis, MO, U.S.A.) gradient consisting of 2 ml each of 3, 10, 15 and 23% (v v^{-1}) Percoll® dissolved in 0.32 M sucrose containing 100 mg l^{-1} EDTA. This was centrifuged at $20{,}000 \times g$ for 5 min at 4°C in a Beckman preparative centrifuge. The 10/15% and 15/23% interfaces were combined and diluted 4 fold with Hanks balanced salt solution (HBSS) at pH 7.3, and then centrifuged at $12{,}500 \times g$ for 25 min. The resulting pellet was resuspended in HBSS. Aliquots of the Percoll® purified synaptosomes were washed twice with 10 vol of HBSS (composition see below) to ensure the removal of all Percoll® and deposited on treated glass microscope slides (500 μl, Cytospin) and used for fluorescence histochemistry (outlined below). The composition of HBSS was as follows (in mM): KCl 5.4, KH_2PO_4 0.5, NaCl 136, $NaHPO_4$ $0{\cdot}7H_20$ 0.34, D-glucose 5.6 and $CaCl_2$ 1.

Calcium influx

The first series of experiments were carried out in choline buffer (composition outlined below) and provided the results described in the first two figures, as well as parts of subsequent figures as described in the text where appropriate. Ca^{2+} influx was carried out according to the method of Blaustein (1975), with modifications (Lundy *et al.*, 1991). In those cases where drug pretreatments were required, the synaptosomes were incubated at 30°C in the presence or absence of antagonist drugs for 15 min. Experiments were carried out using synaptosomes diluted to obtain a final concentration of about 1 mg protein ml^{-1}. Following drug pre-treatment, a 100 μl aliquot of the synaptosomal suspension was quickly injected into an equal volume of resting buffer (5 mM K^+), depolarizing buffer (25 mM K^+, final concentration), or resting buffer to which ATP or its analogues had been added (various concentrations), all containing 0.5 μCi $^{45}Ca^{2+}$ (New England Nuclear, Boston, MA, U.S.A.). Triplicate estimates of basal and of K^+ stimulated Ca^{2+} influx (3 s or adenine nucleotide stimulated influx (60 s) were carried out and terminated by rapid dilution of the buffer with 4 ml ice-cold Ca^{2+}-free buffer containing 4 mM EGTA. Each suspension was rapidly filtered under vacuum through 0.45 μM membrane filters (Gelman Science, Ann Arbor, MI, U.S.A.) using a filtration apparatus (Hoeffer Scientific, San Francisco, CA, U.S.A.). The membrane filters were washed twice with 5 ml normal resting buffer to which excess Ca^{2+} had been added. Membrane filters were allowed to dry, placed in scintillation cocktail, and counted on a Wallac 1500 scintillation counter. Basal influx was subtracted from K^+ or nucleotide-stimulated influx and results were expressed as nmoles Ca^{2+} influx mg protein ml^{-1}. Experimental protocols were designed so that the effects of ATP, as well as five nucleotide analogues could be examined on each synaptosomal preparation. K^+-evoked Ca^{2+} influx was included to assess the viability of each preparation. Subsequent to the first series of experiments, either the sodium chloride or the sucrose-based systems were also used.

Buffer systems

Three buffers were used in the study of calcium influx. The first buffer was choline based and was a buffer that had been utilized in this laboratory for studies of calcium influx for several years. The other two were used as the result of reports in the literature concerning ionic effects on $P2X_7$ receptor activity:

(a) Choline based buffer was of the same composition used previously in this laboratory and is one of three different buffers employed in the measurement of calcium influx. In the results section the various buffers used are identified where appropriate. Choline buffer was made with the following composition (in mM): Choline Cl 132, KCl 5, $MgCl_2$ 1.3, $CaCl_2$ 1.5, NaH_2PO_4 12, D-glucose 10, HEPES 20, brought to pH 7.4 with TRIS base. Choline chloride was originally substituted for NaCl to negate the effects of Na^+/Ca^{2+} exchange (Blaustein, 1975) but also choline has been recently reported to interfere less with ATP induced effects on $P2X_7$ receptors than sodium rich buffer systems (Michel *et al.*, 1996).

(b) Sodium based buffer was identical to the choline buffer but sodium chloride was substituted for choline chloride.

(c) Sucrose buffer was a low ionic strength medium described by Michel *et al.* (1996) and Surprenant *et al.* (1996) in order to maintain lower concentrations of certain ions which interfered with agonist activity. It consisted of the following (in mM): sucrose 280, $CaCl_2$ 0.5, KCl 5, D-Glucose 10, HEPES 10, N-methyl-D-glucamine 5, with the pH adjusted to 7.4.

Fluorescence histochemistry

Immunohistochemical staining was conducted as follows: slides were rinsed in phosphate buffered saline (PBS) for 10 min and blocking/diluent buffer was applied (PBS, 1.5% normal goat

serum (NGS) was applied for 20 min. Primary antibodies (anti-$P2X_7$, anti-syntaxin, and anti-SNAP-25, all rabbit (Alomone Labs, Jerusalem, Israel and Chemicon International Inc., Temecula, CA, U.S.A.) and anti- OX-42 (mouse, ICN Biochemicals, Aurora, OH, U.S.A.) were applied at 1/300 dilution with diluent buffer and incubated for 4 h at room temperature. Slides were rinsed three times with PBS. Secondary antibodies (Oregon Green 488-labelled goat anti-rabbit IgG and goat anti-mouse IgG, Molecular Probes, Eugene, OR, U.S.A.) were applied to sections at 1/200 dilution with diluent buffer for 2 h under the same conditions. Following incubation, the slides were washed in three changes of PBS and coverslipped using Prolong anti-fade mounting media (Molecular Probes, Eugene, OR, U.S.A.).

A negative procedural control, in which the primary antibody was omitted and replaced with diluent buffer only, was used with each series. Slides were visualized using fluorescence microscopy and representative images taken with a Spot 2 digital camera (24 bit colour images, Diagnostic Instruments Inc., Sterling Heights, MI, U.S.A.) Protein concentration was determined using the BCA Protein Assay Reagent kit (Pierce Chemical Co., Rockford, IL, U.S.A.) by the method of Bradford (1976).

Western blot characterization of P2X receptors

Pheochromocytoma PC12 cells (CRL-1721, American Type Culture Collection, Manassas, VA, U.S.A.), vas deferentia, cortical synaptosomes (both crude P_2 and purified homogenates), or whole brain homogenates from the rat were incubated on ice for 20 min in 300–500 μl 1× SDS gel loading buffer of the following composition: 50 mM Tris-HCl (pH 8.6), 100 mM DTT, 2% SDS, 0.1% bromophenol blue and 10% glycerol. Tissues were centrifuged at $12,000 \times g$ for 3 min at 4°C and the supernatant was transferred to a fresh tube. Protein was measured using Coomassie protein reagent (Pierce, Rockford, IL, U.S.A.) according to the method of Bradford (1976). The protein samples were immersed in boiling water for 5 min and equal amounts of protein (20 μg of each) were electrophoresed on 8% SDS polyacrylamide gels and transblotted onto a nitro-cellulose membrane. Prestained protein standards (Bio-Rad, Mississauga, Ontario, Canada) were used to visualize successful transfer and to measure molecular weight of the subsequent signal. The membrane was blocked with PBS containing 0.1% Tween (PBST) and 5% skimmed milk overnight at 4°C, then washed four times at 10 min intervals with PBST. Washed membranes were incubated with 1:300 dilutions of anti-$P2X_1$, anti-$P2X_2$ (Alomone Labs, Jerusalem, Israel), or anti-$P2X_7$ antibody (Alomone Labs, or Chemicon International, Temecula, CA, U.S.A.) in PBST solutions for 90 min. They were then rewashed and incubated with a peroxidase labelled anti-rabbit antibody (1:3000 dilution, included in ECL-kit Amersham Pharmacia Biotech, Baie d'Urfe, Quebec, Canada). The membranes were washed again and protein visualized with the enhanced chemiluminescence reagents according to the instructions of the manufacturer.

In order to test the purity of synaptosomes obtained by the Percoll® gradient method, we detected the expression of the synaptosome specific proteins syntaxin, SNAP-25, and glial fibrillary acidic protein (GFAP) using a Western blot. Rabbit anti-syntaxin, anti -SNAP-25 (Alomone Labs. Jerusalem, Israel) and mouse anti-GFAP (Pharmingen Labs, Mississauga, Ontario, Canada), and the corresponding cognate antibodies (Amersham Pharmacia, Quebec, Canada) were used as primary and secondary antibodies in experiments according to the above-mentioned Western blot protocol. 12% SDS-Poly-acrylamide gels were used for syntaxin, SNAP-25 and GFAP.

Drugs

The following drugs were used: Adenosine 5-triphosphate disodium (ATP), adenosine 5′-O-(3-thiotriphosphate) (ATPγS), 2-methylthio-ATP, 2′ & 3′-O-(4-benzoylbenzoyl)-ATP (BzATP), α,β-methylene ATP, β,γ-methylene-L-ATP; pyridoxal-phosphate-6-azophenyl-2-disulphonic acid tetra sodium (PPADS), ω-conotoxin-MVIIC (ω-CTx-MVIIC) and Brilliant Blue G (BBG) (all purchased from Sigma St Louis, MO, U.S.A). All drugs were dissolved in distilled H_2O and added to the appropriate incubation buffer.

Statistics

Comparisons among data were carried out using a two-way ANOVA. In certain cases a Student's *t*-test was performed where appropriate, as stated in the results. Probability values less than 0.05 were considered significant.

Results

Initial experiments were performed in choline buffer in which cortical synaptosomes were exposed to increasing concentrations of ATP or BzATP (Figure 1A) for 60 s, which was determined as the optimal incubation period (Figure 1B). The maximally effective concentration required for ATP and BzATP stimulated influx (stimulated *minus* resting $^{45}Ca^{2+}$ influx) was determined (nMoles Ca^{2+}mg protein^{-1}). Both nucleotides evoked a dose dependent influx of extracellular Ca^{2+}. Of the agonists examined, only ATP and BzATP acted as full agonists for which an EC_{50} could be calculated. The maximal responses for the two full agonists was achieved at 1 mM ATP or 100 μM BzATP. Dose-effect curves to 2-methylthioadenosine triphosphate (2-me-S-ATP) and to adenosine 5′-O-(3- thiophosphate, (ATPγS) were also carried out however these analogues acted as partial agonists and produced shallow dose response curves which did not reach maximal values at the highest concentration examined (1 mM). Therefore, each analogue was tested at the concentration of ATP which produced maximal effects (ATP EC_{100} or 1 mM). The results in Figure 2 indicate that at 1 mM the order of agonist efficacy was BzATP = ATP > 2-me-S-ATP > ATPγS. The nucleotides α, β-methylene adenosine triphosphate (α,β-me-ATP) and β, γ-methylene-L-adenosine triphosphate (β,γ-me-ATP) were inactive. EC_{50} values for ATP and BzATP were calculated to be 214 and 30 μM (about a 7 fold difference) respectively. Therefore for the two agonists for which an EC_{50} was available, BzATP was considerably more potent (about seven times) than ATP. In each experiment some synaptosomes were exposed to 25 mM K^+ for 3 s to confirm synaptosomal viability and to demonstrate the effective block of neuronal VSCCs by ω-conotoxin-MVIIC (ω-CTx-MVIIC). ATP induced influx

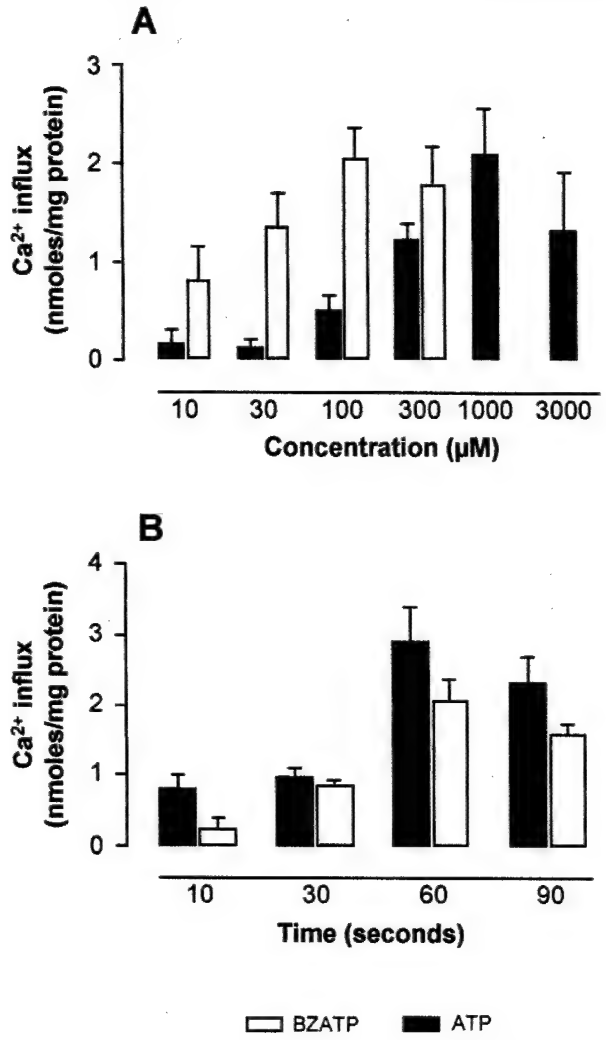

Figure 1 Concentration and time dependence of ATP and BzATP-evoked Ca^{2+} influx in rat brain cortical synaptosomes carried out in choline buffer as outlined in Methods. (A) ATP (solid bars) or BzATP (open bars) were incubated with the synaptosomes for 60 s at the concentrations indicated and calcium influx was measured. (B) Time dependence of ATP and BzATP-evoked Ca^{2+} influx. Synaptosomes were incubated with maximally effective concentrations of ATP (1 mM) or BzATP (100 μM) for 10–90 s as indicated. Values shown are mean ± s.e.mean, $n=4$.

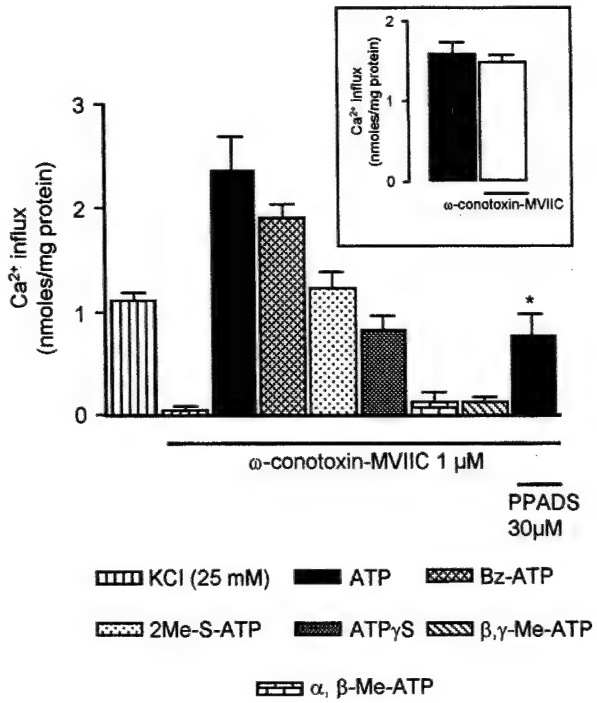

Figure 2 K^+ and adenine nucleotide-evoked Ca^{2+} influx in rat brain cortical synaptosomes. K^+-evoked and adenine nucleotide induced influx was measured in the presence and absence of (ω-CTx-MVIIC, 1 μM) as indicated. ATP evoked influx (solid bar, third bar from left) is shown in the absence and presence (solid bar, far right side) of PPADS (30 μM) $n=4$. Synaptosomes were exposed to 25 mM K^+ for 3 s and 1 mM of the nucleotides for 60 s. The influx induced by maximally effective concentrations of 1 mM ATP or BzATP were not significantly different from one another. Inset: shows lack of effect of ω-CTx-MVIIC on ATP-evoked Ca^{2+} influx (*$P<0.05$, $n=4$).

(Figure 2 inset) was unaffected by a concentration of the VSCC blocker ω-CTx MVIIC (1 μM) sufficient to completely inhibit influx through all of the recognized neuronal VSCCs (Hillyard *et al.*, 1992; Lundy *et al.*, 1994, see also Figure 2). ATP stimulated influx was also unaffected in synaptosomes treated with the L-type calcium channel blocker (−)202−791 (Lundy *et al.*, 1991, present results not shown).

The P2X receptor antagonist pyridoxal-phosphate-6-azophenyl-2′-4′ disulphonic acid (PPADS) (Lambrecht, 1996) at a concentration of 30 μM markedly reduced ATP-evoked Ca^{2+} influx (Figure 2).

Since $P2X_7$ agonist activity has been reported to be greater in physiological buffers containing low concentrations of cations, experiments were repeated in two additional cation modified buffers (see Methods). The dose-effect curve for BzATP-stimulated influx was shifted to the left in sucrose, as compared to both choline and Na^+ based buffers; (difference $P<0.001$, 2-way ANOVA), confirming previous studies concerning $P2X_7$ receptor sensitivity in ionic media (Michel *et al.*, 1998; Virginio *et al.*, 1997). Results are shown in Figure 3A.

Brilliant Blue G (BBG), an antagonist selective for $P2X_7$ receptors (Jiang *et al.*, 2000; Hibell *et al.*, 2001) showed concentration related inhibitory activity towards BzATP-stimulated influx ($P<0.01$, at 1 μM, Figure 3B).

In order to provide more definitive data concerning the receptor subtype involved in the observed influx, lysates and homogenates were prepared from both whole brain and purified synaptosomes and were probed with antibodies for $P2X_2$ and $P2X_7$ receptors (Figure 4). $P2X_2$ receptors were detected in whole brain homogenates (Br) but not in purified synaptosomes (Syn) (Figure 4A). Lysates of whole PC-12 cells served as a positive control for the presence of $P2X_2$ receptors (Brake *et al.*, 1994). $P2X_7$ receptor protein was strongly expressed in both whole brain (Br) homogenates and in synaptosomal preparations (Syn) (Figure 4B). Homogenates of vas deferens (Vas) were used as negative controls for the presence of $P2X_7$ receptors.

The occurrence of $P2X_7$ receptors in brain has been attributed to their presence on microglia (Collo *et al.*, 1997). However, contamination by non-neuronal elements was not detected in purified synaptosomes prepared by similar methods as those described here (Daniels & Vickroy, 1998;

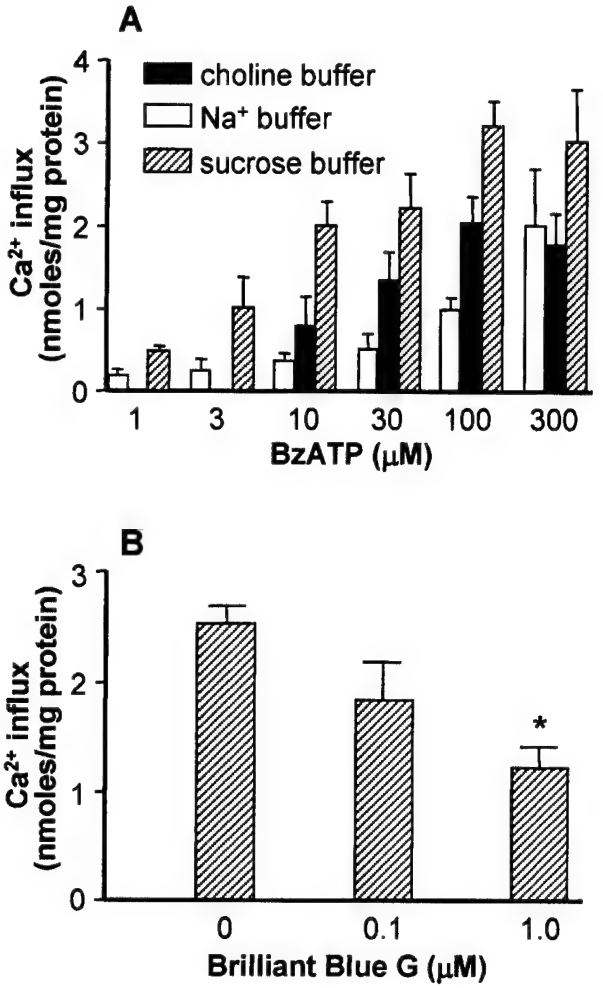

Figure 3 (A) Calcium influx was measured in synaptosomal preparations exposed to increasing concentrations of BzATP in three incubating solutions of different ionic composition. Each bar represents the mean ± s.e.mean, obtained in three experiments carried out in triplicate. BzATP induced influx was significantly greater in sucrose buffer than in the high ionic strength sodium or choline based buffers (2-way ANOVA, $P<0.001$). (B) Calcium influx initiated by BzATP in synaptosomal preparations incubated in the presence of the selective $P2X_7$ antagonist Brilliant Blue G. The influx represented by the bars is the mean ± s.e.mean of three experiments carried out in triplicate. The asterisk denotes a significant reduction in influx as compared to that caused by BzATP alone ($P<0.01$, Student's *t*-test).

Hoogland *et al.*, 1999). However, to preclude this possibility, we examined the presence of contaminants using specific antibodies to $P2X_7$ receptors and OX-42 (specific for microglia). Background immunofluorescence was examined in whole brain (Figure 5A) and synaptosomes (Figure 5B).

Immunofluorescence for $P2X_7$ receptors was located in brain and synaptosomes (Figure 5C, D) while OX-42 fluorescence was evident in whole brain (Figure 5E) but was absent in synaptosomes. The fluorescence in individual synaptosomes appears not to be uniform, probably as the result of the fact that they were concentrated (cytospun) and therefore could be at slightly different planes in the field or in some cases overlap one another. In similar experiments we also detected GFAP immunofluorescence in cortical tissue but not in purified synaptosomes (results not shown).

Although the lack of activity of the $P2X_1$ agonist α,β-me-ATP appears to preclude a role for $P2X_1$ receptors in ATP-stimulated Ca^{2+} influx, $P2X_1$ receptors were weakly detected by Western blot techniques in whole brain and in purified synaptosomal preparations. Rat vas deferens was used as a positive control for $P2X_1$ receptors (results not shown).

Western blots obtained using purified synaptosomal homogenates probed with anti-SNAP 25, anti-syntaxin and anti-GFAP antibodies, provided no evidence for GFAP in the purified synaptosomal preparation, but both synaptic markers were clearly evident (Figure 6). The purity of synaptic elements was further confirmed using immunohistochemistry to visualize the neuronal markers using fluorescent antibodies against SNAP-25 and syntaxin. These findings, which are in accord with the Western blot data, are shown in Figure 7.

Discussion

The present study offers several lines of evidence, which suggests the existence of P2X receptors on presynaptic elements of mammalian brain. In these studies we have examined the effects of ATP analogues on $^{45}Ca^{2+}$ influx, which provides a reliable functional assay for characterizing P2X receptor activity (Michel *et al.*, 1996; 1998). In previous studies, the potency order of ATP and related nucleotides has been used to define P2X receptor subtypes pharmacologically in a variety of tissues (Abbracchio & Burnstock, 1994; Fredholm *et al.*, 1994; 1997; Burnstock, 1999). In the present study, the synaptosomal calcium influx initiated by ATP or ATP analogues suggested both the presence of P2X receptors and a role for a specific subtype.

Dose response curves for calcium influx following ATP and BzATP were constructed. With the exception of BzATP, the remaining analogues were all compared at the same concentration at which ATP produced its maximal effect (the EC_{100}.). This is a similar method of comparison to that employed by other investigators as the result of similar problems obtaining EC_{50} values for these agonists (Surprenant *et al.*, 1996; King *et al.*, 1996; von Külgelgen *et al.*, 1997; Troadec *et al.*, 1998; Wiley *et al.*, 1998; Chung *et al.*, 2000). BzATP was about seven times more effective in evoking calcium influx than ATP while 2-me-S-ATP and ATPαS were less active than ATP probably as the result of their partial agonist properties at the $P2X_7$ receptor (Wiley *et al.*, 1998). These results together with the inactivity of α,β,methylene-adenosine 5'triphosphate, (α,β-me-ATP), and β,γ-methylene-L-adenosine triphosphate (β,γ-me-ATP) were consistent with the activation of a $P2X_7$ receptor subtype (Abbracchio & Burnstock, 1994; Wiley *et al.*, 1996; 1998; Surprenant *et al.*, 1996; Watling, 1998).

The $P2X_2$ receptor subtype has previously been identified on mammalian CNS neurons (see Kanjhan *et al.*, 1999 and references therein; Collo *et al.*, 1996). This receptor subtype has also been proposed to exist both on peripheral nerve endings and a percentage of neurohypophysial neurons (Troadec *et al.*, 1998; Boehm, 1999). These previous studies raise the possibility that $P2X_2$ receptors might be responsible for the calcium influx observed in this synaptosomal preparation. However several observations argue that $P2X_2$ receptors do not exist on presynaptic areas in the cortex and

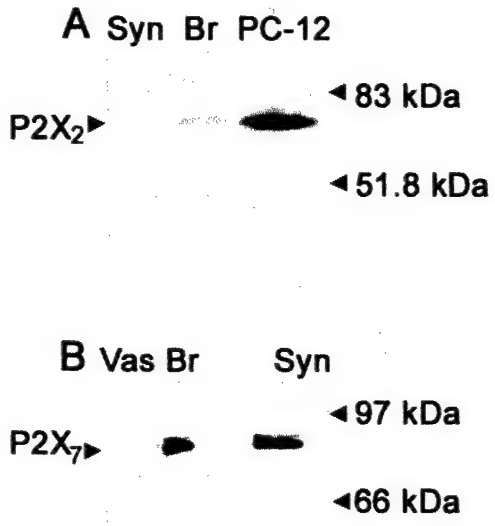

Figure 4 Western blots carried out to detect the presence of $P2X_2$ and $P2X_7$ receptor protein in rat cortical homogenates and synaptosomal preparations. Cortical homogenates and purified synaptosomes were prepared and treated with antibodies to $P2X_2$ and $P2X_7$ receptors. (A) Shows intense staining for $P2X_2$ receptors in PC-12 cells which were used as a positive control, weak detection in brain homogenates (Br), but no evidence of $P2X_2$ subtypes were found in purified synaptosomes (Syn). (B) Shows $P2X_7$ protein in brain homogenates and purified synaptosomes, but not in rat *vas deferens* (Vas) where $P2X_1$ receptors have been located.

are not responsible for the calcium influx observed in the present study. For example, there is ample evidence that BzATP is a much weaker agonist at $P2X_2$ receptors than ATP, 2-me-S-ATP and ATPγS (King *et al.*, 1996; Bianchi *et al.*, 1999; Michel *et al.*, 1996). In the present work, BzATP was found to be approximately seven times more effective as an agonist than ATP, the next most active nucleotide, which was in turn much more active than were any of the other analogues. Moreover western blots from whole brain showed the presence of $P2X_2$ receptors while the synaptosomal preparation did not. The lack of evidence of $P2X_2$ receptors in the synaptosomes corresponds with other important recent studies in which these receptors also could not be identified on midbrain synaptosomes (Gómez-Villafuertes *et al.*, 2001; Diáz-Hernández *et al.*, 2001). Differences between the existence of the same functional structures like $P2X_2$ receptors on peripheral and central nerve endings may be analogous to the situation with calcium channels. In the periphery, the N type VSCC is found almost exclusively in nerve endings whereas the P/Q type appears to be much more prevalent centrally (Lundy & Frew, 1996).

Several other lines of functional evidence all point to the existence of $P2X_7$ receptors on synaptosomes. Ionic composition of the buffer in which P2X receptor/agonist interactions are measured, has a major impact on the effectiveness of these interactions, particularly on the activity of the $P2X_7$ receptor subtype (Michel *et al.*, 1996; 1998; 1999; Surprenant *et al.*, 1996; Virginio *et al.*, 1997). Sodium has been suggested to cause an increase in the interference in $P2X_7$ agonist/receptor interactions (see ref. above and Wiley *et al.*, 1992; Hibell *et al.*, 2001). In our studies, BzATP was much more active in the sucrose based buffer than in either sodium or choline based buffers. The response profile is in good agreement with the activity of BzATP at $P2X_7$ receptors described in previous studies (Michel *et al.*, 1996; 1999). BBG and PPADS also inhibited agonist induced calcium influx. BBG, a selective $P2X_7$ inhibitor (Jiang *et al.*, 2000) was found in this study, to be an effective inhibitor of calcium influx at concentrations similar to those reported previously to be effective (Hibell *et al.*, 2001). The inhibitory effects of BBG at these relatively low concentrations, further mitigates against the presence of most of the other receptor subtypes with the possible exception of $P2X_2$.

Voltage and ligand gated ion channels are the principal Ca^{2+} entry pathways in excitable cells in general and in synaptosomes in particular (Bean, 1992; Benham, 1992). Previous studies have indicated different interactions between P2X receptors and VSCCs. For example, ATP has been reported to activate Ca^{2+} influx by activating both P2X receptors and also VSCCs in some (Rogers *et al.*, 1997; von Külgelgen *et al.*, 1999; Boehm, 1999) but not all peripheral preparations (Sperlágh *et al.*, 2000). In the CNS, the relative role played by calcium channels and P2X receptors in response to nucleotides depends on the neurons examined (Gu & MacDermott, 1997; Khakh and Henderson 1998; 2000; Hugel & Schlicter, 2000). Influx through VSCCs and subsequent neurotransmitter release in rat cortical synaptosomes occurs via activation of three major types of VSCCs (N, P and Q) which are inhibited by ω-CTx-MVIIC (Hillyard *et al.*, 1992; Wheeler *et al.*, 1994; Lundy *et al.*, 1994). In the present study, in order to determine whether nucleotide induced influx was the result of the activation of VSCCs, experiments were carried out in the presence of ω-CTx-MVIIC and the L-type channel blocker (−)202-791. The lack of effect of ω-CTx-MVIIC and (−)202-791 on nucleotide-evoked Ca^{2+} influx would appear to preclude ATP induced activation of VSCCs and suggests that the Ca^{2+} entry observed in the current study occurred directly *via* P2X receptors. These results and those in the literature are consistent with the proposal that various central neuronal populations may utilize different mechanisms to control Ca^{2+} influx following stimulation by ATP and related nucleotides. Therefore, nucleotide induced influx may be the result of activation of VSCCs, activation of P2X receptors or a combination of these two mechanisms, depending on the neurons and the species examined (Khakh and Henderson, 1998; 2000; Gu & MacDermott, 1997; Pintor *et al.*, 1999; Hugel & Schlicter, 2000; Nörenberg & Illes, 2000).

Western blots revealed weak staining for the $P2X_1$ receptor (results not shown) indicating its presence in synaptosomes. $P2X_1$ receptors predominate in smooth muscle, and their existence has also been reported in limited areas of the CNS, such as the cerebellum (Kidd *et al.*, 1995; Burnstock, 1999). However $P2X_1$ (or $P2X_3$) receptor mediated Ca^{2+} influx in this preparation was also precluded as the result of the lack of activity of α, β-me-ATP, a potent agonist at these receptor subtypes (Valera *et al.*, 1994; rev. see Abbracchio & Burnstock, 1994). Furthermore, α,β-me-ATP, which desensitises $P2X_1$ receptors (Kasakov & Burnstock, 1983) also failed to affect subsequent BzATP-evoked influx (P.M. Lundy and R. Frew, unpublished results). In addition, calcium influx was significantly reduced by BBG at concentrations that would not be expected to be active at $P2X_1$ receptors. Effective

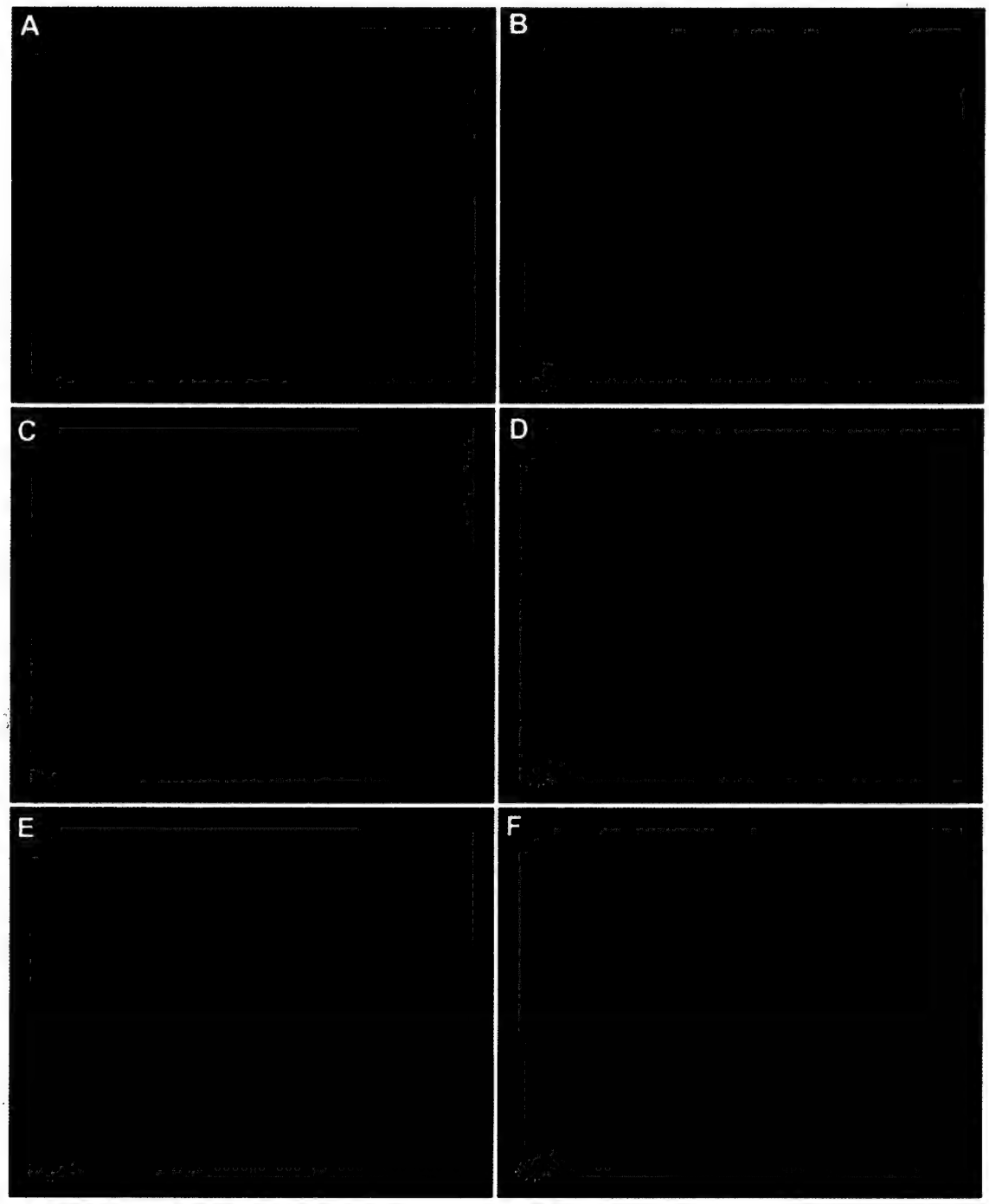

Figure 5 Immunoreactivity in cortical slices or in purified rat cortical synaptosomes treated with fluorescent antibodies to $P2X_7$ receptors or to the microglial marker OX-42. (A and B) show the background fluorescence in the absence of the primary antibodies to $P2X_7$ receptors or to OX-42 in cortical sections or synaptosomes respectively. Immunofluorescence demonstrated following treatment of cortical sections with fluorescent antibodies to $P2X_7$ receptors (C) or cytospun cortical synaptosomes (D). (E) reveals specific immunofluorescence in cortex treated with antibodies to the microglial marker OX-42. This fluorescence is absent from synaptosomal preparations (F).

antagonism of ATP-evoked Ca^{2+} influx by PPADS and the lack of selective activity of certain agonists, appears to preclude a role for $P2X_4$ and $P2X_6$ receptor subtypes (Evans *et al.*, 1998). However, convincing evidence for the existence of $P2X_3$ receptors in synaptosomes from rat midbrain has been recently reported (Gómez-Villafuertes *et al.*, 2001; Díaz-Hernández *et al.*, 2001). Although we did not determine the proportion of $P2X_7$ receptors in our preparation, the presence of a significant proportion of $P2X_3$ receptors on cortical synaptosomes appears unlikely since a high concentration of α-β-me-ATP (1 mM) a potent $P2X_3$ agonist was inactive in the mediation of calcium influx in our studies.

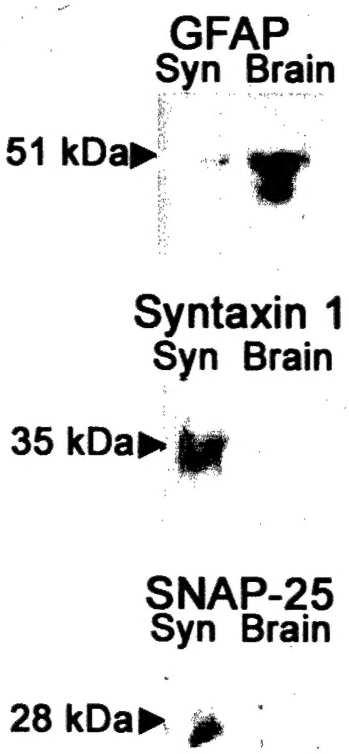

Figure 6 Western blots showing the presence of the synaptic markers syntaxin and SNAP-25 and the virtual absence of glial fibrillary acid protein (GFAP) in purified synaptosomes (Syn). Top panel: GFAP staining in whole cortical homogenates and virtual absence of staining in purified synaptosomes is shown. The figure shows the enhanced concentration of synaptic proteins syntaxin (middle panel) and SNAP-25 (bottom panel) in purified synaptosomes (Syn).

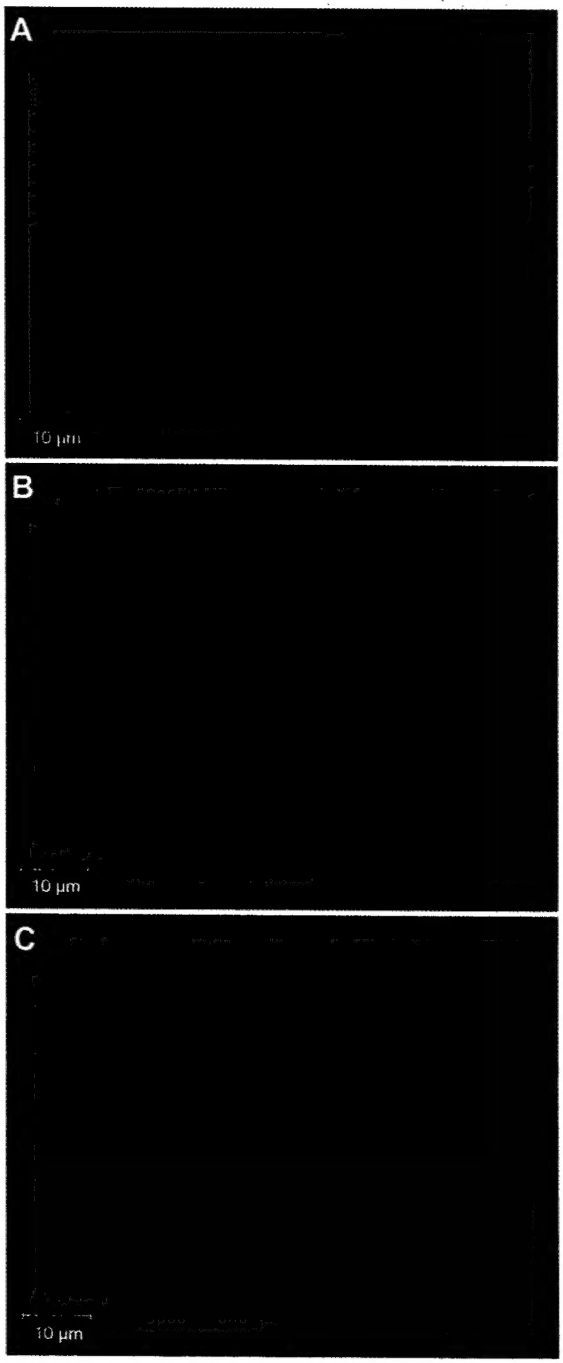

Figure 7 Immunoreactivity of purified synaptosomes treated with antibodies to the synaptic markers syntaxin and SNAP-25. (A) non-specific staining; (B) SNAP 25 staining; and (C) syntaxin staining.

However it appears clear that more than a single P2X receptor subtype likely co-exists at least in certain brain areas (Gómez-Villafuertes *et al.*, 2001; Diáz-Hernández *et al.*, 2001). Determination of the presence of $P2X_3$ receptors in cortical synaptosomes, or conversely of $P2X_7$ receptors in midbrain synaptosomes would be very interesting studies to carry out.

The results which demonstrated that the selective $P2X_7$ receptor agonist BzATP was of the order of seven times more potent with respect to evoking Ca^{2+} influx than ATP, the next most effective agonist, is in good agreement with a number of previous studies in other preparations containing $P2X_7$ receptors (for example, Nuttle & Dubyak, 1994; Wiley *et al.*, 1996; 1998; Evans *et al.*, 1998; Surprenant *et al.*, 1996; Chessell *et al.*, 1998; Chung *et al.*, 2000). However, some doubt has been raised recently concerning the actual $P2X_7$ selectivity of BzATP. For example in certain assays, BzATP has been reported to be more potent at $P2X_1$ than at $P2X_7$ receptors (Bianchi *et al.*, 1999). Reasons for differences reported among a variety of studies concerning the selectivity of BzATP are unclear, but the apparent controversy may complicate use of BzATP as a tool to distinguish between $P2X_1$ and $P2X_7$ subtypes. Oxidized ATP (2,3′-dialdehyde ATP), a $P2X_7$ receptor antagonist, could not be used to further confirm the presence of the $P2X_7$ receptor subtype since its inhibitory activity has been reported to develop only after a 2 h pretreatment period (Murgia *et al.*, 1993) which is inconsistent with synaptosomal viability. Studies using KN-62, which has been reported to be a potent antagonist of the $P2X_7$ receptor of human lymphocytes (Gargett & Wiley, 1997) failed to inhibit ATP-evoked Ca^{2+} influx in synaptosomes (P.M. Lundy and R. Frew, unpublished results) likely due to differences in its inhibitory activity between rat and human receptors (Humphreys *et al.*, 1998).

$P2X_7$ receptor subtypes detected in whole brain homogenates have also been attributed to their presence on microglia (Ballerini *et al.*, 1996; Collo *et al.*, 1997; Ferrari *et al.*, 1997). It was important therefore to ensure that $P2X_7$ protein was indeed located on synaptosomal terminals and was not due to non-neuronal contaminating elements. Percoll® gradient isolation of synaptosomes has been reported to be sufficient to eliminate non-synaptosomal contaminants (Daniels & Vickroy, 1998; Dugar *et al.*, 1998; Hoogland *et al.*, 1999). The presence in the purified synaptosomes of the markedly enhanced concentrations of the synaptic markers syntaxin and SNAP-25, and the almost complete absence of GFAP or the microglial marker OX-42 (Brook *et al.*, 2001) confirmed the lack of glial or microglial contamination in these synaptosomes.

In summary, our study clearly demonstrates that P2X receptors exist on central presynaptic nerve terminals and that the evidence presented here suggests that these receptors are of the $P2X_7$ subtype. This novel finding of $P2X_7$ receptors on cortical synaptosomes suggests that these receptor subtypes play a role in neurotransmission, and probably in other Ca^{2+} dependant events distinct from those mediated by VSCCs in presynaptic terminals in the CNS. We are currently examining the role of this receptor on BzATP induced glutamate release.

This work was supported in part by the U.S. Army Medical Research and Development Command, Award DAMD17-99-2-9010. In performing the research described in this paper, the authors adhered to the 'Guide to the Care and Use of Laboratory Animals' and 'The Ethics of Animal Experimentation' published by the Canadian Council on Animal Care, Ottawa, Ontario, Canada.

References

ABBRACCHIO, M.P. & BURNSTOCK, G. (1994). Purinoceptors: Are there families of P2X and P2Y purinoceptors? *Pharmacol. Ther.*, **64,** 445–475.

BALLERINI, P., RATHBONE, M.P., DIIORIO, P., RENZETTI, A., GIULIANI, P., D'ALIMONTE, I., TRUBIANI, O., CACIAGLI, F. & CICCARELLI, R. (1996). Rat astroglial P2Z ($P2X_7$) receptors regulate intracellular calcium and purine release. *NeuroReport*, **7,** 2533–2537.

BEAN, B.P. (1992). Pharmacology and electrophysiology of ATP-activated ion channels. *TIPS*, **13,** 87–90.

BENHAM, C.D. (1992). ATP joins the fast lane. *Nature*, **359,** 103–104.

BIANCHI, B.R., LYNCH, K.J., TOUMA, E., NIFORATOS, W., BURGARD, E.C., ALEXANDER, K.M., PARK, H.S., YU, H., METZGER, R., KOWALUK, E., JARVIS, M.F. & VAN BIESEN, T. (1999). Pharmacological characterization of recombinant human and rat P2X receptor subtypes. *Eur. J. Pharmacol.*, **376,** 127–138.

BLAUSTEIN, M.P. (1975). Effects of potassium, veratridine and scorpion venom on Ca^{2+} accumulation and transmitter release by nerve terminals in vitro. *J. Physiol.*, **247,** 617–655.

BOEHM, S. (1999). ATP stimulates sympathetic transmitter release via presynaptic P2X receptors. *J. Neurosci.*, **19,** 737–746.

BOEHM, S., HUCK, S. & ILLES, P. (1995). UTP and ATP-triggered transmitter release from rat sympathetic neurones via separate receptors. *Br. J. Pharmacol.*, **116,** 2341–2343.

BRADFORD, M.M. (1976). A rapid and sensitive method for the quantitation of microgram quantities of protein using the principle of protein dye binding. *Anal. Biochem.*, **72,** 248–254.

BRAKE, A.J., WAGENBACH, M.J. & JULIUS, D. (1994). New structural motif for ligand-gated ion channels defined by an ionotropic ATP receptor. *Nature*, **371,** 519–523.

BROOK, G.A., LAWRENCE, J.M. & RAISMAN, G. (2001). Columns of schwann cells extruded into the CNS induce in-growth of astrocytes to form organized new glial pathways. *Glia*, **33,** 118–130.

BURNSTOCK, G. (1999). Current status of purinergic signalling in the nervous system. In *Progress in Brain Research: Nucleotides and their receptors in the nervous system.* eds, Illes P, Zimmerman H. **vol. 120.** pp. 3–10. Amsterdam: Elsevier.

CHESSELL, I.P., MICHEL, A.D. & HUMPHREY, P.P.A. (1998). Effects of antagonists at the human recombinant $P2X_7$ receptor. *Br. J. Pharmacol.*, **124,** 1314–1320.

CHUNG, H.S., PARK, K.S., CHA, S.K., KONG, I.D. & LEE, J.W. (2000). ATP-induced $[Ca^{2+}]_i$ changes and depolarization in GH3 cells. *Br. J. Pharmacol.*, **130,** 1843–1852.

COLLO, G., NEIDHART, E., KAWASHIMA, M., KOSCO-VILBOIS, M., NORTH, R.A. & BUELL, G.N. (1997). Tissue distribution of the $P2X_7$ receptor. *Neuropharmacology*, **36,** 1277–1283.

COLLO, G., NORTH, R.A., KAWASHIMA, E., MERLO-PICH, E., NEIDHART, S., SURPRENANT, A. & BUELL, G. (1996). Cloning of $P2X_5$ and $P2X_6$ receptors, and the distribution and properties of an extended family of ATP-gated ion channels. *J. Neurosci.*, **16,** 2495–2507.

DANIELS, K.K. & VICKROY, T.W. (1998). Simultaneous isolation of glial and neuronal fractions from rat brain homogenates: Comparison of high-affinity L-glutamate transport properties. *Neurochem. Res.*, **23,** 103–113.

DIÁZ-HERNÁNDEZ, M., GÓMEZ-VILLAFUERTES, R., HERNANDO, F., PINTOR, J. & MIRAS-PORTUGAL, M.T. (2001). Presence of different ATP receptors on rat midbrain single synaptic terminals. Involvement of the $P2X_3$ subunits. *Neurosci. Lett.*, **301,** 159–162.

DUGAR, A., PATANOW, C., O'CALLAGHAN, J.P. & LAKOSKI, J.M. (1998). Immunohistochemical localisation and quantification of glial fibrillary acidic protein (mol wt 25,000) in the aging hippocampus following administration of 5,7-dihydroxytryptamine. *Neuroscience*, **85,** 123–133.

DUNKLEY, P.R., HEATH, J.W., HARRISON, S.M., JARVIEM, P.E., GLENFIELD, P.J. & ROSTAS, J.A.P. (1988). A rapid Percoll gradient procedure for isolation of synaptosomes directly from an S_1 fraction: homogeneity and morphology of subcellular fractions. *Brain Res.*, **441,** 59–71.

EDWARDS, F.A., GIBB, A.J. & COLQUHOUN, D. (1992). ATP receptor mediated synaptic currents in the central nervous system. *Nature*, **359,** 144–147.

EVANS, R.J., DERKACH, V. & SURPRENANT, A. (1992). ATP mediates fast synaptic transmission in mammalian neurons. *Nature*, **357,** 503–505.

EVANS, R.J., SURPRENANT, A. & NORTH, R.A. (1998). P2X receptors cloned and expressed. In *The P2 Nucleotide Receptors.*, eds. Turner JT, Weisman GA, Fedan JS. pp. 43–61. Totawa, NJ: Humana Press.

FERRARI, D., CHIOZZI, P., FALZONI, S., DAL SUSINO, M., COLLO, G., BUELL, G. & DI VIRGILLIO, F. (1997). ATP-mediated cytotoxicity in microglial cells. *Neuropharmacology*, **36,** 1295–1301.

FREDHOLM, B.B., ABBRACCHIO, M.P., BURNSTOCK, G., DALY, J.W., HARDEN, T.K., JACOBSON, K.A., LEFF, P. & WILLIAMS, M. (1994). VI Nomenclature and classification of purinoceptors. *Pharmacol. Rev.*, **46,** 143–156.

FREDHOLM, B.B., ABBRACCHIO, M.P., BURNSTOCK, G., DUBYAK, G.R., HARDEN, T.K., JACOBSON, K.A., SCHWABE, U. & WILLIAMS, M. (1997). Towards a revised nomenclature for P1 and P2 receptors. *TIPS*, **18,** 79–82.

GALLIGAN, J.J. & BERTRAND, P.P. (1994). ATP mediates fast synaptic potentials in enteric neurons. *J. Neurosci.*, **14,** 7563–7571.

GARGETT, C.E. & WILEY, J.S. (1997). The isoquinoline derivative KN-62 a potent antagonist of the P2Z receptor of human lymphocytes. *Br. J. Pharmacol.*, **120,** 1483–1490.

GIBB, A.J. & HALLIDAY, F.C. (1996). Fast purinergic transmission in the central nervous system. *Sem. Neurosc.*, **8,** 225–232.

GÓMEZ-VILLAFUERTES, R., GUALIX, J. & MIRAS-PORTUGAL, M.T. (2001). Single GABAergic synaptic terminals from rat midbrain exhibit functional P2X and dinucleotide receptors, able to induce GABA secretion. *J. Neurochem.*, **77,** 84–93.

GU, G. & MACDERMOTT, A.B. (1997). Activation of ATP P2X receptors elicits glutamate release from sensory neuron synapses. *Nature*, **389,** 749–753.

HIBELL, A.D., THOMPSON, K.M., XING, M., HUMPHREY, P.P.A. & MICHEL, A.D. (2001). Complexities of measuring antagonist potency at P2X7 receptor orthologs. *J. Pharmacol. Exp. Ther.*, **296,** 947–957.

HILLYARD, D.R., MONJE, V.D., MINTZ, I.M., BEAN, B.P., NADASDI, L., RAMACHANDRAN, J., MILJANICH, G., AZIMI-ZOONOOZ, A., MCINTOSH, J.M., CRUZ, L.J., IMPERIAL, J.S. & OLIVERA, B.M. (1992). A new conus peptide ligand for mammalian presynaptic Ca^{2+} channels. *Neuron*, **9,** 69–77.

HOOGLAND, G., BLOMENROHR, M., DIJSLBLOEM, H., DE WIT, M., SPIERENBURG, H.A., VAN VEELEN, C.W.M., VAN RIJEN, P.C., VAN HUFFELEN, A.C., GISPEN, W.H. & DE GRAAN, P.N.E. (1999). Characterization of neocortical and hippocampal synaptosomes from temporal lobe epilepsy patients. *Brain Res.*, **837,** 55–66.

HUGEL, S. & SCHLICTER, R. (2000). Presynaptic P2X receptors facilitate inhibitory GABAergic transmission between cultured rat spinal cord dorsal horn neurons. *J. Neurosci.*, **20,** 2121–2130.

HUMPHREYS, B.D., VIRGINIO, C., SURPRENANT, A., RICE, J. & DUBYAK, G.R. (1998). Isoquinolines as antagonists of the $P2X_7$ nucleotide receptor: High selectivity for the human versus rat receptor homologues. *Mol. Pharmacol.*, **58,** 82–88.

JIANG, L-H., MACKENZIE, A.B., NORTH, R.A. & SURPRENANT, A. (2000). Brilliant blue G selectively blocks ATP-gated rat $P2X_7$ receptors. *Mol. Pharmacol.*, **58,** 82–88.

KANJHAN, R., HOUSLEY, G.D., BURTON, L.D., CHRISTIE, D.L., KIPPENBERGER, A., THORNE, P.R., LUO, L. & RYAN, A.F. (1999). Distribution of the $P2X_2$ receptor subunit of the ATP-gated ion channels in the rat central nervous system. *J. Comp. Neurol.*, **407,** 11–32.

KASAKOV, L. & BURNSTOCK, G. (1983). The use of the slowly degradable analog α,β methylene ATP, to produce desensitization of the P_2 purinoceptor: effect of non-adrenergic, non cholinergic responses of the guinea-pig urinary bladder. *Eur. J. Pharmacol.*, **86,** 291–294.

KHAKH, B.S. & HENDERSON, G. (1998). ATP receptor mediated enhancement of fast excitatory neurotransmitter release in the brain. *Mol. Pharmacol.*, **54,** 372–378.

KHAKH, B.S.& HENDERSON, G. (2000). Modulation of fast synaptic transmission by presynaptic ligand-gated cation channels. *J. Aut. Nerv. Syst.*, **81,** 110–121.

KIDD, E.J., GRAHAMES, B.A., SIMON, J., MICHEL, A.D., BARNARD, E.A. & HUMPHREY, P.P.A. (1995). Localization of P_{2x} purinoceptor transcripts in the rat nervous system. *Mol. Pharmacol.*, **48,** 569–573.

KIDD, E.J., MILLER, K.J., SANSUM, A.J. & HUMPHREY. P.P.A. (1998). Evidence for $P2X_3$ receptors in the developing brain. *Neuroscience*, **87,** 533–539.

KING, B.F., ZIGANSHINA, L.E., PINTOR, J. & BURNSTOCK, G. (1996) The sensitivity of $P2X_2$ purinoceptor to ATP revealed by changing extracellular pH. *Br. J. Pharmacol.*, **117,** 1371–1373.

LAMBRECHT, G. (1996). Design and pharmacology of selective P_2 purinoceptor antagonists. *J. Aut. Pharmacol.*, **16,** 341–344.

LÊ, K.T., VILLENEUVE, P., RAMJAUN, A.R., MCPHERSON, P.S., BEAUDET, A. & SEGUELA, P. (1998). Sensory presynaptic and widespread somatodendritic immunolocalisation of central ionotropic P2X ATP receptors. *Neuroscience*, **83,** 177–190.

LUNDY, P.M. & FREW, R. (1996). Review: Ca^{2+} channel sub-types in peripheral efferent autonomic nerves. *J. Aut. Pharmacol.*, **16,** 229–241.

LUNDY, P.M., FREW, R., FULLER, T.W. & HAMILTON, M.G. (1991). Pharmacological evidence of an ω-conotoxin, dihydropyridine-insensitive neuronal Ca^{2+} channel. *Eur. J. Pharmacol. (Mol. Pharmacol.)* **206,** 61–68.

LUNDY, P.M., HAMILTON, M.G. & FREW, R. (1994). Pharmacological identificationof a novel Ca^{2+} channel in chicken brain synaptosomes. *Brain Res.*, **643,** 204–210.

MOTIN, I. & BENNETT, M.R. (1995). Effect of P_2-purinoceptor antagonists on glutamatergic transmission in the rat hippocampus. *Br. J. Pharmacol.*, **115,** 1276–1280.

MICHEL, A.D., CHESSELL, I.P. & HUMPHREY, P.P.A. (1999). Ionic effects on human recombinant $P2X_7$ function. *Naunyn-Schmied. Arch. Pharmacol.*, **359,** 102–109.

MICHEL, A.D., CHESSELL, I.P., SIMON, J. & HUMPHREY, P.P.A. (1998). Identification and characterization of an endogenous $P2X_7$ (P2Z) receptor in CHO-K1 cells. *Br. J. Pharmacol.*, **125,** 1194–1201.

MICHEL, A.D., GRAHAMES, C.B.A.& HUMPHREY, P.P.A. (1996). Functional characterisation of P2 purinoceptors in PC12 cells by measurement of radiolabelled calcium influx. *Naunyn-Schmied. Arch. Pharmacol.*, **354,** 562–571.

MURGIA, M., HANAU, S., PIZZO, P., RIPPA, M. & DI VIRGILIO, F. (1993). Oxidised ATP, an irreversible inhibitor of the macrophage purinergic P2Z receptor. *J. Biol. Chem.*, **268,** 8199–8203.

NÖRENBERG, W. & ILLES, P. (2000). Neuronal P2X receptors: localisation and functional properties. *Naunyn-Schmied. Arch. Pharmacol.*, **362,** 324–339.

NUTTLE, L.C. & DUBYAK, G.R. (1994). Differential activation of cation channels and non-selective pores by macrophage P_{2Z} purinergic receptors expessed in *Xenopus* oocytes. *J. Biol. Chem.*, **269,** 13988–13996.

PINTOR, J., DÍAZ-HERNÁNDEZ, M., BUSTAMANTE, C., GUALIX, J., GÓMEZ DE TERREROS, F.J. & MIRAS-PORTUGAL, M.T. (1999). Presence of dinucleotide and ATP receptors in human cerebrocortical synaptic terminals. *Eur. J. Pharmacol.*, **366,** 159–165.

ROGERS, M., COLQUHOUN, L.M., PATRICK, J.W. & DANI, J.A. (1997). Ca2+ flux through predominantly independent purinergic ATP and nicotinic acetylcholine receptors. *J. Neurophysiol.*, **77,** 1407–1417.

SÉGUÉLA, P., HAGHIGHI, A., SOGHOMONIAN, J-J. & COOPER, E. (1996). A novel neuronal P_{2x} ATP receptor ion channel with widespread distribution in the brain. *J. Neurosci.*, **16,** 448–455.

SILINSKY, E.M., GERZANICH, V. & VANNER, S.M. (1992). ATP mediates fast excitatory synaptic transmission in enteric neurones. *Br. J. Pharmacol.*, **106,** 762–763.

SPERLÁGH, B., ERDELYI, F., SZABÓ, G. & VIZI, E.S. (2000). Local regulation of ^{3}[H]-noradrenaline release from the isolated guinea-pig right atrium by P_{2x} receptors located on axon terminals. *Br. J. Pharmacol.*, **131,** 1775–1783.

SURPRENANT, A., RASSENDREN, F., KAWASHIMA, E., NORTH, R.A. & BUELL, G. (1996). The cytolytic P2Z receptor for extracellular ATP identified as a P2X receptor ($P2X_7$). *Science*, **272,** 735–737.

TROADEC, J-D, THIRION, S., NICAISE, G., LEMOS, J.R. & DAYANITHI, G. (1998). ATP-evoked increases in $[Ca^{2+}]_I$ and peptide release from rat isolated neurohypophysial terminals via a $P_{2\times2}$ purinoceptor. *J. Physiol.*, **511,** 89–108.

UENO, S., HARATA, N., INOUE, K. & AKAIKE, N.J. (1992). ATP-gated current in dissociated rat nucleus solitarii neurons. *J. Neurophysiol.*, **68,** 778–785.

VALERA, S., HUSSY, N., EVANS, R.J., ADAMI, N., NORTH, R.A., SURPRENANT, A. & BUELL, G. (1994). A new class of ligand-gated ion channel defined by a P_{2X} receptor for extracellular ATP. *Nature*, **371,** 516–519.

VIRGINIO, C., CHURCH, D., NORTH, R.A. & SURPRENANT, A. (1997). Effects of divalent cations and protons and calmidazolium at the rat $P2X_7$ receptor. *Neuropharmacology*, **36,** 1285–1294.

VON KÜLGELGEN, I., KURZ, K. & STARKE, K. (1993). Axon terminal P_2-purinoceptors in feedback control of sympathetic transmitter release. *Neuroscience*, **56,** 263–267.

VON KÜLGELGEN, I., NORENBERG, W., MEYER, A., ILLES, P. & STARKE, K. (1999). Role of action potentials and Ca2+ influx in ATP- and UDP-induced noradrenaline release from rat cultured sympathetic neurones. *Naunyn- Schmeid. Arch. Pharmacol.*, **359,** 360–369.

WATLING, K.J. (1998). P_2 receptors. In *The RBI Handbook of Receptor Classification and Signal Transduction*. 3rd edn. pp. 58–60. Natick, MA: RBI.

WHEELER, D.B., RANDALL, A. & TSIEN, R.W. (1994). Roles of N-type and Q-type Ca^{2+} channels in supporting hippocampal synaptic transmission. *Science*, **264,** 107–111.

WILEY, J.S., CHEN, J.R., SNOOK, M.S., GARGETT, C.E. & JAMIESON, G.P. (1996). Transduction mechanisms of P2Z purinoceptors. In: *P2 Purinoceptors: Localization, Function and Transduction Mechanisms*. pp. 149–165. Chichester: Wiley.

WILEY, J.S., CHEN, J.R., WILEY, M.J. & JAMIESON, G.P. (1992). The ATP^{4-} receptor-operated ion channel of human lymphocytes: inhibition of ion fluxes by ameloride analogues and by extracellular sodium ions. *Biochem. Biophys.*, **292,** 411–418.

WILEY, J.S., GARGETT, C.E., ZHANG, W., SNOOK, M.B. & JAMIESON, G.P. (1998). Partial agonists and antagonists reveal a second permeability state of human lymphocyte P2Z/$P2X_7$ channel. *Am. J. Physiol.*, **275,** C1224–C1231.

(Received September 3, 2001
Revised January 11, 2002
Accepted January 23, 2002)